Project Title:	ECOPOTENTIAL: IMPROVING FUTURE ECOSYSTEM BENEFITS THROUGH EARTH OBSERVATIONS
Project number:	641762
Project Acronym:	ECOPOTENTIAL
Proposal full title:	IMPROVING FUTURE ECOSYSTEM BENEFITS THROUGH EARTH OBSERVATIONS
Type:	Research and innovation actions
Work program topics addressed:	SC5-16-2014: “Making Earth Observation and Monitoring Data usable for ecosystem modelling and services”

Deliverable No: 4.2

EO Biophysical Parameters, Land Use and Habitats Extraction Modules

Version:	v1
Main Authors:	UNSW, CNR, UPS, CERTH, EURAC, CSIR, STARLAB, CREAF, ISPRA, DLR, UAB, UFZ, FORTH, ESL, UFZ

This project has received funding from the *European Union’s Horizon 2020 research and innovation programme* under grant agreement No 641762

Table of Contents

1. Executive summary

ECOPOTENTIAL WP4 is responsible for the provisioning of Earth Observation (EO) data and derived products for the Protected Areas (PAs) as well as to support other activities executed in WP6, WP7, WP8, WP9 and WP10. The final objective of the WP is to empower the PA to execute the algorithms presented here and sibling deliverables themselves by transferring the codes to the Virtual Laboratory (WP10). This is complemented by WP5 that provides the necessary in situ data.

Deliverable D4.2 conveys the activities carried out within Task 4.2 and Task 4.3 (first 22 months) of the EU Horizon 2020 ECOPOTENTIAL Project. The Deliverable provides an overview of the algorithms used or developed to retrieve Environmental Variables (EVs) for the 22 PAs distributed across Europe, in Israel and South Africa and selected for study. For classification, the Earth Observation Data for Ecosystem Monitoring (EODESM) system stands out as it makes full use of and integrates all of the EVs retrieved for the different PAs in the classification of lands covers and generally used for monitoring of PAs. Its development also considered the storylines described through ECOPOTENTIAL and outlined in Deliverable 2.2.

One of the main objectives of WP4 was to design and develop the EODESM system to enable quantitative descriptions of land cover for each of the 22 PAs and according to the FAO Land Cover Classification System (LCCS2) taxonomy. An essential component is to ensure that the diverse range of EO data and derived products that are increasingly becoming available from Task 4.2, contributed significant input to the EODESM system. Particular focus is on utilising EO data provided through the European Copernicus project (and particularly Sentinel-1 and -2 radar and optical data).

The retrieval of EVs focused on those that were identified during the development of storylines for each PA and are obtained locally (e.g., using established algorithms including those developed through this project) or from layers generated at the national, European or global level; from EO data acquired across a range of spatial resolutions and temporal frequencies. For the EODESM system, these EVs are categorized according to whether they a) are thematic classifications of LCCS2 components (e.g., plant life form) or continuous surfaces (e.g., of canopy cover %) and b) provide direct input to the classification (e.g., hydro-period) or are simply additional descriptors (e.g., above ground biomass; Mg ha-1). Open source software is then used to combine the individual components of the LCCS2 system (e.g., water state, movement, inundation frequency, sediment loads and depth) into a single class (e.g., flowing, deep and clear water for more than 9 months of the year). All pixels and objects associated with that class are then attributed with information on the different EVs. Comprehensive and detailed land cover maps with a consistent LCCS2 taxonomy are generated for the PAs for which input data are available. The accuracy of the classifications is dependent on that of the input layers combined and is assessed against existing land cover and habitat maps whose diverse taxonomies had been standardized to that of the LCCS2. The assessment of accuracy is complex because of the integration of different layers obtained using a range of approaches and data and will be further reported in Deliverable 4.3.

The following sections detail the concepts behind the EODESM system (Section 2) and provide a list of the key EVs that are of relevance to the storylines and how these have been obtained (Section 3) and used as input (Section 4). Classifications for different PAs and validation techniques applied are illustrated in Section 4. The products provided (and to be updated) to the ECOPOTENTIAL repository as well as the modules to be linked to the Virtual Laboratory (WP10), how and when, are summarized in Section 5. Conclusions are reported in Section 6, with all references in Section 7. Appendix 1, in Section 8, provides the workflow of some modules. Appendix 2 and 3, in Sections 9 and 10, respectively, provide any additional information concerning the FAO LCCS2 taxonomy as well as class codes and map legends used in D4.2. Appendix 4, in Section 11, illustrates the methodology used to assess the Technological Readiness Level (TRL) of the modules discussed in previous sections.

1.1 Abbreviation and acronyms

BIO_SOS project	Biodiversity Multi-Source Monitoring System: from Space to Species, (http://www.biosos.eu/)
CHM	Canopy Height Model
CLC	Corine Land Cover
DEM	Digital Elevation Model
EBONE	European Biodiversity Observation Network (http://www.wur.nl/en/Expertise-Services/Research-Institutes/Environmental-Research/Projects/EBONE-2.htm)
EEA39	European Environment Agency – Wetlands – 100 m.
EO	Earth Observation Data
EODESM	Earth Observation Data for Ecosystem Monitoring
ESA	European Space Agency
EU BON	Building the European Biodiversity Observation Network (http://www.eubon.eu/)
Eunis	European Nature Information System
FAO-LCCS2	Food And Agriculture Land Cover Classification System, version 2
GEE	Google Earth Engine
GRD	Ground Range Detected SAR products
IW-GRD-HR	Interferometric Wide Swath Ground Range Multi-Look Detected High Resolution Sentinel-1 mode
EW-GRD-MR	Interferometric Extra-Wide Swath Ground Range Multi-Look Detected Medium Resolution Sentinel-1 mode
LAIe	effective Leaf Area Index
MCC	Multiscale Curvature Classification
MODIS	Moderate Resolution Imaging Spectroradiometer
MMW	Minimum Mapping Width
MMU	Minimum Mapping Unit
NDVI	Normalized Difference Vegetation Index
NDWI	Normalized Difference Water Index
Ms.MONINA	Multi-scale Service for Monitoring NATURA 2000 Habitats of European Community Interest (http://www.ms-monina.eu/)
NA	Not Available
PA	Protected Area
SAR	Synthetic Aperture Radar
SVM	Support Vector Machine Classifier
TCD	Tree Canopy Density
TRL	Technology Readiness Level
VHR	Very High Spatial resolution
VL	Virtual Laboratory
WPS	Web Processing Service

2. Introduction

A key aim of the EU FP7 Horizon 2020 ECOPOTENTIAL Project was to retrieve environmental variables (EVs) from earth observation (EO) that could be used to describe but also contribute to the classification of landscapes within and surrounding protected areas (PAs) and assessment of change. The study focused on 22 PAs and their surrounds, with these distributed across Europe and also Israel and South Africa and representing a diversity of land covers (LC) and habitats associated with high mountain, marine and coastal, and arid and semi-arid ecosystems. Providing a robust, accurate and relevant classification for this diverse range of PAs was a significant challenge but was addressed by designing and developing the Earth Observation Data for Ecosystem Monitoring (EODESM) system. This system was built on the knowledge driven concepts behind the Earth Observation Data for Habitat Monitoring (EODHaM) system generated as part of the EU FP7 BIO_SOS project (Lucas et al., 2014) and applied to Very High Resolution (VHR) Worldview data. The EODESM system is similar to its predecessor in that it facilitates routine classification of land covers according to *the Food and Agricultural Organisations Land Cover Classification System* (FAO LCCS2) and can translate these to other LC as well as habitat taxonomies with or without the integration of in-situ data (Tomaselli et al. 2013). The EODESM system can also integrate products generated by data driven classifiers and pre-existing validated thematic data. The system facilitates routine detection of change and allows for the generation of maps indicating the causes and consequences of change (to be reported in Deliverable 4.3). The system has been developed in **Task 4.3** and uses, as input, the EVs generated in **Task 4.2**. The resulting maps provide direct input to the modelling activities being undertaken in other WPs (i.e., WP6, WP7, WP8).

The motivations behind the development of the EODESM system was the recognition that:

a) Land cover and change classification could be generated for any area using a consistent and globally-applicable land cover taxonomy (i.e., the FAO LCCS2).

b) The classifications could make direct use of EVs generated within **Task 4.2**, over varying periods of time from EO and other data sources. These included those that were knowledge-driven (e.g., rule-based) or data driven and using algorithms (e.g., through supervised random forest or support vector machine algorithms) that were developed through previous FP6 and FP7 projects (e.g., FP6-EBONE, FP7-BIO_SOS, FP7-MS.MONINA, FP7-EU BON, FP7-TELEIOS).

c) The use of raster attribute tables, through the newly developed KEA format (Bunting et al., 2013), allowed additional EVs from different GEO Societal Benefit Areas (SBAs) to be integrated and made available.

d) The classifications could be applied at any scale and using input from a wide range of multiple-source earth observation data, including from radar and optical sensors.

e) The classifications could be validated by translating existing land cover or habitat maps to the same consistent taxonomy (i.e., FAO LCCS2) or providing validated in situ information (including recent updated data collections) that was equivalent in content to that used for classification and description within the EODESM system.

f) The FAO LCCS2 taxonomy could be largely translated to habitat categories including those described by Annex 1 (Habitat Directive (92/43/EEC) or the European Nature Information System (EUNIS) taxonomies or The General Habitat Categories (GHCs from the EBONE and BIO_SOS projects).

g) LC and habitats are important elements for ecosystem monitoring. In the literature, and for practical purposes, the MAES report (Maes at al., 2014) considers an ecosystem at the scale of habitats, which can be mapped through translation from LC maps (Tomaselli et al., 2013).

h) Open source software (mainly written in python) was available or could be advanced to undertake the development of the EODESM system, which could then be distributed to users.

2.1 Main objectives

The stated operational objectives of WP4, as listed in the DOW, are:

1. Design and develop a pre-operational multi-modular system named EO Data for Ecosystem Monitoring (EODESM) for Level 1, 2, 3 and 4 Remote Sensing (RS) data to quantify Essential Biodiversity Variables (EBVs) and other EVs and document quality and uncertainty. An advancement of the state of the art using both pre-existing and new techniques will be achieved particularly when dealing with Very High spatial Resolution (VHR) (e.g., 3rd Party missions: WorldView-3), temporal Resolution (VHT) (e.g., Sentinel-1/2) and spectral Resolution (VSR) (e.g., DLR's hyperspectral EnMap).
2. Optimise the selection and use of appropriate EO data, considering sensor types, spatial, temporal and spectral resolution, and Copernicus core products for ecosystem classification, mapping and monitoring.
3. Elaborate open source software and products.
4. Support activities in WP6, WP7, WP8 and WP9 and provide results to WP10. Provide EO product validation, inter-comparison and visualization tools for assessing the quality of data products (e.g., land cover and habitat maps). As output, WP4 will provide comprehensive multi-source, multi-scale and multi-temporal EO products (services) for ecosystem monitoring and will distribute them as an ECOPERNICUS service (WP10).

In this framework, Deliverable 4.2 describes the activities carried out within Task 4.2 and Task 4.3.

Task 4.2 focuses on the direct and indirect retrieval of terrestrial (Task 4.2.1) and marine/coastal (Task 4.2.1) bio-geophysical variables at spatial resolutions (grains) and temporal frequencies that are appropriate as input to the activities undertaken in Task 4.3 and other modelling WPs of the project. Section 3 of this document describes the activity carried out in Task 4.2.

Task 4.3 focuses on the EODESM system for the extraction of thematic maps and indicators from multiple-scale EO data (including satellite and *in-situ* data). Land cover and habitats classifications (Task 4.3.1 and Task 4.3.2) and their validation (Task 4.3.5) have been mainly based on the analysis of recent and archived Medium Resolution (MR) and High spatial Resolution (HR) images. Knowledge- and data-driven classification techniques for multi-scale LC maps and LC to habitat conversion have been used. Such maps have been used for landscape and biodiversity indicators extraction carried out in (Task 4.3.3), and will be used in the next months for ecosystem services indicators (Task 4.3.4).

Due to the lack of VHR satellite data from 3rd Party missions (e.g., WorldView2, WorldView3, QuickBird), it has not been possible to carry out the activities related to VHR data analysis in Task 4.3.1 and Task 4.3.2. Access to the ESA Data Warehouse was obtained at the beginning of the project but no quota for new VHR data has been assigned to the project so far. However, given that 10 m Sentinel-2 data given the consistent availability across the all protected areas at no charge to the users, attention focused on generating consistent land cover classifications from these for the PAs.

2.2 Process for satellite EO products identification

According to Objective 2 of WP4, the EO-derived products and services to be delivered and used subsequently within the modelling components of ECOPOTENTIAL were defined through storylines. For the process, a questionnaire exposing WP4 data generation capabilities and pointing out the constraints and the requirements for products delivery was developed. The form was sent to partners involved in WP4, modelling WPs (i.e., WP6, WP7, WP8, WP9) as well as those partners directly or indirectly involved in the management of the project's Protected Areas. The survey tried also to support the conceptual framework built within WP2 for linking EO satellite data/products and in-situ data to the concept of EVs, by contributing to their extraction within WP4. The questionnaire was successfully filled for all PAs.

The output of this process was a tabular description of the products explicitly required for each PA and storyline, including temporal and spatial resolution requirements as well as the time interval of observation and the priority level according to the PA. The Table has been regularly updated within ECOPOTENTIAL meetings (e.g., the General Assembly held on June 2016; the Review Meeting held on January 2017) and improved with information concerning the partner in charge of the production, the status of the production (pending to be assigned, assigned/to be generated, in process, available on the FTP), the expected deliverable date, the link to the data repository and a tag for metadata: (http://twiki.ECOPOTENTIAL.creaf.cat/foswiki/pub/ECOPOTENTIAL_WP4/ProductsAndPartners/Responsibles_vs_PA_Storylines.xlsx) .

2.3 Software and taxonomies

2.3.1 Software

Open source software (e.g. Python, RSGISLib) has been mainly adopted for data processing. Web Processing Services (WPS) have been developed or are in progress in order to guarantee open access, through the Virtual Laboratory (WP10), to modules still based on commercial software (e.g., Matlab).

As many organisations may not be in a position to provide their modules to the ECOPOTENTIAL project, all products provided by such modules for ECOPOTENTIAL PAs have been and will be (updating) uploaded on the project ftp site for access from the Virtual Laboratory. In Appendix 1, most of the modules used are described using a data-flow diagram. In Section 3, for each product generated in WP4, the use of commercial or proprietary software has been indicated as well as the use of existing Copernicus services. Section 5 summarizes the preliminary list of modules that the Virtual Laboratory will access, how and when. Such list will be updated by the end of WP4 (M40).

2.3.2 Taxonomies of Land Cover, Habitats and Ecosystems

In the previous FP7 BIO_SOS project, an in-depth analysis and comparison of LC and habitat taxonomies was carried out (Tomaselli et al., 2013). As a result, the FAO LCCS2 taxonomy proved to be the most useful for LC map production and subsequent LC to habitats translation, with the latter requiring additional thematic and in-situ data (in some cases; e.g., water salinity, lithology; Tomaselli et al., 2013; Kosmidou et al., 2013; Adamo et al., 2014).

LC and habitats are important elements for ecosystem monitoring. As well known, for practical mapping and assessment purposes, the MAES report (Maes at al., 2014) considers an ecosystem at the scale of habitats, which can be mapped through translation from LC maps (Tomaselli et al., 2013). To this purpose, the EODESM system provides a general framework for ecosystem monitoring.

2.3.3 Overview of Study Areas

The ECOPOTENTIAL project focuses on 22 protected areas that are associated with 11 biogeographic regions across Europe but also including the Caribbean, the Canary Islands, Kruger National Park and Le Reunion (Figure 2. 1). A full description of the protected areas, the ecosystems and habitats occurring and the particular pressures placed on ecosystem services is given at http://www.ECOPOTENTIAL-project.eu/2016-05-24-14-52-12/protected-areas and reported also in Deliverable 2.2.

Figure 2.1. Protected areas considered by the ECOPOTENTIAL project

3. Retrieval of bio-geophysical variables (Task 4.2)

For all PAs, a number of environmental (primarily bio-geophysical) variables have been generated through ECOPOTENTIAL but existing global and European datasets (e.g. Copernicus) have been also considered. Both sets of variables have been used as input to the EODESM system. The following sections give a detailed perspective of those that have been produced by ECOPOTENTIAL WP4 partners, with focus on a) Terrestrial bio-geophysical variables retrieval (Task 4.2.1) and marine, coastal and transitional water monitoring (Task 4.2.2).

Variable	Code	Year	Example Reference
Tree canopy cover	CC	2000	Hansen *et al.* (2013)
Tree cover density	TCD	2012	Hansen *et al.* (2013)
Vegetation Continuous Fields (VCF) tree cover	CC	2000-2010	Sexton *et al.* (2013)
Forest/non-forest cover	FN	2010	Shimada *et al.* (2014
Canopy height	HT	2004-2008	Lefsky (2010)
Canopy height	HT	2005	Simard *et al.* (2011)
Leaf type	LT	2012	Langanke (2013)
Forest fragmentation	FF	2013	Potapov *et al.* (2008)
Boreal forest biomass	AGB	2000s	Santoro *et al.* (2015)
Bare ground	BG	2010	Hansen *et al.* (2013)
Urban and settlement map	UR	2010-2013	Copernicus[1]
Impervious surface	IM	2011-2012	Langanke (2013)
Hydroperiod	HY	2009-2014	Pekel *et al.* (2016)
Surface water	SW	2000-2012	Hansen *et al.* (2013)
Surface water	SW	2006-2012	Pekel *et al.* (2016)
Inland water	SW	2000	Feng *et al.*, (2016)
Water	SW	2000-2002	Carroll *et al.* (2009)
Inland water bodies	SW	2014-present	Gond *et al.*, (2004)
Glaciers	GL	1850-present	GLIMS and NSIDC (2005)
Snow and ice cover[2]	SC	1966-present	Hall *et al.* (2016)

[1]http://land.copernicus.eu/pan-european/GHSL/view

[2]http://nsidc.org/data/search/#keywords=snow/sortKeys=score,,desc/facetFilters=%257B%2522facet_parameter%2522%253A%255B%2522Snow%2520Cover%2522%255D%257D/pageNumber=1/itemsPerPage=25

Table 3.1. Summary of variables provided for use in EODESM and derived from global and European layers.

3.1 Terrestrial bio-geophysical variables retrieval (Task 4.2.1)

This section includes a detailed product card for each of the terrestrial geophysical variables generated in the context of ECOPOTENTIAL PAs requests. The card includes:

- the Technology Readiness Level (TRL) of the module used to retrieve each specific variable. The TRL follows the accepted metrics for HORIZON2020 projects (See Section 11). Not Applicable (NA) indicates variables retrieved as open access services (e.g., Copernicus service or MODIS products);
- the type of software used (Open Access, Commercial or Proprietary (C/P));
- the label Background/Foreground knowledge (B/F) is adopted to indicate whether the Virtual Laboratory (in WP10) will not access/access the module.

The list of the bio-geophysical variables described in subsequent sub-sections is reported in Table 3.2.

Life Forms: woody, herbaceous, cryptograms	UNSW, UPS, EVS, EURAC, CREAF, UAB, UiB
Life Form*: semi-natural and natural grassland	EURAC, CNR
Tree Cover Density (%)*	UPS
Leaf Type*	UPS
Vegetation height (m.)	UPS, CSIR, TdV, ESL
Leaf Area Index (m^2 m^{-2})	UPS
Vegetation Phenology - 1	UAB, CREAF, CSIC-EBD, UFZ, CSIR
Vegetation Phenology - 2	CERTH, CSIC
Invasive Plant Species	CNR, ICETA-InBIO
Above Ground Biomass (Mg ha^{-1})	UPS, CSIR
Herbaceous Biomass (g m^{-2})	CSIR
DEM (m.)	UPS
Soil moisture (%): Time series approach	CNR
Soil Moisture: Data driven approach	EURAC
Vegetation moisture content	UPS, UAB, CREAF
Land Surface Temp.	FORTH
Albedo	FORTH
Water State	CSIC, CERTH
Water Extent	CERTH, CSIC
Water Hydro-period	CSIC, CERTH, UIB, EURAC
Hydroperiod and seasonality maps estimation	CERTH
Water turbidity and sediment loads	UNSW, CSIC (EBD), CREAF
Water depth	CSIC (EBD)
Snow cover from optical data	EURAC
Snow cover from SAR data	STARLAB
Ocean Color Products (CHL-a, CDOM, TSM)	ISPRA
Wind fields	CNR
Sea Surface Temperature	ISPRA
Chlorophyll-a	ISPRA, CREAF, HIO
Shoreline delineation	STARLAB
Bathymetry	ISPRA
Cloudiness	CNR

* Data from 3rd parties.

Table 3.2. List of bio-geophysical variables retrieved.

3.1.1 Vegetation

Life Forms

Algorithms/Methods: For vegetated areas[1], a random forests classification has been applied to differentiate lifeforms (e.g., for Northern Limestone), with these including woody (trees or shrubs), herbaceous (grasses or forbs) and cryptophytes (mosses or lichens).

Woody: As an alternative, the extent of woody vegetation can be extracted from maps of canopy cover[2] (> 20 %), height[2] (> 2 m) and above ground biomass[2] (e.g. > 5 Mg ha^{-1}), with shrubs and trees also differentiated using these layers (e.g., based on thresholds of 5 m).

Herbaceous: Associated with vegetation not mapped as woody, particularly in areas where cryptograms have limited distribution and extent (e.g., in semi-arid areas). For the Camargue[3], changes in the extent of reedbeds were mapped using classifications of Sentinel-1 SAR. For the EEA39 area, Copernicus High Resolution European Layers (namely Landsat sensor data from 2006, 2009 and 2012) were used to map the extent of semi-natural and natural grassland. A subset was extracted for Gran Paradiso[4],

Cryptograms: For the Hardangervidda[5,6,7], the extent of lichens was mapped using 66 Landsat 5, 7 and 8 sensor data acquired in 2000, 2003, 2006, 2010 and 2015 (with less than < 50 % cloud cover), the Normalised Difference Lichen Index (NDLI) and Normalized Difference Moisture Index (NDMI) were used in a regression algorithm with three normal distribution parameters) to estimate lichen volume (Falldorf et al. 2014, Falldorf et al. 2015).

Validation: For random forest classifications of lifeforms, validation has been undertaken with reference to LCCS2 maps generated from existing land cover maps. For NDLI and NDMI indices in Hardangervidda (66 NDLIs and 66 NDMIs, 2003 to 2016) an uncertainty product at pixel level, based on error propagation, has been designed[5,6]. For lichen maps in Hardangervidda[7], validation was based on expert knowledge and field data. The grassland maps generated for the EEA39 were validated using more than 20,000 sample points stratified across the area. Samples with a disagreement of more than 25 % (more than 6,000) were reinterpreted as part of a plausibility check. The overall accuracy was 80 %. No specific regional discrepancies in accuracies were observed among the different biogeographical zones, countries and group of countries larger than 90,000 km^2. For more information, see http://land.copernicus.eu/user-corner/technical-library/hrl-ngr-2012-validation-report.

Technological readiness level: 5 (UNSW[1])
Open source (Y/N): Y
Commercial or proprietary (C/P):
Background or Foreground knowledge (B/F): F

Partners: UNSW[1], UPS[2], EVS[3], EURAC[4], CREAF[5], UAB[6], UiB[7]

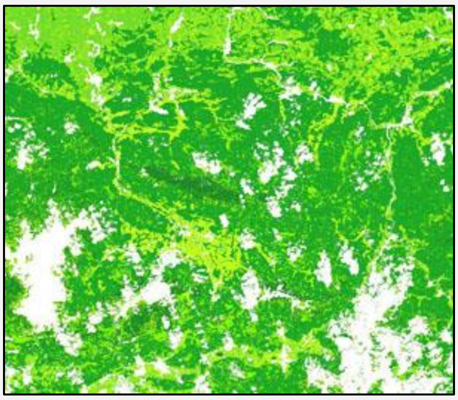

Life form classification for Northern Limestone generated using a random forest algorithm

2 CTV Herbaceous
3 CTV Graminoids
5 NTV Trees
6 NTV Shrubs
7 NTV Graminoids
8 NTV Herbaceous
9 NAV Trees

Extent of lichens (white) for 1990 Hardangervidda

Life Form: semi-natural and natural grassland

Algorithms/Methods: Occurrence of semi-natural and natural grassland as binary product (1: presence, 0: absence) was provided by EURAC[1] and CNR[2] for Gran Paradiso and Murgia Alta PAs, respectively. The production workflow was based on initial image segmentation. Information derived from the biophysical parameter layers is added to the objects from the image segmentation. Then a semi-automated classification of multispectral satellite data (derived from Image 2012-2009-2006) is applied, followed by manual editing (aided by individual country assessments). Spatial resolution: 20m.

(a)

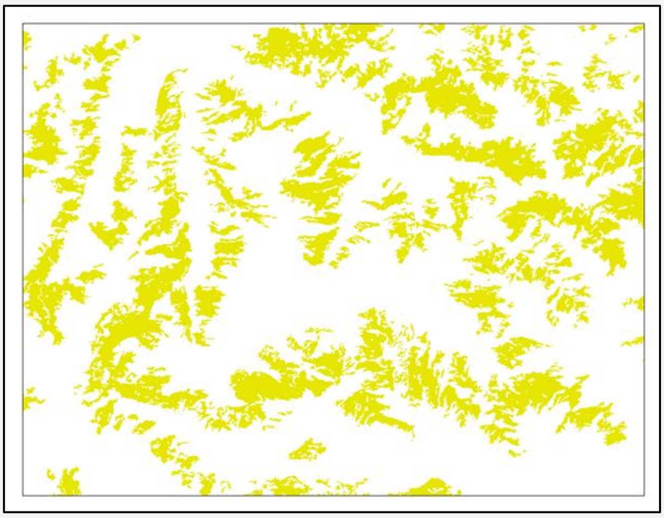

natural grassland
all none-grassland areas

1:250.000

(b)

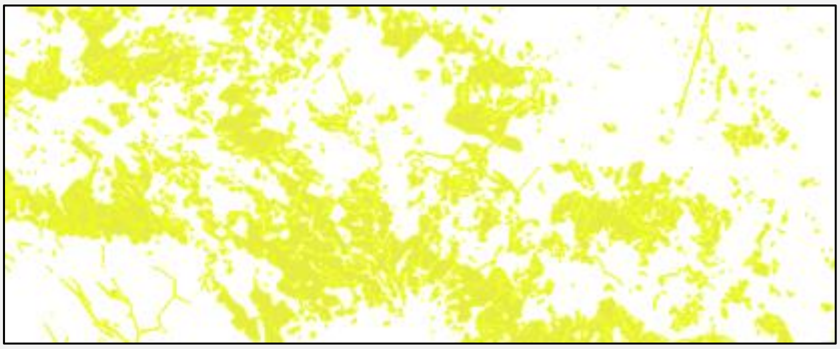

Semi-natural and natural grassland derived from VHR imagery in (a) Gran Paradiso National Park and (b) Murgia Alta. Data provided by Copernicus High Resolution European layers.

Validation: (1) Qualitative assessment: review of the available datasets and the existing documentation prepared as part of the semantic checks performed during the production. (2) Quantitative assessment: blind interpretation of more than 20,000 sample points stratified across the EEA39 area that were compared against different reference data. Samples with a disagreement of more than 25 % (more than 6,000) were reinterpreted as part of a plausibility check. Overall accuracy of 80 %. No specific regional discrepancies in accuracies among biogeographical zones, countries and group of countries larger than 90,000 km^2. For more information, see http://land.copernicus.eu/user-corner/technical-library/hrl-ngr-2012-validation-report.

Source: High Resolution Layer: Natural Grasslands (NGR) 2012, Copernicus Land Monitoring Service.

Technological readiness level: NA
Open source (Y/N): Y (Access to data is based on a principle of full, open and free access as established by the Copernicus data and information policy Regulation (EU) No 1159/2013 of 12 July 2013)
Commercial or proprietary (C/P):
Background or Foreground knowledge (B/F):

Partner: EURAC[1], CNR[2]

Tree Cover Density (%)

Algorithms/Methods: Tree cover density was estimated (Copernicus Land Services) for all protected areas with woody vegetation using a semi-automated classification and computer-aided visual refinement based on high resolution satellite imagery provided by ESA (DWH_M62_CORE_01), mainly IRS RS2 and SPOT 4/5 (COV 1) and RapidEye (COV2) at 20, 25 and 5 m spatial resolution respectively. Stepwise-wise enhancement was achieved using the Corine Land Cover (CLC) maps for 2006 and 2012, within this allowing adjustment for cloud covered areas and where gaps in the data occurred. Additional earth observation (EO) data were also used to refine the mapping for the 39 member states and affiliated countries to the European Environment Agency (EEA39). The resulting estimates were then combined into a European mosaic. The minimum mapping width (MMW) was 20 m. For each PA, a subset was extracted and re-projected (UPS) to the corresponding UTM zone.

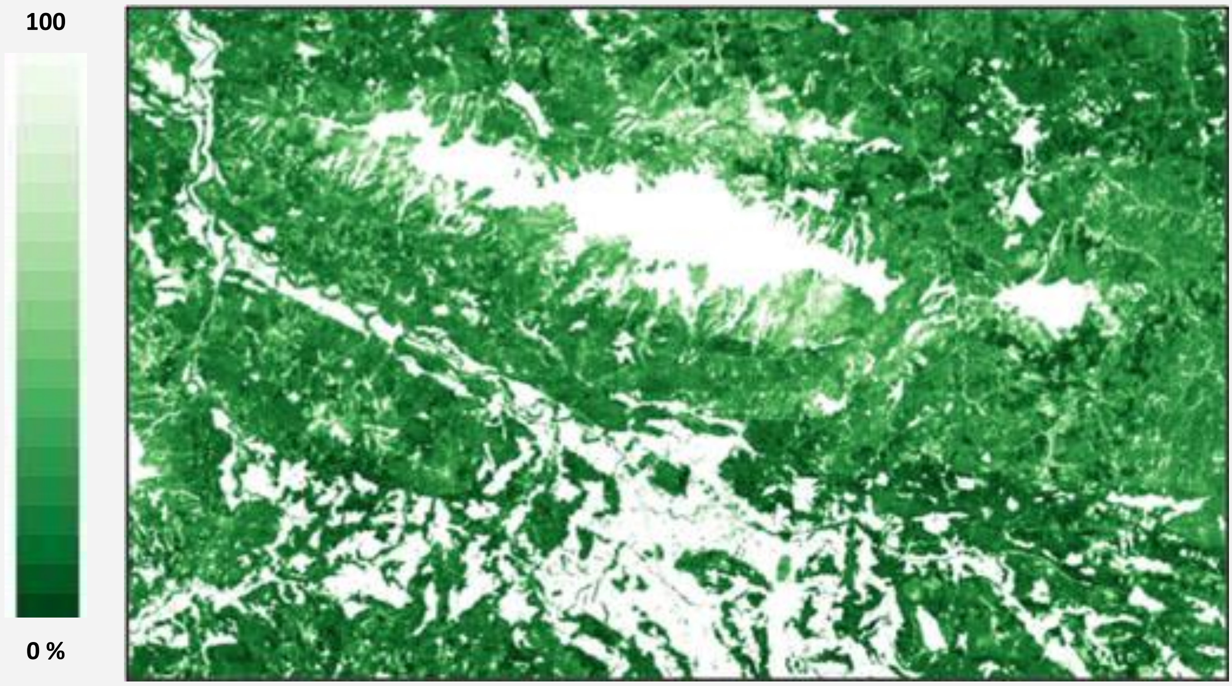

Tree cover density map, Northern Limestone National Park.

Validation: Undertaken based on a dedicated stratified systematic sampling design based on two levels (strata): a) areas greater than 90,000km² and b) omission and commission probability (high and low). Thematic accuracy assessments performed through independent visual interpretation of higher resolution imagery by trained interpreters leading to an overall accuracy of 60 %. For more information, see [http://land.copernicus.eu/user-corner/technical-library/hrl-forest-2012-validation-report-1.](http://land.copernicus.eu/user-corner/technical-library/hrl-forest-2012-validation-report-1)

Technological readiness level: NA
Open source (Y/N):
Commercial or proprietary (C/P):
Background or Foreground knowledge (B/F):

Partner: UPS

Leaf Type

Algorithms/Methods: For all protected area, using the same data used to retrieve Tree Canopy Density (TCD), and for TCD values ≥10 and <100%, a classification of broadleaved and needle-leaved (coniferous) forests was generated (Copernicus Land Services) for Europe with a Minimum Mapping Unit (MMU) at 0.5 ha with a MMW of 20 m. For each PA, a subset was extracted and re-projected (UPS) to the corresponding UTM zone.

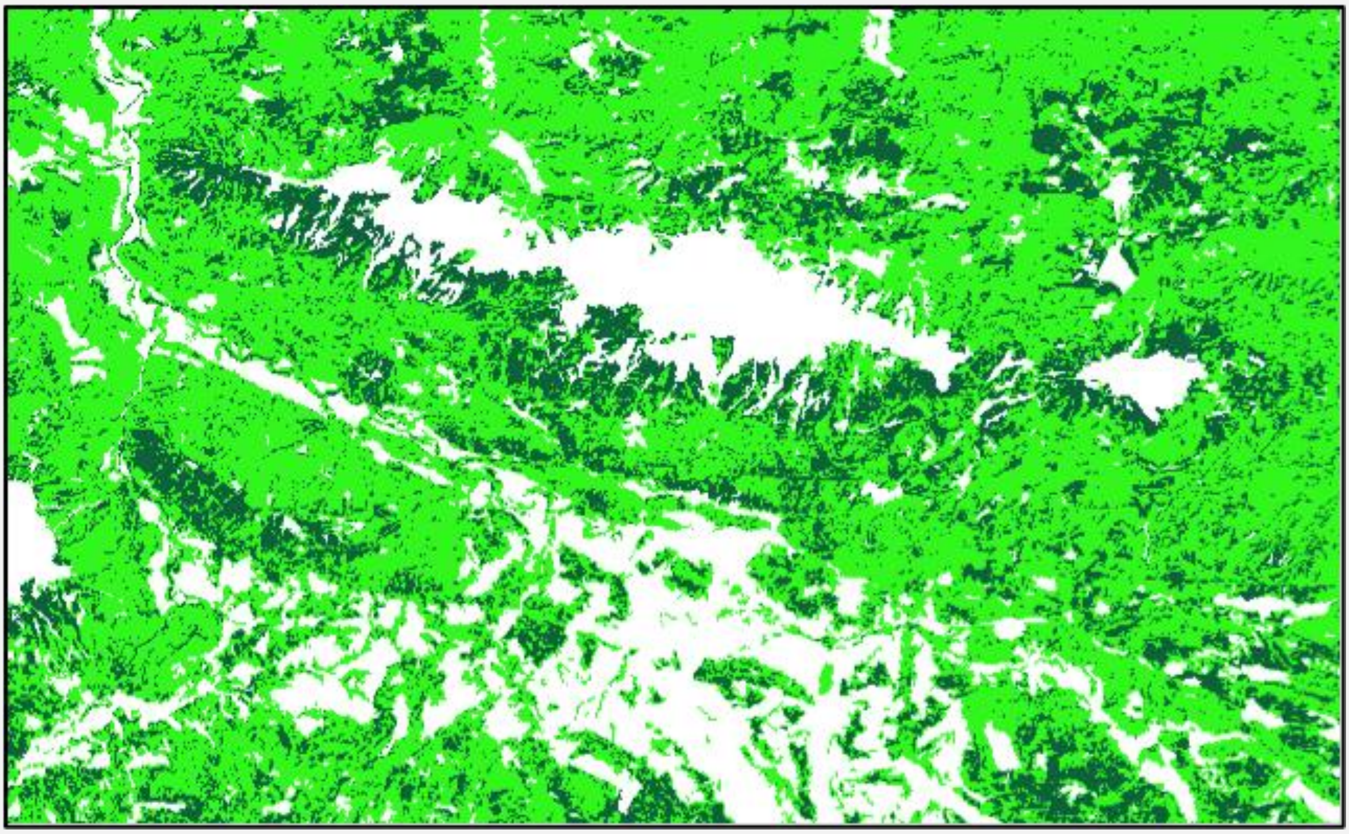

Leaf type classification, Northern Limestone National Park.

Validation: The overall accuracy was assessed using the same stratified sampling design as for TCD, giving an overall accuracy of 82%, with the greatest confusion occurring between the forest types. For more information, see http://land.copernicus.eu/user-corner/technical-library/hrl-forest-2012-validation-report-1.

Technological readiness level: NA
Open source (Y/N):
Commercial or proprietary (C/P):
Background or Foreground knowledge (B/F):

Partner: UPS

Vegetation Height (m.)

Algorithms/Methods: LiDAR data have been used to retrieve canopy height models (CHM) for a) the mountainous PAs of Northern Limestone, Sierra Nevada/Sierra de Baza and Swiss National Park/Davos[1] and b) Kruger NP[2]. In each case, the data were examined for extent, consistency, overlaps or gaps. Overlapping points and 'noise' were removed and gap filling was undertaken. A ground/non-ground classification was also undertaken, if considered to be too coarse, using the open source Multiscale Curvature Classification (MCC) algorithm. Depending on the flight characteristics, the point density and topography parameters were determined for each ALS flight through iterative testing. Following classification, digital elevation models (DEMs) were interpolated at various spatial resolutions and used to compute the normalized height (i.e., height above ground). The normalised point cloud was used subsequently to produce generic LIDAR-based metrics, including canopy closure, canopy density and percentiles of returns at different height levels, with these representing proxies of forest structural characteristics. These data were then used within parametric (e.g., linear regression) or non-parametric (e.g., random forest, support vector machines) models to map forest structural characteristics of interest. For Camargue[3,4], green reed height (*Phragmites australis;* in cm) was mapped using SPOT-5 data based on the algorithm of Poulin et al. (2010).

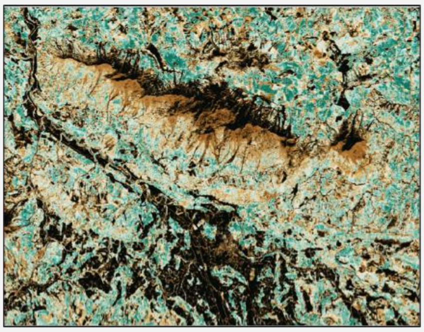

Canopy height model derived from LIDAR, Northern Limestone

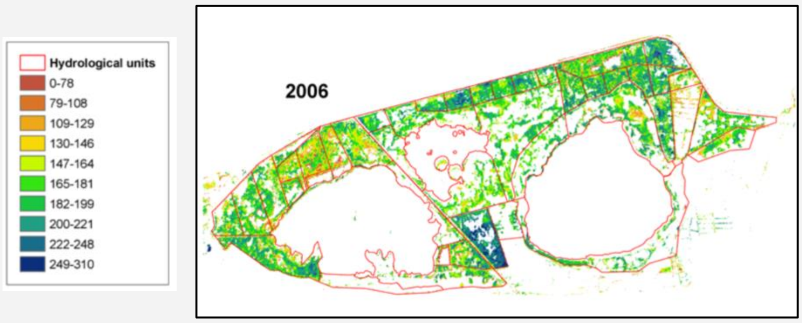

Green reed height (cm) estimated from SPOT-5 data, Camargue

Validation: Product validation was carried out for PAs with available in-situ data. Details regarding validation are available in the product accompanying ReadMe files.

Technological readiness level: NA
Open source (Y/N): Y
Commercial or proprietary (C/P): P
Background or Foreground knowledge (B/F): B

Partner: UPS [1], CSIR[2], TdV[3], ESL[4]

Leaf Area Index (m^2 m^{-2})

Algorithms/Methods: Using the full point cloud LiDAR data processed for Sierra Nevada, Sierra de Baza and La Palma, the effective leaf area index (LAIe) was computed from the gap probability (P) as **LAIe=-ln(P)**, with this being the ratio of ground returns to the total number (Fieber et al., 2014). The aggregation cell was set at 20 m in consideration of saturated cells (i.e., those with no ground returns because of the high density of the canopy and hence low point cloud density). A 10 m spatial resolution LAIe was produced but the higher number of saturated cells restrained its usability.

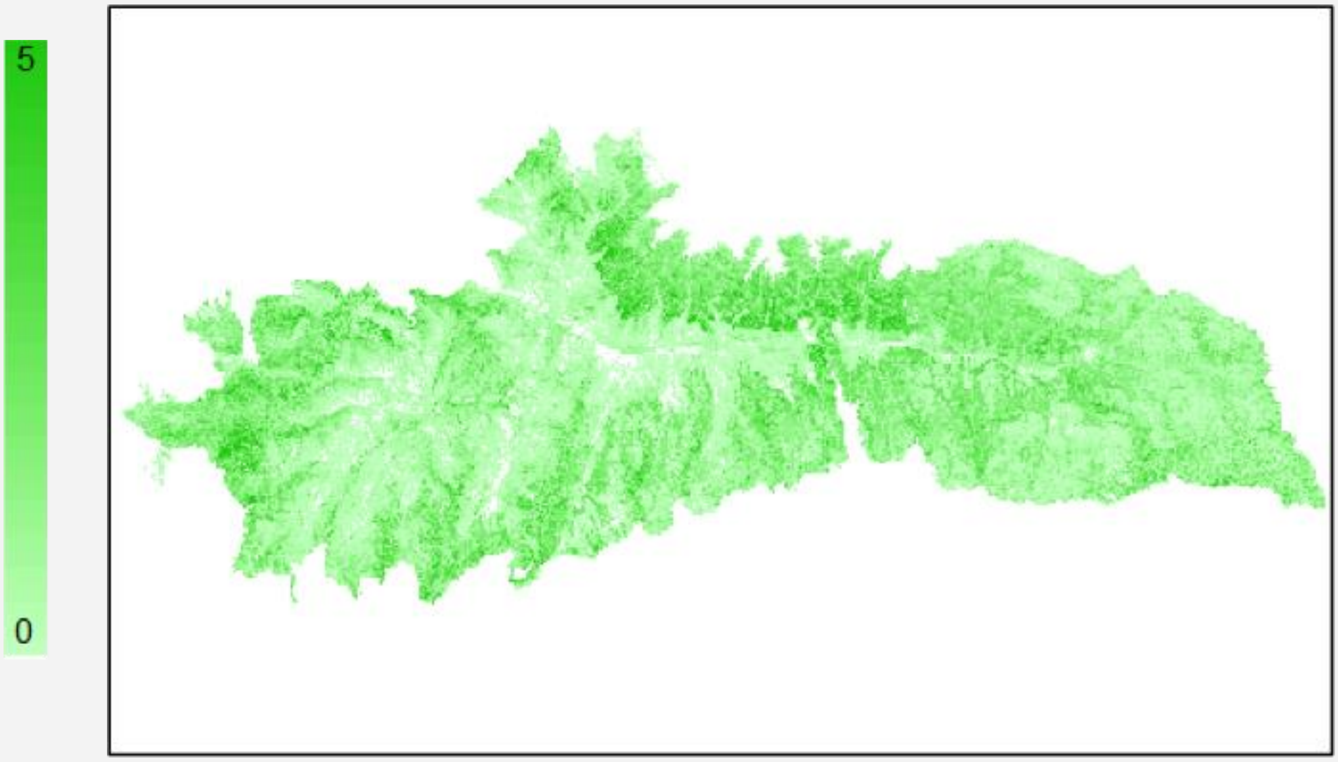

Effective LAI derived from LIDAR, Sierra Nevada

Validation: The lack of reference data (March 2017) prevents validation activities. Other authors showed that LAIe obtained from the gap probability is closely related with reference data from hemispherical photographs (Fieber et al., 2014, Fieber et al. 2016, Morsdorf et al. 2006).

Technological readiness level: NA
Open source (Y/N): Y
Commercial or proprietary (C/P): P
Background or Foreground knowledge (B/F): B

Partner: UPS

Vegetation Phenology_1

Algorithms/Methods: Measures of vegetation phenology were determined by considering temporal and annual variations in the Normalized Difference Vegetation Index (NDVI) or Enhanced Vegetation Index (EVI) derived from Landsat, Sentinel-2 or MODIS data (EVI computed as in Jiang et al., 2008). NDVI time-series were generated[1,2] for Northern Limestone (21 NDVIs and 21 EVIs, 2002 to 2014), La Palma (93 NDVIs, 1988 to 2016), Hardangervidda (66 NDVIs, 2003 to 2016), Sierra Nevada (157 NDVIs, 1984 to 2011), Kruger (67 NDVIs, 1987 tot 2016), Montado (15*2 NDVIs -2 scenes for each date-, 1984 to 2015), Bayerisher Wald (86 NDVI, 1985 to 2016) and Doñana[3]. A total of 541 phenology indices (520 NDVIs and 21 EVI) have been computed [1,2]. A processing chain that uses the R package "phenex" has been developed[4] from deriving phenological metrics from MODIS AQUA and TERRA and Sentinel-2 data. These products were generated[4] for Abisko, Bayerischer Wald, Camargue, Curonian Lagoon, Danube Delta, Donana, Gran Paradiso, Hardangervidda, High Tatra, Montado Alentejo, Northern Limestone, Ohrid Prespa, Peneda Geres, Samaria, Sierra Nevada and Wadden Sea, for the years 2002 to 2016. For Kruger, leaf area index (LAI) time series data (2001-2015) derived from MODIS and Gaussian modelling was used[5] to estimate various phenometrics including start and peak of growing season, maximum senescent rate, end of growing seasons.

(a)

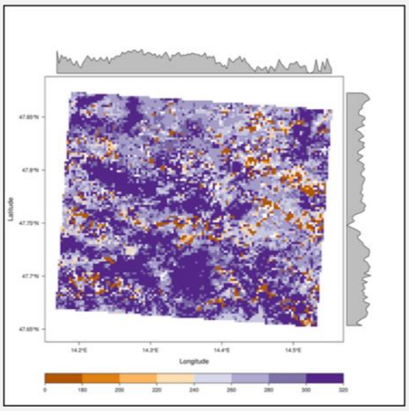

(b)

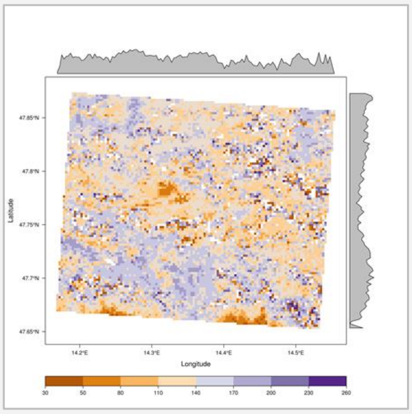

(c)

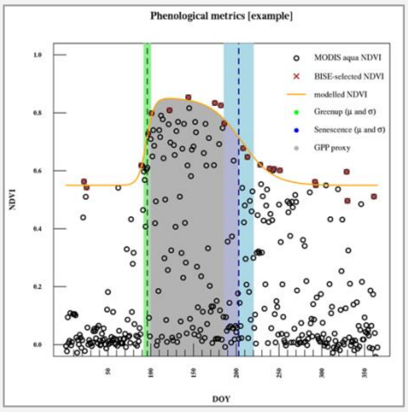

(d)

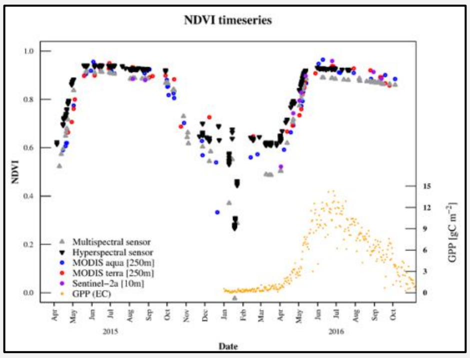

(e)

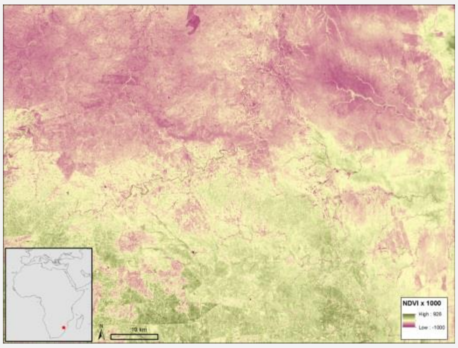

(a) Senescence measures for Northern Limestone (2003); (b) phenology-based GPP proxy (dimension less value) from Northern Limestone (2002); (c) example NDVI time series, filtered values and modelled NDVI curve as well as phenological metrics (green-up and senescence date, GPP proxy; (d) NDVI and GPP time series from validation site "Hohes Holz" (2015-2016). GPP derived by Corinna Rebmann and colleagues (UFZ ; (e) NDVI corresponding to Kruger NP (L8 15/11/2013).

Validation: For NDVI and EVI indices, an uncertainty product at pixel level based on error propagation has been designed[5] For forest and pasture sites in Northern Germany ("Hohes Holz" and "Grosses Bruch" respectively), validation data were collected at sub-daily resolution (2015-2016).

Technological readiness level: 4 (UAB[1])
Open source (Y/N):
Commercial or proprietary (C/P):
Background or Foreground knowledge (B/F): F

Partner: UAB[1], CREAF[2], CSIC-EBD[3], UFZ[4], CSIR[5]

Vegetation Phenology_2

Algorithms/Methods: An algorithm for generating phenology curves relying on annual time series of Sentinel 2 data was implemented. Six indices provided information for phenology estimation for the calculation of the phenology curves: (a) NDVI index, (b) Water content Index, (c) Maturity Index, (d) Biomass Index 1, and (e) Biomass Index 2. The additional information provided by the indices, other than the commonly applied NDVI, is used to fine tune the phenology depiction through the annual vegetative cycle. In order to estimate a curve point for a specific index, date and habitat class, the indices values of pixels belonging to polygons of this class are averaged, while at the same time the standard deviation of the values is estimated as the uncertainty associated with the average value. In the phenology curve, x-axis indicates the date and y-axis indicates the average index value. Around each curve point there is a bar showing the standard deviation of the index values across the polygons of the specific class. The final phenology curve is generated by fitting a smoothing spline to the initial curve points, which may be noisy. The work flow is shown in Appendix 1, section 8.2.

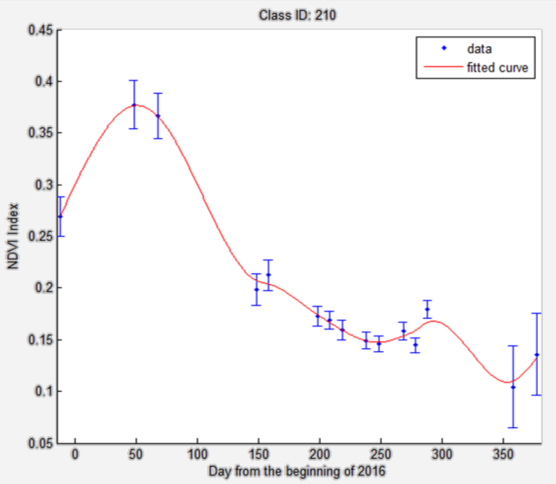

Phenology curve for Class with ID:210 (Marshland area in Donana PA) relying on NDVI Index (each blue point show the average NDVI index value in a class for a date and its blue bar is the standard deviation of the index values across the polygons of the specific class)

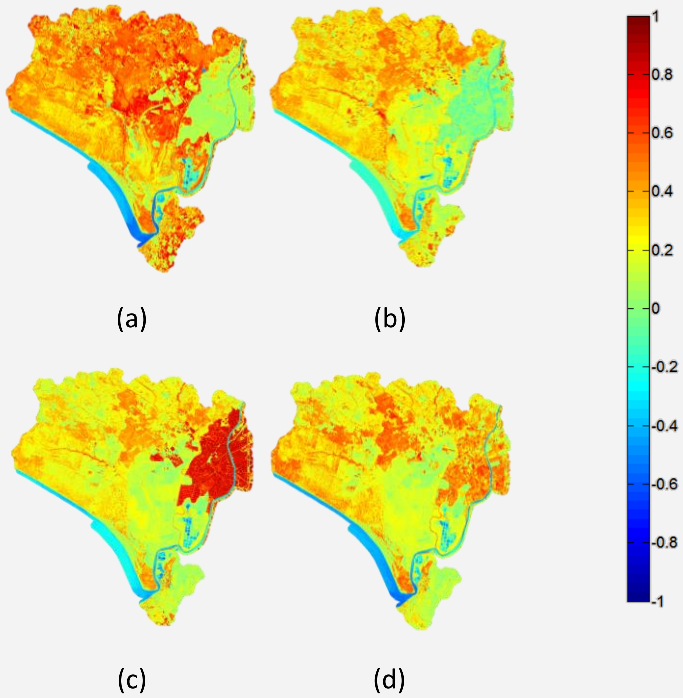

Series of NDVI maps on (a) 17/02/2016; (b) 06/06/2016; (c) 05/08/2016 and (d) 14/10/2016. The legend shows the NDVI value corresponding to each colour in the map.

Validation: The phenology curves of 66 classes containing vegetation have been sent to CSIC[2] for evaluation and selection of best correlated indices with the classes' phenology.

Technological readiness level: 4 (CERTH[1])
Open source (Y/N): N
Commercial or proprietary (C/P): Some components of the software are to be executed via commercial software, because of the availability of resources. It is intended to convert the algorithm to an open source for the Virtual Laboratory Platform.
Background or Foreground knowledge (B/F): F

Partner: CERTH[1], CSIC[2]

Invasive Plant Species

Algorithms/Methods: For Murgia Alta[1], a two-stage classifier was used to differentiate the invasive species *Ailanthus altissima.* First, *a knowledge driven classifier* was applied to analyse 4 multi-temporal WorldView2 images (Adamo et al. 2015). Then, the original winter and summer image pixels belonging to the deciduous layer, in the first stage LC map, were used as input to the second *data driven* classification stage. However, only pixels characterised by NDVI values greater than 0,4 in the summer image were analysed. A set of training reference data was used to train the *data driven* two-classes classifier. At Peneda Geres[2], the combination of machine learning classifier (random forests) feed by WorldView-2 data and species distribution modelling quantified spatially-explicitly at fine-scale invasion extent (2m) and invasion success (200m) of Acacia species (http://www.mdpi.com/1424-2818/9/1/6).

(a)

The invasive species Ailanthus altissima

(b)

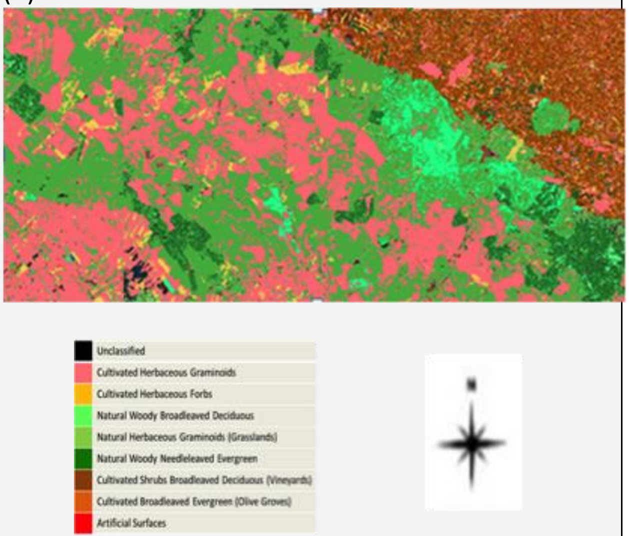

(c)

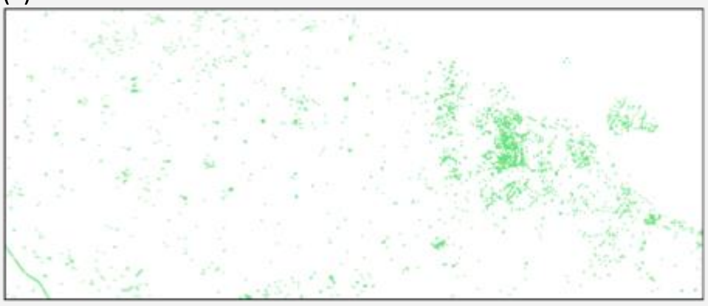

Classification of Ailanthus altissima

(a) The invasive species Ailanthus altissima; (b) land cover map, Murgia Alta National Park, Italy. The layer of deciduous vegetation was used for subsequent classification of Ailanthus altissima, shown in (c).

1:250.000

Validation: The LC map overall accuracy (OA) was 92.77 % ± 0.04%; b) Invasive species map. The OA was 97.07±0.19%. Validation data provided by the LIFE Alta Murgia – LIFE12 BIO/IT/000213 (http://lifealtamurgia.eu/). For Peneda Gerês, in-field validation based on 60 locations estimated an OA of 91.3% and kappa coefficient of 0.81% of invasion map.

Technological readiness level: 4 (CNR[1])
Open source (Y/N): N
Commercial or proprietary (C/P): P
Background or Foreground knowledge (B/F): F

Partner: CNR[1], ICETA-InBIO[2]

Co-funded by the European Union

Above Ground Biomass (Mg ha^{-1})

Algorithms/Methods: For Kruger NP[1,2] and Montado NP[1], above ground biomass (AGB) was retrieved for relatively flat or gently undulating terrain from Advanced Land Observing Satellite (ALOS) Phased Arrayed L-band Synthetic Aperture Radar (SAR) using water cloud semi-empirical models. In mountainous areas of Northern Limestone and Swiss National Park/Davos[1], AGB was estimated by applying a non-parametric support vector regression to LiDAR-derived metrics with field based measurements. AGB maps will also be generated for Sierra Nevada and Sierra de Baza following acquisition of field measurements in 2017.

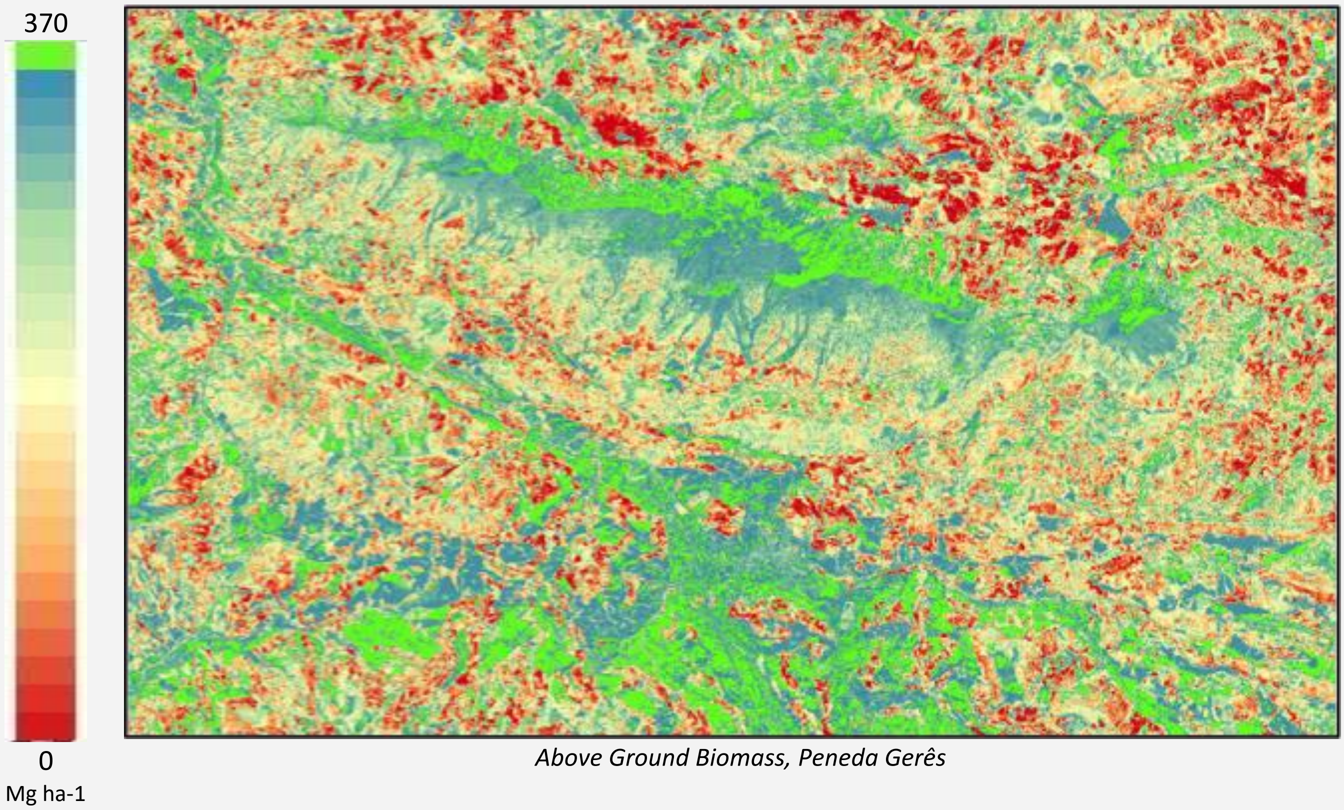

Above Ground Biomass, Peneda Gerês

Validation: Based on comparisons with in situ data (when available) with cross validation achieved using an iterative random splitting of samples. Measures included models R^2, the Root Mean Square Error (RMSE; 70-100 Mg ha^{-1}), RMSE (%); 30-40%), bias and r for observed versus predicted (0.6-0.8). More details regarding validation are available in the product accompanying ReadMe files.

Technological readiness level: NA
Open source (Y/N):
Commercial or proprietary (C/P):
Background or Foreground knowledge (B/F): B

Partner: UPS[1], CSIR[2]

Herbaceous Biomass (g m^{-2})

Algorithms/Methods: For Kruger NP, herbaceous biomass was predicted for 2001 to 2016 using estimates of leaf area index (LAI) inverted from the PROSAIL radiative transfer model and 500 m spatial resolution MODIS data. Semi-empirical models were then used to relate LAI to herbaceous biomass, with these based on field data collected in 2009, 2013 and 2014.

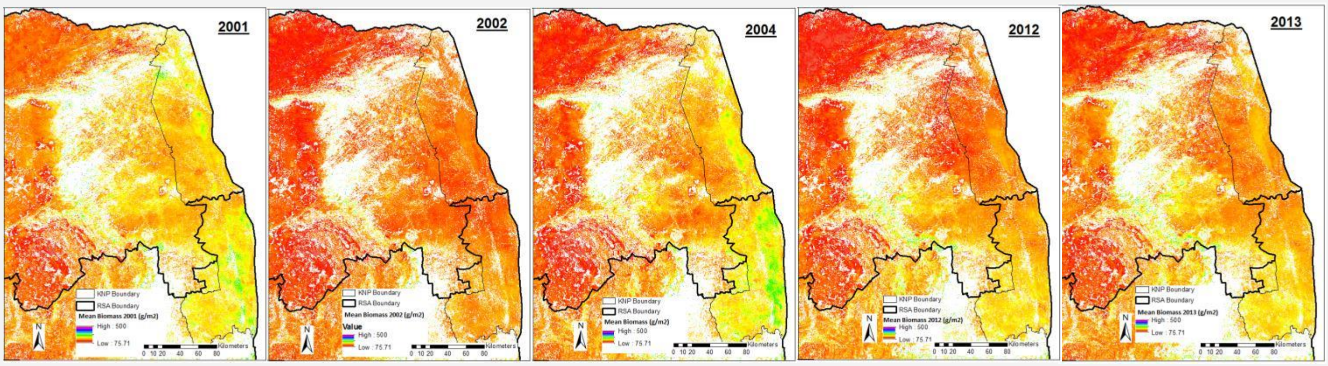

Validation: The LAI explained 50 to 80 % of herbaceous biomass and, using bootstrapping cross-validation, the relative error of the models range from 21 – 30 % of the observed mean.

Technological readiness level: NA
Open source (Y/N): Y
Commercial or proprietary (C/P): P
Background or Foreground knowledge (B/F): B

Partner: CSIR

3.1.2 Digital Elevation Model, Soil and Vegetation Moisture, Land Surface Temperature and Surface Albedo

Digital Elevation Models (m.)

Algorithms/Methods: As a product of airborne LiDAR data processing, high resolution (5 to 20 m) digital elevation models (DEMs) have been produced for Northern Limestone, Swiss National Park/Davos, Sierra Nevada/Sierra de Baza and La Palma island. The ground terrain was interpolated from ground returns classified using the open source Multiscale Curvature Classification (MCC) algorithm. Depending on flight characteristics, point density and topography MCC parameters were determined for each ALS flight through iterative testing.

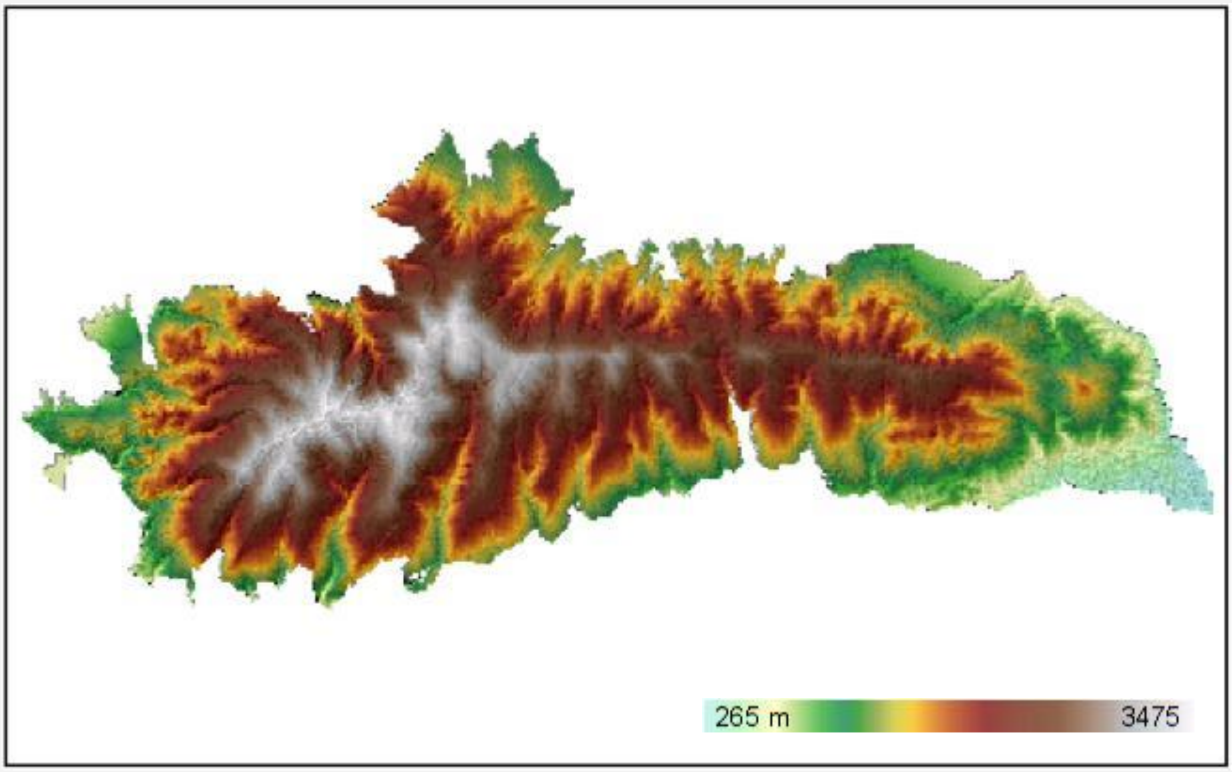

Digital Elevation model (5 m.), Sierra Nevada National Park, Spain.

Validation: ALS data precision (horizontal and vertical) allows for accurate estimates of land surface height. Horizontal and vertical precision better than ± 50 cm and ± 20 cm respectively are generally expected from commercial ALS flights. As a result, the precision of the interpolated surfaces (e.g., DEM, DSM) is significantly higher when compared to DEMs derived from optical stereo imagery or interferometric radars.

Technological readiness level: NA
Open source (Y/N):
Commercial or proprietary (C/P):
Background or Foreground knowledge (B/F): B

Partner: UPS

Soil Moisture (%): Time series based approach

Algorithms/Methods: Surface soil moisture is considered an essential variable in many GEO Societal Benefit Areas (SBAs), such as climate. Soil moisture has been retrieved using two different techniques based on: a) the analysis of dense time-series of Sentinel-1 SAR data and b) the application of a data driven neural network algorithm. For Murgia Alta (a) and Har HaNegev (b), soil moisture in the upper 0-5 cm of the profile was retrieved from time-series of Sentinel-1 SAR using the SMOSAR algorithm of Balenzano et al. (2011; 2013). The retrieval was based on the assumption that the C-band backscatter change (observed every 6-12 days) between dense time-series of C-band SAR data was related to the temporal change of soil moisture (mv) and not that of vegetation or surface roughness changes (which occur over periods exceeding 12 days).

(a)

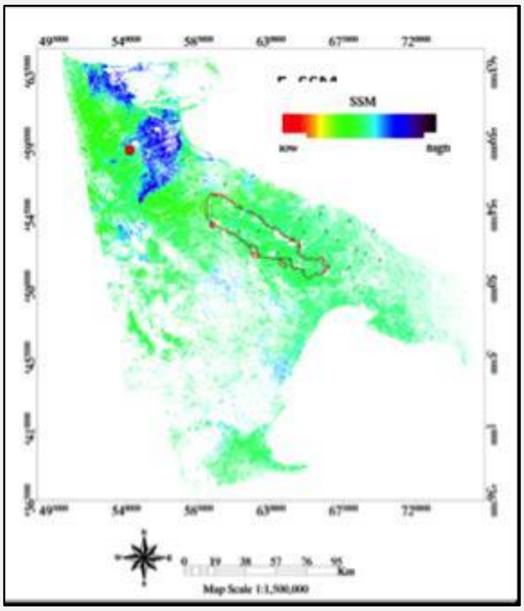

(b)

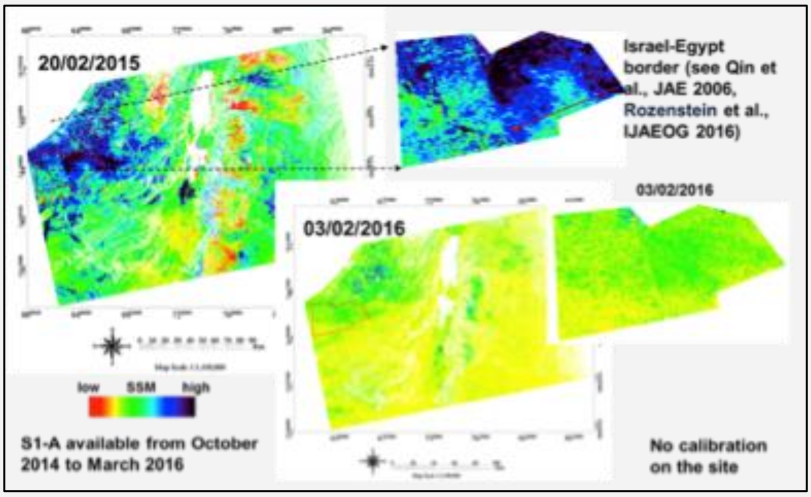

SMM product from Sentinel-1A: (a) Murgia Alta, Italy, and (b) Har HaNegev, Israel

Validation: Monthly measurements of soil moisture from July to October 2016 for Murgia Alta.

Technological readiness level: 3
Open source (Y/N): N
Commercial or proprietary (C/P): P
Background or Foreground knowledge (B/F): B

Partner: CNR

Soil moisture: Data driven approach

Algorithms/Methods: The algorithm of Pasolli et al (2015) for retrieving soil moisture is being applied to several protected areas, including Sierra Nevada, Peneda-Gêres, Har HaNegev and Gran Paradiso. The algorithm requires the establishment of an empirical Support Vector Regression (SVR) model (Drucker et al., 1997) between C-band Synthetic Aperture Radar (SAR) backscatter intensity and surface soil moisture. Instead of using in situ data, a coarse resolution surface soil moisture model (SMAP L4 SM; Reichle et al., 2016) is used during the learning phase. The algorithm requires time-series of Sentinal-1A data, the SMAP L4 reference soil moisture and, ideally, *in situ* data as input. Algorithms have been developed to remote thermal noise, filter, radiometrically calibrate and geometrically correct each Sentinel-1A scene. For the selected protected areas, all available Sentinel-1A 1W GRDH time-series data (October 2014 - October 2015) have been corrected and from these, several temporal parameters have been derived as a first step in the estimation of SSM. Such parameters have been used to compensate for the influence of different surface roughness conditions, land cover classes and topographic distortions, thereby leading to improvements in the SSM estimation. Where available, a subset of in situ data have been used to train the algorithm whilst the remainder have been reserved for validation. Such data have already been obtained for Sierra Nevada (up to 2014 and from autumn 2016) and Peneda-Gêres (June-July 2016). For Gran Paradiso, soil moisture measurements will be collected in2017. The training dataset, combined with the soil moisture reference, is used to establish the SVR model and soil moisture is then estimated at the spatial resolution (sampling of 10 m from the nominal 20 m resolution) of the Sentinel-1A GRDH data. Accuracy is assessed by first using the test data to show how well the reference datasets can be produced and demonstrate the validity of the model. Following adjustments, the in situ test data are used to provide the final validation.

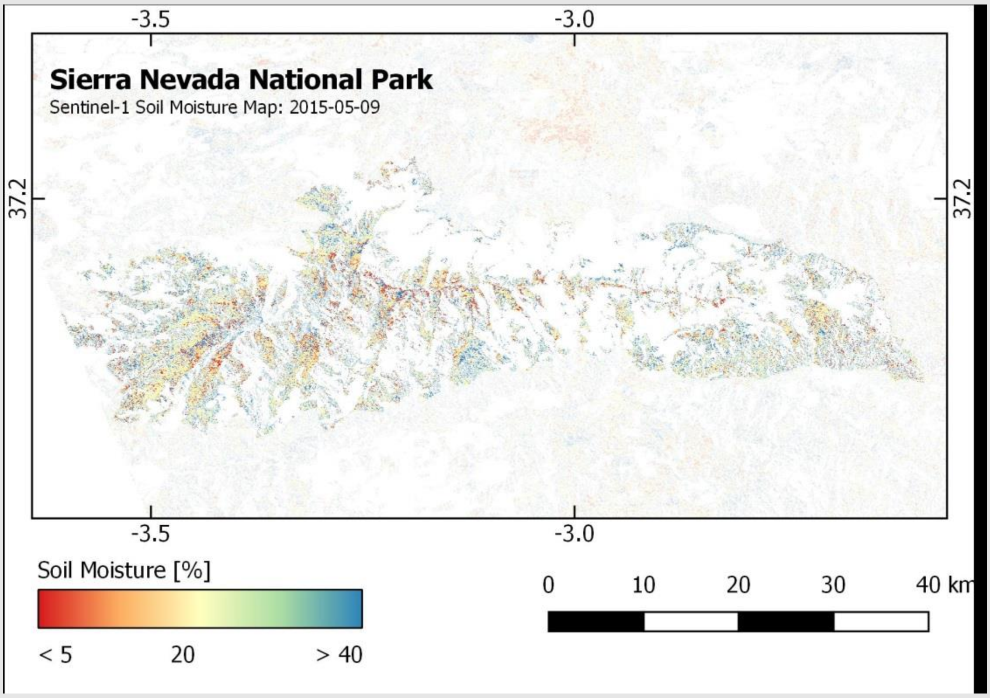

Soil moisture (%) retrieved from Sierra Nevada National Park using time-series of Sentinel-1A data.

Validation: It is ongoing and based on the collection of in-situ data.

Technological readiness level: 6
Open source (Y/N): Y
Commercial or proprietary (C/P): P
Background or Foreground knowledge (B/F): B

Partner: **EURAC**

Vegetation moisture content

Algorithms/Methods: Vegetation moisture content is to be generated using time-series of Sentinel-1 backscatter intensity data for Peneda Gerês and Montado, with calibration from ground-based measurements taken during a dedicated field campaign (2016-2017). The field campaign is still on-going and empirical statistical modelling will be performed to estimate vegetation moisture content. Preliminary results may become available during the first half of 2017. For La Palma, the Normalized Difference Water Index (NDWI) (Gao, 1996), was used as a proxy for changes in water content of leaves, NDWI has been computed [2,3] for a total of 93 images 1988 to 2016. The same is scheduled to be undertaken for the following PAs: Gran Paradiso, Sierra Nevada, Bayerischer Wald, Lake Ohrid and Prespa, High Tatra Mountains, Samaria, Danube Delta.

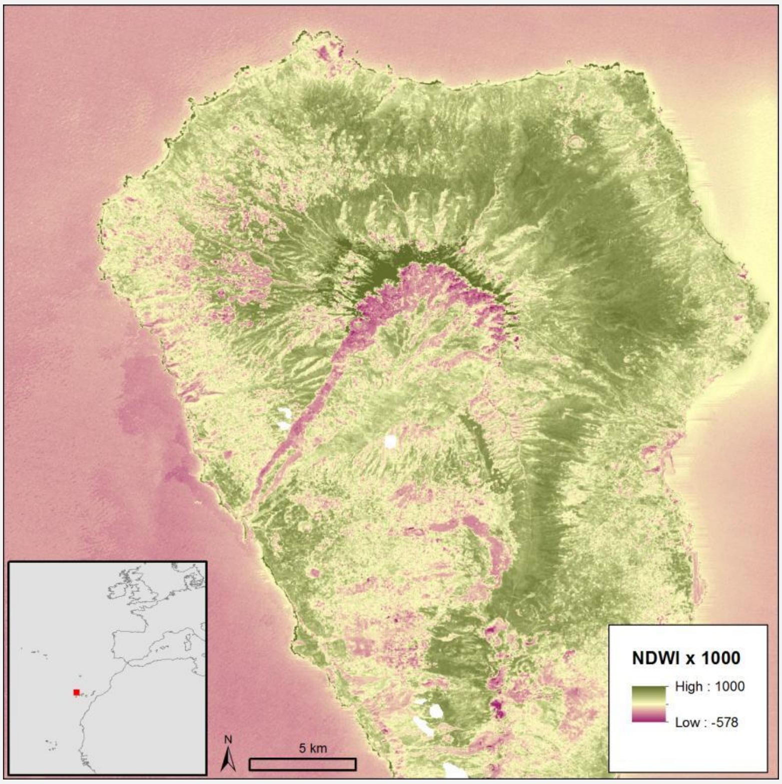

Normalized Difference Water Index for La Palma, Canary Island (L8 10/01/2014)

Validation: For Peneda Gerês and Montado, ground validation data were collected. Product development in Samaria has been cancelled upon agreement with the collaborating partners (PA support for field data collection was not possible during the period of interest). For NDWI validation, in situ data has to be collected. Discussions and collaboration with local partners is expected.

Technological readiness level: 3 (UPS[1])
Open source (Y/N): Y
Commercial or proprietary (C/P):
Background or Foreground knowledge (B/F): F

Partner: UPS[1] , UAB [2], CREAF[3]

Land Surface Temperature

Algorithms/Methods: Land Surface Temperature (LST) is one of the key variables for studying the Earth surface energy processes and surface – atmosphere interactions. Satellite thermal sensors measure the thermal radiation emitted from the Earth's surface and remote sensing techniques allow the estimation of the LST. MODIS (Moderate Resolution Imaging Spectroradiometer) measures the thermal radiation four times per day with two satellites in orbit, Terra and Aqua, since 2000 and 2002 respectively, in 1 km spatial resolution. Averages from the daily MODIS LST products for the entire globe are available to visualize and download All computations are performed in the Google Earth Engine (GEE).

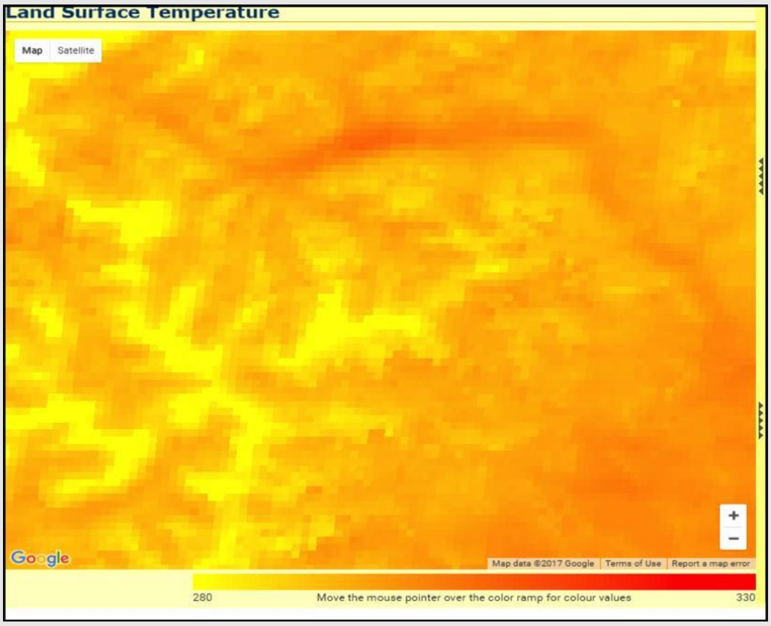

Mean Land Surface Temperature (LST), Gran Paradiso NP.

Validation: Not available

Technological readiness level: 5
Open source (Y/N): Y (Google Earth Engine)
Commercial or proprietary (C/P): P (The product is provided by rslab.gr for free use in ECOPOTENTIAL as well as in any other person/institute needs this information)
Background or Foreground knowledge (B/F): F

Partner: FORTH

Albedo

Algorithms/Methods: For Gran Paradiso, yearly (2000-2015) and monthly means and trends in blue-sky albedo have been generated using the Google Earth Engine cloud platform. The broad-band surface albedo is defined as the ratio of up-welling to down-welling radiation fluxes in a given wavelength range. It is not a true surface property, but rather a characteristic of the coupled surface-atmosphere system, therefore defined as Blue-Sky Albedo (BSA). The BSA is a critical physical variable, which influences the Earth's climate by affecting the energy budget and distribution in the Earth-atmosphere system. Its role is highly significant in both global and local scales; hence, BSA measurements provide a quantitative means for better constraining global and regional scale climate modelling efforts. The Moderate Resolution Imaging Spectroradiometer (MODIS) sensor, on board NASA's Terra and Aqua platforms, provides the parameters needed for the computation of BSA on an 8-day temporal scale 500 x 500 m spatial resolution. Here, the evaluation of BSA is based on albedo model parameters available from the MODIS Bidirectional Reflectance Distribution Function (BRDF) product (product code: MCD43B1), on an 8-day basis at 500 x 500 m on a global basis. These parameters are derived from multi-angular reflectance observations, through the inversion of a BRDF model, after atmospheric correction and cloud screening. The algorithm makes use of a kernel-driven, linear BRDF model, whereby kernel weights are derived from a best fitting procedure to observational data. For each 500 x 500 m pixel, these weights are included in the MCD43A1 product at seven wavelengths in the visible, near infrared and shortwave infrared. Using these weights, and after applying the corresponding quality flags, the broadband (0.25-4.0 μm) directional-hemispherical surface reflectance (Black-Sky Albedo: BSA) for all possible solar zenith angles (in hourly basis) and the bi-hemispherical surface reflectance (White-Sky Albedo: WSA) are computed. Then, the true BSA is estimated using a linear relationship of BSA and WSA, depending on the fraction of diffuse radiation, which is a function of the Aerosol Optical Thickness (AOT). For the BSA computation, AOT data came from the MODIS Level 3 product; among other parameters, this product includes AOT at 550 nm, on an 8-day average basis that temporally coincides with the BSA, and at 1° X 1° spatial resolution. All computations are performed in the Google Earth Engine (GEE).

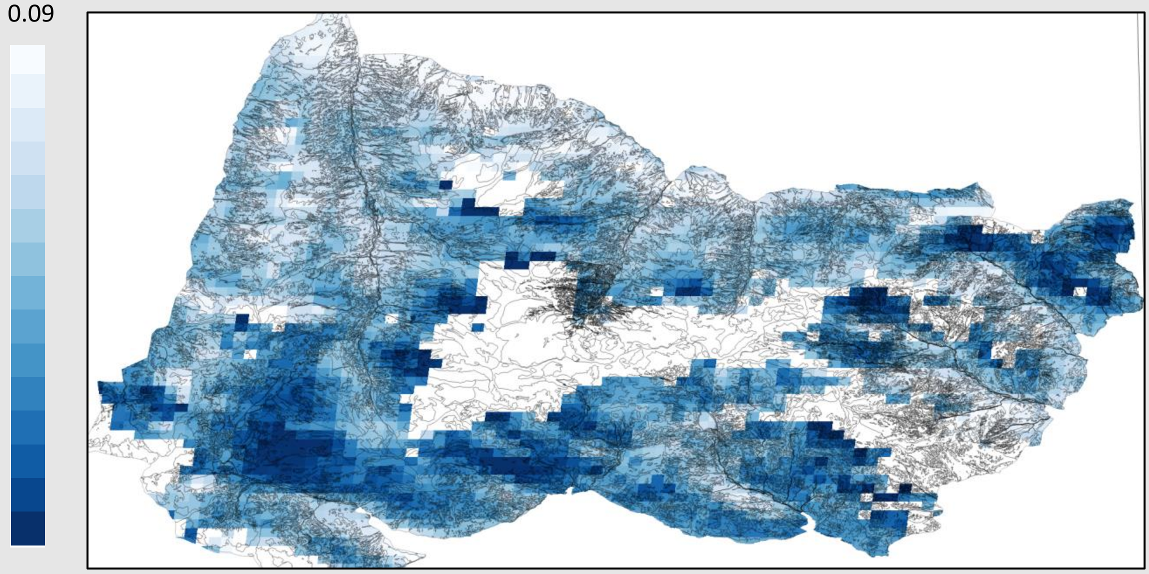

Blue Sky Albedo (2000), Gran Paradiso National Park

Validation: Not available

Technological readiness level: 4
Open source (Y/N): Y (Google Earth Engine)
Commercial or Proprietary (C/P): P (The product is provided by rslab.gr for free use in ECOPOTENTIAL as well as in any other person/institute needs this information)
Background or Foreground knowledge (B/F): F

Partner: FORTH

3.1.3 Inland water and snow

Water State

Algorithms/Methods:

Liquid water: For Donana National Park[1], Delgado et al. (2016) used a Landsat TM and ETM+ shortwave infrared (band 5) threshold of $\rho < 0.186$ to delineated flooded area. A joint TM-MSS acquisition was used to identify the MSS band 4 (near infrared) threshold. Using Landsat OLS data for Donana NP[2], a semi-automated histogram thresholding method was applied to map flooding extent in the Park. Areas (segments) with a high percentage of pixels associated with water are identified and patches around the segment centroids are selected. From these histograms of the combined data are generated and used to define the optimal (mean) thresholds for separating water and non-water. The algorithm has been tested using different datasets, including the polarization channels of Sentinel-1 (and their algebraic combinations) and Sentinel-2 bands (and indices derived from these). Combinations of data (e.g., Sentinel-1 and Sentinel-2) have also been evaluated to establish whether improvements can be made when using each singularly or in combination. For the Wadden Sea, coastal water and land separation has been achieved using Sentinel-1 SAR data.

Snow: For Hardangervidda, maps of snow extent were spatially extrapolated, using snow models that use interpolations of precipitation and air temperate and Bayesian methods, from daily snow depth data provided by the Norwegian Water Resources and Energy Directorate (NVE). The snow maps were generated using V1.1.1 of the snow model but with V2.0 precipitation and air temperature and revised correction factors for precipitation. For Gran Paradiso and Northern Limestone National Parks[3], snow maps were generated using the algorithm developed Notarnicola et al., (2013a, 2013b). In contrast to the 500 m resolution MODIS snow products of NASA (MOD10 and MYD10), this algorithm provides map at the higher 250 m spatial resolution using the red (B1) and infrared (B2) wavebands and the NDVI to allow for a more accurate detection of snow-covered area (SCA). Clouds are classified using also bands at 500 m and 1 km resolution. This is especially important in mountainous regions characterized by extreme landscape heterogeneity and topography. MODIS AQUA and TERRA data are also combined to mask clouds and increase the number of usable pixels for mapping SCA.

Ice: For Gran Paradiso and Northern Limestone National Parks[3], maps of glacier extent were extracted from the GLIMS Glacier database. GLIMS is generating areas of glacial area, geometry, surface velocity and snow line elevation, primarily from the Advanced Spaceborne Thermal Emission and Reflection Radiometer (ASTER) and the Landsat Enhanced Thematic Mapper Plus (ETM+) as well as historical information derived from maps and aerial photographs.

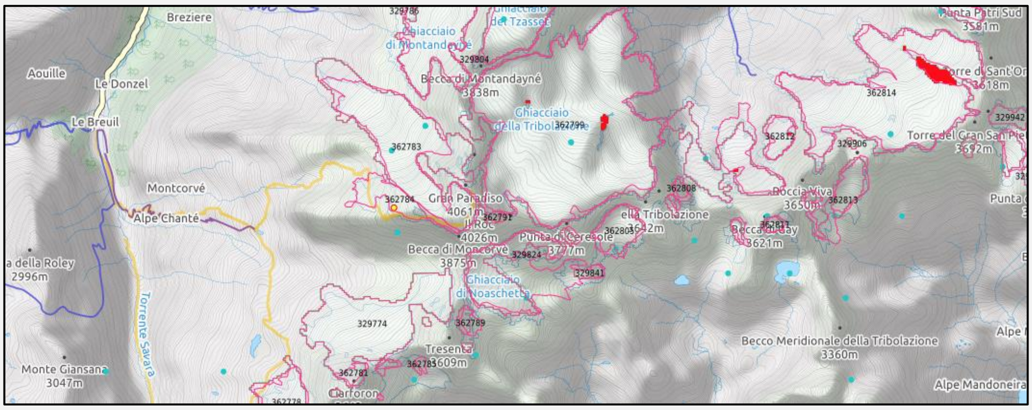

Glacier extent, Gran Paradiso NP, Italy.

Validation: Not completed

Technological readiness level: 3 (CSIC[1])

Open source (Y/N):

Commercial or proprietary (C/P):

Background or Foreground knowledge (B/F): B

Partner: CSIC[1], CERTH[2]

Water Extent

Algorithms/Method: For Donana (Spain)[1,2], a supervised and unsupervised approach for mapping water extent from both Sentinel-1 SAR and/or Sentinel-2 optical data. In the supervised approach, selected pixels representing water identified and, for each, a vector of attributes (based on Sentinel bands and indices) was computed. These were then used as input to the WEKA Data Mining Software to train a range of classification algorithms. The second approach, which is more transferable between sites, applied an unsupervised thresholding to either Sentinel-1 VV and VH data or Sentinel-2 spectral data and derived indices. An initial threshold (**T_{init}**) was used to separate inundated from non-inundated areas and then segments with a high percentage of pixels exceeding or below this threshold (depending on the data inputs) were selected. Patches around the centroids of the selected segments were established and thresholds that effectively split the histograms for each of these were estimated. The final threshold derived from the splitting (**T_{final}**) was then used to separate inundated and non-inundated areas. The work flow of both approaches is shown in Appendix 1, section A1.7, work flows (a) and (b).

(a) (b) (c)

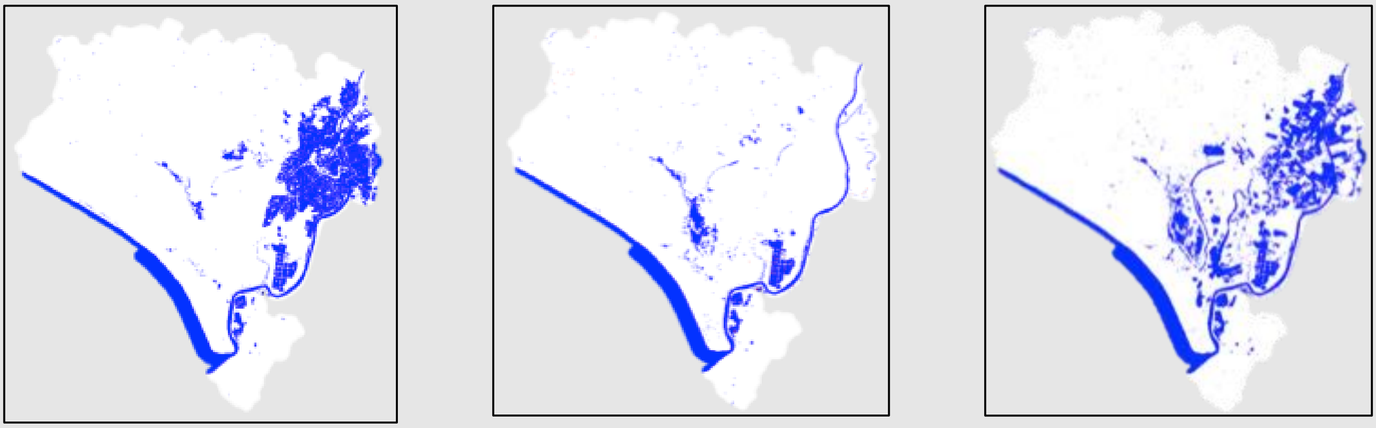

Water extent mapped for the Donana PA on (a) 19th December 2015, (b) 8th March 2016 and (c) 6th June 2016; (a) 19/12/2015, (b) 08/03/2016 and (c) 06/06/2016 relying on the unsupervised approach and S2 input data. Water covered areas are denoted with blue.

Validation: Inundation maps generated from Landsat and validated through field observations (provided by CSIC) are used. Errors are represented by a confusion matrix and the average class producers' accuracy for the supervised approach and using Sentinel-2 and both Sentinel-1/2 was 94.6 % and 93.4 % respectively. The performance of the unsupervised approach was similar when Sentinel-2 data were used as input. Accuracies can be increased when a digital elevation model and/or other land cover classifications are included.

Technological readiness level: 5 (CERTH[1])
Open source (Y/N): N
Commercial or proprietary (C/P): Some components of the software are to be executed via commercial software, because of the availability of resources. The algorithm will be converted to an open source module for the Virtual Laboratory Platform.
Background or Foreground knowledge (B/F): F

Partner: CERTH[1], CSIC[2]

Co-funded by the European Union

Water Hydro-period

Algorithms/Methods:

Water: For Doñana NP[1,2], and for most years between 1974 and 2014, maps of inundation were generated from individual Landsat scenes and combined to generate hydroperiod maps (Delgado *et al*., 2017). Similar maps[2] were generated using combinations of Sentinel-1 and -2.

Snow: For Hardangervidda[3], annual snow cover maps showing the number of days where the snow depth was above 1 mm in each month were generated by summarising daily maps. Two measures of snow cover per year were generated; the number of days with snow cover per calendar year and per season (i.e., September of the previous year to August of the present year). The spatial resolution of the data was the native resolution of Norwegian weather data; 1 x 1 km. For Gran Paradiso (b) and Northern Limestone[4], hydroperiods for snow were generated for 2002 to 2014.

(a)

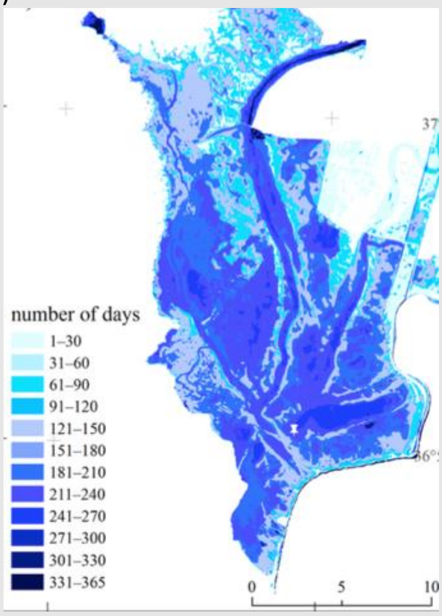

Water hydroperiod (in days), Donana NP.

(b)

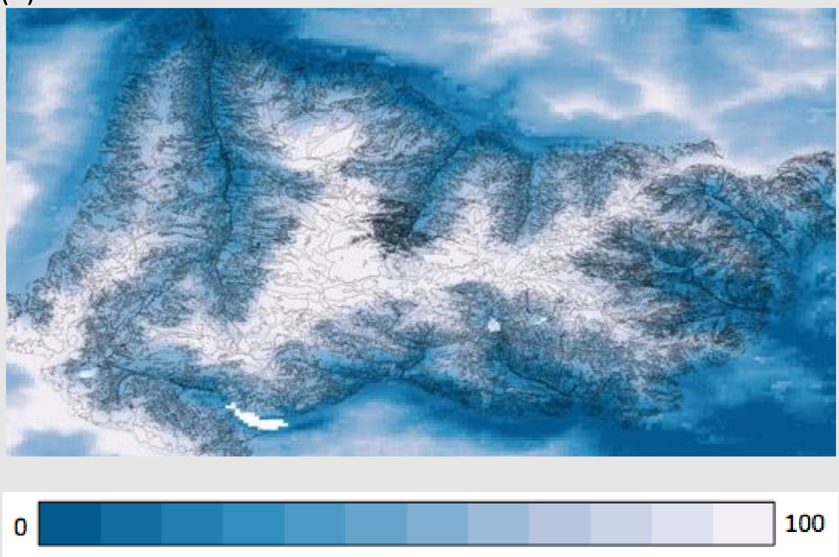

Snow hydroperiod (in days), Gran Paradiso NP.

Validation: For the Landsat-based classification[1] (Delgado *et al*., 2017), the Kappa for flooded areas was 0.65. For Donana[2], field-based, airborne (including drone) and satellite (Landsat) measures of open water were used.

Technological readiness level: NA
Open source (Y/N): For water, raster algebra is used and hence the algorithm is open source.
Commercial or proprietary (C/P): The flooding layers are WMS available at http://venus.ebd.csic.es/imgs
Background or Foreground knowledge (B/F): F

Partner: CSIC[1], CERTH[2], UIB[3], EURAC[4]

Hydroperiod and Seasonality maps estimation

Algorithms/Methods: For Doñana, the hydroperiod has been mapped using water masks generated for different dates. For two dates (herein referred to as A and B) time-separated by X days, the occurrence of water is compared. If a pixel is inundated on both dates, then it is assumed inundated for X-days but X/2 days otherwise (e.g., A and not B or B and not A). The total number of days of inundation is determined by accumulating the water masks throughout the year. The resulting hydroperiod maps indicate the seasons when a pixel is flooded, changes in inundation relative to previous seasons (i.e., the number of times per year) and the periodicity of flooding (number of dry periods). The workflow behind the hydroperiod and seasonality estimation is provided in Appendix 1, Section A1.6.

(a)

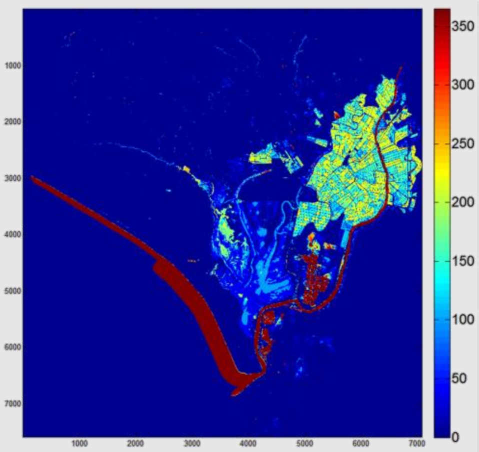

(b)

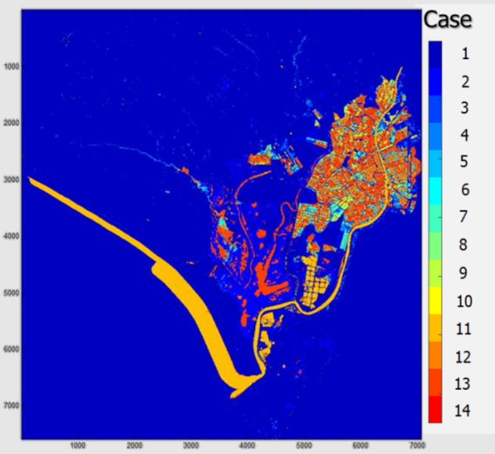

(c)

Case	Flooded seasons of the year	Flooding Increment in relation to previous season	Periodicity of flooding
1	0	0	0
2	1	0	0
3	2	0	0
4	2	1	0
5	2	1	1
6	3	0	0
7	3	1	0
8	3	1	1
9	3	2	0
10	3	2	1
11	4	0	0
12	4	1	0
13	4	2	0
14	4	3	0

Hydroperiod map for Donana PA for Year 2016.The legend shows the duration of inundation days corresponding to each color in the map.

Hydroperiod seasonality map of Donana PA in 2016(winter)-2016(fall). The legend shows the colors that correspond to the cases summarized on the right table.

Validation: No ground truth data are yet available for assessing hydroperiods and associated seasonal variations.

Technological readiness level: 4
Open source (Y/N): N
Commercial or proprietary (C/P): Some components of the software are to be executed via commercial software, because of the availability of resources. It is intended to convert the algorithm to an open source module for the Virtual Laboratory Platform.
Background or Foreground knowledge (B/F): F

Partner: CERTH

Water Turbidity and Sediment Loads

Algorithms/Methods: For protected areas, including the Camargue[1], areas of clear and turbid water were discriminated from Sentinel-2 data by applying a random forest algorithm. For Donana, an empirical model relating water turbidity to Landsat 5 Thematic Mapper (TM) and Landsat-7 Enhanced TM (ETM+) radiometrically normalised images was used for discriminating turbidity classes. Initially, areas of flooding were identified using a red (R; band 5) and short wave infrared (SWIR; band 5) reflectances lower than 30 % and 9 % reflectance respectively (Diaz-Delgado et al., 2006). Nefelometric Turbidity Units (NTU) were then determined by including the near infrared (NIR; band 4) and using:

$$Log(NTU + 0.01) =$$
$$4.1263 + 18.8113 * R - 32.2615 * SWIR - 0.6114 * (\frac{R}{NIR})$$

For pixels that were not within the areas defined by the R and SWIR thresholds, the following was used:

$$Log(NTU + 0.01) = 4.1263 - 0.6114 * (\frac{R}{NIR})$$

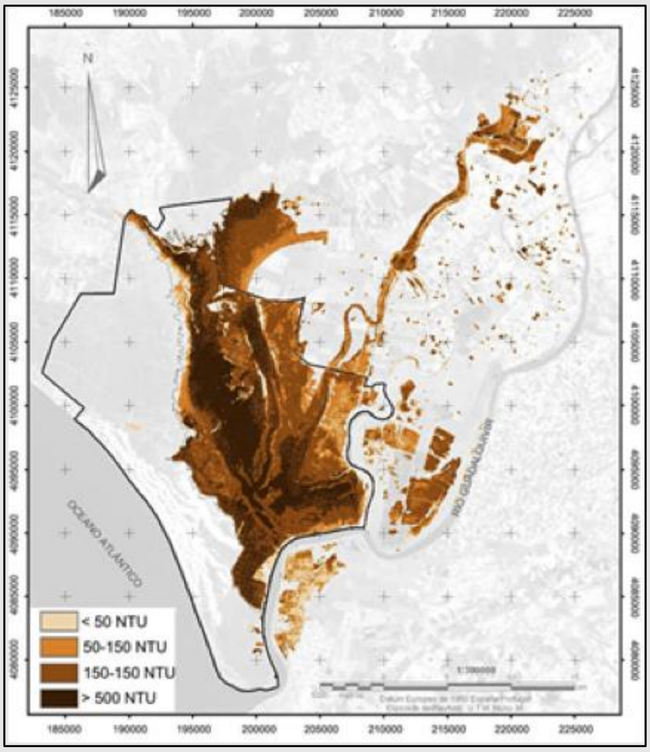

Estimates of Nefelometric Turbidity Units (NTU), Doñana marshes.

Validation: To be undertaken.

Technological readiness level: **5 (UNSW[1])**
Open source (Y/N): Y; algebraic equations
Commercial or proprietary (C/P): The NTU products are available at http://venus.ebd.csic.es/imgs
Background or Foreground knowledge (B/F): F

Partner: UNSW[1] , CSIC (EBD)[2], CREAF[3]

Water Depth

Algorithms/Methods: For Doñana marshes, the water depth (cm) was estimated using Landsat 5 Thematic Mapper (TM) and Landsat-7 Enhanced TM (ETM+) radiometrically normalised images and for pixels identified as flooded (Díaz-Delgado et al. 2006; with a blue (B, band 1) reflectance of < 12 % and where the green (G) and near infrared (NIR) ratio was less than 2.5). For retrieval, the following relationship was used:

$$Log(Depth + 0.01) =$$
$$(0.039 * R) + (0.028 * SWIR) - 0.0075 * (\frac{B4}{B4S}) + \left(1.023 * \frac{G}{NIR}\right) + (-1.042 * B4) + 5.2937$$

where B4S represents the reflectance of the soil surface (when dry), which was obtained from a September Landsat-5 TM image.

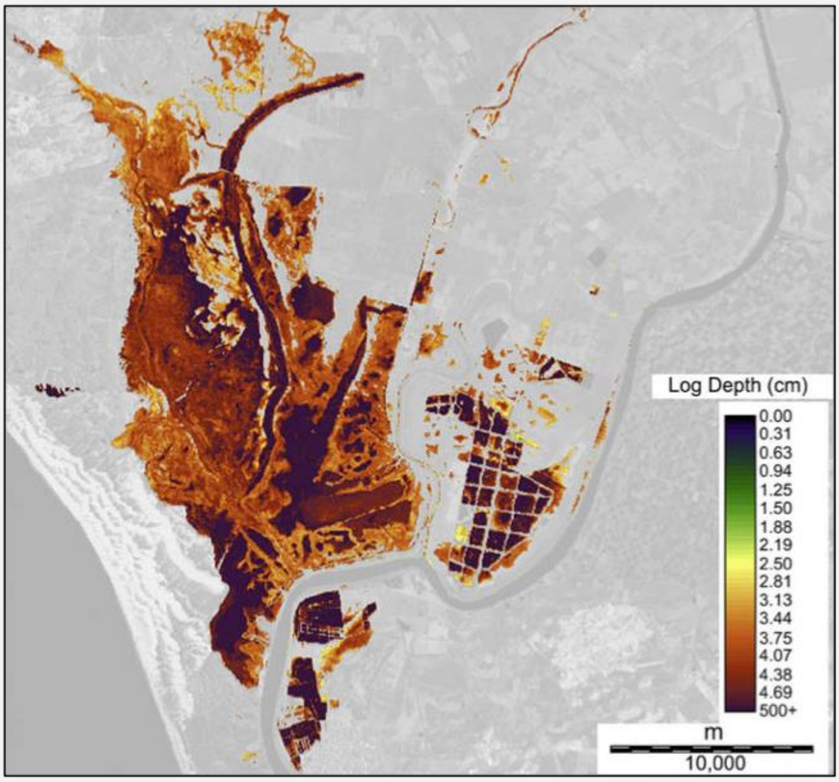

Estimated water depth (cm), Doñana marshes

Validation: Based on in situ data, with water turbidity (in NTU) measured for samples collected at points 60 m apart along 20 walked transects, each of ~3 km. The model explained 75.42% of the variance. More information in (Bustamante *et al*., 2009).

Technological readiness level: 3
Open source (Y/N): Y; algebraic equations.
Commercial or proprietary (C/P):
Background or Foreground knowledge (B/F): B

Partner: CSIC (EBD)

Snow cover from optical data

Algorithms/Methods: For Gran Paradiso, Northern Limestone and Sierra Nevada as well as Hardangervidda National Parks, snow cover area has been mapped over using an existing algorithm developed by Notarnicola et al. (2013a, b). The algorithm exploits the MODIS AQUA and TERRA 250 m red (B1) and near infrared (B2) regions as well as the Normalized Difference Vegetation Index (NDVI). Clouds are classified using these but also other bands at 500 m and 1 km resolution.   Snow has been mapped for the entire period of the MODIS operation (since 2000). In the Hardangervidda NP, areas of snow and ice and also free of both water states have also been separated. The maps are of finer resolution that the 500 m resolution MODIS snow products generated by NASA (MOD10 and MYD10).

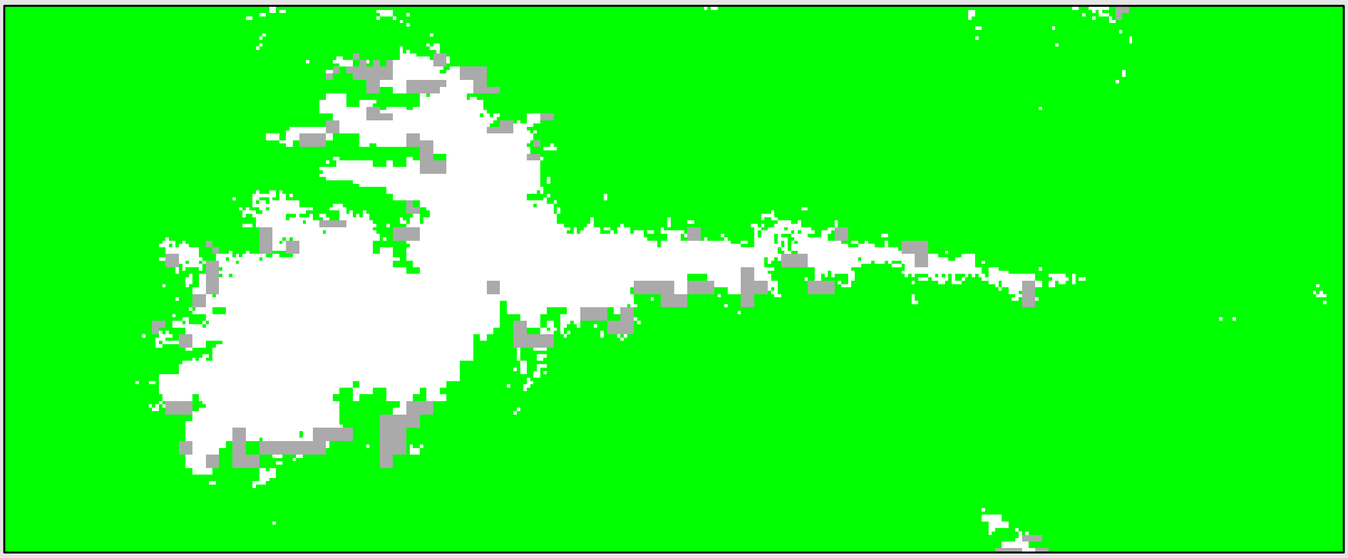

Snow cover over Sierra Nevada on March 2nd 2016, as mapped from MODIS data.

snow

snow free

clouds

Technological readiness level: 7
Open source (Y/N): N
Commercial or proprietary (C/P): P
Background or Foreground knowledge (B/F): B

Partner: EURAC

Snow Cover from SAR data

Algorithms/Methods: Sentinel-1 Interferometric Wide (IW) Ground Range Detected (GRD) SAR products (~20x20m spatial resolution, 250 km swath) are used to generate snow cover maps in Sierra Nevada (Spain), Hardangervidda (Norway) and Tatra Mountains (Poland) national parks. SAR acquisitions are suitable to identify wet snow covered areas through a change detection approach. However, in order to classify the snow wetness (i.e. wet or dry snow), temperature maps and digital elevation model (DEM) are needed. The implemented algorithm requires snow-free reference images of the area of interest generally taken in summer. Both summer and winter images undergo a pre-processing phase including calibration, terrain correction, geolocation (Small et al. 2008). Areas affected by layover and shadowing SAR effects cannot provide any reliable information and therefore are masked out. A single reference image is then generated by temporally averaging the set of no-snow images, with a consequent reduction of the speckle noise. A spatial speckle filter is instead applied to each winter acquisition, achieving a better image quality, at the cost of slightly degraded spatial resolution. The identification of pixels covered in wet snow is made by carrying out a comparison between the ratio between the backscattering of the reference acquisition and of each winter image, and an empirical threshold. Pixel values larger than the threshold and characterised by a temperature below an empirical threshold which is slightly higher than the freezing temperature, are initially classified as wet snow. Digital elevation model (DEM) and temperature maps related to the same date as the winter image are needed to identify dry snow covered areas. To this purpose, pixels affected by a significant variation in the backscattering value, are further analysed together with their neighbours (75x75 window size). When the pixel is located at higher altitude than the average altitude of the surrounding snow covered area, and exhibits a temperature lower than the freezing point, it is classified as dry snow. The final snow cover maps are thematic maps labelled as: Layover/Shadowing= -50, No snow =0, Wet Snow= 50, Dry Snow= 200. The implemented algorithm based on the method presented in (Nagler et al., 2000) needs to be adapted to the characteristics of each observed area by setting proper backscattering ratio and temperature thresholds, by using ground truth data during the calibration phase.

(a) *(b)* *(c)*

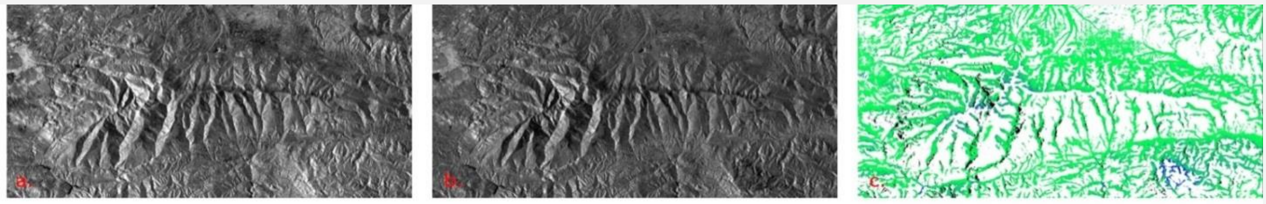

Pre-processed and despeckled reference (a) and winter (b) Sentinel-1 IW GRD HR images of the Sierra Nevada National Park (Spain); (c) example of snow cover map derived from the Sentinel-1 acquisition taken on 23rd December 2016(black: layover/shadowing; blue: no snow; green: wet snow; white: dry snow).

Validation: To carry out as soon as the ground truth will be available for all sites. Liquid Water Content maps (1000x1000 m grid) are available for the Hardangervidda National Park and can be used for the validation activity.

Technological readiness level: 3 The algorithm is currently implemented. However, temperature maps are still not
Open source (Y/N): Y (Python)
Commercial or proprietary (C/P): P
Background or Foreground knowledge (B/F): F

Partner: STARLAB

3.2 Marine, coastal and transitional water monitoring (Task 4.2.2)

This section includes a detailed product card for each of the marine, coastal and transition water monitoring variables generated in the context of ECOPOTENTIAL PAs requests.

Ocean Color Products (CHL-a, CDOM, TSM)

Algorithms/Methods: Optically speaking, waters can be generally divided into two different classes (Morel and Prieur, 1977): *case 1* waters, those dominated by phytoplankton (e.g. open oceans); *case 2* waters, optically deep and complex waters that contain not only phytoplankton but also other constituents such as suspended sediments, dissolved organic matters, and anthropogenic substances.
The variety within *case 2* waters, generally related to the coastal domain, is large because concentrations as well as specific Inherent Optical Properties (IOPs) of Chlorophyll-a (CHL-a), Total Suspended Matter (TSM) and Colored Dissolved Organic Matter (CDOM) concentrations are subject to potentially large and independent variations (Odermatt et al., 2012). Universally applicable algorithms for the retrieval of water constituents from *case 2* waters are not known (IOCCG, 2006). Odermatt et al. (2012) provided a comprehensive overview of water constituent retrieval algorithms and models for optically deep and complex *case 2* waters using Remote Sensing data.

Currently, the empirical model is still the most widely used tool to infer water constituents from Remote Sensing data, even if the accuracy of semi-empirical models is better than that of empirical algorithms (Bukata et al., 1995), and these models are more applicable for different water types with the capability to account for the effects of water depth, particle size, and water-air interface. Spectral inversion procedures match spectral measurements with bio-optical forward models by means of inversion techniques, in order to generate standard Ocean Color products. The spectral IOPs of all three constituents are thereby retrieved at once from one spectral AOP. Among the several inversion techniques applied for this procedure, the CoastColour algorithm (Brockmann et al., 2012) was selected to estimate water constituents concentrations of the Wadden Sea Dutch Delta site from MERIS data.
The CoastColour algorithm is freely available as a plugin of the BEAM VISAT software (http://www.brockmann-consult.de/cms/web/beam; http://www.coastcolour.org).

Validation:

Technological readiness level: NA
The Brockmann Consult algorithm was used.

Open source (Y/N): Y
Commercial or proprietary (C/P):
Background or Foreground knowledge (B/F):

Partner: ISPRA

(a)

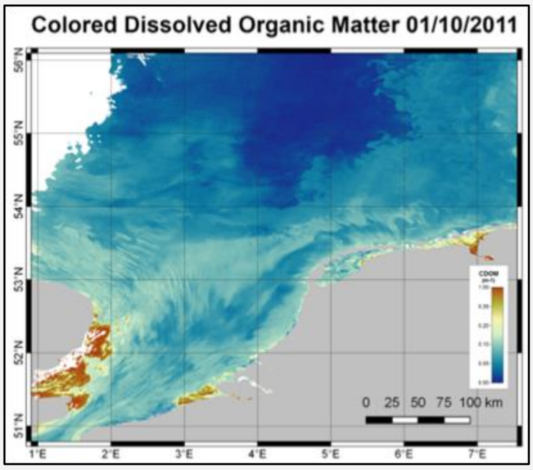

(b)

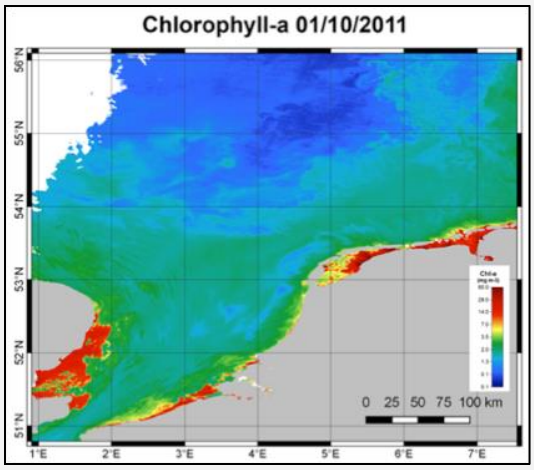

(c)

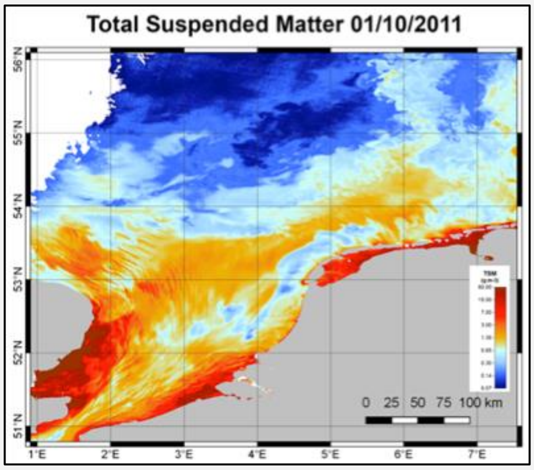

Products for Wadden Sea (Dutch Delta)

Wind Fields

Algorithms/Methods: High resolution offshore and coastal sea surface winds (directions and speeds) have been retrieved from co-polarised VV and HH Sentinel-2 SAR data for the Mediterranean Sea, south of the Camargue, and the Wadden Sea using the SARWIND LG-Mod (Rana et al., 2016). Validation has been achieved through cross comparison with numerical weather re-analyses and or predictions (e.g., ECMWF and SKIRON wind data; (Kallos, 1997)). The wind direction component was retrieved directly from Sentinel-1 data and then used as input to the backscattering Geophysical Model Functions (GMFs) for retrieving the wind speed component by (Li and Lehner, 2014). SSW fields derived from Sentinel-1 data seem to better reproduce the spatial characteristics of local winds at both high and medium output resolutions, compared to the ones obtained from the weather models considered, i.e. SKIRON (Kallos, 1997) and ECMWF. More details in the paper (Rana et. al, 2017), which is under revision. The algorithm work flow is shown in Appendix 1.

(a)

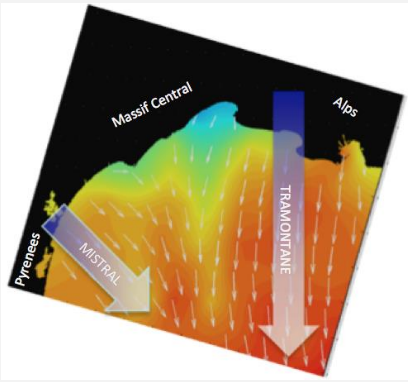

(b)

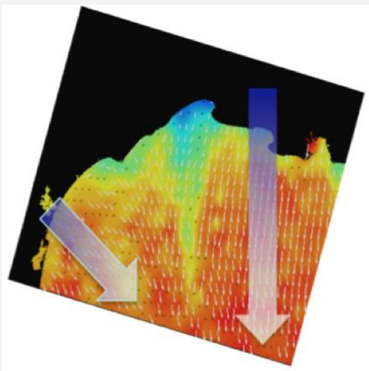

SSW wind direction and speed components at 12,5km (a) and 5km spatial resolution (b) retrieved offshore from the Camargue by descending IW-GRD-HR Sentinel-1 data

(c)

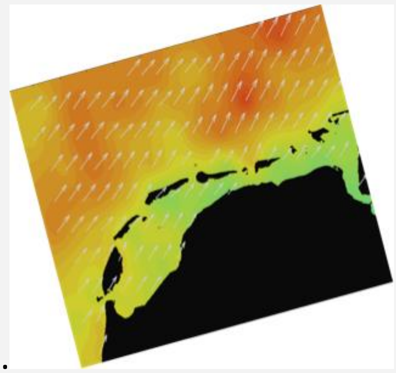

(d)

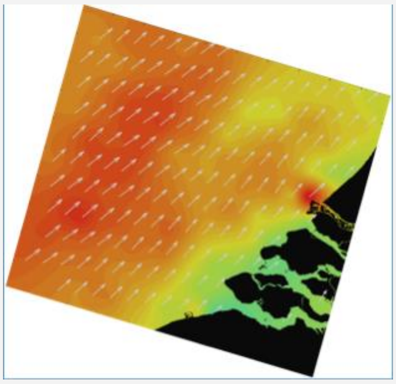

SSW products for the Wadden Sea at 12.5 km spatial resolution from ascending (c) and descending (d) IW-GRD-HR Sentinel-1 data

Validation: Details are provided in Section 4.7.6

Technological readiness level: 4
Open source (Y/N): N
Commercial or proprietary (C/P): P Some components of the software are to be executed via commercial software but the intention is to provide WPS for the Virtual Laboratory Platform.
Background or Foreground knowledge (B/F): F

Partner: CNR

Sea Surface Temperature

Algorithms/Methods: Sea Surface Temperature (SST) has been mapped from both weather and earth observation satellite thermal infrared data, initially using algorithms developed by, for example, by Andling and Kauth (1970) and later improvements of these (e.g., Merchant et al., 2008). For European seas, the Copernicus Marine Environment Monitoring Service (CMEMs) currently employs operational processing chains for SST retrieval (known as the Level 4 product) from multiple thermal infrared sensors (referred to as L2P) including the AATSR (ENVISAT), AVHRR (METOP_A, NOAA-17, NOAA-18), MODIS (TERRA, AQUA) and SEVIRI (MSG) (Buongiorno Nardelli et al., 2013; Pisano et al., 2016). The highest quality SST data are acquired between 9 pm and 6 am local (pixel) time. For each pixel and acquisition time, SST are first extracted and spatially correlated errors are then removed using a bias adjustment procedure. Successive supercollating algorithms are then utilized to generate Level 3 multi-sensor SST (Buongiorno Nardelli *et al.*, 2013). Finally, interpolation procedures are optimized to generate the gap filled SST Level 4 dataset on a daily basis and at 1/100° spatial resolution. For the protected areas of the Wadden Sea (Dutch Delta) and the Mediterranean Sea (Large Marine Area), SST Level 4 data were extracted from CMEMS following application of offset and scale factor values.

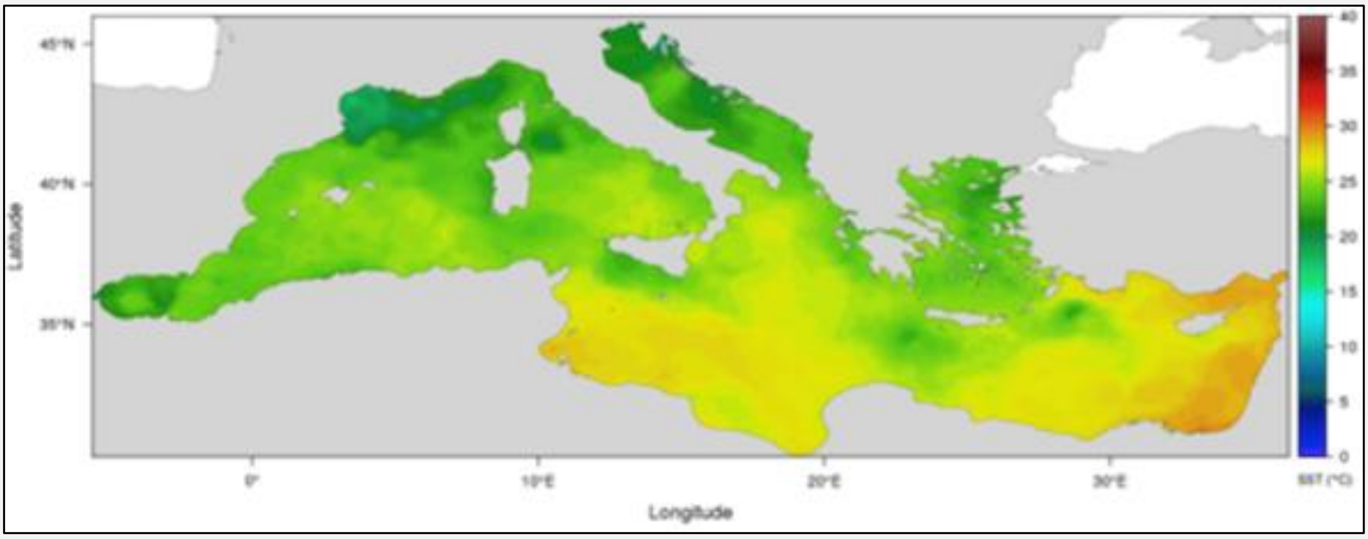

Sea Surface Temperature for the Mediterranean Sea, 20th September, 2008.

Validation:

Technological readiness level: NA - CMES product source
Open source (Y/N):
Commercial or proprietary (C/P):
Background or Foreground knowledge (B/F):

Partner: ISPRA

Chlorophyll-a (open waters and inland waters)

Algorithms/Methods: Optical oceanography aim to operate accurate estimation concentrations of the water constituents from optical measurements. Absorption and scattering properties of sea water are described by its inherent optical properties, (IOPs). Based on the IOPs, waters can be classified in two main classes: Case 2 waters, vertically mixed coastal waters dominated either by suspended inorganic material or biogenic particulate material, and Case 1 waters, influenced by biogenic materials only. Depending on the concentrations of the constituents, the water changes its color from blue to green to light brown. Different bands from optical multispectral sensors are used to estimate surface concentration of photosynthetic pigment chlorophyll-a, yellow substance and suspended inorganic sedimentary particles. Algorithms are applied to derive the concentrations of the three different groups of substances in Case 2 waters from the water-leaving radiance, and of Chl-a concentration in Case 1 waters, after an atmospheric correction is performed (Doerffer, 2009). The Copernicus Marine Environment Monitoring Service (CMEMS) employs operational processing chains for the production, validation and dissemination of the multi-sensor Chl-a Level 3 (L3) products covering the European Seas. For the Mediterranean Sea, the combination of MedOC4 (Case 1; Volpe et al., 2007) and AD4 (Case 2; Berthon and Zibordi, 2004) algorithms are used to generate and distribute the L3 ESA CCI 8-days and monthly average composites of Chlorophyll-a concentration data. Input TOA radiance data are collected from SeaWiFS (R2010.0), MODIS (R2013.1) and MERIS L1B (3rd reprocessing). MedOC4 is the best algorithm matching the requirement of unbiased satellite chlorophyll estimates for the Mediterranean Sea (Volpe et al., 2007). For Lake Ohrid and Lake Prespa (inland waters)[2,3], monthly means of Chlorophyll A product derived from MERIS, at a 300 m spatial resolution from 2002 to 2012 have been computed in collaboration of Brockmann Geomatics Sweden AB from H2020 SWOS Project.

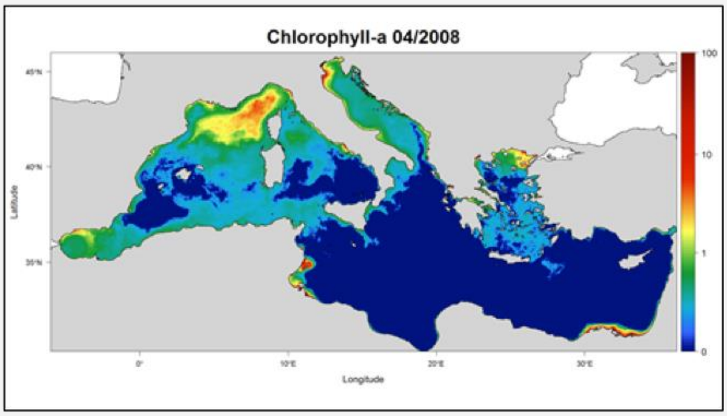

Chlorophyll a concentrations obtained for the Mediterranean Sea.

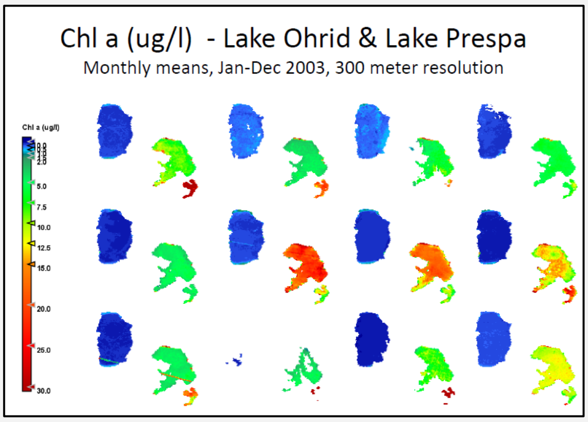

Chlorophyll a for Lake Ohrid and Prespra (SWOS Collaboration product)

Validation: Chl a Product for Lake Ohrid and Prespa is being validated through in-situ data for several years, comparing it to monthly MERIS based estimates.

Technological readiness level: NA - CMEMS product source
Open source (Y/N):
Commercial or proprietary (C/P):
Background or Foreground knowledge (B/F):

Partner: ISPRA[1], CREAF [2], HIO [3]

Shoreline delineation

Algorithms/Methods: Sentinel-1 Interferometric Wide (IW) Ground Range Detected (GRD) (https://sentinel.esa.int/web/sentinel/user-guides/sentinel-1-sar) products are used for the shoreline delineation of the Wadden Sea area. The frequent availability of such products with a spatial resolution of ~20x20m (10x10m pixel spacing) make them particularly suitable to the coastline detection. The default dual polarisation VV+VH of Sentinel-1 IW is used. However, while VH (HV) polarisation provides high land-sea contrast, VV polarisation is more sensitive to sea surface roughness, providing higher sea backscattering values (especially in presence of strong wind) comparable to the land backscattering values. The chain of processing starts with a typical pre-processing phase including SAR calibration, terrain correction and geolocation (Small et al., 2008). Afterwards, each band of the Sentinel-1 product is processed separately to generate the shoreline map. To this aim, the images are firstly enhanced to increase the land/sea contrast through the scaling of SAR backscattering values. The resulting images are then converted to grayscale (0-255) without loss of significant information, but with a gain in next algorithm steps computational effort. A further improvement of the images is achieved by applying a despeckle filter to reduce typical noise affecting SAR acquisitions. A median-filtering (21x21 pixels kernel) approach has been selected for this application. Land/sea discrimination is carried out through an image binarisation approach based on the pixel intensity values which are assumed being characterised by a bimodal probability density function. Under such assumption, the Otsu's method (Otsu, 1975) is applied to automatically derive the optimum threshold allowing the discrimination between land and sea pixels. The output binary images may present artefacts due to the presence of ships or to SAR noise, resulting in small isolated areas or in gaps which can be removed by applying morphological filters (i.e. opening and closing operations). The Canny edge detector (Canny, 1986) is finally applied to the binary water masks (land=0, sea=1) to generate the correspondent shoreline images. Each dual polarisation Sentinel-1 product will provide one water mask and one shoreline image. These results are also combined through logical operators in a third pair of products. If the water mask outputs obtained from both the polarisations agree, the pixel values are set to 0 (land) or to 255 (sea) in the combined water mask image, otherwise the uncertainty areas are highlighted by pixels whose values are set to 127. The correspondent combined shoreline result is derived from only the common outcomes in the combined water mask image.

(a) (b) (c) (d)

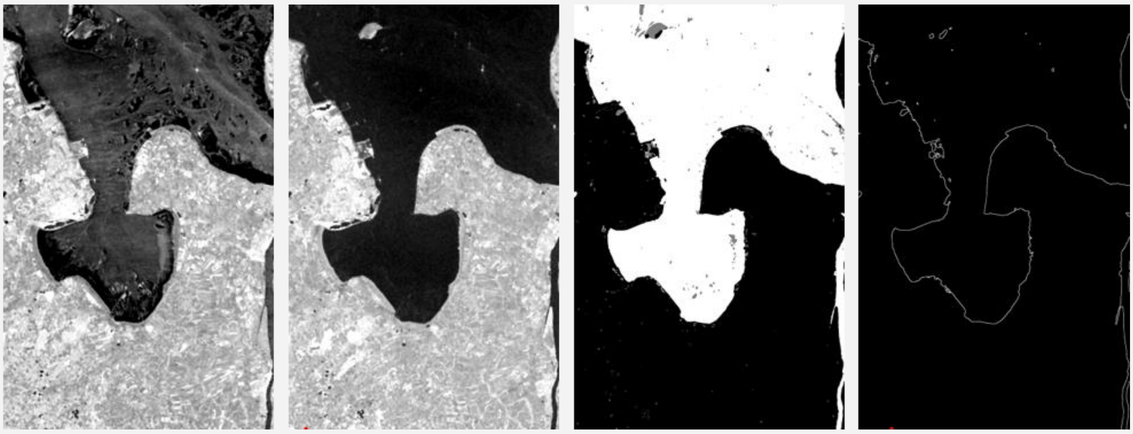

Sentinel-1 IW GRDH images (VV (a); VH (b)) after pre-processing and despeckle filtering; (c) combined water mask (White: sea; Black: land; Grey: uncertainty areas); (d) shoreline image derived from (c).

Validation: To be carried out as soon as the ground truth will be available. Difficulties may arise due to the need of having reference data related to the same date and time as the Sentinel-1 acquisition, and therefore to the same moment of the tidal cycle.

Technological readiness level: 3
Open source (Y/N): Y , in Python
Commercial or proprietary (C/P): P
Background or Foreground knowledge (B/F): F

Partner: STARLAB

3.3 Other: bathymetry and cloud cover

Bathymetry

Algorithms/Methods: The bathymetry of the Mediterranean basin was collected from the EMODnet bathymetry portal (EMODnet Bathymetry Consortium, 2016). It represents the elevation in meters of the sea bottom and with reference to Lowest Astronomical Tide (LAT). EMODnet Digital Terrain Model (DTM) is generated for European sea regions by harmonizing more than 7700 bathymetric survey datasets collated from public and research organizations. Bathymetric survey data are derived from either high resolution datasets from single- and multi-beam surveys or bathymetric database of National Hydrographic Offices based on historic surveys. Sea bottom elevation was smoothed by means of a spline function and areas with no survey data coverage are completed by integrating the GEBCO 2014 Digital Bathymetry at 30 sec spatial resolution.

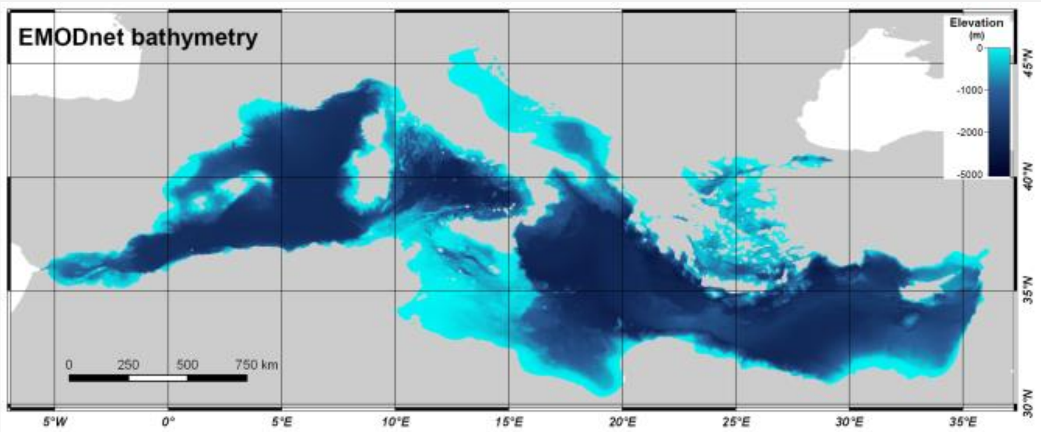

Tiles of the EMODnet Digital Terrain Model (DTM) were mosaicked after applying offset and scale factor.

Technological readiness level: NA – EMODnet product source
Open source (Y/N):
Commercial or proprietary (C/P):
Background or Foreground knowledge (B/F):

Partner: ISPRA

Cloudiness

Algorithms/Methods: For La Palma, the F-mask algorithm of Zhu et al., (2015) has been used to map cloud cover in each Landsat-8 Operational Land Imager (OLI) data acquired between August and December 2015. By combining the cloud masks over the time-series, maps of cloud persistence and periodicity have been generated for the island and convey the greater frequency of occurrence on the mid-western section.

(a)

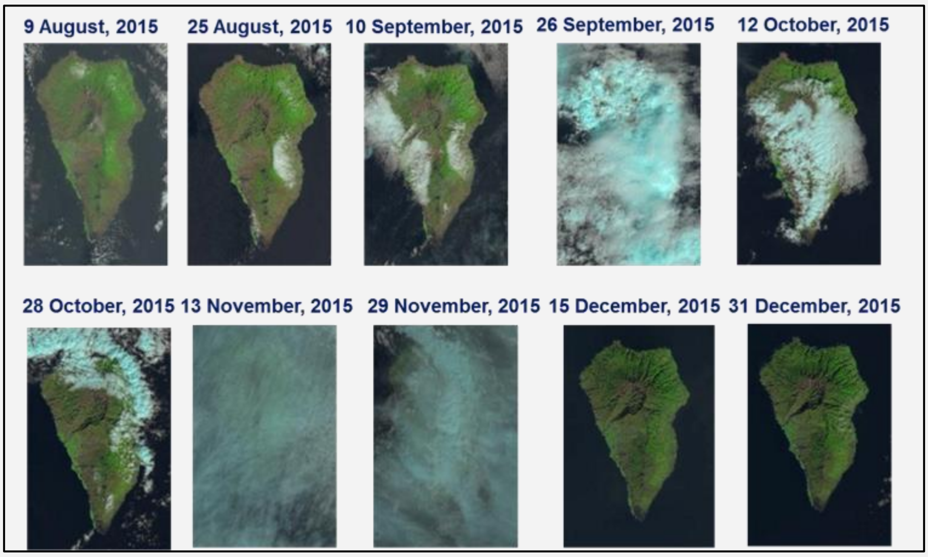

(b)

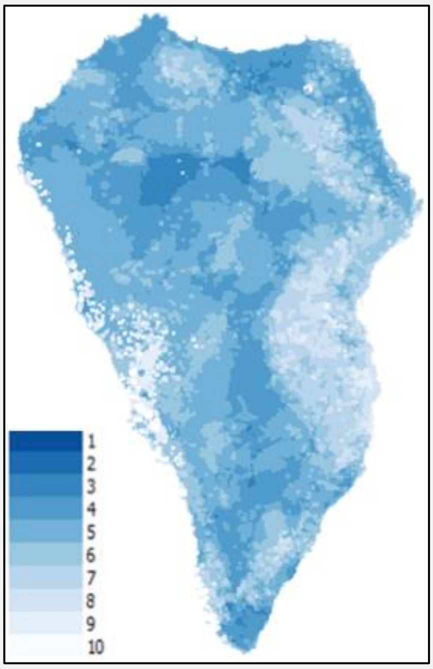

(a) The 10 Landsat images considered for La Palma and (b) the cloud cover frequency.

Technological readiness level:
Open source (Y/N): Y available as an algebraic formulation.
Commercial or proprietary (C/P): C
Background or Foreground knowledge (B/F): F, through WPS

Partner: CNR

4. The EODESM system: a new approach to Land Cover and Change classification (Task 4.3)

4.1 Land Cover/Land Use (Task 4.3.1)

The EODESM developed through ECOPOTENTIAL builds on the previous EODHAM system developed through the FP7 BIO_SOS project (www.biosos.eu; Lucas et al., 2014). The system consists of several modules that focus on a) the classification of land covers from thematic (e.g., leaf type, water state) and continuous layers (e.g., hydro-period, canopy cover) and b) the detection of change based on LCCS2 categories, component codes and environmental variables. The classification of land cover is based mainly on the knowledge driven hierarchical implementation of the Food and Agricultural Organisation's (FAO's) Land Cover Classification System (LCCS2), which was developed using LCCS2 Version 2 and can be modified to integrate the more recent Land Cover Macro Language (LCML). An overview of the LCCS2 Taxonomy is given in Figure 4.1. However, land cover maps produced by other data driven classifiers (e.g., Support Vector Machine, Random Forest) from both optical and Radar data e.g., Sentinel-1) can be integrated into the system.

EODESM is based on open source software (i.e., python) and the Virtual Laboratory will access the system by an http web interface.

The following sections describe the EODESM system and then present the output classifications according to the LCCS2 taxonomy. The approach to validation is also described, with this making reference to both in situ and existing habitat (thematic) classifications. The overall approach is discussed in relation to previous efforts at land cover mapping.

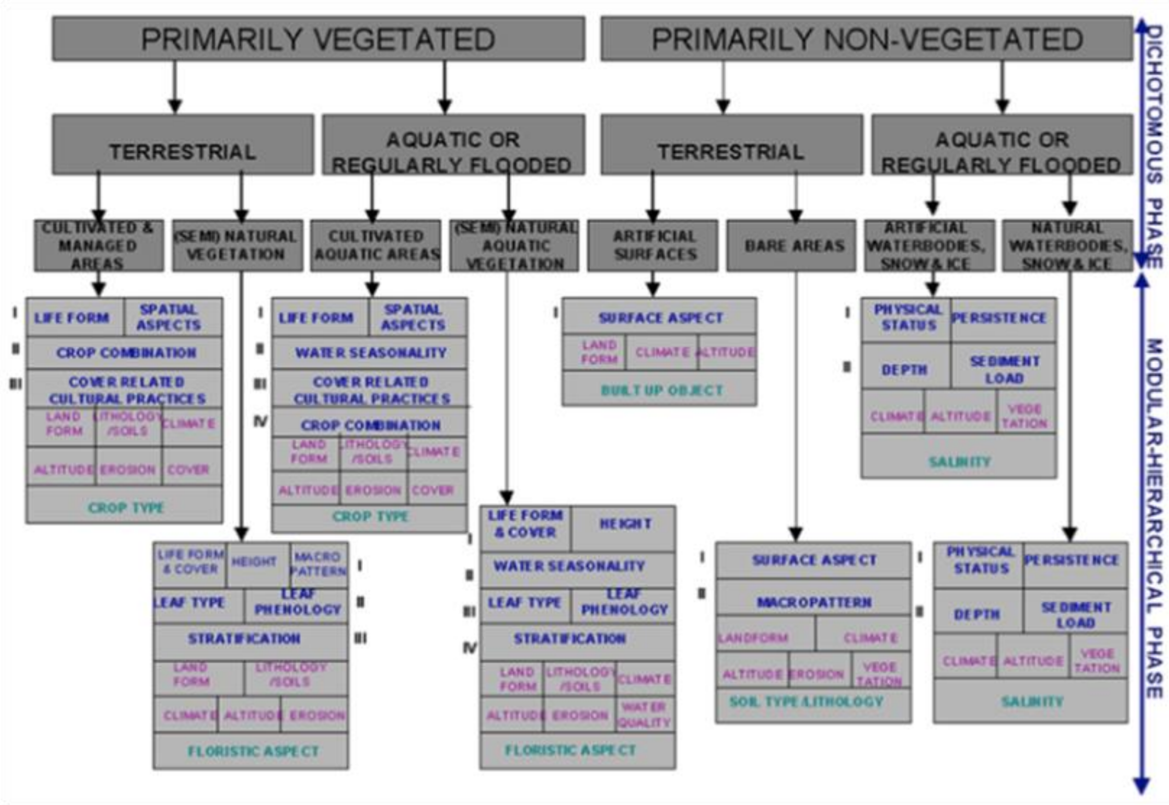

Figure 4.1. The FAO LCCS Taxonomy

The LCCS2 taxonomy (see also Deliverable 2.2) is hierarchical and allows for the progressive classification of a comprehensive range of land covers at the ground level but also from Earth Observation (EO) data. The LCCS2 system has been used as the basis for EO-based classifications in many studies but the approach has typically been to establish training areas for the 'end classes' of the taxonomy (such as broadleaved evergreen forests). The

EODESM (Figure 4. 2) takes a different approach in that it follows the sequences of classifications through the hierarchy using directly EO images or derived products from EO data but also other ancillary spatial information, such as cadastral and urban maps, models (e.g., of hydrology) and knowledge. This is the unique advantage of EODESM, in that the classification algorithm does not require modification by the user; rather, the user has the opportunity to develop or obtain their own input layers by whatever means they consider best. The EODESM system is particularly attuned to ingest biophysical information obtained from remote sensing data (Task 4.2).

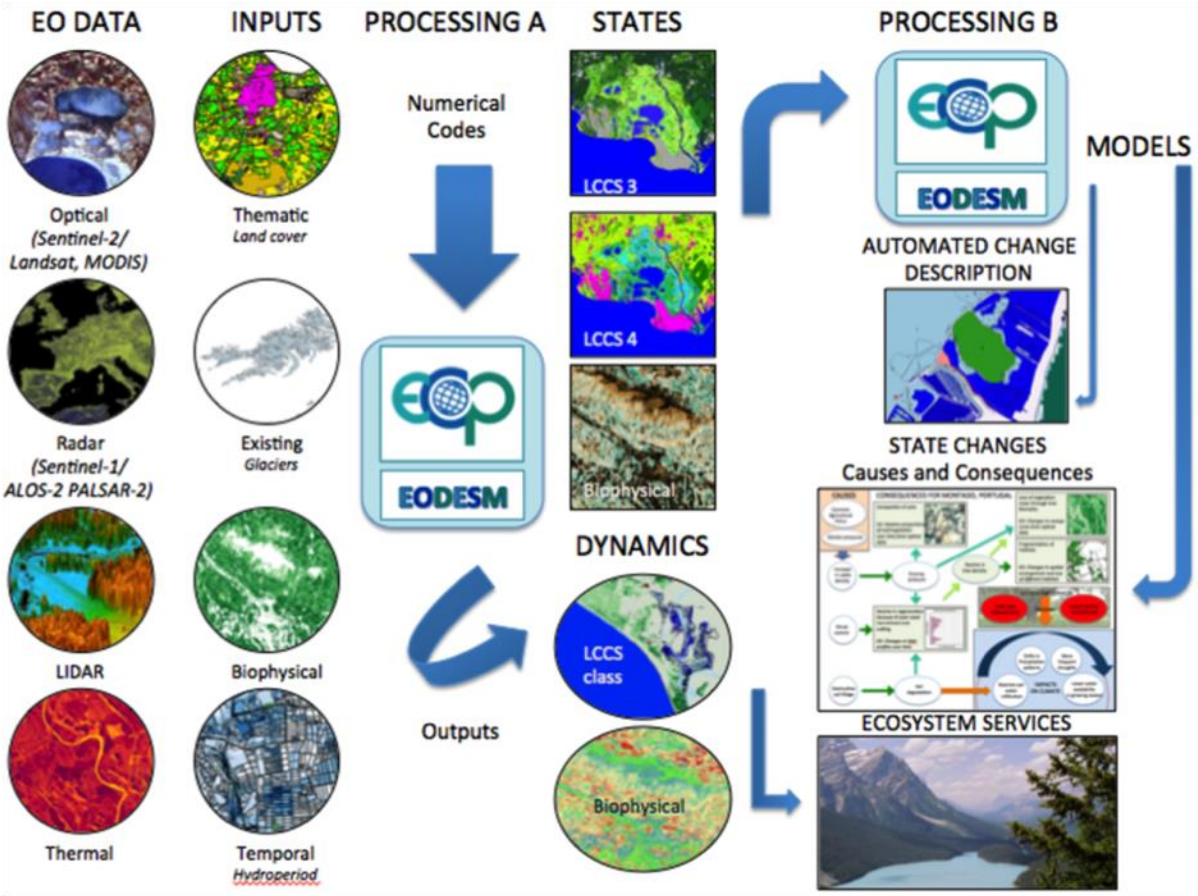

Figure 4.2. An overview of the EODESM system.

4.2 Environmental Variables (EVs)

The EODESM system has been designed such that it maximises uses and also sets out the requirements for EVs and other biophysical parameters. A summary of how variables are integrated within the EODESM system is provided in Figure 4.3.

In the first instance, EODESM uses some EVs as direct input to the classification, with these relating to agriculture (e.g., crop area and phenology, biodiversity (e.g., phenology, vegetation height), climate (e.g., glacial and lake extent and snow cover), renewable energy (e.g., tidal areas) and water (turbidity). In the second case, EVs and biophysical variables are not used in the classification but are nevertheless included as attributes to provide fuller descriptions of land covers and change. Examples are crop type, above ground biomass (AGB; Mg ha-1), Leaf Area Index (LAI, m2 m-2) and ocean colour. In the third case, the EODESM system actually generates the EVs, including disturbance regime, habitat structure, fire disturbance, land cover and water use.

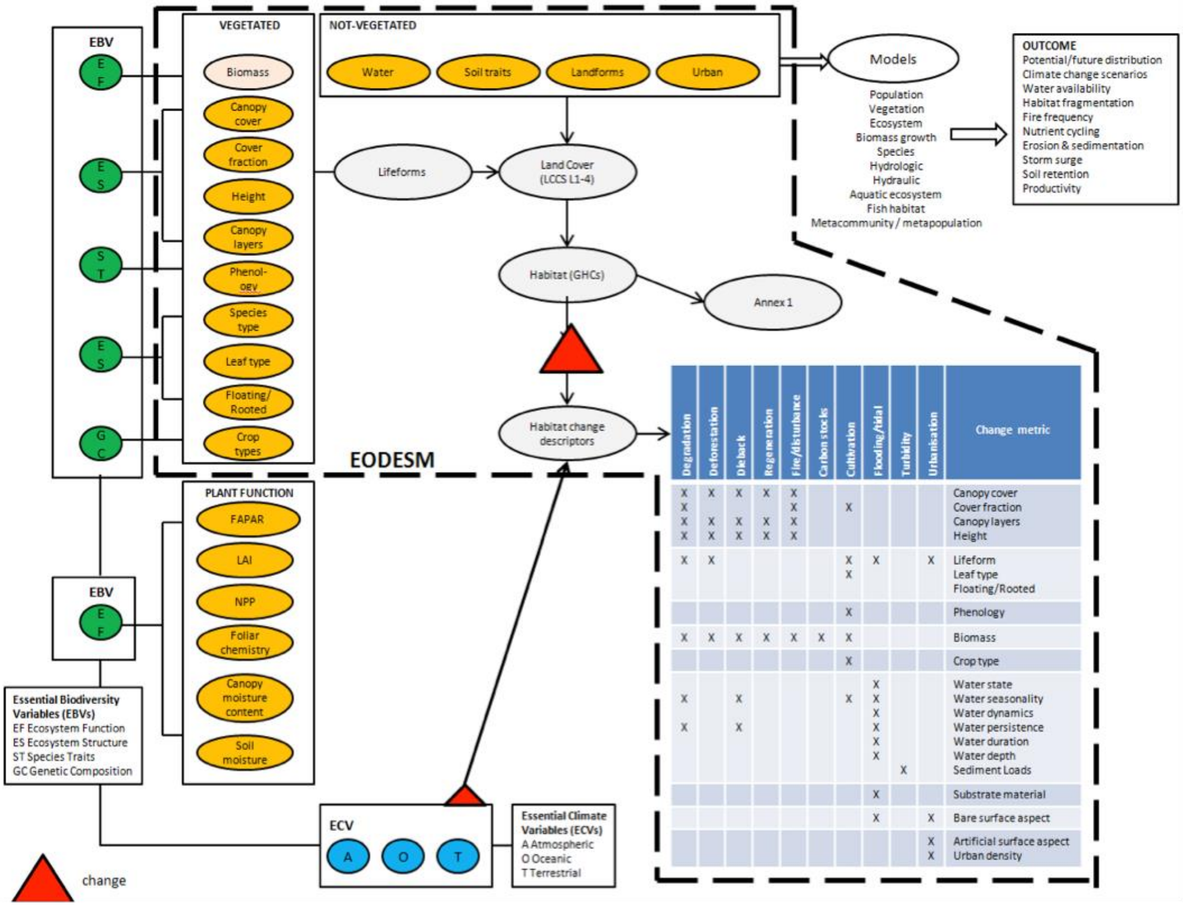

Figure 4.3. How EODESM fits in with EBVs and ECVs: the latter are used, in some cases, to drive the inputs for the LCCS classification; the results of which are used in modelling change scenarios.

4.2.1 Variables used directly in the EODESM classification

From the storylines and process described in Section 2.2, for each of the PAs a number of variables (including some EBVs) were identified as being important, with some able to be retrieved from EO data, including optical, radar and LiDAR imagery. The sources for each of the variables differed and was specified within EODESM as being derived at local (L), Regional (R; or European if applicable; E) and/or Global (G) scales and from data from satellite sensors (S; including Landsat (LS) and Sentinel (SN) optical (O) or radar (R)), airborne sensors(A; including LIDAR (LD)), existing thematic layer (including habitat and land cover maps; GI) or a combination (hybrid) of these (HY).

The EODESM system accepts up to 45 inputs (e.g., relating to hydroperiod, leaf type, cadastral information, if updated), with these provided as thematic and continuous (typically biophysical) layers. The EODESM system can ingest locally derived layers (e.g., by the user through supervised classifications or spectral unmixing) or those extracted from European or global datasets (e.g., the University of Maryland's tree cover density layer or the European Commissions (EC) Joint Research Centre (JRC) global hydroperiod; refer to Table 3.1). A time-series of vegetation indices may provide information on phenology and cropping combinations. Polygons representing cultivated lands can be attributed with geometric features (e.g., field dimensions and area) and thresholds applied to generate layers of field size and distribution. In some cases, user knowledge comes into play, for example, when defining cultural practices (e.g., water supply and time factor). Natural vegetation can be described on the basis of stratification (including height and cover of strata), however, these layers are subject to availability of, for example, LiDAR data. Existing layers representing artificial surfaces (e.g., roads, urban, non-built up) can be used, or alternatively generated through classification where spectrally distinct (e.g., white roofs of industrial buildings).

Proportions can be used to designate urban density classes. Both global and European data sources representing surface water, persistence and seasonality exist, and can complement local data sources (e.g., satellite derived hydroperiod and inundation maps). Turbidity can be retrieved using a combination of reflectance and spectral indices, and water dynamics (whether flowing or standing) can be identified by whether water bodies are entirely or partially enclosed by land.

Thematic layers are recoded to achieve appropriate input to the EODESM system, whilst continuous layers are summarised into different categories within the system (e.g., relating to canopy cover or hydroperiod). Once entered, the system automatically translates the inputs to individual LCCS2 codes (e.g., A4 for shrubs, A5 for forbs), combines these to form a string (e.g., A3.A10.B2.C1.D1.E1.F1.F9.G7) and then translates the string to a descriptive name (in this case, Trees closed canopy (>70-60 %) tall (14-30 m) continuous broadleaved evergreen with 2nd layer supporting open canopy 7-3 m in height). An example is given in Figure 4.4.

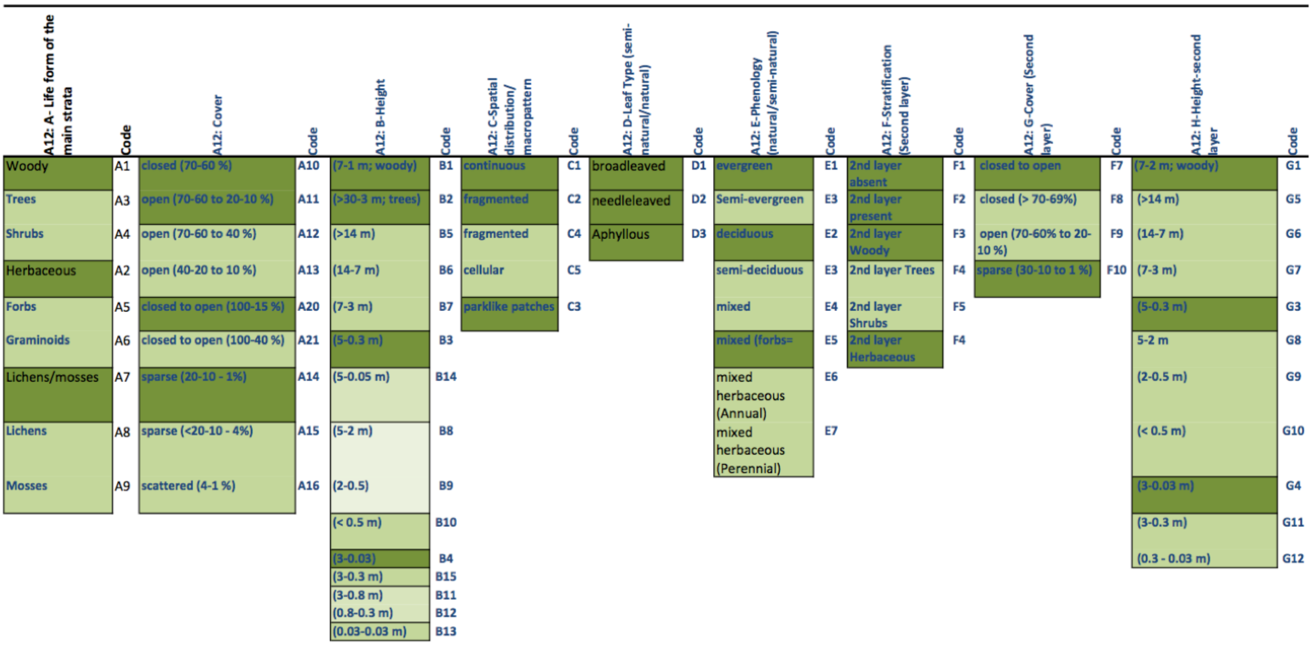

Figure 4.4. LCCS codes for natural terrestrial vegetation.

4.2.2 Variables as attributes to the classification

For many regions, a diverse range of other variables can be obtained from EO data but these cannot be used to establish the LCCS2 categories. Nevertheless, they can be included as attributes within the EODESM system and used to provide additional descriptors of land covers and also changes. Vegetation attributes may include, for example, Leaf Area Index (LAI), moisture content, species and Above Ground Biomass (AGB). Land descriptors may include topographic data (DEMs, slope and aspect), soil moisture, land surface temperature and albedo. Atmospheric attributes of cloudiness, wind speed and direction may be included. Marine attributes may include sea surface temperature, chlorophyll and coloured dissolved organic matter (CDOM). In some cases, these data have been requested by the PA to fulfil a particular mapping objective.

4.2.3 Variables resulting from the classification

A number of variables are generated from the change classification including deforested and disturbed areas and these will be discussed in Deliverable 4.3.

Layer Category	CROPS						VEGETATION										URBAN				BARE			WATER							
Layer Type*	T	T	T	T	T	T	T	M	D	D	T	T	T	T	D	D	T	M	M	M	T	M	M	D	T	T	T	T	T	T
	Combinati ons	Sequences	Irrigation	Cultural	Spatial	Spatial size	Lifeform	Lifeform	Canopy	Canopy	Leaf type	Phenology	Layers	Layers(lifef	Layers	Layers	Artificial	Linear	Non-built	Density	Bare	Macropatt	Bare	Hydroperio	Diurnal	Annual	Water	Water	Water	Water
Mountain																														
Austrian Alps			E L	L		L	L		E		E						E L	L		E	E L			G			GL		GL	
Bavarian Forest							L		E		E									E				G						
Gran Paradiso							L		E		E									E				G						
Hardangervidda			E	L		L	L		E		E						GL			E	L			G			GL		L	
High Tatra Mountains							L		E		E						EL			E				G						
La Palma	L		L	L		L	L		E		E	L					EL	L		E	L			G			GL		GL	
Ohrid and Prespa							L		E		E									E				G						
Peneda-Gerês	L				L		L		E		E						L			E	L			G					LG	
Samaria							L		E		E									E				G						
Sierra Nevada							L		E		E									E				G						
Swiss National Park			E	L		E L	L		E	L	E						E L	L		E	L		L	G			GL		GL	

ocal.

Layer Category	CROPS						VEGETATION										URBAN				BARE			WATER						
Layer Type	T	T	T	T	T	T	T	M	D	D	T	T	T	T	D	D	T	M	M	M	T	M	M	D	T	T	T	T	T	T
	Combinations	Sequences	Irrigation	Cultural practice	Spatial distribution	Spatial size	Lifeform	Lifeform (aquatic)	Canopy cover	Canopy height	Leaf type	Phenology	Layers (number)	Layers (life form)	Layers (cover)	Layers (height)	Artificial surface	Linear	Non-built up	Density	Bare surface	Macropattern	Bare materials	Hydroperiod	Diurnal variations	Annual variations	Water state	Water depth	Water movement	Water sediments
Arid/semi-arid																														
Har HaNegev						L	L																							
Kruger NP						L	L																							
Montado							L		E		E									E				G						
Murgia Alta							L		E		E						EL			E	L			G			GL			

*Layer Type: 'T' Thematic, 'M' Modifier, 'D' Derivative

Table 4.2. Summary of variables used in the classification (for arid/semi-arid PAs). Notation indices for the scale of the input data source: 'G' Global, 'E' European, 'L' Local.

Layer Category	CROPS						VEGETATION										URBAN				BARE			WATER						
Layer Type	T	T	T	T	T	T	T	M	D	D	T	T	T	T	D	D	T	M	M	M	T	M	M	D	T	T	T	T	T	T
	Combinations	Sequences	Irrigation	Cultural practice	Spatial distribution	Spatial size	Lifeform	Lifeform (aquatic)	Canopy cover	Canopy height	Leaf type	Phenology	Layers (number)	Layers (life form)	Layers (cover)	Layers (height)	Artificial surface	Linear	Non-built up	Density	Bare surface	Macropattern	Bare materials	Hydroperiod	Diurnal variations	Annual variations	Water state	Water depth	Water movement	Water sediments
Wetland/marine																														
Camargue						L	L		E		E									E				G						
Curonian Lagoon						L	L		E		E									E				G						
Danube Delta	L		E L	L		E L	L		E		E	L					G E L	L		E	L	L		G	L		G		G	L
Doñana			L	L		L	L		E		E	L					G L	L	L		L			G L	L	G L	L	L	G L	

*Layer Type: 'T' Thematic, 'M' Modifier, 'D' Derivative

Table 4.3. Summary of variables used in the classification (for wetland/marine PAs). Notation indices for the scale of the input data source: 'G' Global, 'E' European, 'L' Local.

Caribbean LME																														
Mediterranean LME																														

*Layer Type: 'T' Thematic, 'M' Modifier, 'D' Derivative

Layer Category	VEGETATION				LAND				ATMOS.			MARINE		
Layer Type	Leaf Area Index	Moisture content	Species	Biomass	DEMs	Soil Moisture	Land surface temp.	Albedo	Cloudiness	Wind speed	Wind direction	Sea surface temp.	Chlorophyll	CDOM
Mountain														
Austrian Alps					•		•							
Barvarian Forest	•	•	NR		•	•	•	NR	NR					
Gran Paradiso	•	•	NR	NR	•	•	•	•	NR					
Hardangervidda	NR	NR	NR		•	NR	•	NR	NR					
High Tatra Mountains	•	•	NR		•	•	•	NR	NR					
La Palma	•	•	NR	•	•	•	•	NR	•					
Northern Limestone	NI	NR	NR	•	•	•	•	NR	NR					
Ohrid and Prespa	NR	•	NR		•	•	•	NR	NR					
Peneda-Gerês	NR	•	NR		•	•	•	NR	NR					
Samaria	•	•	NR	NR	•	•	•	•	NR					
Sierra Nevada	•	•	NR	NR	•	•	•	•	NR					
Swiss National Park	•	NR	NR	•	•	NR	•	NR	NR					

Table 4.4. Summary of attributes not used for the LCCS classification (for mountain PA). (NR= not requested)

Co-funded by the European Union

Layer Category	VEGETATION				LAND				ATMOS.			MARINE		
Layer Type	Leaf Area Index	Moisture content	Species	Biomass	DEMs	Soil Moisture	Land surface	Albedo	Cloudiness	Wind speed	Wind direction	Sea surface temp.	Chlorophyll	CDOM
Arid/semi-arid														
Har HaNegev	NR	NR	NR		•	•	•	NR	NR					
Kruger NP	•	NR	NR	•	•	NR	•	NR	NR					
Montado	•	•	NR	•	•	•	•	NR	NR					
Murgia Alta			•		•	•	•							
Wetland/marine														
Camargue					•		•	NR	NR	•	•	•	•	•
Curonian Lagoon					•			NR	NR	•	•	•	NI	•
Danube Delta		•		•	•		•	NR	NR	NR	NR	NR	NR	NR
Doñana					•			NR	NR	NR	NR	NR	NR	NR
Wadden Sea					•			NR	NR	•	•	•	•	•
Oceanic														
Caribbean LME												•		
Mediterranean LME								NR	NR	•	•	•	•	NR

Table 4.5. Summary of attributes not used for the LCCS classification (for arid/semi-arid, wetland and oceanic PA). (NR= not requested)

4.3 Implementation of Land Cover Classifications and output maps

The knowledge driven classification is implemented in a three-step process, comprising segmentation, calculation of object statistics and translation to LCCS2 classes. The algorithm of Shepherd et al. (2015) is applied to divide the landscape into units that are spectrally homogeneous. The segmentation procedure uses just the Sentinel-2 reflectance data (e.g., two images representing the pre- and peak-vegetation flush periods), although it can integrate ancillary data layers such as those representing field (cadastral) boundaries and urban areas, if frequently updated, as in UK or the NL. Following segmentation, statistics are calculated for objects based on available data layers and used as input to the classification. The majority class and proportion are calculated for every object and using available thematic layers. The mean value of objects is calculated from continuous layers such as canopy cover, urban density and bare ground. Object statistics are stored in a raster attribute table (RAT), with one row per object and one column for each class.

The classification of LCCS2 categories comprises three main stages according to the LCCS2 hierarchy. The classification can be based either on spectral reflectance values and context-related features or the integration of available updated layers (e.g., from Task 4.2, Copernicus layers, updated ancillary layers). In the first step, the classification of Level 1 categories is performed, with the main focus being the separation of vegetated and non-vegetated areas. This is achieved using either image spectral values or vegetated areas derived from an existing data layer generated in an external classification process (e.g., data driven random forests, SVM). Non-vegetated areas are assigned by way of an exclusion rule, so if they are not classified as vegetated, then they are considered non-vegetated. Similarly in the second step, aquatic and terrestrial environments are separated using a defined mask for aquatic areas. Level 3 classes are assigned on the basis of whether they are cultivated/managed or natural, artificial or natural/semi-natural. Beyond Level 3, the Level 4 classes are classified using any number of separate layers relating to key descriptors within the LCCS2 classification. Rules are applied to generate the codes representing the LCCS2 categories. For example, woody shrubs are assigned a code of 'A4' if the supercategory (from the Level 3 classification) is 'A12' and the integer value in the lifeforms layer corresponds to woody shrubs.

```
lifeForm = numpy.where(((supercategory == "A12") | (supercategory == "A24")) & (LLifeform == 4), "A4",lifeForm)
```

Canopy cover is classified into categories such as 'closed to open (40-100%), 'open (70-60 - 40%)', 'open (40-20 - 10%)' and so on, and assigned the appropriate LCCS2 code. An existing layer, e.g., UMD global tree canopy cover, can be used for this purpose. Similarly, canopy height is categorised if the data layer (e.g., a LiDAR derived canopy height model, CHM) exists. Individual LCCS2 codes are applied to each layer and combined to form a summary class code (e.g., A11.A1.B4.C1.D9.D1) and an associated descriptor (e.g., Single crop Permanently cropped area with Rainfed Tree crops). A pre-defined colour scheme is applied to the result. The LCCS2 classification has the capacity to significantly increase the information content by describing each habitat with species, biophysical and environment information as available. It allows for direct comparison between sites and regions by applying a standardised and consistent classification scheme. LCCS2 codes are described in Appendix 2, Section 9. The translation from to LCCS2 categories and habitats defined by one-to-one LC to habitat relation (Tomaselli et al., 2013) are reported in Appendix 3, Section 10.

The following sections present examples of the LCCS2 output maps. The legend is detailed and comprehensive and will be available with each of the data products (on the ftp site). However, the maps can be broadly interpreted as water (blue), snow and ice (white), cultivation (yellow), herbaceous vegetation (including in cultivated areas; light green), woody vegetation (darker greens), urban (grey), bare ground (browns to orange).

Figure 4.5 shows the colour legend for the LCCS2 categories used for all the LC maps presented in the following subsections.

Figure 4.5. An example of the LCCS2 categories generated by the EODESM system. Each classification is associated with between 50 and 200 classes depending on the complexity of the land covers occurring.

4.3.1 Curonian Lagoon, Lithuania

Coastal lagoons are important contributors to core ecosystem functions (e.g., habitat, biodiversity, productivity) and services (e.g., provisioning, regulating and maintenance and cultural). Anthropogenic activities that interfere with the natural state are leading to a loss of intertidal wetlands and altered tidal regime. LCCS2 classifications for Curonian lagoon subject can be used to study habitat availability following disturbance. Hydro-period information and the distribution of aquatic vegetation biophysical characteristics are required to understand and quantify such changes.

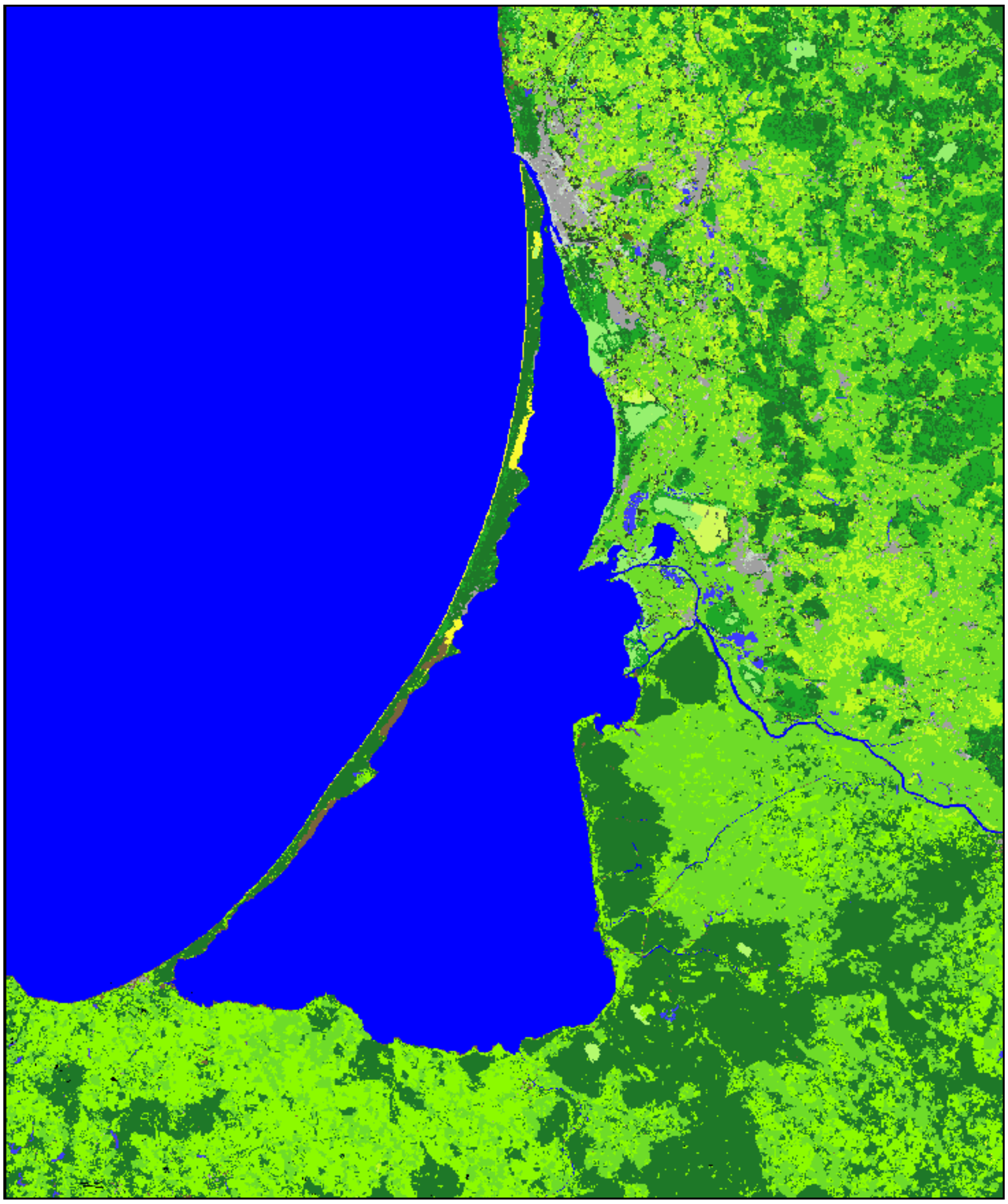

Figure 4.6. LCCS Level 4 classification of the Curonian Lagoon, Lithuania (for the nominal year of 2016).

4.3.2 Camargue, France

The Camargue Biosphere Reserve in the Rhone delta covers an area of 193,000 ha, largely dominated by lagoons, brackish/freshwater marshes with emergent or aquatic vegetation, as well as halophilous scrubs and steppes. These systems are intermingled with agro-systems dominated by irrigated rice crops. Wetlands of the Camargue are important for a range of regulating ecosystem services, provisioning and cultural services, but are under threat from agricultural land use and changes in hydrological conditions. LCCS2 Level 3 and 4 classifications have been produced using a time-series of Sentinel-2 images (5 February and 7 July 2016; Figure 4.7) and external data layers and provide useful information for studies exploring the evolution in the state of wetlands and services.

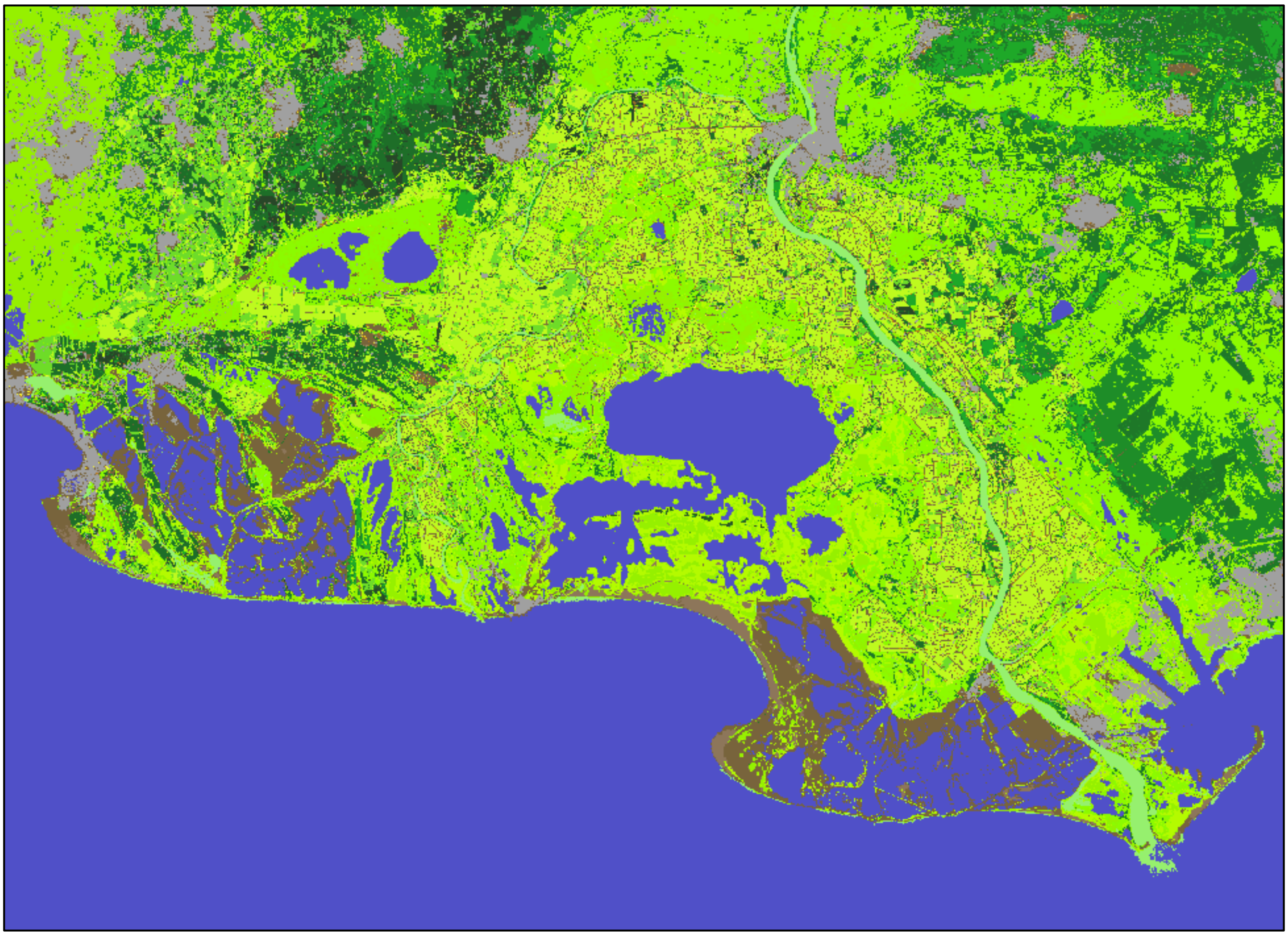

Figure 4.7. LCCS Level 4 classification of the Camargue National Park (for the nominal year of 2016).

4.3.3 Danube Delta

The Danube River delta is an area of approximately 5,100 km^2 that consists of complex alluvial systems, dominated by wetland ecosystems of great socio-ecological and economic importance. The area is under threat from human activity, including, for example, drainage for agricultural and urban development, hydrological alteration (channelization, embankments, dikes etc.), habitat fragmentation, climate change, nutrient and sediment inputs, and invasive species. A time-series of Sentinel-2 imagery (28 April and 16 August 2016) and various data layers including global (e.g., surface water, hydroperiod), European (e.g., forest type, canopy cover, settlements) and derived (e.g., lifeforms, water dynamics, bare materials) layers were combined to produce the LCCS2 Level 3 and 4 classifications (Figure 4.8). The LCCS2 provides a baseline for tracking and understanding the processes and impacts of change on intertidal wetland ecosystems.

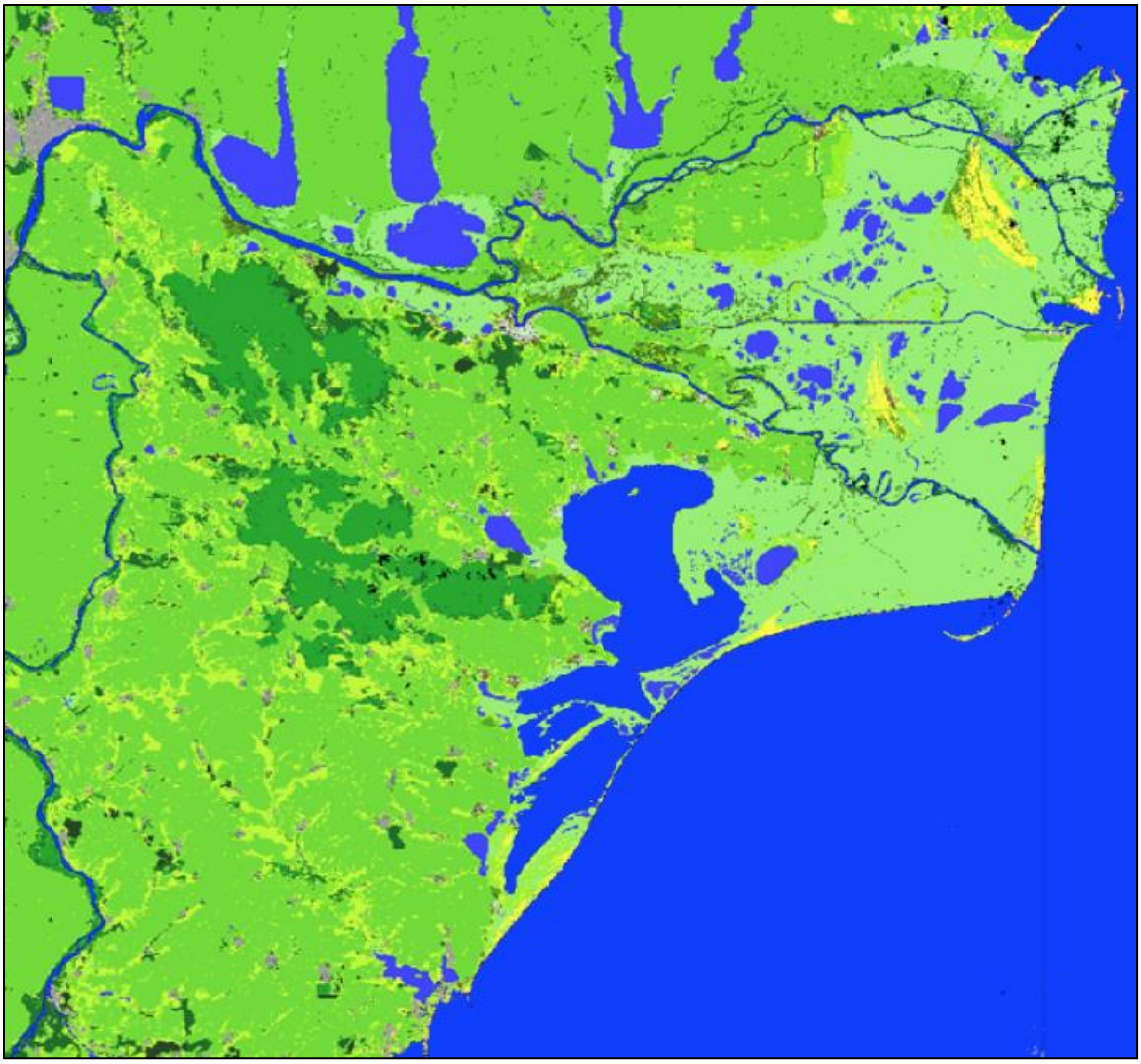

Figure 4.8. LCCS Level 4 classification of the Danube Delta Biosphere (for the nominal year of 2016).

Co-funded by the European Union

4.3.4 Doñana National Park, Spain.

Doñana is dominated by a diverse array of wetland ecosystems. The area was declared a national park in the 1960s to assist the protection of waterbirds after two-thirds of the original area was drained for agriculture. Multiple stressors are affecting the vitality of the wetlands, including, for example, water diversion and extraction, pollution, overgrazing, introduction of exotic species and climate change. A time-series of Sentinel-2 imagery (8 March and 5 August 2016) and various external data layers, including an existing habitat map (Organismo Autónomo de Parques Nacionales, 2013) were available, from which LCCS2 Level 3 and 4 classifications were generated (Figure 4.9). The LCCS2 maps provide baseline information on habitat and landscape diversity and agricultural use.

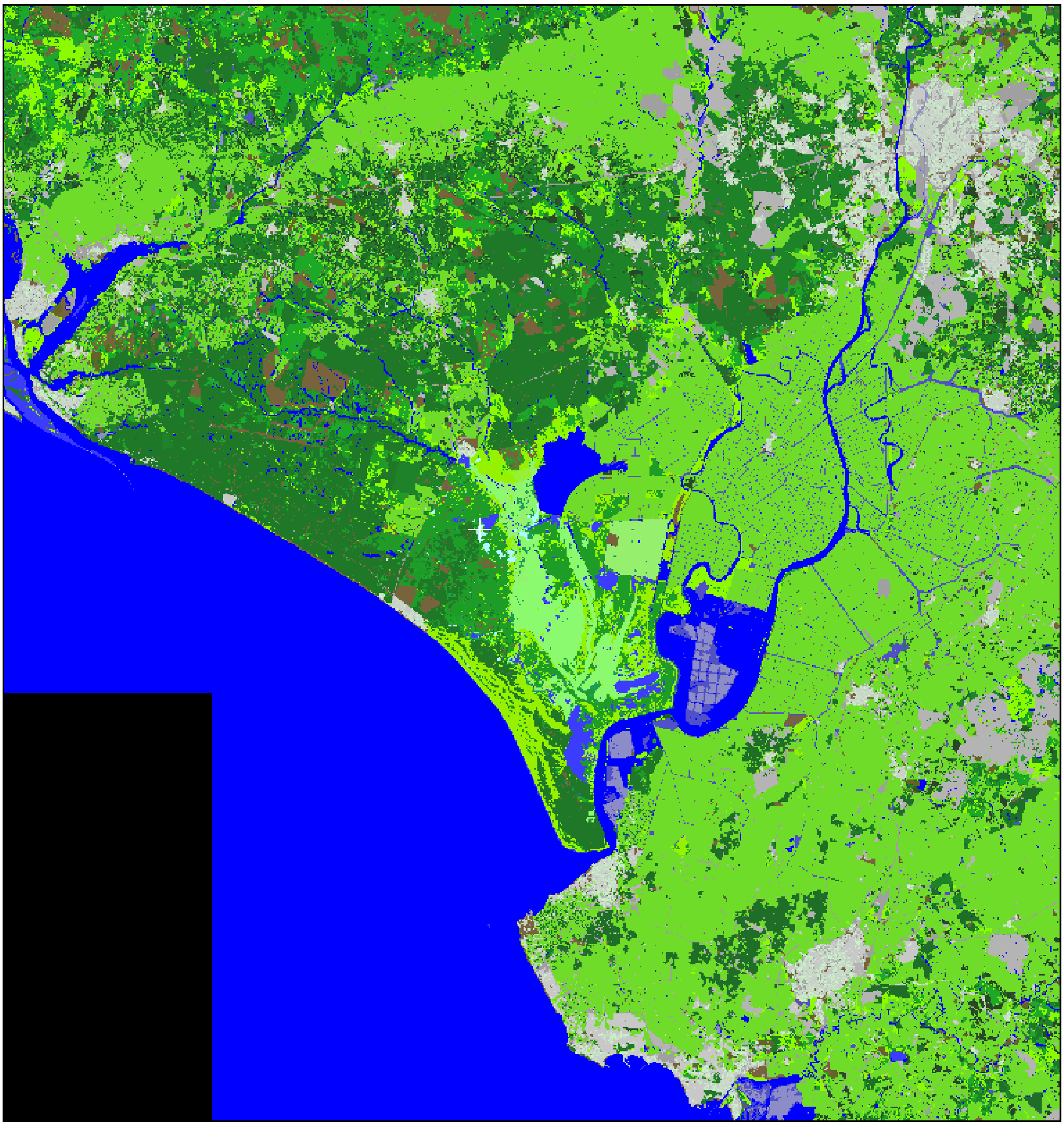

Figure 4.9. LCCS Level 4 classification of the Doñana National Park (for the nominal year of 2016).

4.3.5 Gran Paradiso National Park, Italy.

The progressive abandonment of certain management practices has resulted in modifications to grassland that affect its forage value for wild herbivores such as alpine ibex and chamois in high altitude mountainous areas such as Gran Paradiso National Park. Changes in plant species and richness and fragmentation of semi-natural grasslands are also observed. Climate change is another risk factor in these environments, with changes in community composition, soil moisture, vegetation structure and productivity anticipated. The LCCS2 classification for Gran Paradiso (Figure 4.10) was generated using Sentinel-2 data and external data layers and attributed with information on, for example, blue sky albedo and snow cover period. Such maps provide a baseline against which to quantify the diversity of changes occurring in the PA and surrounds.

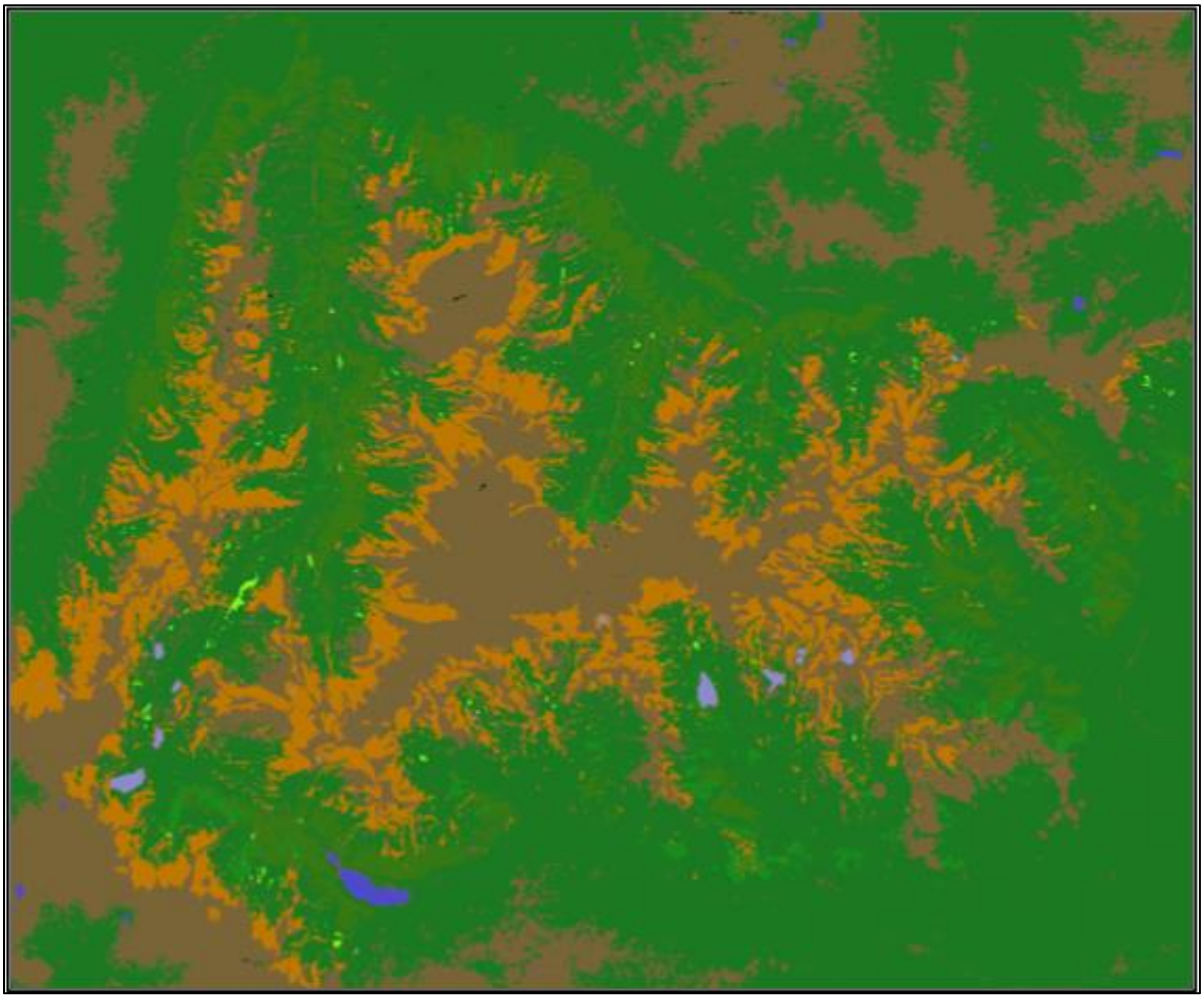

Figure 4.10. LCCS Level 4 classification of Gran Paradiso National Park (for the nominal year of 2016).

4.3.6 The Har HaNegev Reserve, Israel.

Located in the central Negev Highlands of Israel, the Har HaNegev Reserve is threated by human settlement and infrastructure development, mining, hunting and agriculture. The area also contains many natural springs and water holes, which are vital to the flora and fauna but also are used for human recreation. Grazing is also undertaken by the Bedouins that are living in small settlements close to the reserve, which places pressure on the natural vegetation. The LCCS2 classification of the Har HaNegev Reserve was undertaken using a single RapidEye scene (approximately 6 m spatial resolution).

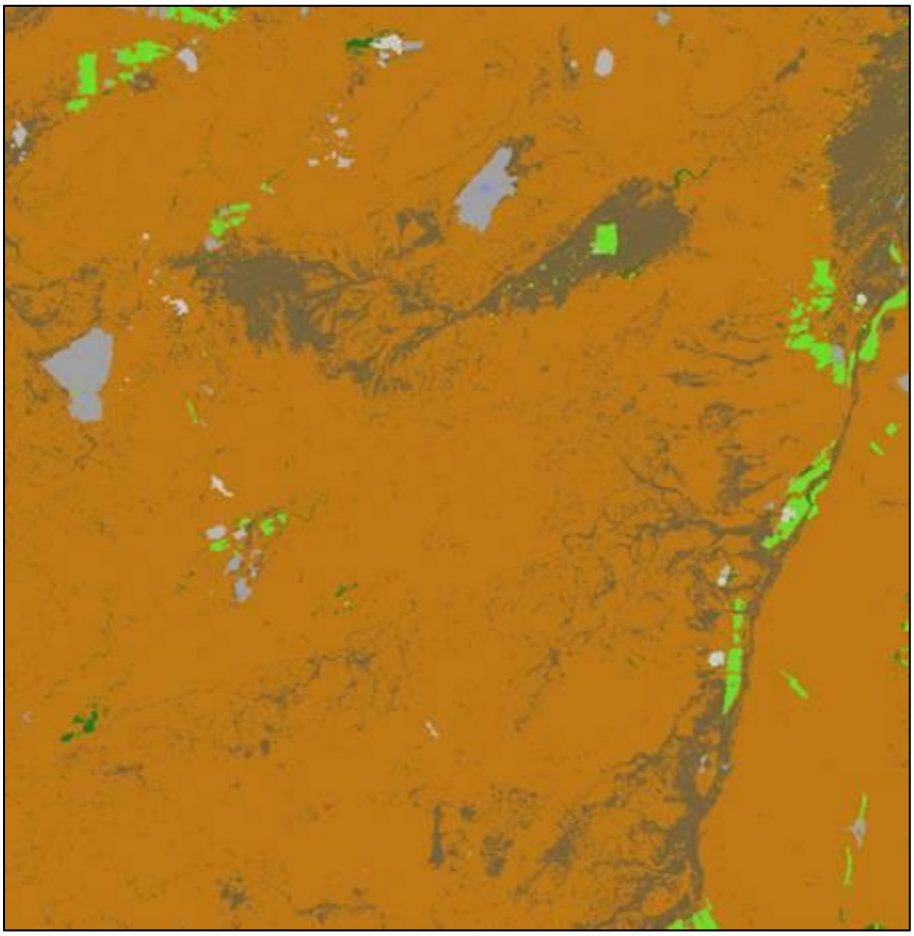

Figure 4.11. LCCS2 Level 4 classification of a subset of the Har Negev Reserve, Israel, generated from RapidEye

4.3.7 Hardangervidda National Park, Norway

Hardangervidda National Park is Norway's largest national park and is an important area for conservation and human use. Wild reindeer, a keystone species in the Park, are sensitive to human disturbance and modification, climatic variation and suitability of winter pastures. Black grouse in the area are also under threat for similar reasons. Monitoring of factors relating to pasture quality, lichen biomass and health and habitat heterogeneity are key to conservation of these species. LCCS2 Level 3 and 4 classifications (Figure 4.12) have been produced using available Sentinel-2 imagery (18 September 2016) and other environmental variables (e.g., lichen index and snow cover maps). The LCCS2 outputs provide a baseline map for 2016 against which to quantify past and future changes in ecosystem state and dynamics and faunal (e.g., reindeer movements).

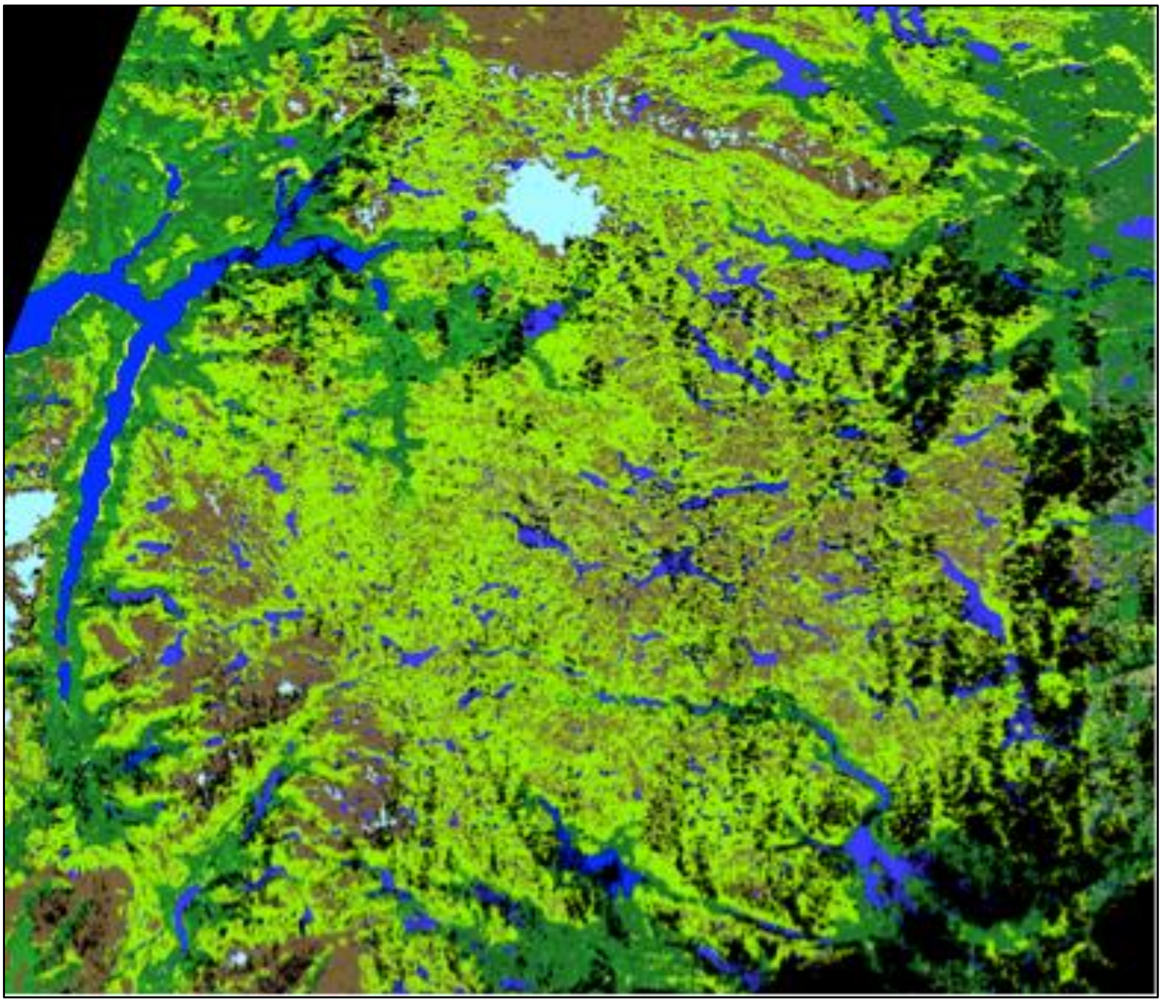

Figure 4.12. LCCS2 Level 4 classification of Hardangervidda National Park (nominal year of 2016).

4.3.8 High Tatra Mountains, Poland, Slovakia

The High Tatra Mountains National Park has protected many of the regions natural habitats, with a clear demarcation between areas influenced by human activities (e.g., agricultural expansion and urban development). A windstorm in November 2004 led to substantial damage to the forests on the Slovak side, resulting in a large-scale forests loss across a large area. In the years following, the frequency of landslides and flooding increased, which were exacerbated during periods of snowmelt, and massive bark beetle infestations occurred within the area of dieback. Whilst considered initially to be a major setback, the storm has provided an opportunity to re-establish forests of more mixed species composition. The LCCS2 maps provide a baseline against which the past impacts on and recovery of the forests in the years following can be quantified.

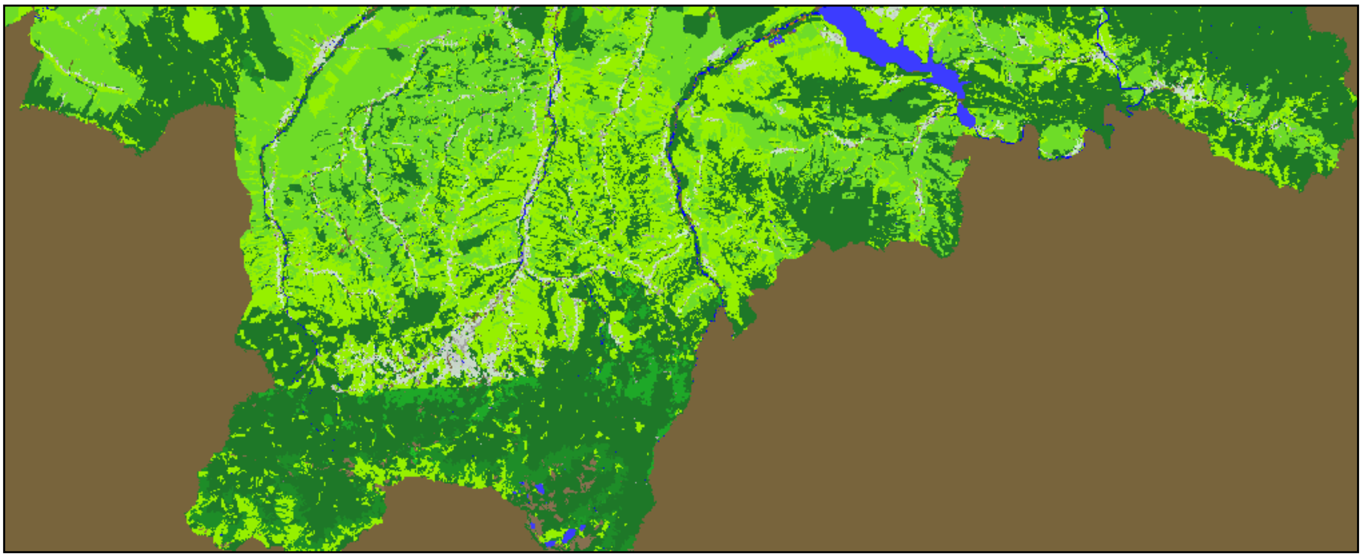

Figure 4.13. LCCS2 Level 4 classification, High Tatra Mountains NP, Poland/Slovakia (nominal year of 2016).

4.3.9 Lake Orhid and Prespa National Park, Balkans region

Despite Lake Ohrid being the most diverse lake in the world, with 212 known endemic species, it is facing a biodiversity crisis. The increasing pressure on the lake ecosystem from competing uses (tourist/recreation, water supply, rapid urbanization) is rendering the biodiversity particularly sensitive to environmental and climate changes. Catchment scale information on, for example, land cover, land use, water quality and vegetation status, is needed to better understand the links between current and future state and adoption of appropriate management strategies. The LCCS2 classifications being produced through a combination of Sentinel-2 time-series and external data layers allow issues relevant to land use change and loss of habitat and habitat diversity in the National Park and surrounds to addressed.

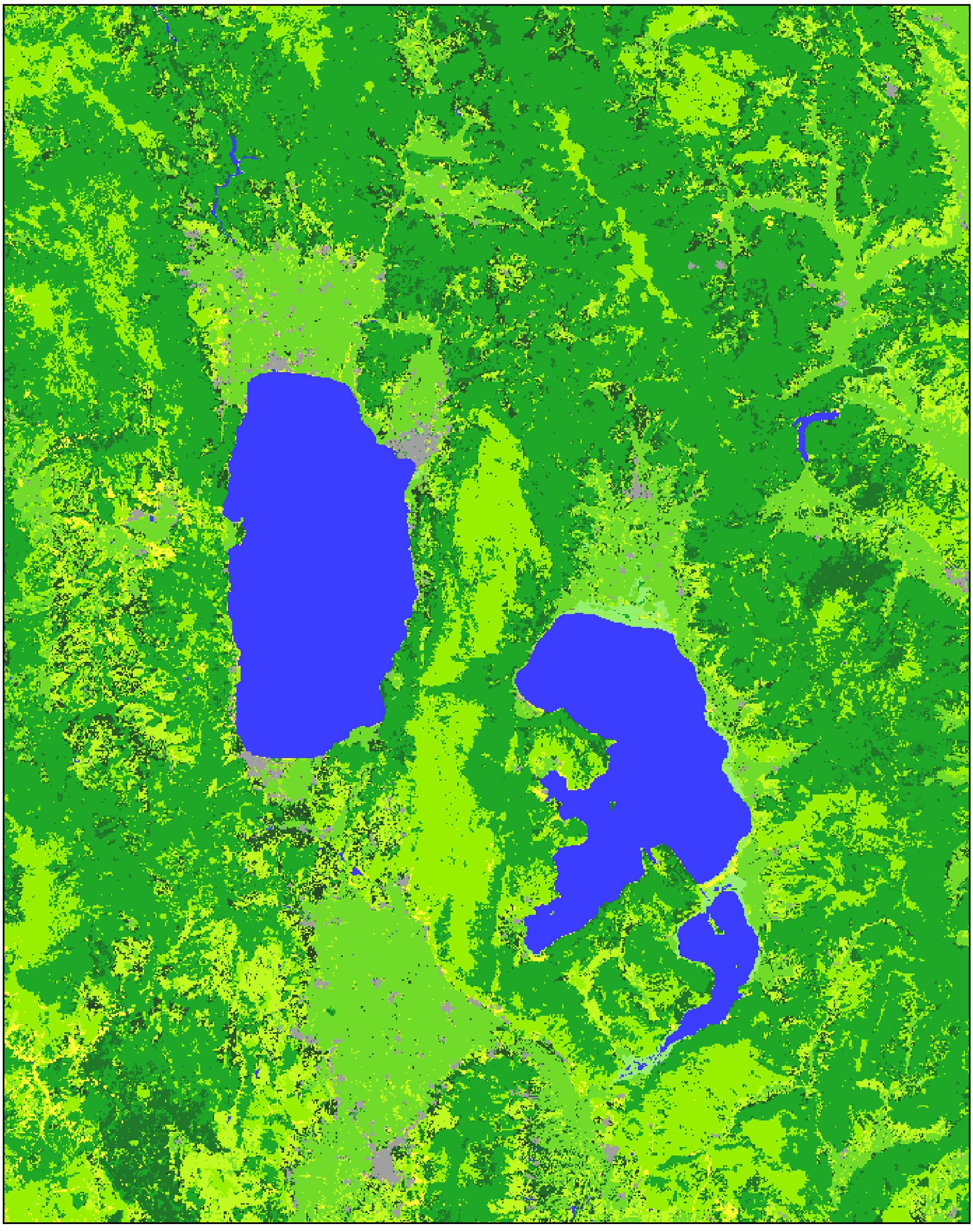

Figure 4.14. LCCS2 Level 4 classification of Lake Orhid and Prespa National Park, Balkans region (nominal year of 2016).

4.3.10 La Palma, Canary Islands, Spain

La Palma, as one of the Canary Islands, hosts a high diversity of taxa of aesthetic and commercial importance. Non-native herbivory and invasive species are having an adverse impact on vegetation richness, with losses of biodiversity, ecosystem functioning and services observed. LCCS2 Level 3 and 4 classifications have been produced using available Sentinel-2 imagery and existing data layers (see Figure 4.15) and can be used to better understand the spatial-temporal distribution in natural and semi-natural ecosystems in response to change.

Figure 4.15. LCCS2 Level 4 classification of La Palma, Canary Island (nominal year of 2016).

4.3.11 Montado National Park, Portugal

Montados (or dehesas in Spanish) are traditional wood-pasture systems with a savanna type structure that are characteristic of the Mediterranean Basin The main threats are the higher frequency and duration of water stress periods, soil degradation caused by overgrazing and tillage (for purposes of crop seeding and shrub control), increased tree vulnerability to pests and diseases, low tree recruitment for stand regeneration, and increased fire risk due to warmer summer temperatures. More specifically, declining trends in stand density, caused by adult tree mortality and the lack of recruitment, are alarming and may lead to an eventual loss of Montado and their replacement by shrublands. The LCCS2 classes of most important for Montado are canopy cover and lifeform and information on the structural composition of the understorey (where present).

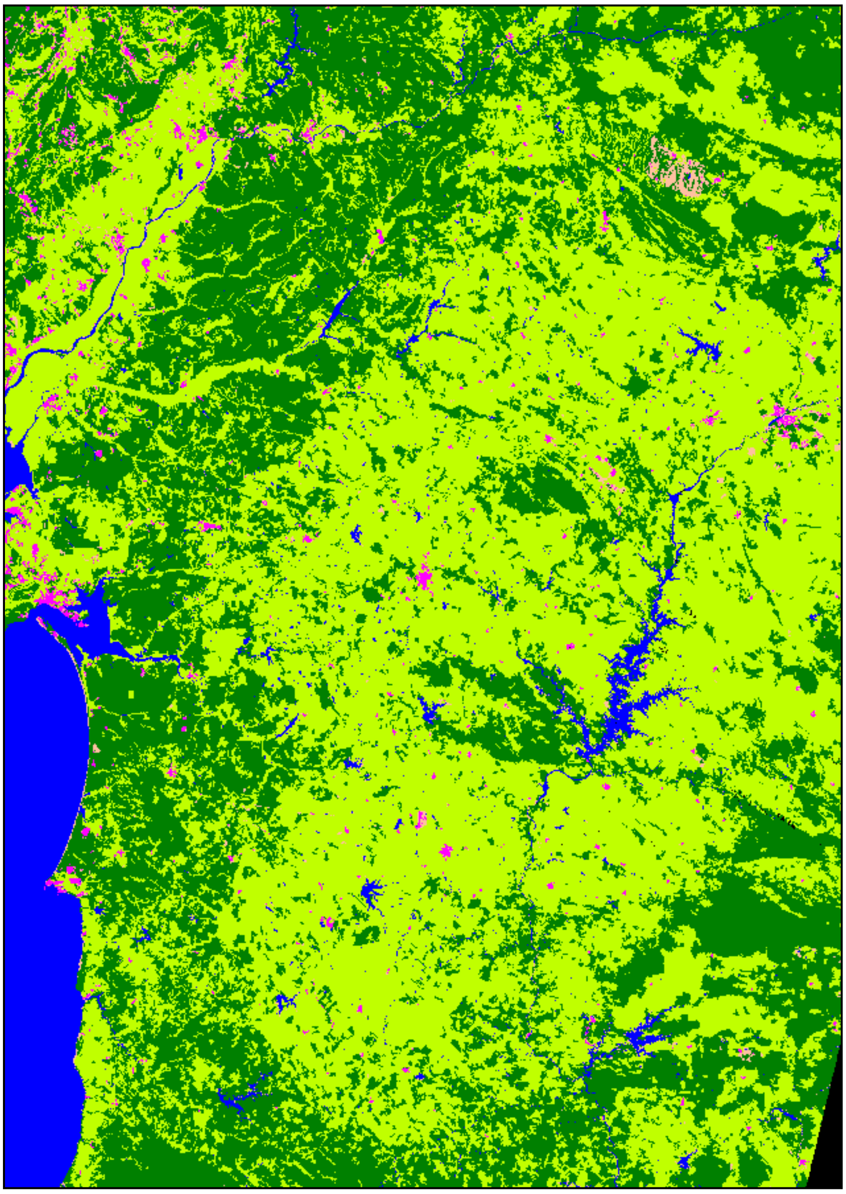

Figure 4.16. LCCS2 Level 3 classification of Montado, Portugal (nominal year of 2016).

4.3.12 Murgia Alta Natura 2000 site, Italy

The Site of Community Importance Murgia Alta IT9120007 is located in Puglia, Italy, and it has an area of 1258,89 km2. The most important habitat types in this site, according to 42/93/EEC directive are 6210(*) Semi-natural dry grasslands and scrubland facies on calcareous substrates (Festuco-Brometalia) (*important orchid sites) and 6220* Pseudo-steppe with grasses and annuals of the Thero-Brachypodietea. The main impacts associated with human activity have been habitat fragmentation and contamination both within what is now the Natura 2000 site and at its borders by a number of combined pressures including transformation of grassland pastures into agricultural (cereal) crops with this involving graining (clearance) of rock and lead to soil erosion and sediment deposition in the aquifers. Illegal waste and toxic mud dumping caused heavy contamination of the soils and aquifers and legal and illegal mining activities also contributed to pollution. Wind farms have also increased the precipitation has been below average for many years. The LCCS2 map for 2016 provides considerably more detail on the distribution of land covers compared to previous studies and provide an up-to-date baseline against which to quantify change.

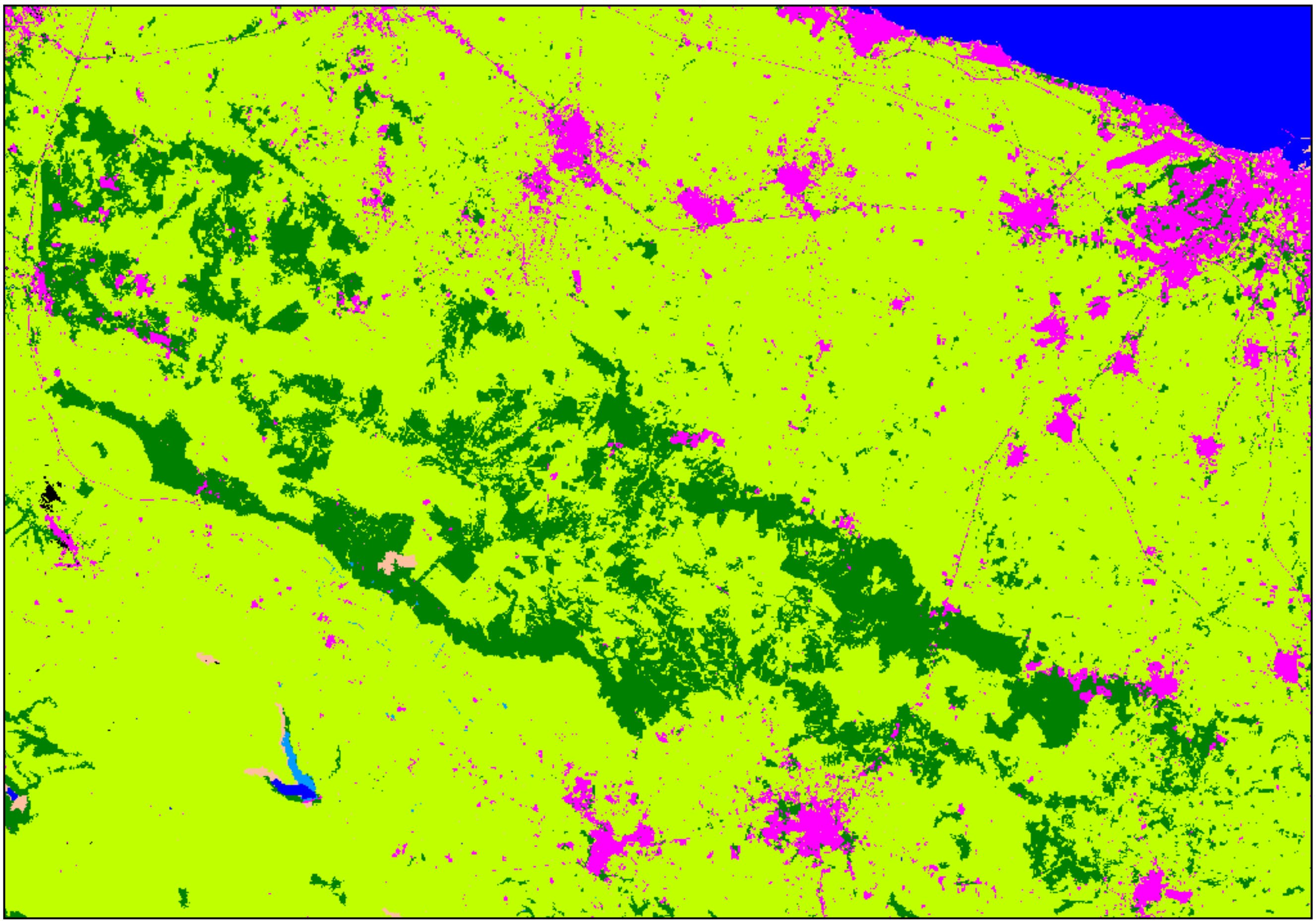

Figure 4.17. LCCS2 Level 3 classification of Murgia Alta, Italy (nominal year of 2016).

4.3.13 Northern Limestone National Park, Austria

Alpine forests provide a wealth of ecosystem services, including carbon storage and sequestration, biodiversity hotspots and landscape stability. The integrity of these services is continually compromised however by human exploitation, with large-scale clear cutting and planting of monoculture conifer forests, and natural disturbances such as drought, storms and insect infestations. LCCS2 Level 3 and 4 classifications have been produced for Northern Limestone using a combination of satellite imagery and available data layers (Figure 4.18). The LCCS2 maps provide useful information on habitat suitability and biodiversity and can contribute to understanding the impacts of disturbance and links with forest management.

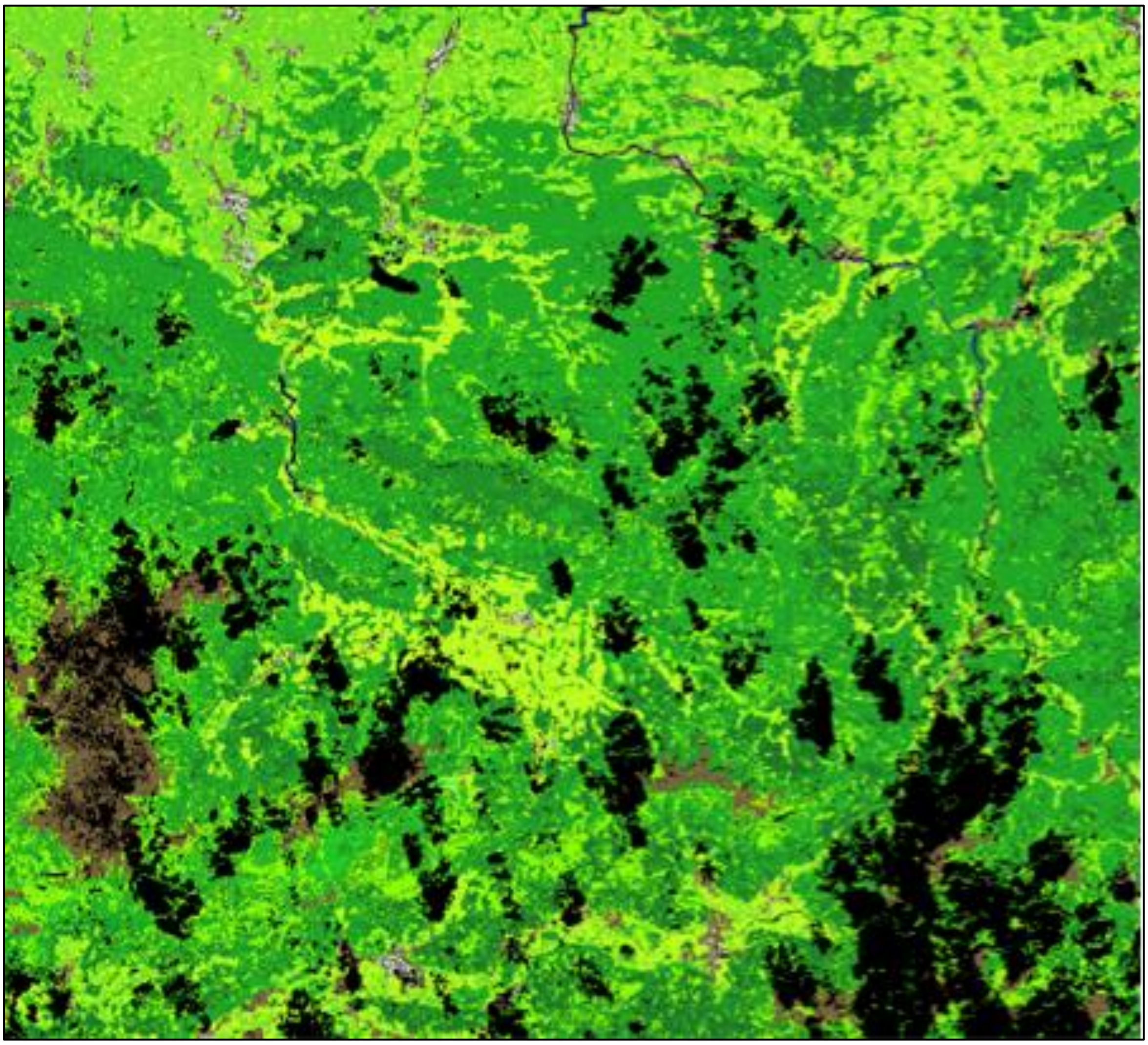

Figure 4.18. LCCS2 Level 4 classification of Northern Limestone Alps National Park (nominal year of 2016).

4.3.14 Peneda Gerês National Park, Portugal

The decline of traditional agro-pastoral systems changed vegetation characteristics and dynamics as well as social expectations to Portuguese mountains. The introduction of new dimensions (ecosystem services), concepts (rewilding of mountain areas) and societal expectations (nature conservation) to mountain protected areas makes the comparison of multiple management scenarios an essential task to the future of mountain areas. At Peneda-Gerês, main societal expectations rely on two groups of benefits: conservation of natural heritage, and supply of regulating and cultural ecosystem services. The multi-temporal (1987, 2002 and 2016) classification of LCCS2 Level 3 and 4 performed using available Landsat, Sentinel-2 and external data layers provide a baseline for land cover and grassland habitat, their change in time and for the development of future land cover scenarios under different management options to be used in the modelling stage.

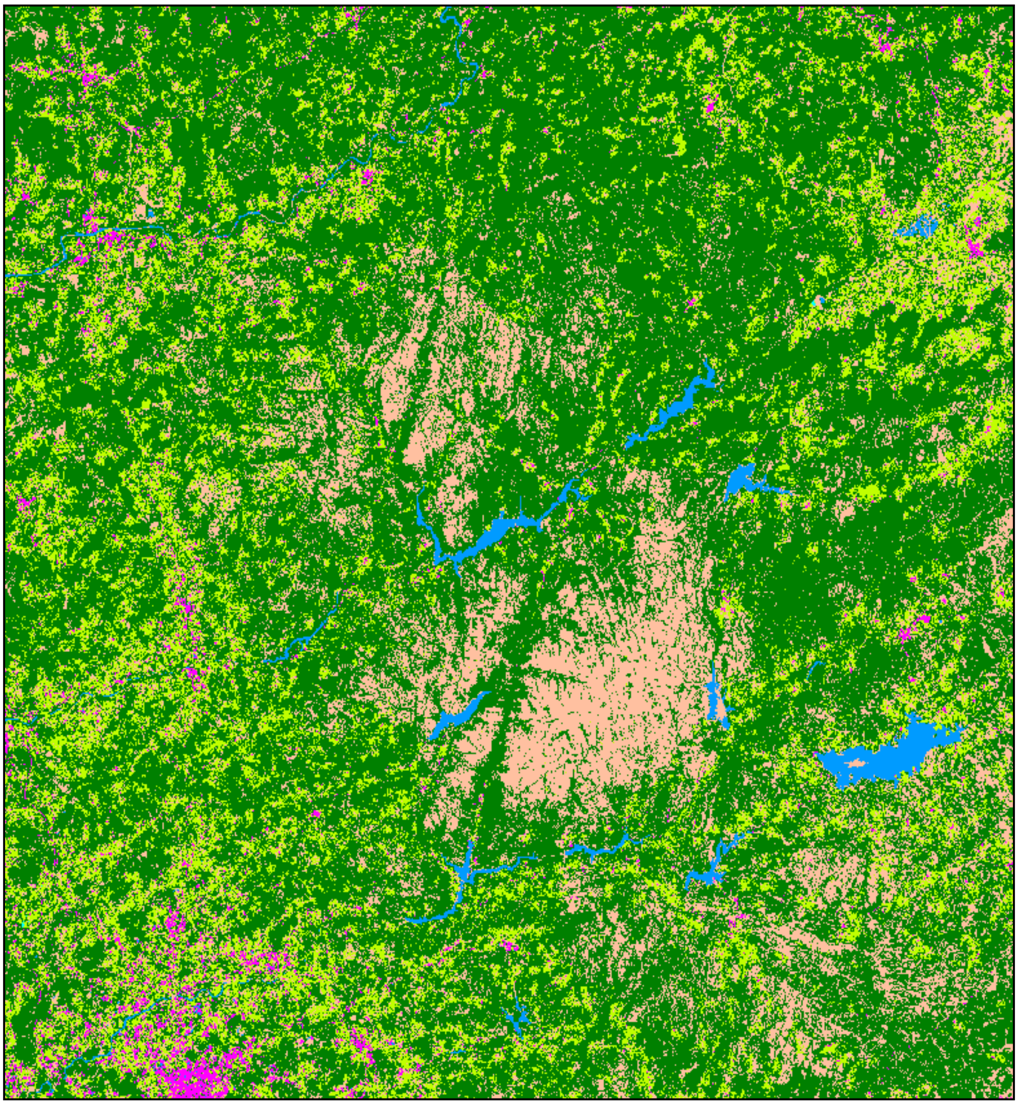

Figure 4.19. LCCS2 Level 3 classification of Peneda Gerês National Park (nominal year of 2016).

4.3.15 Samaria National Park, Crete

Samaria (White Mountains) National Park is located on the West part of island of Crete and was declared as a National Park via a Royal Decree in 1962. It is a multi-designated area and specifically a National Park, Landscape of Outstanding Beauty, Natura 2000 site coded GR 4340008 and GR4340014 and Biosphere Reserve in the framework of the "Man and Biosphere" Programme of UNESCO. Threats to the flora and fauna include landscape fragmentation, desertification induced by overgrazing and uncontrolled fire, modifications in water and groundwater regime induced by large scale infrastructure, poaching and uncontrolled abstraction of endemic species of flora, massive touristic flow and relative medium and large-scale touristic infrastructures.

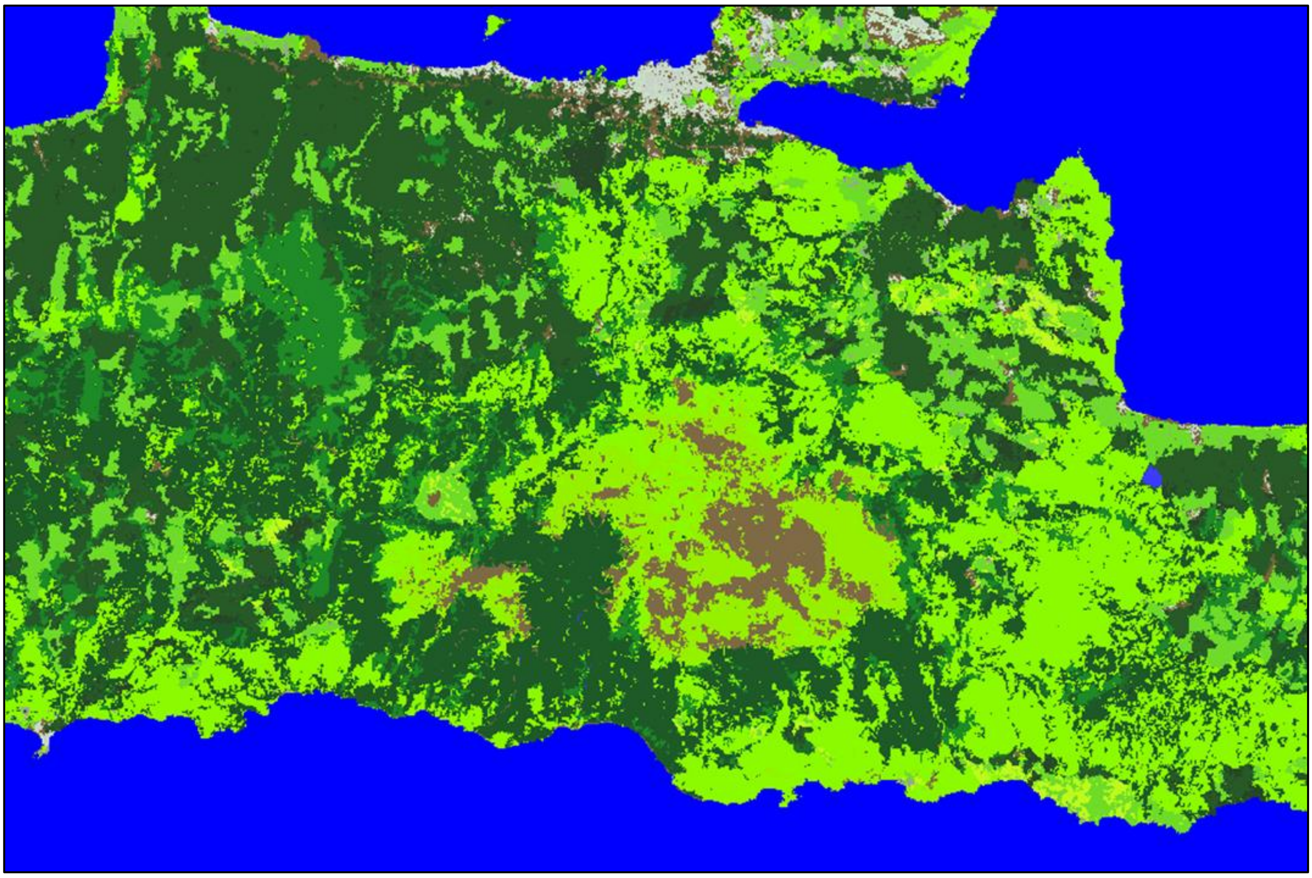

Figure 4.20. LCCS2 Level 3 classification of Samaria Gorge National Park (nominal year of 2016).

4.3.16 Swiss National Park and Davos, Switzerland

Alpine forest and grasslands provide essential services such as food, timber, protection from natural hazards, biodiversity, recreation and carbon sequestration. These values are under threat by human development, agricultural expansion, land abandonment, tourism and climate change. LCCS2 classifications have been produced for Swiss and Davos NP using available data layers and Sentinel-2 imagery. LCCS2 outputs will provide information on the spatial distribution and structure of forests and semi-natural grassland, and their response to change in the face of disturbance.

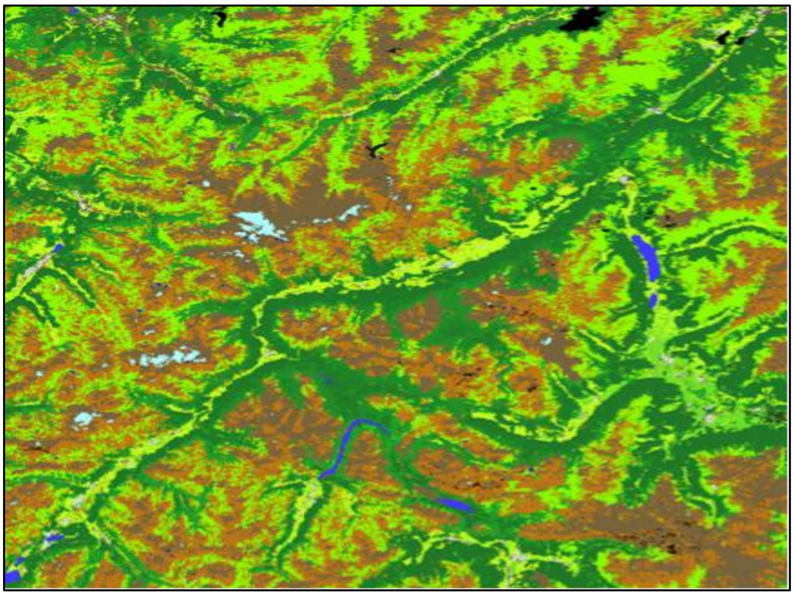

Figure 4.21. LCCS2 Level 4 classification of Swiss NP (nominal year of 2016).

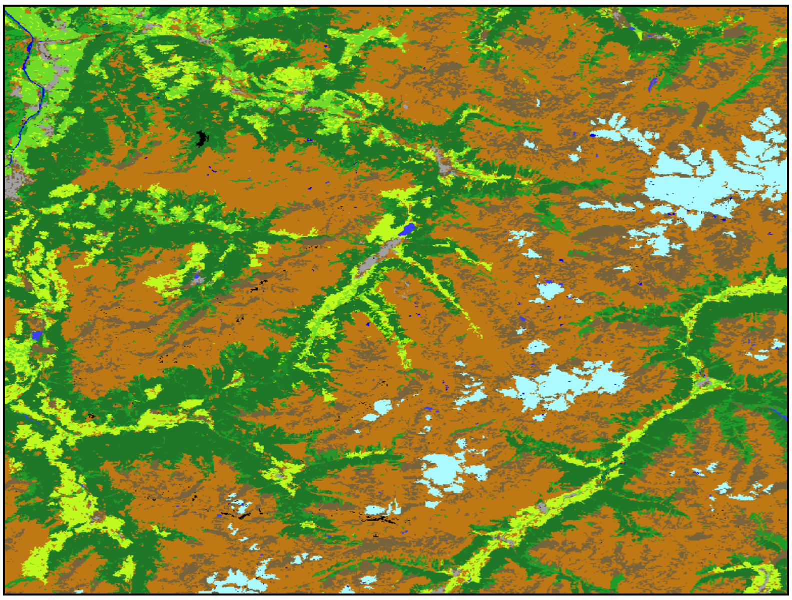

Figure 4.22. LCCS2 Level 4 classification of Davos NP (nominal year of 2016).

4.3.17 Wadden Sea, The Netherlands

The Wadden Sea is an international, highly productive estuarine area, and one of the largest coastal wetlands in the world. Situated abreast mainland Europe in the south-eastern portion of the North Sea, it borders Germany, the northern portion of the Netherlands, and western Denmark, thereby requiring tri-lateral cooperation in the management and protection of the system. This coastal area is a biodiversity hotspot due to its positioning as a convergence point of multiple domains, including terrestrial, fresh water, brackish and marine habitats. This multi-faceted combination allows for the support of a wide breadth of biota. Commercial activities include industrial fishing for commercial fish and shellfish; recently aquaculture for shellfish has been introduced. One of the objectives of the application of protected area status to the Wadden Sea is to limit the degree of exploitation by the commercial shellfish industry whose high degree of pressure through mussel extraction has significantly impacted the system's capacity to support the large volume of migratory birds. The classification will be provided soon.

4.3.18 Bayerwische Wald, Germany

In recent years, increasingly mild winters combined with prolonged warm and dry summers and the predominance of certain trees species (spruce), have led to outbreaks of bark beetles that have decimated high altitude forest ecosystems in protected areas such as the Bavarian Forest National Park (Bayerischer Wald). Monitoring is a key part of the management process, as is understanding the historic, current and future ecosystem response in these wilderness areas. LCCS2 classifications for Bayerischer Wald form the basis for tracking changes in vegetation cover and better understanding ecosystem resilience. Input layers of particular importance include life form, canopy cover, vegetation phenology and leaf type. The classification will be provided soon.

4.3.19 Kruger National Park, South Africa

Kruger National Park (KNP) and surrounds support both high wildlife diversity (in the park) and livestock production (in adjacent areas). KNP represents a typical South African savanna ecosystem, and presents an opportunity to assess savanna dynamics and ecosystem services. Key influential factors on the savanna landscape and vegetation productivity are edaphic, climatic, biotic and anthropogenic (e.g., fire, grazing, fuelwood collection) in origin. LCCS2 maps generated for KNP represent an integration of inputs that can inform on activities within KNP's savanna ecosystems and their impact on key ecosystem services (e.g., ecotourism, grazing and browsing resources, wood resources and water). Key layers used for the classification included canopy cover, the height of woody vegetation, phenology and above ground biomass. The classification will be provided soon.

4.4 Data driven classification from optical and SAR data

A number of EO data-driven classifications have been generated from the range of EO data. These can be used as input to the EODESM system such that they align with the LCCS2 for subsequent change detection. The following sections provide examples from Doñana, the Wadden Sea, Danube Delta and Har HaNegev.

4.4.1 Doñana

Six Landsat-5 images (from October 2009 to August 2010) were obtained for Doñana National Park in the south of Spain, from which the Normalized Difference Vegetation Index (NDVI), a green vegetation indicator, and two variations of Normalized Difference Water Index (NDWI), related to liquid water) were calculated. For each pixel and for each index band, a neighbourhood of 3x3 pixels was vectorized and concatenated to form a vector of 27 elements. A k-means clustering was then applied to 30% of the local feature vectors computed (using all six images) to identify semantic classes and associate these with clusters. The remaining local feature vectors were then assigned to their closest clusters. Change was then assessed based on transitions between semantic classes, with these measured by counting the number of times the semantic class assigned to each pixel changed in every image. Observed changes included inundation of marshlands and bare soils in winter, drainage of water in the summer. Phenological changes were also evident in spring and late summer and often associated with agricultural production. This example showed that the computation of local descriptors from indices can assist the identification of different land cover classes which can also be used as input to the EODESM system, including the forthcoming change component.

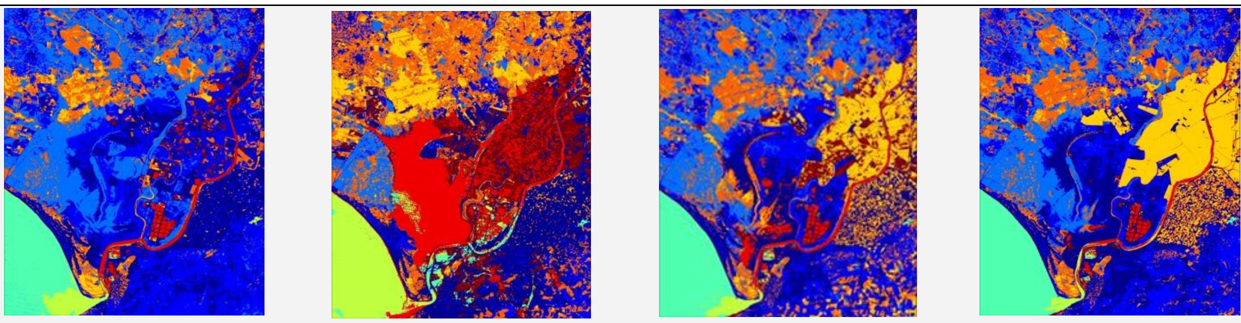

October 2009 | February 2010 | June 2010 | August 2010

Land cover classification of the Doñana protected area for four months: a) Bare soil, b) Very sparse vegetation, c) Marshland, d) Deep water such as Ocean, e) Sediments, f) Forest, g) Bushes, h) Mid-level water, i) Shallow water.

Technological readiness level: 3 (DLR[1])
Open source (Y/N): Y
Commercial or proprietary (C/P): P
Background or Foreground knowledge (B/F): F

Partner: DLR[1] use case and validation jointly with CSIC[2]

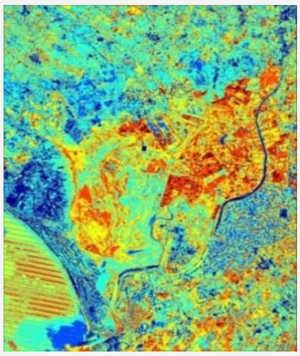

LC change map from October 2009 to August 2010. The minimum through maximum changes are depicted in the range between dark blue to red

4.4.2 Wadden Sea from SAR data

For the Wadden Sea as well as other wetland sites (Lake Ussel and Marker Lake), a systematic feature extraction and classification approach described in Espinoza-Molina et al. (2016) was used to generate and semantically annotate a classification of Sentinel-1A data. The classification is based on four modules; a data model generation (DMG), a database management systems (DBMS), knowledge discovery in databases (KDD) and statistical analysis (SA) (Dumitru et al. 2017). These modules are operated automatically although user interaction is possible. The DMG module transforms the original format of the EO products into smaller and more compact product representations that include image descriptors, metadata and image patches. The DBMNS module is used to store all of the information generated and allows query and retrieval of data. The KDD module is based on cascaded learning and is designed to find patterns of interest from the processed data at multiple resolutions and present the data to the user in a readily interpretable manner. The KDD module also allows semantic annotation of the image content using machine learning algorithms and human interaction. The SA module provides classification maps of the input dataset, the distribution results of the retrieved categories in an image, and the classification accuracy of selected descriptors (primitive features) by computing different metrics (Bahmanyar et al. 2017). Where Sentinel-1A data are used, the number of categories retrieved is lower compared to when higher resolution data (e.g., TerraSAR-X) are used and many are quite general (e.g., inhabitat built up; Dumitru et al., 2016). The classification accuracy for the Wadden Sea was 90 % for precision and 85 % for recall.

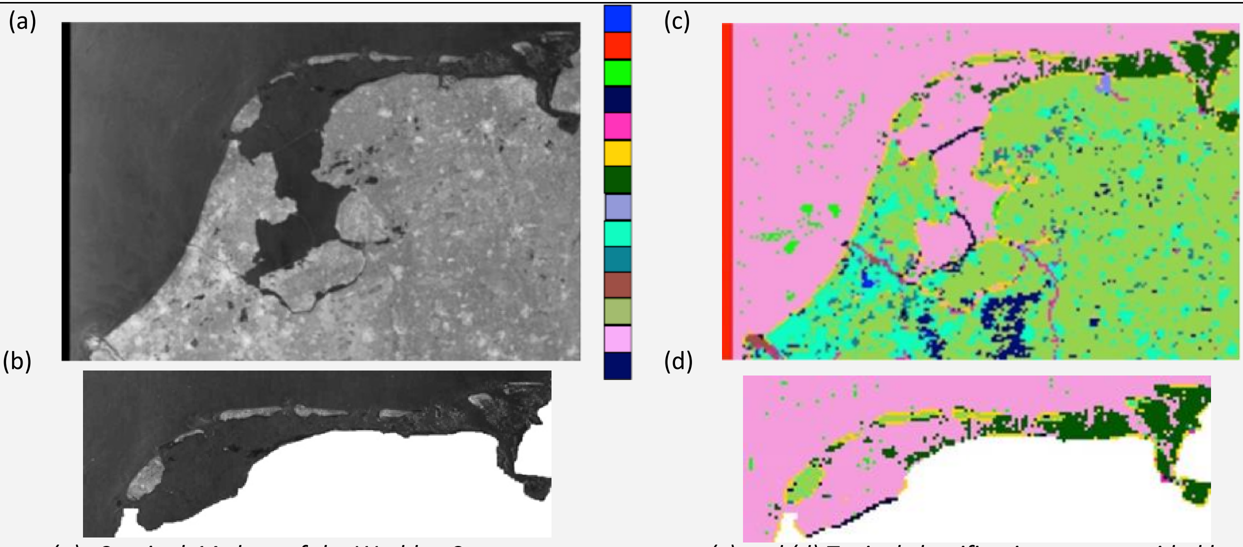

(a) Sentinel-1A data of the Wadden Sea
(b) Detail of the Dutch part

(c) and (d) Typical classification map provided by the first component of the SA module.

(e)

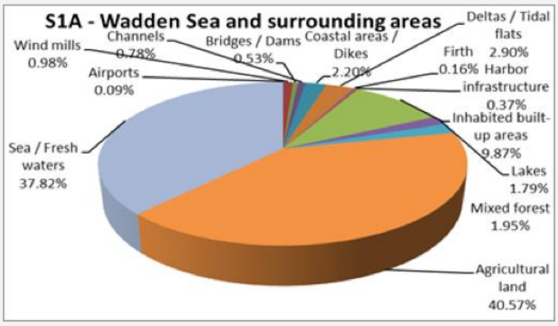

Technological readiness level: 3 (DLR[1])
Open source (Y/N): Y
Commercial or proprietary (C/P):
Background or Foreground knowledge (B/F): F

Partner: DLR[1] use case and validation jointly with **NIOZ[2]** in Netherlands

The diversity of retrieved and semantically annotated categories is shown in (e), which shows the high level of detail generated. The colour legend labels range from blue (top) to dark blue (bottom) and represent airport-runways, Black edge (image edge effect), Wind mills, Bridges or Dams, Channels, Coastal areas / Dunes or Dikes, Deltas / Tidal flats, Firth, Inhabited built-up areas, Lakes, Harbor infrastructure, Agricultural land, Sea / Fresh waters, and Natural vegetation.

4.4.3 Danube Delta

As with the Wadden Sea, land cover classifications were generated for the Danube Delta which can also provide input to the EODESM system.

(a)

(b)

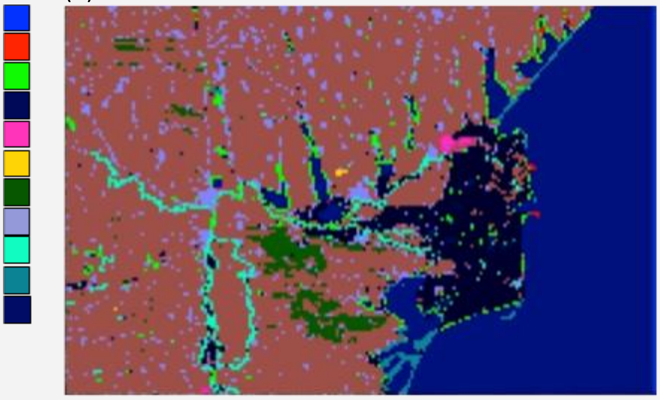

(a) Sentinel-1A data of the Danube Delta

(b) Typical classification map provided by the first component of the SA module.

(c)

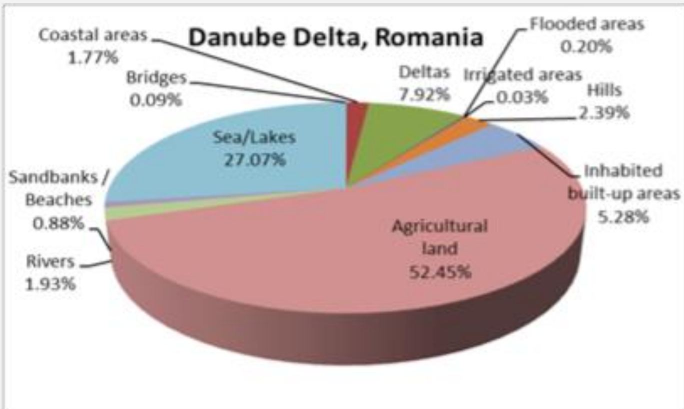

Technological readiness level: 3 (DLR[1])
Open source (Y/N): Y
Commercial or proprietary (C/P):
Background or Foreground knowledge (B/F): F

Partner: DLR[1] in collaboration with **UB[2]**

The diversity of retrieved and semantically annotated categories is shown in (c), which shows the high level of detail generated. The colour legend labels range from blue (top) to dark blue (bottom) and successively represent airport-runways, Black edge (image edge effect), Wind mills, Bridges or Dams, Channels, Coastal areas / Dunes or Dikes, Deltas / Tidal flats, Firth, Inhabited built-up areas, Lakes, Harbor infrastructure, Agricultural land, Sea / Fresh waters, and Natural vegetation.

4.4.4 Har HaNegev, Israel

Israel study area Har HaNegev in the southern arid part of Israel is the largest land resource in the country. The area offers an opportunity to better understand the consequences of residential development on the fragile arid environment at various levels of ecological organization and landscape scales and the LCCS2 classifications provide a baseline against which changes can be quantified. Classification was conducted by the BGU Partner based on a RapidEye image of April 2014 with 5 m resolution. Pre-processing involved atmospheric correction using the ATCOR software. Support Vector Machine (SVM) technique was used for classification. Long-term change detection of NDVI was conducted using two Landsat images from 1987 and 2017. Both are summer images. Although the area is defined as a protected area, several hot-spots can be observed.

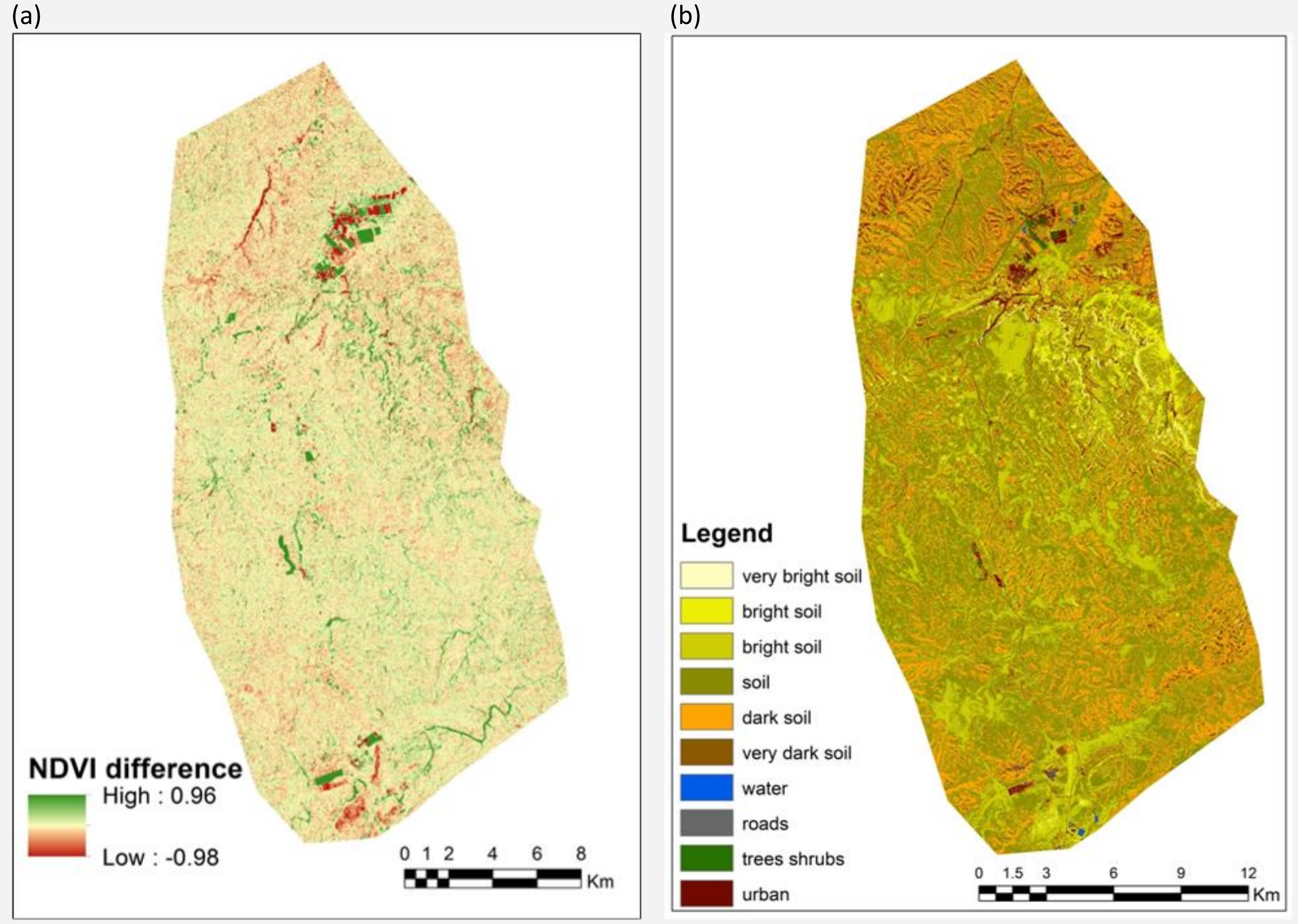

(a) The NDVI difference and (b) classification of land covers generated for Har HaNegev, Israel.

Technological readiness level: 4 (BGU)
Open source (Y/N): N
Commercial or proprietary (C/P): C
Background or Foreground knowledge (B/F): B

Partner: BGU

4.4.5 Kruger National Park, South Africa.

For Kruger NP, the Normalized Burn Ratio (NBR) has been computed (as in Escuin et al., 2008). The NBR, designed to highlight burned areas and estimate fire severity, has been calculated for a total of 67 Landsat scenes (1987 to 2015), covering an important part of the Kruger National Park. Burned areas identified in the maps have been validated through filed work and local partners expertise.

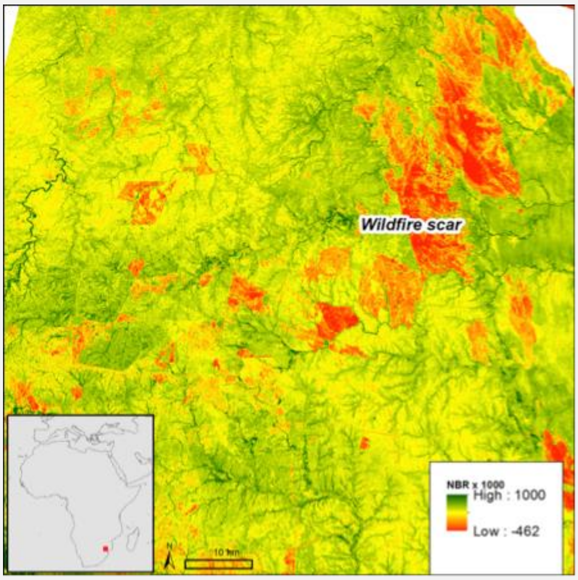

Normalized Burn Ratio for Kruger National Park from Landsat-8 OLS for 15th September, 2014.

Technological readiness level: 4 (BGU)
Open source (Y/N): N
Commercial or proprietary (C/P): C
Background or Foreground knowledge (B/F): B

Partner: BGU

4.5 Translation to Habitats (Task 4.3.2)

The maps generated using the EODESM system use the LCCS2 taxonomy but the code also allows for their translation to General Habitat Categories (GHCs), as well as Annex 1 and Eunis categories, as developed through the BIO_SOS project (Kosmidou et al., 2013; Adamo et al. 2014, Petrou et al. 2014). In some cases, there is a one-to-one translation but this is not always the case and often there are ambiguities (Tomaselli et al., 2016; Adamo et. al. 2016). To resolve these, other environmental and contextual information is needed as well as expert knowledge, as indicated in Figure 4.23 for a wetland Mediterranean site.

LCCS Dichotomous phase	LCCS Mod Hier phase Level II-III	EUNIS	Annex I	ENVIRONMENTAL ATTRIBUTES				EXPERT PRIOR INFORMATION	
				Lithology-Parent material	Soil - surface aspect	Soil - suburface aspect	Water quality	Phenology - vegetative stages	Water seasonality flooding period
A 12	A2A5A10B4E5-B12E7	E16	X	Calcareous rock - Calcarenite	/	/	/	March-June	/
A 12	A1A4A10B3-D1E2B9	F5.51	X	Calcareous rock - Calcarenite	/	Leptosols	/	March-October	/
A 12	A1A4A10B3D2E1-B9	B1631	2250	Unconsolid- Clastic sedimentaryrock - Sand	/	Arenosols	/	Full year	/
A 12	A1A4A10B3D1E1-B9	F5.514	X	Calcareous rock - Calcarenite	/	Leptosols	/	Full year	/
A 12	A1A4A11B3D1E1-B10	F6.2C	X	Calcareous rock - Calcarenite	Soil surface, stony(5-40%)	Leptosols	/	Full year	/
A 12	A2A5A11B4E5-A13B13E7	B11	1210	Calcareous rock - Calcarenite	Loose and shifting sands	Arenosols	/	April-September	/
A 12	A2A6A11B4E5-A12B12E6	B131	2110	Unconsolid- Clastic sedimentaryrock - Sand	Loose and shifting sands, with dunes	Arenosols	/	April-August	/
A 12	A2A6A10B4E5-B11E6	B132	2120	Unconsolid- Clastic sedimentaryrock - Sand	Loose and shifting sands, with dunes	Arenosols	/	April-August	/
A 12	A2A5A11B4E5-A13B13E7	B148	2230	Unconsolid- Clastic sedimentaryrock - Sand	Loose and shifting sands	Arenosols	/	April-May(June)	/
A 12	A2A5A11B4E5-A13B13E7	E13.13	6220	Calcareous rock - Calcarenite	Soil surface, very stony(40-80%)	Leptosols	/	March-May(June)	/
A 24	A2A5A13B4C2E5-B13E7	C3.421	3170	Calcareous rock - Calcarenite	Soil surface	Leptosols	Fresh water	March-May(June)	nov-feb
A 24	A2A5A13B4C2E5-B13E7	A2.55	1310	Unconsolid- Clastic sedimentaryrock - Sand	Soil surface	Solonchaks	Saline water	June-October	(no v) dec-apr (may)
A 24	A1A4A12B3C2D3-B10	A2.526	1420	Unconsolid- Clastic sedimentaryrock - Sand	/	Solonchaks	Saline water	June-September (Oct)	(depending on veg.type)
A 24	A2A6A12B4C2E5-B11E6	A2.522	1410	Unconsolid- Clastic sedimentaryrock - Sand	/	Solonchaks	Brakish/Saline water	June-September	(no v) dec-mar (apr)
A 24	A2A6A12B4C2E5-B11E6	D5.24	7210	Calcareous rock - Calcarenite	/	Histosols	Fresh/Brakish water	June-September	(no v) dec-mar (apr)
A 24	A2A6A12B4C2E5-B11E6	A2.53 A2.53C	X	Calcareous rock - Calcarenite	/	Histosols	Fresh/Brakish water	June-September	(no v) dec-mar (apr)
A 24	A2A6A12B4C2E5-B11E6	A2.53 A2.53D	X	Calcareous rock - Calcarenite	/	Solonchaks	Brakish/Saline water	June-September	(no v) dec-mar (apr)
A 24	A2A6A12B4C2E5-B12E6	C2	X	Calcareous rock - Calcarenite	/	Histosols	Fresh water	June-September	(no v) dec-mar (apr)
A 24	A2A5A16B4C1E5-A17B12E6	X03	1150	/	/	/	Brakish water	June-September	Full year

Figure 4.23 An example of the translation from the same LCCS2 category to different Annex I and EUNIS habitat categories, as undertaken for a Mediterranean PA site in Italy.

Habitat maps will be provided at the end of the LC validation process by integrating LC maps with environmental LCCS2 attributes. Expert knowledge will be used for such integration (Tomaselli et al., 2013), according to the approach developed in the previous BIO_SOS project. For comparison purposes, such expert knowledge-based approach has been compared with a data driven Hierarchical Random Forests (HRF) classifier when mapping the habitats within a Mediterranean wetland PA. The rules obtained by the HRF seem reproduce the expert knowledge rules with comparable results. The research activity carried out with links to the EUBON Project Partners has been recently submitted (Gavish et al., 2017) for review.

4.6 Landscape and biodiversity indicators (Task 4.3.3)

The input to the landscape indicators estimation approach is comprised of land cover (LC) or habitat maps. In this approach, study area in its entirety is split into square-shaped cells that represent smaller areas in the region. From the splitting of the site into cells, several patches of the selected LC or habitat classes may split into several cells to allow consideration of adjacent cell. This property may be undesired for the calculation of certain landscape analysis measures. For this reason, overlapping cells are considered, in order to increase the possibility that patches, which would have otherwise split into different cells, may be entirely included in one or more overlapping cells. The cell size and the step distance (i.e., the distance between the centres of two consecutive cells, both in the left-right and top-bottom directions) are parameters defined by the user according to preferences, or the particular characteristics of the site or the target class under consideration. A graphical illustration of the site splitting into cells is presented in Figure 4.24.

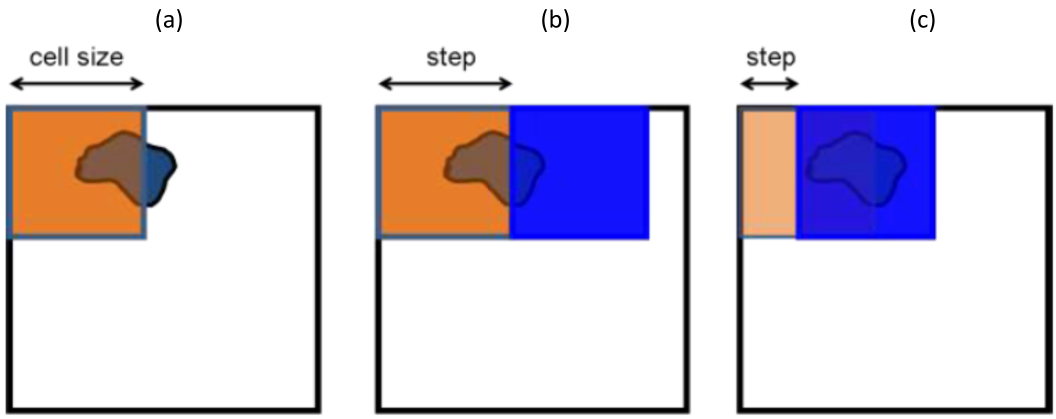

Figure 4.24. Splitting the site in cells. (a) First cell, in orange colour; (b) second cell, in blue, adjacent with the previous one; (c) second cell, in blue, overlapping the previous one; in (c), the patch of the target class falls entirely in the blue cell.

Within each individual cell, class- and landscape-level indicators are calculated for a specific class depicted in the mask image. The calculated indicator values are assigned to the pixels of the cell that belong to the selected class. The same process is performed for all defined cells. When overlapping cells are used, some pixels of patches of the selected class may fall in more than one cell. In this case, the average value of the measure of all cells within which the pixel falls, is assigned to the pixel. Through this procedure, an image map per indicator is estimated. In parallel with the indicator maps, indicator uncertainty maps are also estimated (see Section 4.7.5). The selected FRAGSTATS landscape indicators include: (a) percentage of landscape (PLAND), (b) patch density (PD), (c) mean shape index distribution (SHAPE_MN), (d) total class area (CA), (e) mean patch size (MPS), (f) effective mesh size (MESH), and Area-Weighted Mean Patch Fractal Dimension (AWMPFD). The workflow of Landscape indicator maps estimation is shown in Appendix 1, Section 8, sub-section 8.10, workflow (a). PLAND images for four PAs are illustrated in the Figure hereafter.

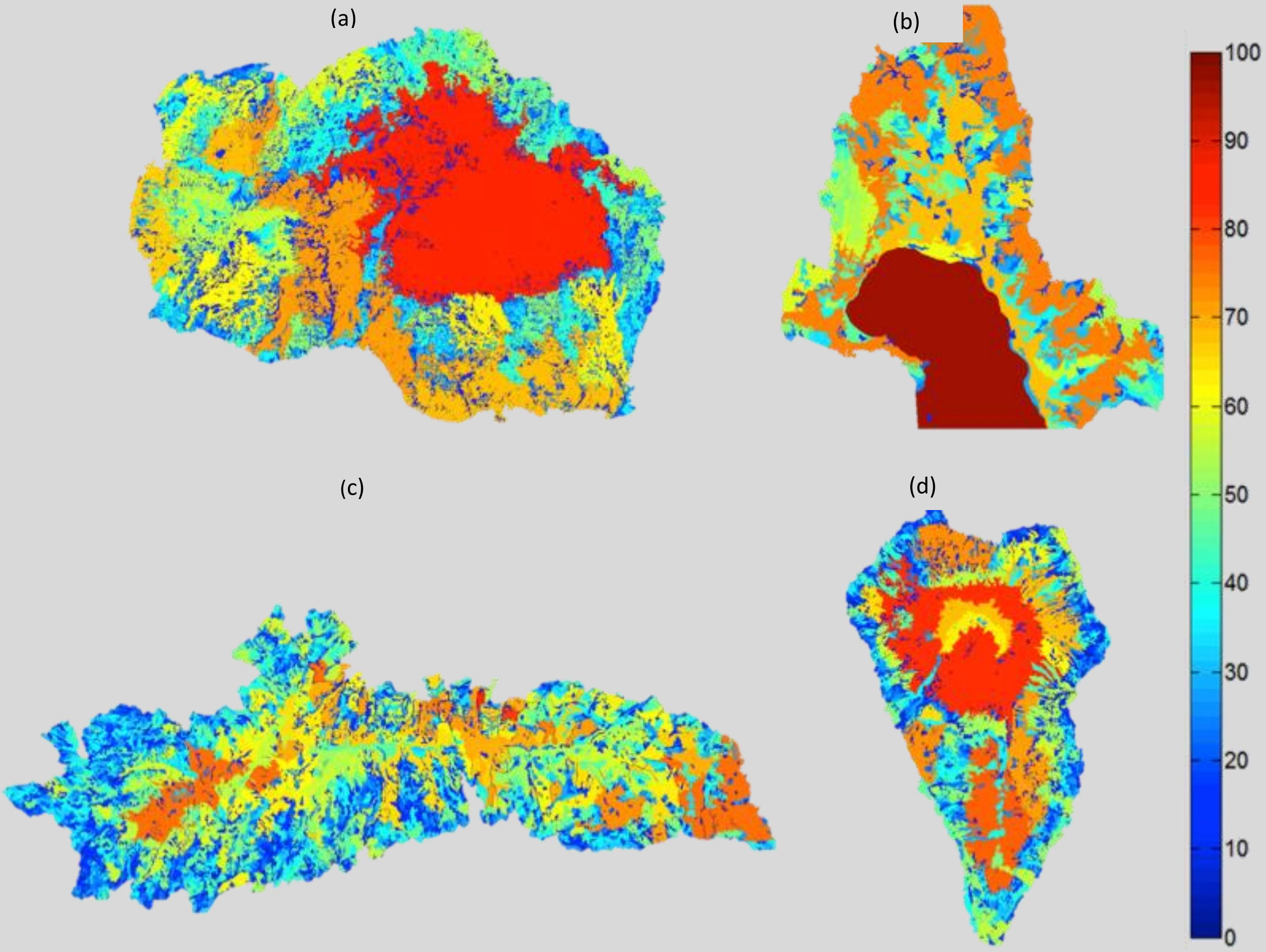

PLAND (%) image maps for: (a) Samaria (year 2015); (b) Prespa (year 2012); (c) Sierra Nevada (year 2007) and (d) La Palma (year 2007) PAs.

Technological readiness level: 5
Open source (Y/N): Y
Commercial or proprietary (C/P):
Background or Foreground knowledge (B/F): F

Partner: CERTH

4.7 Validation (Task 4.3.5)

4.7.1 Thematic and continuous layers

To generate the LCCS2 classifications for each PA, both continuous (representing EVs) and thematic layers are used (e.g., from data driven classifiers), with these often generated from different sources (e.g. optical, SAR or LiDAR data). Where feasible, each of these inputs has been (or will be) associated with an estimate of error or uncertainty, with these typically generated through reference to in situ data or other validated datasets. As an example, the Root Mean Square Error (RMSE) is commonly used to describe the differences between estimates (e.g., from an established relationship between L-band backscatter and above ground biomass) and actual measures on the ground. For thematic maps or specific target categories, standard confusion matrices have been generated, with these indicating measures such as overall, users' and producers' accuracies (Congalton, 1988). Each of these layers (whether continuous or thematic) is combined within the EODESM system to generate a comprehensive descriptor of the land cover occurring at a particular location. For example, the class "Trees closed canopy (>70-60 %) tall (14-30 m) continuous broadleaved evergreen with 2nd layer supporting open canopy 7-3 m in height" can be derived from a classification of lifeform (e.g., from Sentinel-2), cover (from Landsat), height (LIDAR), fragmentation (FRAGSTATS), leaf type (Sentinel-2), and phenology (Landsat/Sentinel-2 time-series of NDVI) and the metrics describing the second layer (e.g., as generated from LIDAR). This integration of multiple layers from a wide range of sources increases the complexity of quantifying the uncertainty of the overall (final) class. The following sections outline the approach to assessing the accuracy of both the continuous and thematic layers used as input to the EODESM system and the final output maps.

4.7.2 Thematic classifications: use of existing land cover and habitat maps

For the majority of the PAs, maps of land cover already exist, with these typically generated from local surveys, visual interpretation of aerial photography or satellite image analysis, either by organizations running or associated with the PAs or by independent organizations focusing on mapping the local, national or regional area. For example, the Corine Land Cover Map 2012 is available for all of Europe. Many of these maps, including the majority currently available for the PAs use different land cover taxonomies and have different legends; hence, these are unable to be compared. Additional maps may have been generated by data driven classifiers (Section 4.4).

Maps of land cover are different from those describing habitat. For some PAs, habitat as well as land cover maps are available but in most cases, only one of these exists. Standardization of habitat classifications across Europe has been facilitated by the development of the EUNIS habitat classification system, which provids over 5000 separate descriptions but these are not easily mapped, particularly from remote sensing data alone, and are not available for the PAs. Increasingly, approaches to translating from land cover to habitat maps are being developed within previous BIO_SOS project (Kosmidou et al., 2013; Tomaselli et al., 2013, Adamo et al. 2016). For each of the PAs, existing land cover or habitat maps were requested for the following reasons:

a) To establish the current state of land cover or habitat mapping and then extract changes in comparison to recent maps produced by EODESM.

b) To provide comparison with the LCCS2 maps generated by the EODESM system and extract reference no-change samples to be used in the validation of new maps.

c) To demonstrate the transferability and consistency of the LCCS2 taxonomy.

An overview of the maps and the taxonomies used are provided in Tables 4.5 and 4.6. An example of the translation to the LCCS2 taxonomy is provided for the Camargue PA in Figure 4.25, and those for other PAs can be viewed in Appendix 2 (Section 9).

Mountain PAs	Existing land cover map	Semi-arid PAs	Existing land cover map
		Har HaNegev	
Austrian Alps	Corine CLC (2012)	Kruger NP	LC (2015)
Barvarian Forest	Corine CLC (2012)	Samaria	Corine CLC (2012)
Gran Paradiso	Corine CLC (2012)		
Hardangervidda	AR50, Corine CLC (2012)	**Wetlands PAs**	
High Tatra Mountains	Corine CLC (2012)	Camargue	Corine CLC (2012)
La Palma	Corine CLC (2012)	Curonian Lagoon	Plotai
Montado	LC (2007), Corine CLC (2012)	Danube Delta	Corine CLC (2012)
Murgia Alta	Corine CLC (2012)	Doñana	SIOS LC, Corine CLC (2012)
Ohrid and Prespa	Macedonia LC, Corine CLC (2012)	Wadden Sea	
Peneda-Gerês	Corine CLC (2012)		
Samaria	LC (1985/95/00/05/10/15), Corine CLC (2012)	**Maritime PAs**	
Sierra Nevada	Corine CLC (2012)	Caribbean LME	
Swiss National Park	LC, Corine CLC (2012)	Mediterranean LME	

Table 4.6 Existing land cover maps for each PA

Mountain PAs	Existing land cover map	Semi-arid PAs	Existing land cover map
		Har HaNegev	
Austrian Alps	EUNIS (2012)	Kruger NP	
Barvarian Forest		Samaria	
Gran Paradiso			
Hardangervidda		**Wetlands PAs**	
High Tatra Mountains		Camargue	
La Palma	Disvva1nombre, Vegetacion	Curonian Lagoon	
Montado		Danube Delta	DD Habitats (2006/12)
Murgia Alta		Doñana	Habitats
Ohrid and Prespa	Galitcicia	Wadden Sea	
Peneda-Gerês	Habitats		
Samaria		**Maritime PAs**	
Sierra Nevada		Caribbean LME	
Swiss National Park	Habitatalp	Mediterranean LME	

Table 4.7 Existing habitat maps for each PA

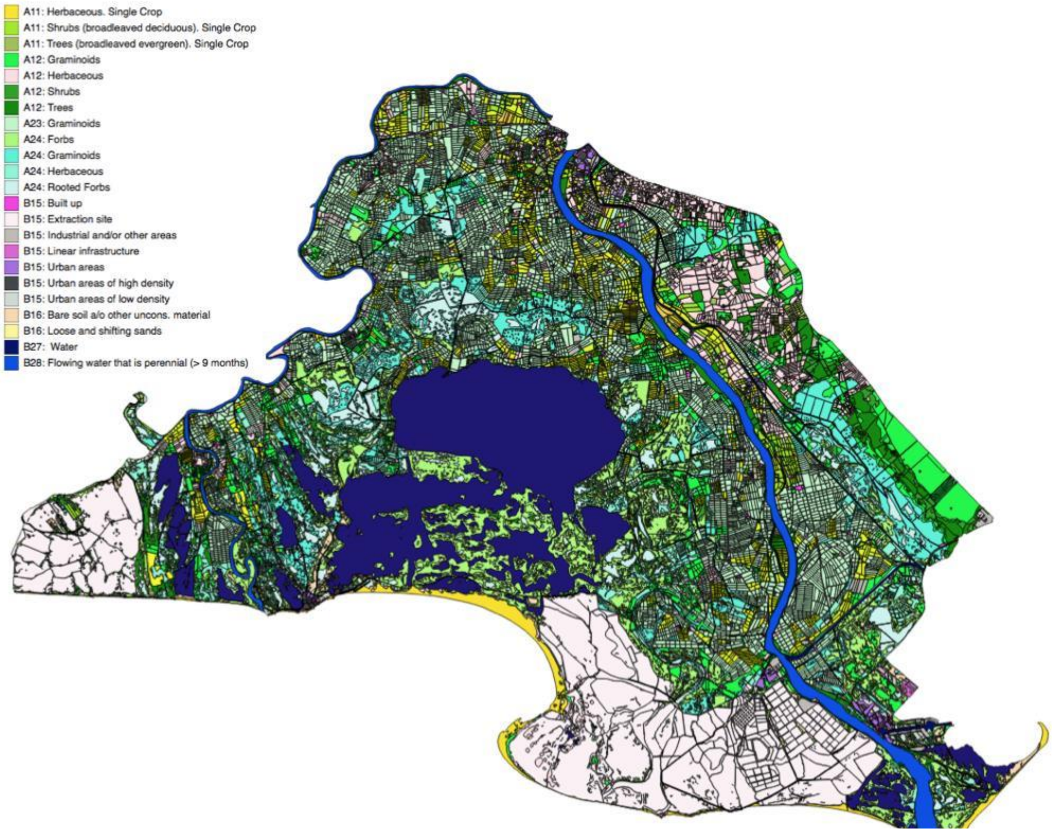

Figure 4.25. LCCS2 map of the Camargue BRD translated from the existing land cover map.

Using the existing land cover and habitat maps (translated to LCCS2 categories) no-change reference samples were extracted as ground truth. Standard confusion matrices (based on overall, users' and producers' accuracies; Congalton, 1988) were generated for the main thematic layers used as input to the EODESM system, with these primarily being lifeform, consolidated/unconsolidated materials and water sediment loads. An example confusion matrix is provided in Table 4.8 for Donana in Spain (overall accuracy of 81 %; with users' and producers' accuracies varying from 57 % to 99 % and 48 % to 100 % respectively). Overall accuracies for other PAs were also above 65 %, including for Danube Delta (77 %), Hardangervidda (66 %), La Palma (77 %), Northern Limestone (74 %), Davos (66 %) and Swiss National Park (69 %). Validation of other maps is still ongoing.

	Classification translated from existing land cover map												
	Cultivated Terrestrial			Natural Aquatic			Bare	Natural Terrestrial					
Classification using the EODESM system	Herbaceous	Shrubs	Trees	Graminoids	Herbaceous	Woody	Bare	Graminoids	Herbaceous	Shrubs	Trees	TOTAL	Users Accuracy
Herbaceous	93	1	21	0	0	0	0	0	0	0	0	115	80.9
Shrubs	1	98	0	0	0	0	0	0	0	0	0	99	99.0
Trees	6	1	29	0	0	0	0	0	0	0	0	36	80.6
Graminoids	0	0	0	36	0	1	0	0	2	3	0	42	85.7
Herbaceous	0	0	0	5	200	0	0	1	1	2	0	209	95.7
Woody	0	0	0	0	0	9	0	1	0	0	0	10	90.0
Bare	0	0	0	0	0	0	98	0	0	1	0	99	99.0
Graminoids	0	0	0	0	0	0	1	77	3	33	21	135	57.0
Herbaceous	0	0	0	1	0	0	0	4	28	2	7	42	66.7
Shrubs	0	0	0	7	0	0	0	9	8	48	12	84	57.1
Trees	0	0	0	1	0	0	1	8	8	11	60	89	67.4
TOTAL	100	100	50	50	200	10	100	100	50	100	100	960	
Producers Accuracy	93.0	98.0	58.0	72.0	100.0	90.0	98.0	77.0	56.0	48.0	60.0	Overall	80.8

Table 4.8 Confusion matrix generated for Donana National Park for lifeforms and bare surfaces (unconsolidated materials).

Validation of the thematic layers can also be undertaken with reference to *in situ* data and also airborne imagery. Where *in* situ data or aerial imagery is used, the information collected or extracted should be the same as, or at least commensurate, with the classifications generated from the EODESM system. Hence, for the class "Trees closed canopy (>70-60 %) tall (14-30 m) continuous broadleaved evergreen with 2nd layer supporting open canopy 7-3 m in height", ground truth information needs to be collected on each of the components (i.e., lifeform, canopy cover, canopy height, fragmentation status, leaf type, phenology and characteristics of understory layers). Each layer can then validated separately with an overall accuracy then given to the final class. A stratified random sampling, according to the sampling protocol developed within the FP7 BIO_SOS project (See Deliverable D4.3, Part 2, at http://www.biosos.eu/deliverables/D4-3.pdf), is also recommended.

As indicated, calculating the accuracy of the final LCCS2 class is complex and there is the argument to instead consider the accuracies of the contributory layers separately. This is particularly relevant when the inclusion or exclusion of a contributory layer occurs. For example, the overall accuracy might decrease if height is excluded or increase if phenology is included, or the accuracy of the classification will be lower if forests are described by a single variable (e.g., lifeform Trees) as compared to when more detailed descriptions are provided (e.g., of leaf type, cover, phenology). Future focus will therefore be on achieving a robust and consistent assessment of accuracy for LCCS2 classes generated from the EODESM system.

For a more accurate quantification of map accuracy the protocol described in Olofsson et al. (2013; 2014) has been investigated. The protocol uses the information obtained for map accuracy assessment to estimate the area of each land cover class (or of land change), and construct confidence intervals that reflect the uncertainty of the area estimates obtained. While accuracy measures (i.e., overall map accuracy, class omission and commission errors), based on a probability sample of reference observations, provide important information on how to use and interpret the map, they do not provide an adjustment or correction for estimated bias in the areas of mapped classes. This requires construction of an unbiased area estimator that excludes the area committed and includes the area that was omitted in the classification. The protocol, proposed by Olofsson et al. (2013), allows to construct an area estimator to be constructed directly from the error matrix (Congalton, 1988).

According to the protocol, when map categories are the rows (*i*) and the reference categories are the columns (*j*), the sample error matrix is reported in terms of the unbiased stratified estimator of the proportion of area ($\hat{p}_{ij}$) in each cell i,j of the matrix and estimates of the overall accuracy, user's accuracy and producer's accuracy with confidence intervals.

A_{tot} represents the total area of the map, $A_{m,i}$ is the mapped area (ha) of category *i* in the map and $W_i = \frac{A_{m,i}}{A_{tot}}$ is the proportion of the mapped area as category *i*, $\hat{p}_{ij}$ is then:

$$\hat{p}_{ij} = W_i \frac{n_{ij}}{n_{i\cdot}} \qquad (1)$$

The unbiased stratified estimator of the area of category *j* is obtained as:

$$A_j = A_{tot} \times \hat{p}_{\cdot j} = A_{tot} \sum_i W_i \frac{n_{ij}}{n_{i\cdot}} \qquad (2)$$

where $\hat{A}_j$ can be viewed as an "error-adjusted" estimator of area because it includes the area of map omission error of category *j* and leaves out the area of map commission error.

The estimated standard error of the estimated proportion of area is:

$$S(\hat{p}_{\cdot j}) = \sqrt{\sum_{i=1}^{q} W_i^2 \frac{\frac{n_{ij}}{n_{i\cdot}}\left(1 - \frac{n_{ij}}{n_{i\cdot}}\right)}{n_{i\cdot} - 1}} \qquad (3)$$

Finally, the standard error of the stratified area estimate can be expressed as:

$$S(\hat{A}_j) = A_{tot} \times S(\hat{p}_{\cdot j}) \qquad (4)$$

and an approximate 95% confidence interval for A_j is:

$$\hat{A}_j \pm 2 \times S(\hat{A}_j) \qquad (5)$$

Such protocol can be used also for the validation of the change maps (Tarantino et al., 2016) to be produced in Task 4.4.

4.7.3 Vegetation phenology uncertainty estimation

A model to compute and map uncertainty at pixel level has been developed. The model is based on error propagation formulas and could be adapted to other quantitative remote sensing products. The error model uses the radiometric error for a given sensor and spectral bands and it is modulated according to the incidence angle (taking into account the day and hour of the acquisition of image as well as the geographic location of the pixel). For very large images it is necessary to consider different times for different pixel locations. The model also adds a digital projected shadow model to take into account cast shadowed pixels. Once the maximum error is computed, it is conveniently rescaled (lineal fitting) according to the incidence angle of each pixel (the bigger the angle the more specular effects in reflectance and the higher the error expected). The model it also takes into accounts the behaviour of Lambertian surfaces and diffuse radiation. An example of the uncertainty propagation computing process is the following:

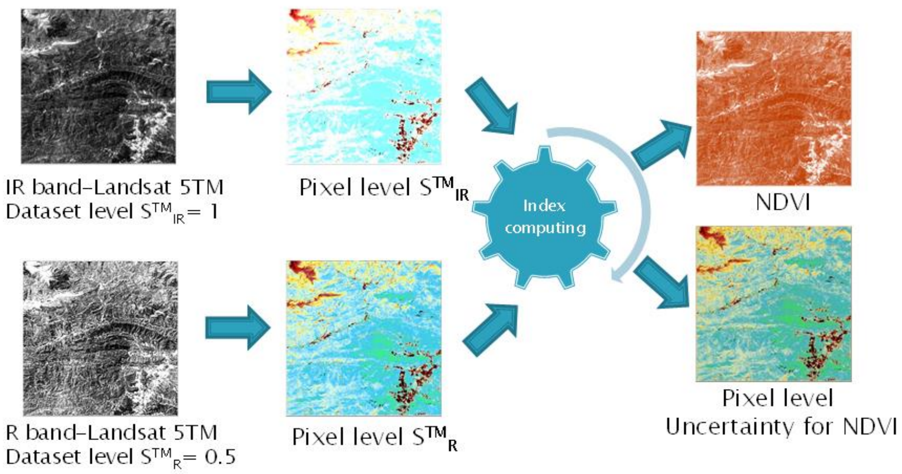

Figure 4.26. Uncertainty workflow

As a result, the index is computed with an ancillary band corresponding to the uncertainty at pixel level.

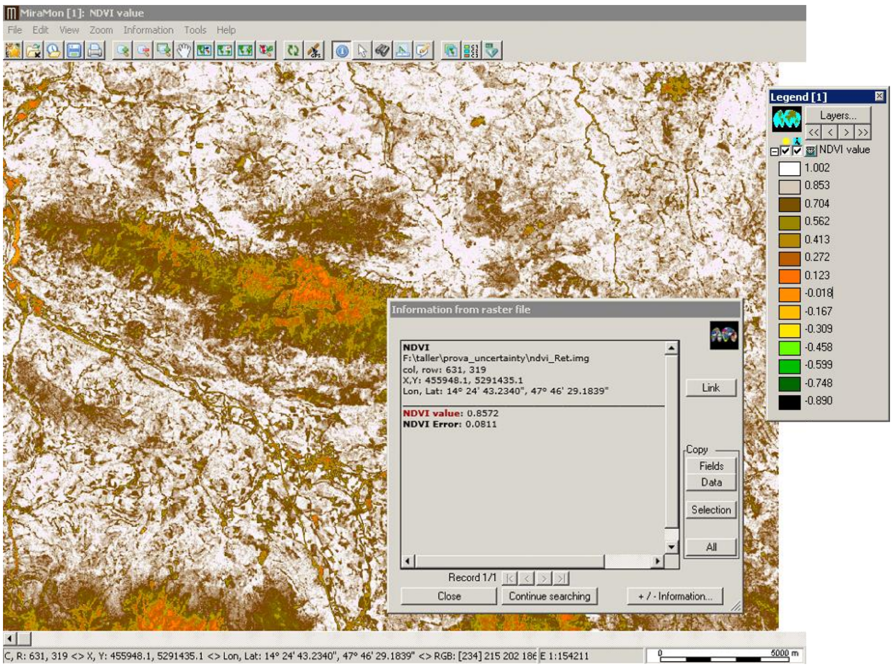

Figure 4.27. Final result of the uncertainty computed as ancillary data

4.7.4 Water and water-vegetation mask uncertainty estimation

An approach to estimating uncertainty in the classification of water and aquatic vegetation was developed by CERTH. Significant bands for assessing water, vegetation and soil presence are selected. These are used in combination for making decisions on the land cover per pixel. Each feature significant band is analyzed based in the emerging valleys in their histogram. An initial and a final band threshold T_{init}, T_{final} are estimated based on the unsupervised approach described in the Water mask delineation. Pixels that have a band value below T_{init} are assumed to have 0 % uncertainty, while as pixels' value approaches T_{final} uncertainty approaches 50 %. Assuming that uncertainty increases linearly from 0 % to 50 % as the band value increases from T_{init} to T_{final}, uncertainty maps accompanying the water mask are generated. Especially for the water-vegetation mask uncertainty map the estimation of uncertainty is related to the existence of both water and vegetation via combined analysis of the valleys' of histograms corresponding to the bands/ indices used. Whilst providing a map of uncertainty, independent validation has not been undertaken. The workflow of water and water-vegetation is shown in Appendix 1, section 8.7, workflow (c).

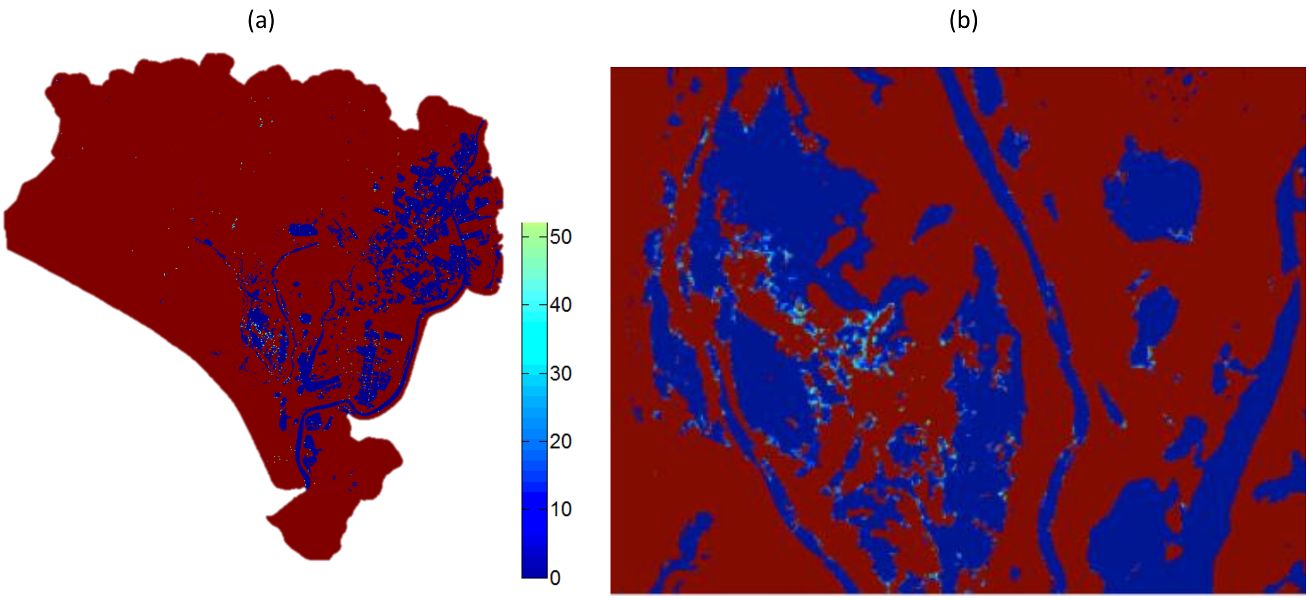

Figure 4.28. Uncertainty map (in %) for the water mask generated for the Donana PA using Sentinel-2A data from 6th June 2016 using an unsupervised classification is shown in (a); a subset of the image is shown in (b).

4.7.5 Landscape biodiversity indicators uncertainty estimation

An approach for assessing the uncertainty of the landscape biodiversity measures has been developed by CERTH. Initially, for each indicator included within each object/path, the number of pixels having a value is estimated. Each indicator value and the corresponding number of pixels are stored into an array, which is sorted into descending order. Depending upon the values where most pixels are allocated, averages are generated in a two-sample size approach. The variation is registered along with the form and width of the distribution of pixels across values. For the Lake Prespa PA, objects in the landscape are shown in Figure 4.29(a) and the PLAND measure map in Figure 4.29(b). Pixels omitted from the averaging procedures are also counted. Both the variation and the percentage of the omitted (erroneous) pixels are used to generate a coefficient indicative of the variability (CVB) of the values across pixels of the object in question (Figure 4.29(c)). At the same time for the elimination of erroneous cases the coefficient of variation (CV) is calculated (Figure 4.29 (d)). Their combination, as a mean of uncertainty, may be applied to the patch, class or landscape level (Figure 4.29 (e)). The workflow for indicator uncertainty estimates and maps is provided in Appendix 1, Section 8.10 and workflow (b).

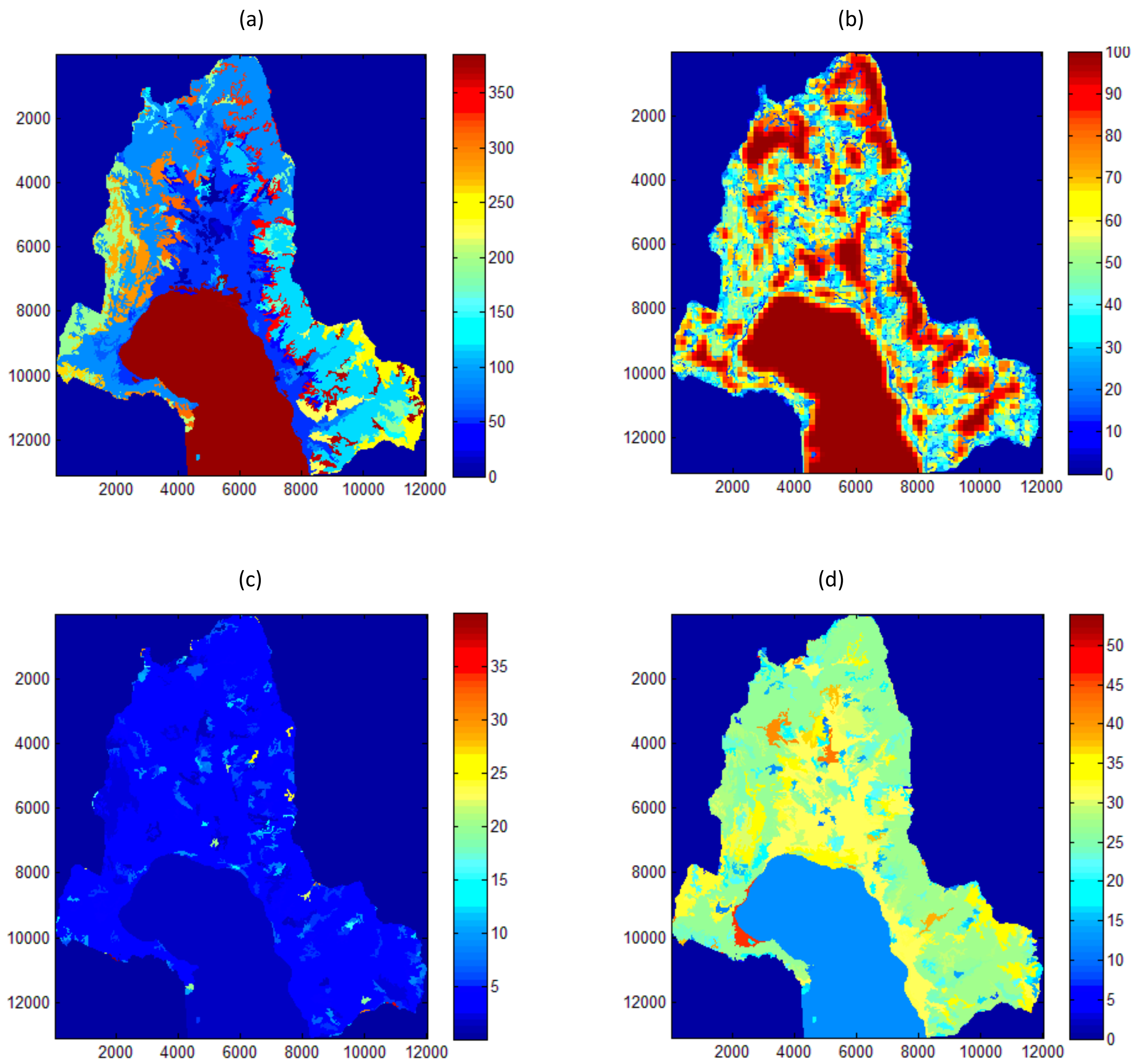

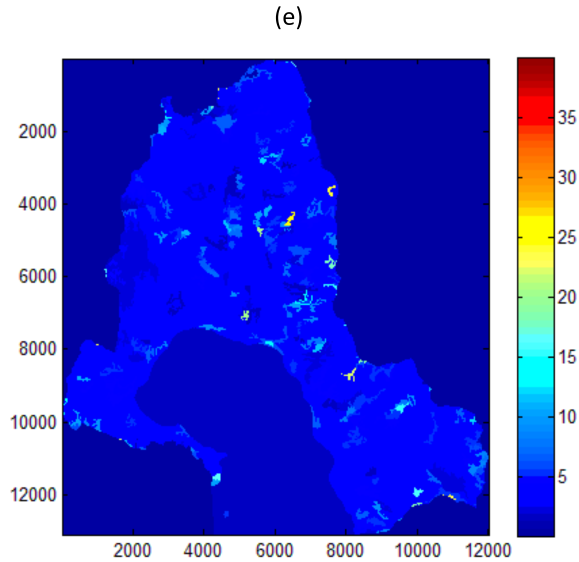

Figure 4.29. For the Lake Prespa PA: (a) objects in the landscape; (b) the PLAND measure map; (c) uncertainty based on CVB; (d) uncertainty based on CV and (e) integrated uncertainty.

4.7.6 Validation of environmental variables

For each of the EVs generated, estimates of error in retrieval have or are being provided to support the overall error associated with each LCCS2 class generated through the EODESM system as well as the attributes associated with each class (e.g., wind fields). The following provides an example of the validation for wind fields undertaken by CNR.

High precision/accuracy measurements of wind are generally available from in situ instrumented stations (e.g., buoys or platforms) but these are relatively sparse and insufficient for validating the wind field products generated from Sentinel-1A SAR data. So, first comparisons between different Sentinel-1 image modes, i.e. IW-GRD-MR data and EW-GRD-MR data, analysed by the SARWIND LG-Mod algorithm (see Section 3.1) were carried out at both 5km (red diamonds) and 12.5km (blue squares) output resolutions for the Camargue site. Results (Figure 4.30) indicated better percentage of wind direction estimation from IW-GRD-MR than EW-GRD-MR data at both (a) 5 km (88.5 % compared to 28.5 %) and (b) 12.5 km (99.6 % compared to 86.3 %). These findings satisfy the users' requirement of wind directional accuracy of less or equal to 20° for each direction estimate, with 95% confidence level. For the Wadden Sea, only IW-GRD-MR data were used at medium resolution with similar estimation percentage (i.e. 98.6%).

Then, Sentinel-1 wind direction and speed estimates obtained through the SARWIND LG-Mod algorithm were compared with those provided by both regional (i.e., SKIRON by Kallos et al. (1997)), and global (i.e., ECMWF) weather models at 5km and 12.5km grid respectively. Summary statistics (expressed in terms of RMSE and mean bias error (MBE) are provided in Table 4.9.

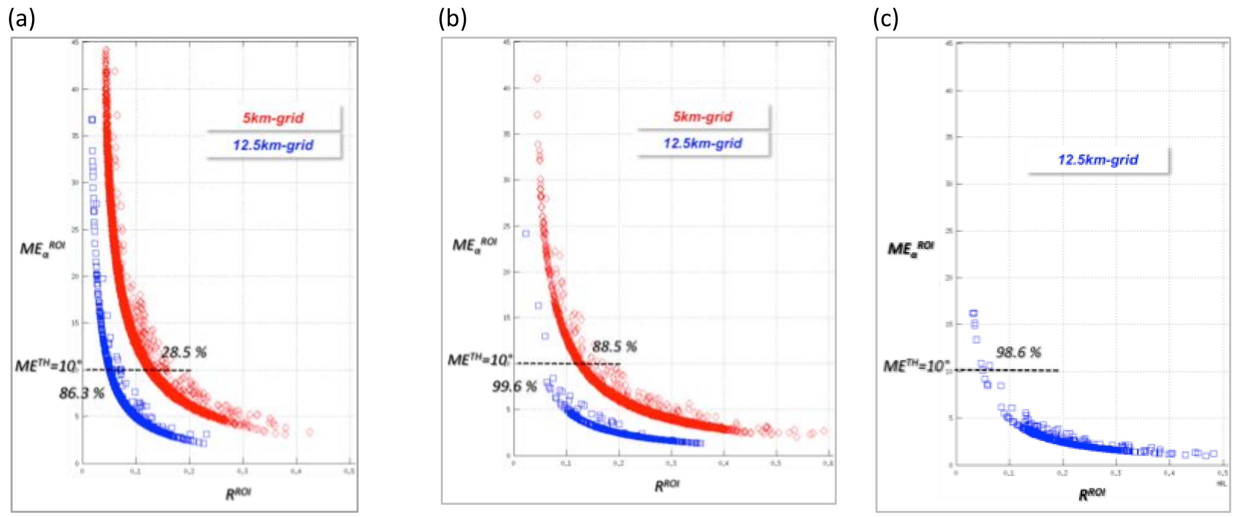

Figure 4.30. Trends of the wind directional accuracy measures $\mathrm{ME}_\alpha^{\mathrm{ROI}}$ (y-axis) plotted as function of the concentration parameter $\mathrm{R}^{\mathrm{ROI}}$ (x-axis). Plots refer to directional estimations obtained from: (a) EW-GRD-MR and (b) IW-GRD-HR images at both 5km (red diamonds) and 12.5km (blue squares) grids for the Camargue site; (c) directions estimated from IW-GRD-HR images at 12.5km grid for the Wadden Sea. All percentages correspond to the application of a threshold $\mathrm{ME}^{\mathrm{TH}}$=10° (95% confidence level fixed).

Site	Sentinel-1 Data	Wind Field Output Resolution	NWM Data	Wind Direction RMSE [°]		Wind Direction MBE [°]		Wind Speed RMSE [m/s] [CMOD4]		Wind Speed MBE [m/s] [CMOD4]		Number Of Samples N	
				NoTH	TH	NoTH	TH	NoTH	TH	NoTH	TH	NoTH	TH
Camargue	EW subset	5km x 5km	SKIRON	23.8	20.6	-5.9	-7.4	4.4	4.2	1.2	1.4	8520	2431 (28.5%)
	IW subset			16.3	15.1	-5.4	-5.1	2.8	2.7	1.0	1.0	3789	3355 (88.5%)
	All			21.8	17.7	-5.7	-6.1	4.0	3.4	1.2	1.2	12309	5786 (47.0%)
	EW subset	12.5km x 12.5km	ECMWF	20.9	19.2	-8.4	-7.9	4.6	4.6	3.0	3.2	1503	1297 (86.3%)
	IW subset			18.9	18.9	6.8	6.7	4.6	4.6	2.8	2.8	560	557 (99.6%)
	All			20.4	19.1	-4.3	-3.6	4.6	4.6	3.0	3.1	2063	1854 (89.9%)
Wadden Sea	IW subset	12.5km x 12.5km	ECMWF	9.5	9.3	1.3	1.0	3.4	3.5	2.5	2.5	567	559 (98.6%)

Table 4.9. Wind direction and speed RMSE and MBE values from Sentinel-1 for Camargue and the Wadden Sea. The estimates are compared with SKIRON wind predictions at 5km and ECMWF wind re-analyses at 12.5km- without ("NoTH") and with ("TH") final threshold applied ME^{TH}=10° (with 95% confidence level fixed).

4.8 Discussion of the approach

The EODESM system facilitates the generation of LCCS2 categories from a diverse range of inputs and has additional capacity to translate these to habitat categories. An overview of the Scheme is provided in Figure 4.31.

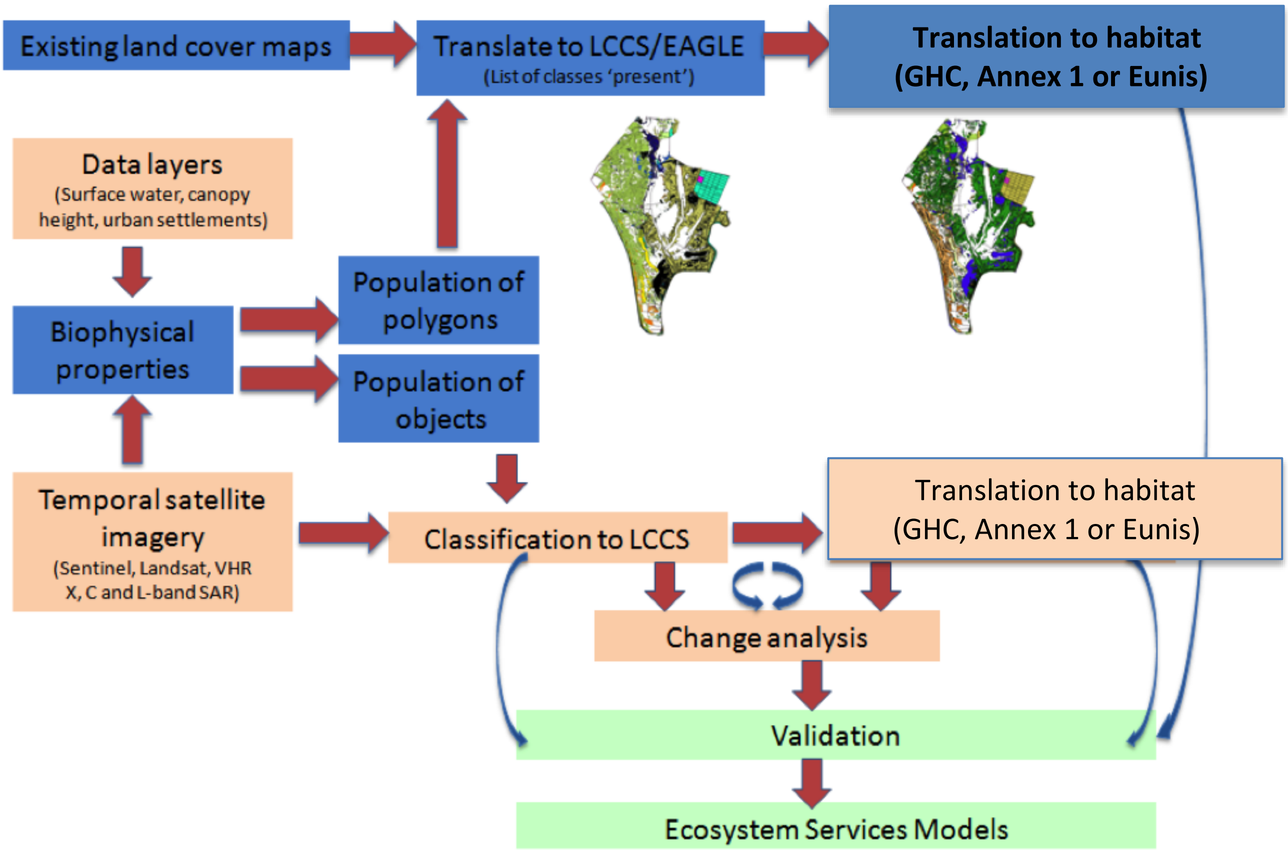

Figure 4.31. Schematic of the LCCS2 classification procedure showing the two main streams: (i) translation of existing land cover maps, or (ii) classification of LCCS2 classes using satellite imagery and input data layers. Following classification of LCCS2 Level 3 and 4 classes, these can be translated to habitat categories and used in change analysis.

The following sub- sections present the LCCS2 output maps. A unified legend is provided in Appendix 2.

4.8.1 Biophysical attributes

The approach within ECOPOTENTIAL has been to obtain (from existing sources) or retrieve (primarily from EO data) a diverse range of biophysical attributes for the protected areas. Such retrieval has only been possible over the past 3-5 years because of data availability and processing capability.

The public release of the Landsat archive from 1985 to the present has allowed multi-temporal classifications of components of the land surface to be undertaken at regional to global levels on a regular basis, with these including forest cover (Hansen et al. 2013), inundation (Hansen et al. 2013; Feng et al. 2016) and urban extent (Copernicus HRL: http://land.copernicus.eu/pan-european/GHSL/view). The introduction and greater availability of high performance computing and data storage facilities, including through cloud processing, has also allowed classification and time-series comparisons of these data and the retrieval of change summary layers (e.g., hydroperiod; Pekel et al., 2016) and forest losses and gains. In some cases (e.g., for forest cover), regular updates are being provided which allow ongoing monitoring of land surfaces.

The successful launch of the Sentinel-1 and 2 radar and optical data as well as the Landsat-8 Operational Land Imager (OLI) and their free provision to the global community has significantly increased the capacity for near daily observations of the earth's surface (cloud permitting and based on observation times). The acquisition of data in new wavelength regions (particularly the coastal and red edge bands) has also provided new opportunities for retrieving biophysical attributes of land surfaces but also for classification of components of land covers (e.g., plant lifeforms and dominant species).

In many countries, complete or partial coverage of airborne LIDAR data have been obtained, and open access provided in some cases, which has facilitated better discrimination of woody (forest and woody shrubs) from herbaceous vegetation, direct measurement of vegetation (stand) height and profiles and also canopy cover. Indirect estimates of above ground biomass have also been obtained. This information can significantly enhance the number and diversity of inputs to classification systems.

The increased willingness to develop and share software (e.g., for pre-processing of satellite sensor data, image analysis) has provided capacity to create end-to-end processes for retrieving biophysical attributes, classifying land covers, detecting change and quantifying uncertainty. The release and sharing of processing tools (e.g., through the Google Earth Engine) has also increased the willingness and ability of groups and individuals to generate outputs from Landsat and Sentinel data in particular.

4.8.2 Classification of land covers

The classification of land covers through the EODESM system is a new approach that differs from the majority of those that have occurred previously for the following reasons.

Most land cover classifications have focused on the use of one or several images, mainly from either spaceborne optical or radar data. In seasonal environments, images acquired during the pre-flush and peak-flush period are used to classify vegetation whilst snow cover classifications, for example, might use several (daily to weekly) images acquired from the start to the end of the snow covered period. In less seasonal environments (e.g., areas occupied by deserts or tropical forests), images from any season can generally be used although this depends upon cloud cover, with drier season imagery often used in the case of many tropical regions.

Whilst a wide range of classification algorithms have been developed, these broadly consist of those that are unsupervised or supervised, with these applied to one or several images from single or multiple sensors. In the former case, no training data are used to support the classification although data from the ground or high resolution imagery (for example) are typically referenced for validating the output maps. For supervised classifications, including using machine-learning algorithms, training data are essential. However, given the complexity of many land covers, the training classes are often very broad. For example, many will focus on discriminating broadleaved evergreen forests but there is limited capacity to provide more information on, for example, canopy cover and height within the same classification. This is because the number of classes that required training data exceeds the capacity of the EO data or the ability or willingness of users to collect the required amount of information needed for training at the ground level. Hence, many classifications, particularly those generated at national, regional or country levels, use relatively broad taxonomies, with these including the global land cover maps (e.g., GlobeLand30; Jun et al. 2014), the European Corine Land Cover (http://land.copernicus.eu/pan-european/corine-land-cover/view) and the Land Cover Maps for the United Kingdom. Several studies have based classifications on the FAO LCCS2 system but have generally taken training data for areas that represent some classes associated with different levels of the LCCS2 (e.g., broadleaved evergreen forests).

The EODESM system has taken the approach of using information that is now available from a diverse range of sources, including EVs and thematic classifications. The data layers used in the classification have been generated by experts that have often dedicated years or even decades to formulate algorithms and approaches for their retrieval and are often fine-tuned at particular scales, whether local or global. Increasingly, the output products are of finer spatial resolution and some are even generated at < 1 m resolution particularly when airborne data (e.g., LIDAR) are used. The advantage of the EODESM system, and particularly the LCCS2 taxonomy, is that it can be applied at any scale. Hence, LCCS2 classifications have been generated from both Sentinel-2 and RapidEye data.

Within the EODESM system, layers representing several retrieved environmental variables are used directly in the classification of land covers, with these including canopy height and cover, water and snow hydroperiods and urban density. Several of these layers are available at the global or European level and so all protected areas are classified using a dataset that has been generated using the same algorithm and consistently within and between protected areas and also their surrounds. Many of the data layers will continue to be generated in future years (e.g., hydroperiod), even though some projects may have come to an end. What is certain is that many of the products will be generated routinely, particularly given the ongoing promise of Sentinel and Landsat availability for several decades to come. Data from future satellite sensors (e.g., JEDI, BIOMASS) may also contribute to generation of biophysical layers (canopy height and AGB) for use in EODESM. As well as providing input to classifications, these products also play a major role in the detection and description of change.

The environmental layers that are used in the classification are continuous in nature (e.g., canopy cover in percent, height in metres, hydroperiod in days, water turbidity) and are summarised into discrete classes automatically within the EODESM system. However, the system also requires thematic classifications (e.g., of leaf type, water state, unconsolidated material). These can be generated from unsupervised or supervised classifications of specific components of the landscape and using any available algorithm. For example, leaf type would only be classified in vegetated areas but not non-vegetated areas where information on the different types of unconsolidated material is needed. Such an approach to classification is greatly assisted by the hierarchical nature of the LCCS2 system.

Once all layers have been generated, with these amounting to about 24 for a full classification, each of the pixels or objects can be associated with environmental variables (referred to as attributes) that are not used in the classification. Multiple types and sources of information can be attributed to the classification, with this practically assisted by the use of the raster attribute tables associated with the KEA format (Bunting & Gillingham, 2013). Such variables include above ground biomass, species types, coloured dissolved organic matter (CDOM) and even wind speed and direction. These variables can then be collected over time and added into the attribute table as needed. For example, a forest may be classified and the attributes might include phenology (which varies regularly over the year) or above ground biomass (which decreases or increases depending on disturbance events/processes or growth). These layers can also be used to support further classifications (e.g., of species types) and to facilitate translation to other taxonomies, including those relating to habitat categories.

A recognised limitation of the system is that the input layers may be generated for different times and at different spatial resolutions or modes (e.g., hydro-period retrieved from optical, radar or both). In Hardangervidda, for example, snow cover data are provided daily whilst lichen cover is obtained using temporal Landsat sensor data acquired through the snow cover period. The difference in spatial resolution does, of course, compromise the classification but how else can the snow cover information be obtained to address issues such as lichen availability to reindeer in this particular case. It is therefore better to use all of the available information to address an issue, particularly given the increased urgency to do so in light of population increases and climate change. The EODESM system provides capacity to achieve this. A further potential issue is that the classifications are far too detailed for purpose. However, the advantage of the system is that the classifications can be made broader as and when required. Furthermore, by having access to the full range of retrieved environmental variables with a single file (i.e., the KEA), then a class can be associated with multiple subclasses. For example, a flooded forest can be described by its cover (which would give it a two dimensional description) but also by its hydroperiod (which then increases the dimensions of description; Figure 4.32).

(a) (b)

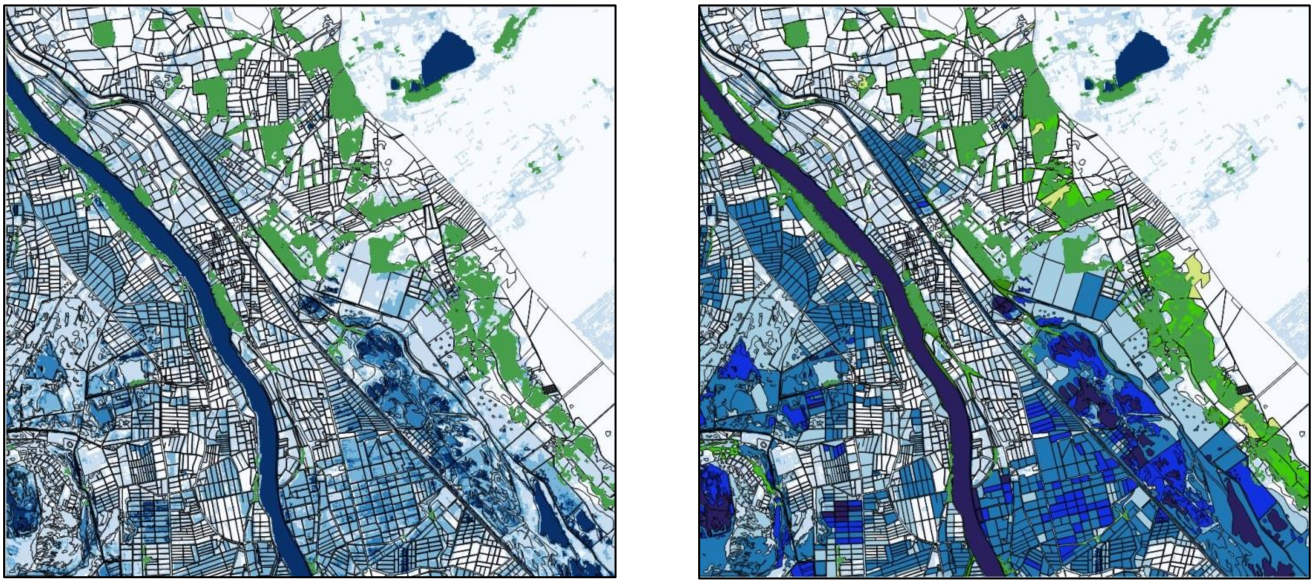

Figure 4.32 (a) Continuous layers of hydroperiod (blue) and canopy cover (green) for a section of the Camargue and (b) the classes generated from these continuous layers. Note that, if flooded, the forest can be described in terms of its hydroperiod in addition to its cover.

4.8.3 Assessment of accuracy

The classes generated by the EODESM system are detailed and comprehensive but the validity of each is complex to describe. For this reason, validation of the individual and different components of the class codes is advocated. A limitation is that many in situ measurements that already exist often only record part of the class code and, for this reason, future validation needs to focus on all components of the code. By assessing the accuracy of each component separately, the overall accuracy of the combined class can be calculated depending on which components are contributing. The assessment of the accuracy of biophysical variables (including those used as input to the EODESM system) could contribute to evaluate the accuracy of the components of each class associated with each object. Confusion matrices and more involved algorithms (e.g. Olofsson et al.; 2013; 2014) can be generally applied.

5. Summary: how the Virtual Laboratory can access data, variables, modules

For the protected areas considered by the ECOPOTENTIAL project, a wide range of biophysical variables have been retrieved for all or for a select few (Section 3). These biophysical variables as well as thematic classifications of several land cover components (e.g., lifeform, bare surfaces) have been used as input to the EODESM system to classify land covers but also included as attributes associated with pixels/objects for use in other WPs. The EODESM system has generated detailed and very comprehensive classifications of land covers, that can be translated into habitats, for the PAs and also their surrounds. The legends are complex but highly interpretable and can be reduced to avoid confusion where necessary.

All input data and thematic layers as well as output products (variables) described in D4.2, and their associated metadata, are available on the ECOPOTENTIAL ftp repository site. These products will be updated up to Month 40 (end of WP4). The VL can access the ftp site and then all products.

Concerning the modules used/developed for variables and land cover production, Table 5.1 summarizes those that WP4 Partners will provide to the VL, according to the information collected so far. The Table includes the TRL index (see Appendix 4, section 11); the internet or web based interface that will be used for making the modules accessible by the VL. Additional modules may be provided by the end of the project through WPS.

Modules for retrieving/mapping:	**Lead**	**TRL**	**WHEN Month**	**Internet interface**	**WEB based interface**		
				FTP	**GitHub**	**WPS**	**http**
Vegetation moisture content	UPS	3	M30	O			
Snow cover	STARLAB	3	M30	O		O	
Shoreline delineation	STARLAB	3	M30	O		O	
Land Cover from Radar data (*data driven*)	DLR	3	M30	O			
Vegetation Phenology -1	UAB	4	M32		O		
Vegetation Phenology -2	CERTH	4	M32		O		
Albedo	FORTH	4	A				http://rslab.gr/downloads_blue_sky.html
Hydroperiod and seasonality	CERTH	4	M32		O		
Wind fields	CNR	4	M32			O	
Invasive Plant Species detection	CNR	4	M32			O	
Life Form	UNSW	5	M32				O
Land Surface Temp.	FORTH	5	A				http://rslab.gr/downloads_lst.html
Water extent and uncertainty estimation	CERTH	5	M36		O		
Landscape indicators and uncertainty estimation	CERTH	5	M36		O		
Water turbidity and sediment	UNSW	5	M36				O
R-Package "phenex" for deriving phenological metrics	UFZ	7	A				(https://cran.r-project.org/)
EODESM	UNSW	9	M36				O

Table 5.1. Modules accessible through the Virtual Laboratory (VL). A for Available

6. Conclusions

A key advance within ECOPOTENTIAL has been the concept that the EODESM classification system, which is open source, provides a unified framework for ecosystem monitoring ready for end users. The system does not require any modification by the user but, instead, the user has the opportunity to develop or obtain their own output layers/variables by whatever means they consider the most reliable (i.e., of the greatest accuracy). These data can be obtained from EO, with different knowledge driven or data driven techniques, but also from other sources, including knowledge, modelled outputs and Copernicus strata or existing data. This is in line with the main achievement of Deliverable D11.1, which states that: “The results of the online survey show that for PA managers online format of communication was considered more efficient than printed and oral communication. Especially maps and graphics are seen as useful when provided online”. Consequently, ECOPOTENTIAL can provide tools and products that can easily support decision-making. The LCCS2 taxonomy supports classification from EO data and associated information. Future work is also considering the translation of FAO-LCCS2 to the new FAO Land Cover Meta Language (LCML), with this being undertaken in coordination with the SWOS project. The EODESM system also accommodates for change and the approaches will be described in Deliverable 4.3.

7. References

Anding, D., Kauth R. (1970). Estimation of sea surface temperature from space. Remote Sensing of the Environment, vol. 1, pp. 217–220. doi: 10.1016/S0034-4257(70)80002-5.

Adamo, M., Tarantino, C., Tomaselli, V., Kosmidou V., Petrou Z., Manakos, I., Licas, R.M., Mucher, C. A., De Pasquale, V., Blonda, P. (2014). Expert knowledge for translating land cover/ use maps to General Habitat Categories (GHCs). Landscape Ecology, Vol. 29 (6), pp. 104-1067. DOI: 10.1007/s10980-014-0028-9.

Adamo, M., Tarantino, C., Lucas, R.M., Tomaselli, V., Sigismondi, A., Mairota, P., Blonda, P. (2015). Combined use of expert knowledge and earth observation data for the land cover mapping of an Italian grassland area: An EODHaM system application. Geoscience and Remote Sensing Symposium (IGARSS), pp. 3065 – 3068. ISBN: 978-1-4799-7929.

Adamo, M., Tarantino, C., Tomaselli, V., Veronico, G., Nagendra, H., Blonda, P. (2016). Habitat mapping of coastal wetlands using expert knowledge and Earth observation data. *Journal of Applied Ecology*, Vol. 53, pp. 1521-1532. DOI: 10.1111/1365-2664.12695.

Bahmanyar, R., Datcu, M., Dumitru, O., Espinoza-Molina, D., Schwarz, G., Hummel, C., Hummel, H., Blonda, P., Diaz-Delgado, R. (2017). Analysis of Protected Areas: The Use of Satellite Images for Data Mining within ECOPOTENTIAL. Proceedings of WorldCover, Rome, online.

Balenzano, A., Mattia, F., Satalino, G., Davidson, M. W. J. (2011), Dense temporal series of C- and L-band SAR data for soil moisture retrieval over agricultural crops, *IEEE Jou. of Selected Topics in Applied Earth Obs. and Remote Sensing (J-STARS)*, Vol. 4, No. 2, pp. 439-450, DOI: 10.1109/JSTARS.2010.2052916.

Balenzano, A., Satalino, G., Lovergine, F., Rinaldi, M., Iacobellis, V., Mastronardi, N., Mattia, F. (2013). On the use of temporal series of L- and X- band SAR data for soil moisture retrieval. Capitanata plain case study. *European Jou. of Remote Sensing*, Vol. 46, pp. 721-737, 2013, DOI: 10.5721/EuJRS20134643.

Berthon, J.F., Zibordi, G. (2004). Bio-optical relationships for the northern Adriatic Sea. *International Journal of Remote Sensing*, 25(7-8), 1527-1532. doi:10.1080/01431160310001592544.

Brockmann, C., Doerffer, R., Sathyendranath, S., Ruddick, K., Brotas, V., Santer, R. & Pinnock, S. (2012). The CoastColour dataset. In *Geoscience and Remote Sensing Symposium* (IGARSS), 2012 IEEE International, pp 2036-2039. IEEE. doi:10.1109/IGARSS.2012.6350976.

Bukata R.P., Jerome, J.H., Kondratyev, A.S., Pozdnyakov, D.V. (1995). Optical properties and remote sensing of inland and coastal waters. CRC, 1995. ISBN: 0849347548

Bunting, P., & Gillingham, S. (2013). The KEA image file format. Computers & Geosciences, 57, 54–58. https://doi.org/10.1016/j.cageo.2013.03.025.

Bustamante, J., Paciso F., Diaz-Delagado R., et al. (2009). Predictive models of turbidity and water depth in the Doñana marshes using Landsat TM and ETM+ image, *Journal of Environmental Management*, Vol. 90, pp 2219-2225. http://dx.doi.org/10.1016/j.jenvman.2007.08.021

Canny, J. (1986). A computational approach to edge detection. *IEEE Transactions on pattern analysis and machine intelligence*, 6, 679-698.

Carroll, M., Townshend, J., DiMiceli, C., Noojipady, P., Sohlberg, R. (2009). A New Global Raster Water Mask at 250 Meter Resolution. *International Journal of Digital Earth*, 2 (4).

Congalton, R.G. (1988). Using spatial autocorrelation analysis to explore the errors in maps generated from remotely sensed data. *Photogramm. Eng. Remote Sens*. 54, 587–592.

Doerffer R., Sørensen, K., Aiken, J., 2009. MERIS potential for coastal zone applications. *Intenational Journal of remote sensing*, 1999, vol. 20, no. 9, 1809-1818. doi: 10.1080/014311699212498.

Dumitru, G., Schwarz, D. Espinoza-Molina, M. Datcu, H. Hummel, and C. Hummel, (2017), Classification and Semantic Annotation of Extended Wadden Sea Features Using SAR Images and their Environmental Interpretation, *International Journal of Remote Sensing*, submitted.

Dumitru G., Schwarz, G., and Datcu, M. (2016), Land Cover Semantic Annotation Derived from High-Resolution SAR Images, *IEEE Journal of Selected Topics in Applied Earth Observations and Remote Sensing*, vol. 9(6), pp. 2215-2232.

Dumitru O., Schwarz, G., Espinoza-Molina, D., Datcu, M., Hummel, H., Hummel, C. (2017), "Classification and Semantic Annotation of Extended Wadden Sea Features Using SAR Images and their Environmental Interpretation". Submitted to *International Journal of Remote Sensi*ng.

EMODnet Bathymetry Consortium (2016). EMODnet Digital Bathymetry (DTM). EMODnet Bathymetry. doi:10.12770/c7b53704-999d-4721-b1a3-04ec60c87238.

Escuin, et al. (2008). Fire severity assessment by using NBR (Normalized Burn Ratio) and NDVI (Normalized Difference Vegetation Index) derived from LANDSAT TM/ETM images. *International Journal of Remote Sensing*, 29 (4), 1053–1073.

Espinoza-Molina, D., Manilici, V., Dumitru, O., Reck, C., Cui, S., Rotzoll, H., Hofmann, M., Schwarz, G., and Datcu, M. (2016), "The Earth Observation Image Liberian (EOLIB): The Data Mining Component of the TerraSAR-X Payload Ground Segment", in *Proceedings of BiDS*, Santa Cruz de Tenerife, pp. 228-231.

Espinoza-Molina D., Bahmanyar, R., Diaz-Delgado, R., Bustamante, J., and Datcu, M. (2017). Land Cover Change Detection Using Local Feature Descriptors Extracted from Spectral Indices, submitted to *IGARSS 2017.*

Falldorf, et al. (2014). Estimating lichen volume and reindeer winter pasture quality from Landsat imagery, *Remote Sensing of Environment*, 140 (2014) 573–579.

Falldorf, et al., (2015). Corrigendum for the paper "Estimating lichen volume and reindeer winter pasture quality from Landsat imagery, *Remote Sensing of Environment*, 140, 573–579

FAO (2005). Land Cover Classification System. Classification Concepts and user manual. Software version 2. FAO Rome.

Feng, M., Sexton, J.O., Channan, S. and Townshend, J.R. (2016). A Global, High-Resolution (30 m) Inland Water Body Dataset for 2000: First Results of a Topographic-Spectral Classification Algorithm.' International Journal of Digital Earth, 9 2, 113-133. doi:10.1080/17538947.2015.1026420.

Fieber, et al. (2014). Effective LAI and CHP of a Single Tree From Small-Footprint Full-Waveform LiDAR. IEEE Geoscience and Remote Sensing Letters, 11, No 9, pp 1634-1638.

Fieber et al. (2016). CHP Toolkit: Case Study of LAIe Sensitivity to Discontinuity of Canopy Cover in Fruit Plantations, IEEE Transactions of Geoscience and Remote Sensing, in press.GEO BON , 2015. GEO BON (2015) An Essential Biodiversity Variable Approach to Monitoring Biological Invasions: Guide for Countries. At: http://www.geobon.org/Downloads/reports/GEOBON/2015/MonitoringBiologicalInvasions.pdf

Gavish, Y., O'Connell, J., Marsh, C.J., Tarantino, C., Blonda, P., Tomaselli, V., Kunin, W.E. (2017). Comparing the performance of flat and hierarchical habitat/land-cover classification models in a Natura 2000 site. Submitted to *ISPRS Journal of Photogrammetry and Remote Sensing.*

Gond, V. , Bartholomé, E., Ouattara, F., Nonguierma, A., Bado, I. (2011). Surveillance et cartographie des plans d'water et des zones humides et inondables en régions arides avec l'instrument VEGETATION embarqué sur SPOT-4. International Journal of Remote Sensing, 25, pp. 987–1004. Pekel, J. - F. ; Cressman, K. ; Ceccato, P. ; Vancutsem, C. ; Vanbogaert, E. ; Defourny, P. Development and application of multi-temporal colorimetric transformation to monitor vegetation in the desert locust habitat. *Journal of Selected topics in Applied Earth Observations and Remote Sensing*, 4, 318-326.

Hall, D.K., and Riggs, G.A. (2016). MODIS/Terra Snow Cover 8-Day L3 Global 500 m Grid, Version 6. Boulder, Colorado, USA. *NASA National Snow and Ice Data Center Distributed Active Archive Center*. Doi: http://dx.doi.org/10.5067/MODIS/MOD10A2.006.

Hansen, M.C., Potapov, P.V., Moore, R., Hancher, M., Turubanova, S.A., Tyukavina, A., Thau, D., Stehman, S.V., Goetz, S.J., Loveland, T.R., Kommareddy, A., Egorov, A., Chini, L., Justice, C.O., and Townshend, J.R.G. (2013). High-Resolution Global Maps of 21st-Century Forest Cover Change: *Science*, 342, no. 6160, p. 850-853, at http://www.sciencemag.org/content/342/6160/850.abstract

IOCCG (2006). Remote sensing of inherent optical properties: Fundamentals, tests of algorithms, and applications. In Z. P. Lee (Ed.), Reports of the *International Ocean-Colour Coordinating Group*: IOCCG, 122.

Jiang, et al, 2008, Development of a two-band enhanced vegetation index without a blue band, Remote Sensing of Environment, 112, pp. 3833–3845.

Jun, C., Yifang, B., Songnian, L. (2014). China: Open access to Earth land-cover map. *Nature*, 514(7523), 434.

Langanke, T., Büttner, G., Dufourmont, H., Iasillo, D., Probeck, M., Rosengren, M., Sousa, A., Strobl, P. and Weichselbaum, J. (2013). GIO land (GMES/Copernicus initial operations land) High Resolution Layers (HRLs) – summary of product specifications. ESA GIO Land Team. 16p.

Lefsky, M.A. (2010). A global forest canopy height map from the Moderate Resolution Imaging Spectroradiometer and the Geoscience Laser Altimeter System. Geophysical Research Letters, 37, 15.

Lucas R., Blonda P., Bunting P., Jones G., Inglada J., Arias M., Kosmidou V., Petrou Z., Manakos I., Adamo M., Charnock R., Tarantino C., Mucher C.A., Jongman R., Kramer H., Arvor D., Honrado J., Mairota P., 2014. The Earth Observation Data for Habitat Monitoring (EODHaM) System, JAG *International Journal of Applied Earth Observation and Geoinformation, Special Issue on earth observation*, Vol. 37, pp. 17-28, November 2014, doi:10.1016/j.jag.2014.10.011.

Maes, J., Teller, A. Markus, E. M. Murphy, P.; Paracchini, M. L., Barredo, J.I, Grizzetti, B., Cardoso, A., Somma, F., Petersen, J.E., Meiner, A., Gelabert, E.R., Zal, N.; Kristensen, P.;Bastrup-Birk, A.; Biala, K.;Romao, C.;Piroddi, C.; Egoh, B.; Fiorina, C.; Santos, F.; Naruševičius, V.; Verboven, J.; Pereira, H.; Bengtsson, J.; Kremena, G.; Pedroso, C.M.; Snäll, T.; Estreguil, C.; San Miguel, J.; Braat, L.; Grêt-Regamey, A.; Perez-Soba, M.; Degeorges, P.; Beaufaron, G.; Lillebø, A.; Abdul Malak, D.; Liquete, C.; Condé, S.; Moen, J.; Östergård, H.; Czúcz, B.; Drakou, E.G.; Zulian, G.; Lavalle, C. (2014). Mapping and Assessment of Ecosystems and their Services (MAES). Indicators for ecosystem assessments under Action 5 of the EU Biodiversity Strategy to 2020. *Second Technical Report (2014-080).* Publications office of the European Union, Luxembourg. DOI: 10.2779/75203.

Kallos, G., Nickovic, S., Papadopoulos, A., Jovic, D., Kakaliagou, O., Misirlis, N., ... and Anadranistakis, E. (1997). The regional weather forecasting system SKIRON: An overview. In Proceedings of the symposium on regional weather prediction on parallel computer environments (Vol. 15, p. 17).

Kosmidou, V., Petrou, Z., Bunce, R.G., Mucher, C., Jongman, R.H., Bogers, M.M., Lucas, R.M., Tomaselli, V., Blonda, P., Pado-Schioppa, E., Manakos, I. and Petrou, M. (2013). Harmonization of the Land Cover Classification System (LCCS2) with the General Habitat Categories (GHC) classification system. Ecological Indicators, 36, 290-300.

McGeoch, M.A. and Squires, Z.E. (2015). An Essential Biodiversity Variable approach to monitoring biological invasions: Guide for Countries. GEO BON Technical Series 2, 13 pp. At:

http://www.geobon.org/Downloads/reports/GEOBON/2015/MonitoringBiologicalInvasions.pdf

Merchant, C.J., Le Borgne, P., Marsouin, A., Roquet, H. (2008). Optimal estimation of sea surface temperature from split-window observations, *Remote Sensing of Environment*, 112(5), 2469-2484. doi:10.1016/j.r2007.11.011.

Morel, A., Prieur, L. (1977). Analysis of variations in ocean color. *Limnology and Oceanography*, 22(4): 709–722. doi: 10.4319/lo.1977.22.4.0709.

Nagler, T., Rott, H. (2000). Retrieval of Wet Snow by Means of Multitemporal SAR Data, IEEE Trans. On *Geosc. And Rem. Sens*., 18 (2), 754-763.

Nardelli, B.B., Tronconi, C., Pisano, A., Santoleri, R., 2013. High and Ultra-High resolution processing of satellite Sea Surface Temperature data over Southern European Seas in the framework of MyOcean project. Remote Sensing of Environment, 129, 1-16. doi:10.1016/j.rse.2012.10.012.

Odermatt, D., Gitelson, A., Brando, V., Schaepman, M. (2012). Review of constituent retrieval in optically deep and complex waters from satellite imagery. *Remote Sensing of Environment*, 118: 116-126. doi: 10.1016/j.rse.2011.11.013.

Olofsson, P., Foody, G. M., Herold, M., Stehman, S. V., Woodcock, C. E., & Wulder, M. A. (2014). Good practices for estimating area and assessing accuracy of land change. *Remote Sensing of Environment*, 148, 42–57.

Olofsson, P., Foody, G. M., Stehman, S. V., & Woodcock, C. E. (2013). Making better use of accuracy data in land change studies: Estimating accuracy and area and quantifying uncertainty using stratified estimation. *Remote Sensing of Environment,* 129, 122–131.

Otsu, N. (1975). A threshold selection method from gray-level histograms. Automatica, 11(285-296), 23-27.

Pasolli, L., Notarnicola, C., Bertoldi, G., Bruzzone, L., Remelgado, R., Greifeneder, F. , Niedrist, G., Della Chiesa, S., Tappeiner, U., Zebisch, M. (2015). Estimation of soil moisture in mountain areas using SVR technique applied to multiscale active radar images at C band, *IEEE Journal of Selected Topics in Applied Earth Observations and Remote Sensing*, Vol. 8, No. 1, pp. 262-283.

Pekel, J., Cottam, A., Gorelick, N. and Belward, A.S. (2016). High-resolution mapping of global surface water and its long-term changes. Nature, 540, 418-422;

Petrou, Z., Kosmidou, V., Manakos, I., Stathaki, T., Adamo, M., Tarantino, C., Tomaselli, V., Blonda, P. , Petrou. M. (2014). “A rule-based classification methodology to handle uncertainty in habitat mapping employing evidential reasoning and fuzzy logic”, Pattern Recognition Letters – doi: http://dx.doi.org/10.1016/j.patrec.2013.11.002, Special Issue: MP, Vol. 48, pp. 24-33, I.F. = 1.586.

Pisano, A., Nardelli, B. B., Tronconi, C., Santoleri, R. (2016). The new Mediterranean optimally interpolated pathfinder AVHRR SST Dataset (1982–2012). *Remote Sensing of Environment*, 176, 107-116. doi:10.1016/j.rse.2016.01.019.

Potapov, P., Yaroshenko, A., Turubanova, S., Dubinin, M., Laestadius, L., Thies, C., Aksenov, D., Egorov, A., Yesipova, Y., Glushkov, I., Karpachevskiy, M., Kostikova, A., Manisha, A., Tsybikova, E., Zhuravleva, I. 2008. Mapping the World's Intact Forest Landscapes by Remote Sensing. *Ecology and Society*, 13 (2)

Poulin B., Davranche A. & Lefebvre G. (2010). "Ecological assessment of Phragmites australis wetlands using multi-season SPOT-5 scenes. *Remote Sensing of Environment.* 114: 1602-1609.

Rana, F. M., Adamo, M., Pasquariello, G., De Carolis, G., & Morelli, S. (2016). LG-Mod: a modified local gradient (LG) method to retrieve SAR sea surface wind directions in marine coastal areas. Journal of Sensors, 2016. http://dx.doi.org/10.1155/2016/9565208.

Rana, F.M., Adamo, M., Richard, L., Blonda, P. (2017). Sea Surface Winds Retrieval from ESA Sentinel-1 Data. Under revision, *Remote Sensing of Environment* on 17 Feb. 2017.

Santoro, M., Beaudoin, A., Beer, C., Cartus, O., Fransson, J.E.S., Hall, R.J., Pathe, C., Schmullius, C., Schepaschenko, D., Shvidenko, A. et al. (2015). Forest growing stock volume of the northern hemisphere: Spatially explicit estimates for 2010 derived from Envisat ASAR. *Remote Sensing of Environment*, 168, 316-334.

Sexton, J. O., Song, X.-P., Feng, M., Noojipady, P., Anand, A., Huang, C., Kim, D.-H., Collins, K.M., Channan S., DiMiceli, C., Townshend, J.R.G. (2013). Global, 30-m resolution continuous fields of tree cover: Landsat-based rescaling of MODIS Vegetation Continuous Fields with lidar-based estimates of error. *International Journal of Digital Earth*, 130321031236007. doi:10.1080/17538947.2013.786146.

Shepherd, J.D., Bunting, P. and Dymond, J.R. (2015). Operational large-scale segmentation of imagery based on iterative elimination. *Journal of Applied Remote Sensing*.

Shimada, M., Itoh, T., Motooka, T., Watanabe, M., Tomohiro, S., Thapa, R. and Lucas, R. (2014). New global forest/non-forest maps from ALOS PALSAR data (2007-2010). *Remote Sensing of Environment*, 155, 13-31.

Simard, M., Pinto, N., Fisher, J. B., and Baccini, A. (2011), Mapping forest canopy height globally with spaceborne lidar, *J. Geophys. Res*., 116, G04021, doi:10.1029/2011JG001708.

Small, D., Schubert, A. (2008). Guide to ASAR geocoding. Issue, 1(19.03).

Tarantino, C., Adamo, M., Lucas, R., Blonda P. (2016). Detection of changes in semi-natural grasslands by Cross Correlation Analysis with WorldView-2 images and new Landsat 8 data. *Remote Sensing of Environment*. Vol. 175, 15 March 2016, Pages 65–72, DOI:10.1016/j.rse.2015.12.031.

Tomaselli, V., Panayotis, D., Marangi, C., Kallimanis, A., Adamo, M., Tarantino, C., Panitsa, M., Terzi, M., Veronico, G., Lovergine, F., Nagendra, H., Lucas, R., Mairota, P., Mucher ,S., Blonda, P. (2013). Translating land cover/land use classifications to habitat taxonomies for landscape monitoring: a Mediterranean assessment, *Landscape Ecolog*y, Vol. 28, Issue 5, pp 905-930.

Tomaselli, V., Adamo, M., Veronico, G., Sciandrello, S., Tarantino, C., Dimopoulos, P., Medagli, P., Nagendra, H., Blonda, P.. **(2016)**. Definition and application of expert knowledge on vegetation pattern, phenology and seasonality for habitat mapping, as exemplified in a Mediterranean coastal site, *Plant Biosystems*, pp. 1-13, doi: 10.1080/11263504.2016.1231143, I.F.=1.360

Volpe, G., Santoleri, R., Vellucci, V., d'Alcalà, M. R., Marullo, S., d'Ortenzio, F. (2007). The colour of the Mediterranean Sea: Global versus regional bio-optical

Zhu, Z., Wang, S., Woodcock, C.E. (2015). Improvement and expansion of the Fmask algorithm: cloud, cloud shadow and snow detection for Landsats 4-7, 8 and Sentinel 2 images. *Remote Sensing of Environment*, 159, pp. 269-277.

8. Appendix 1. Work flows for retrieving terrestrial and marine environmental variables.

8.1 Canopy height, LAI and additional vegetation metrics

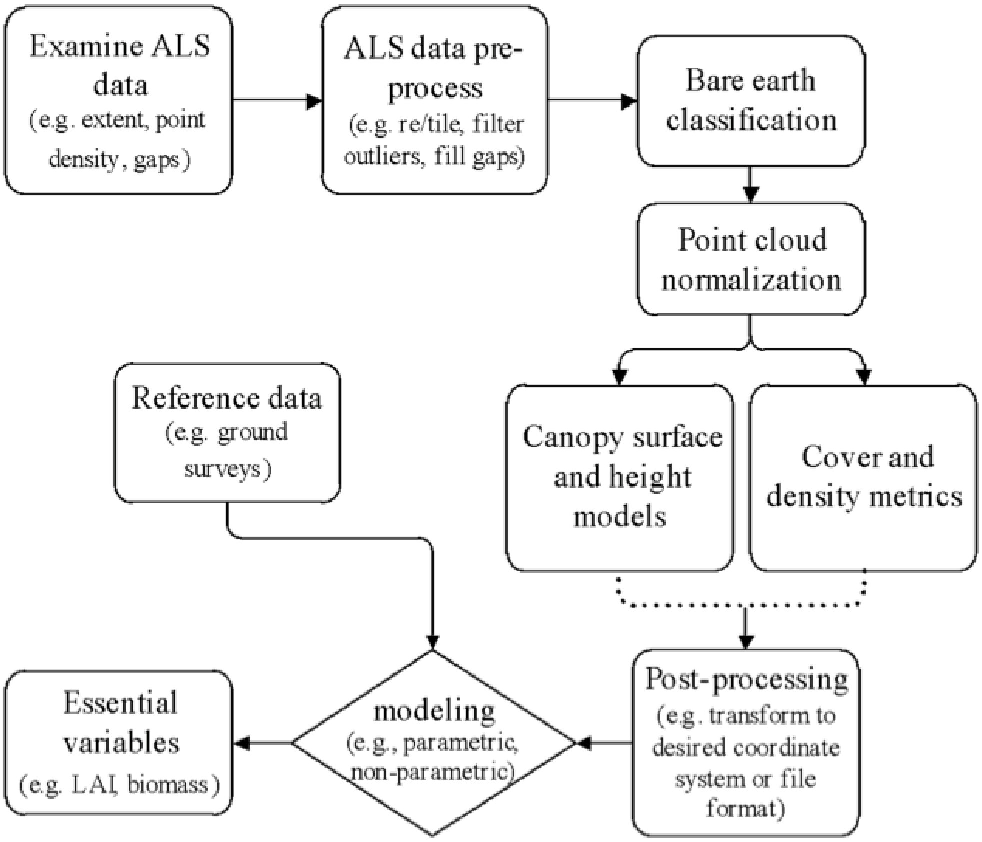

Figure 8.1. EV modelling from LiDAR data

8.2 Vegetation phenology

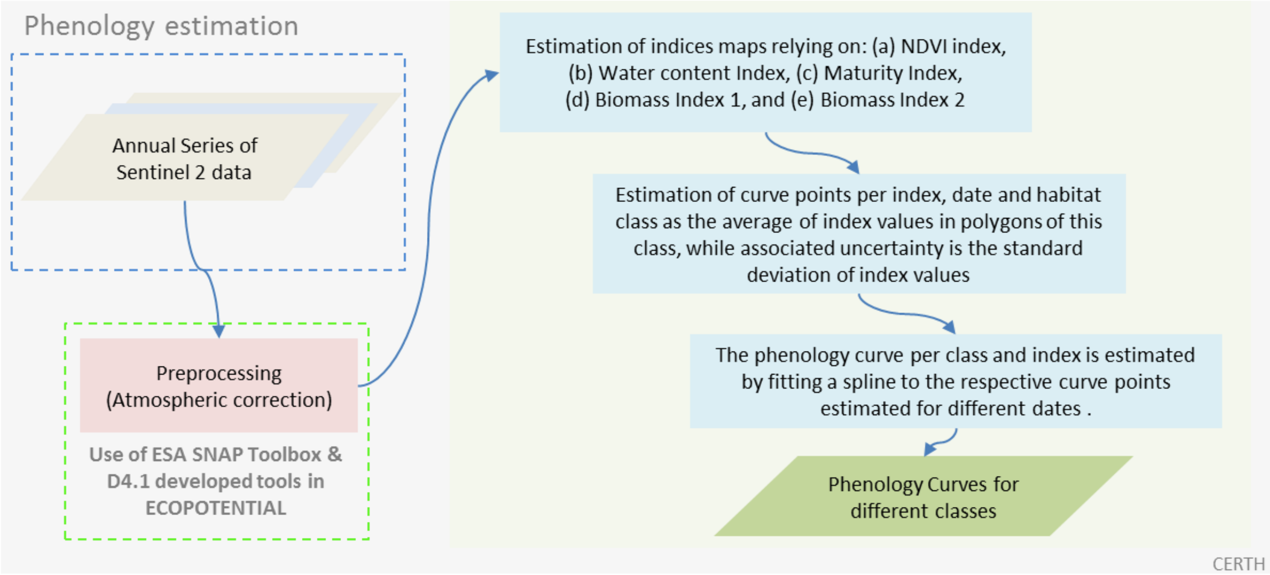

Figure 8.2. Phenology estimation

8.3 Invasive species

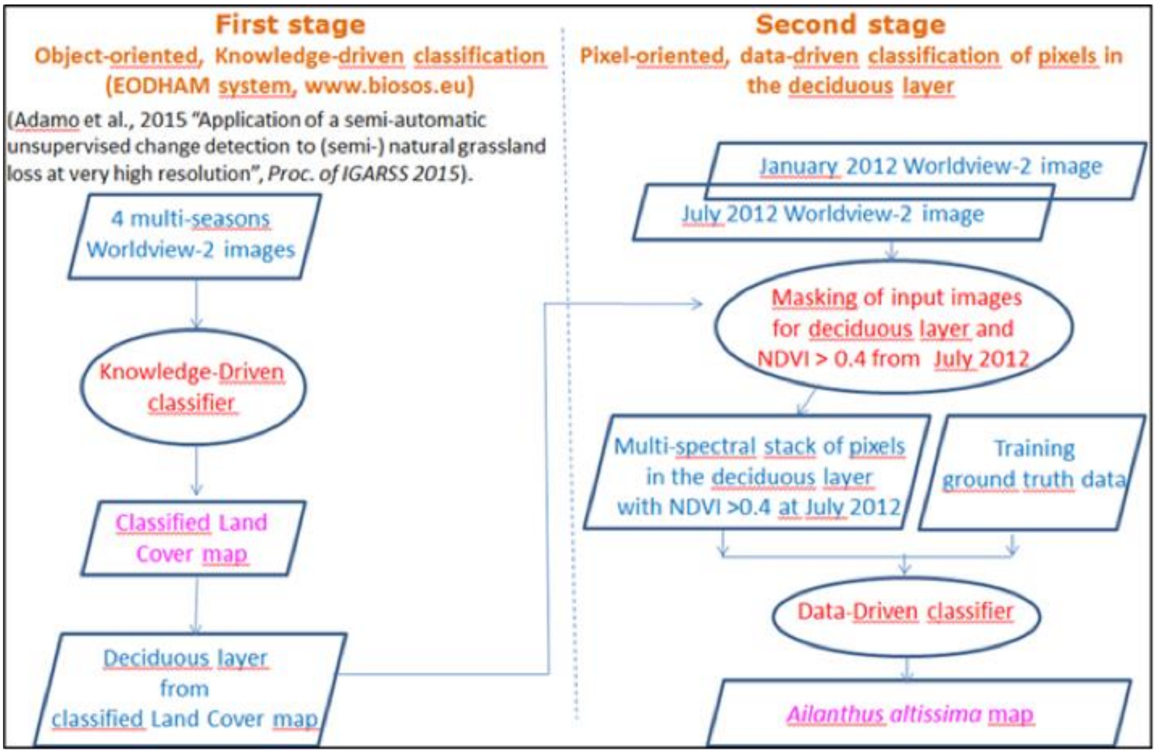

Figure 8.3. Two-stage classification of invasive species detection

8.4 Herbaceous biomass

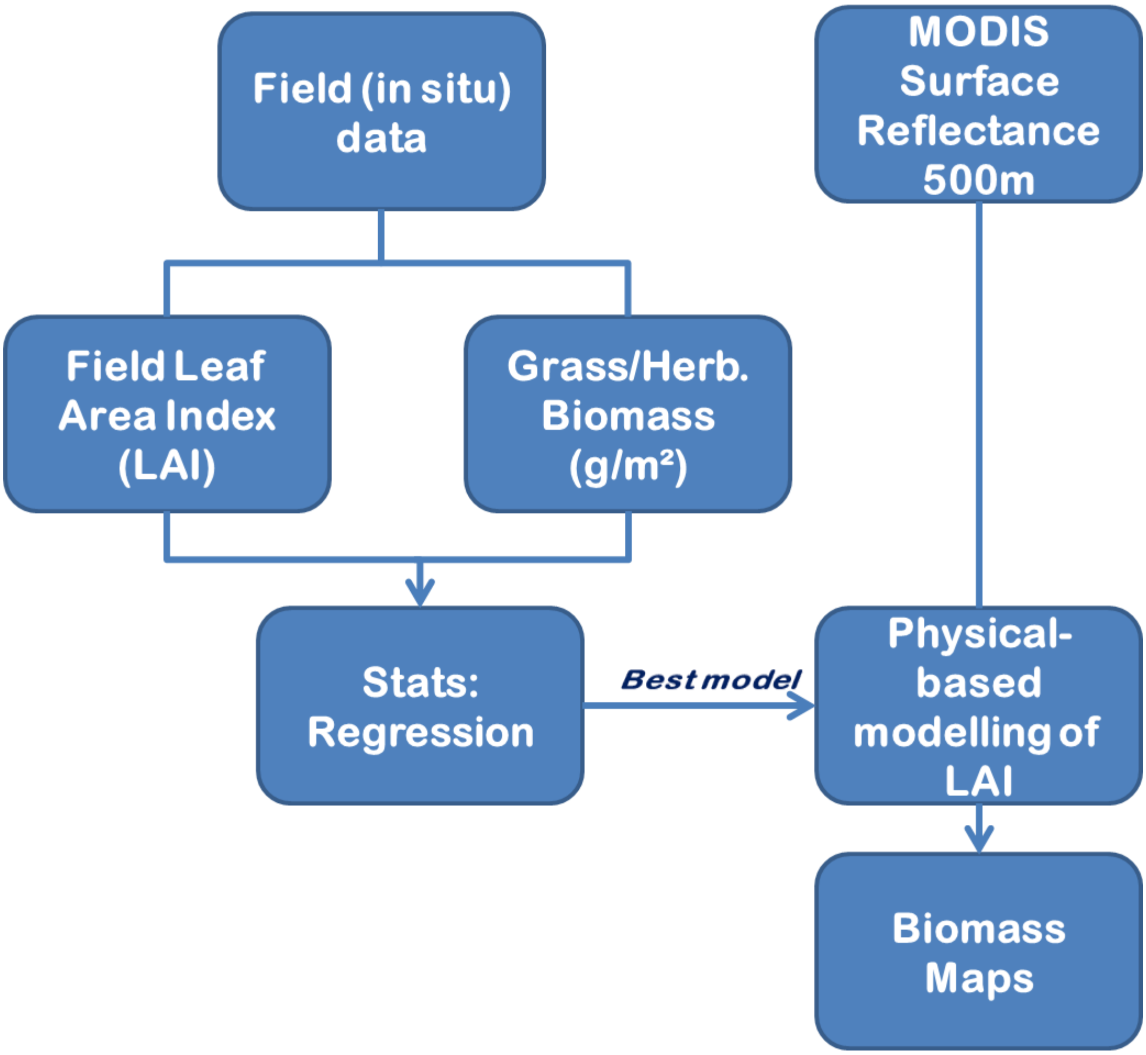

Figure 8.4. Flowchart of the herbaceous biomass

8.5 Above ground biomass

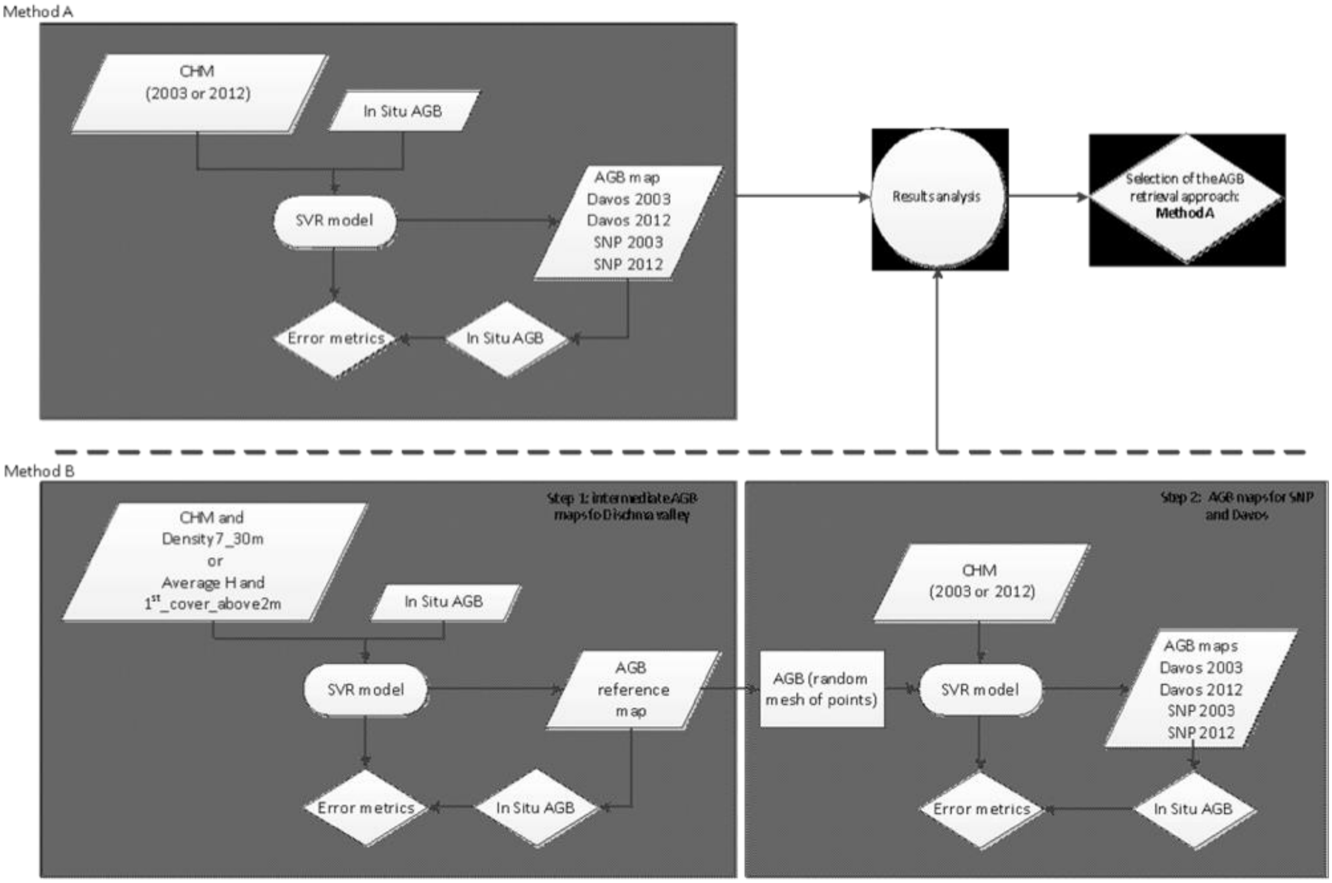

Figure 8.5. Flowchart for methods used to retrieve AGB in Davos and Swiss NP areas

8.6 Surface Soil Moisture

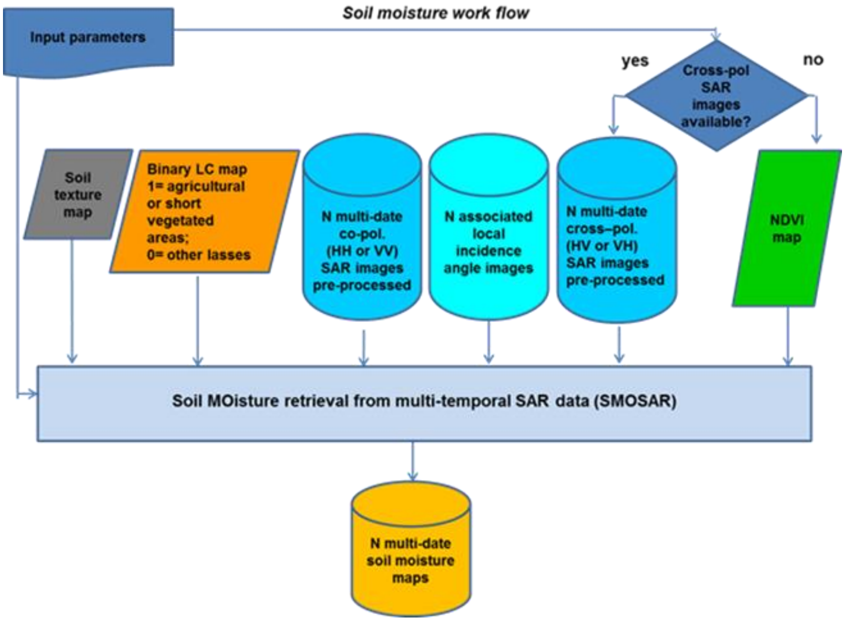

Figure 8.6. SARWIND LG-Mod processing scheme

Co-funded by the
European Union

8.7 Hydroperiod and Seasonality maps estimation

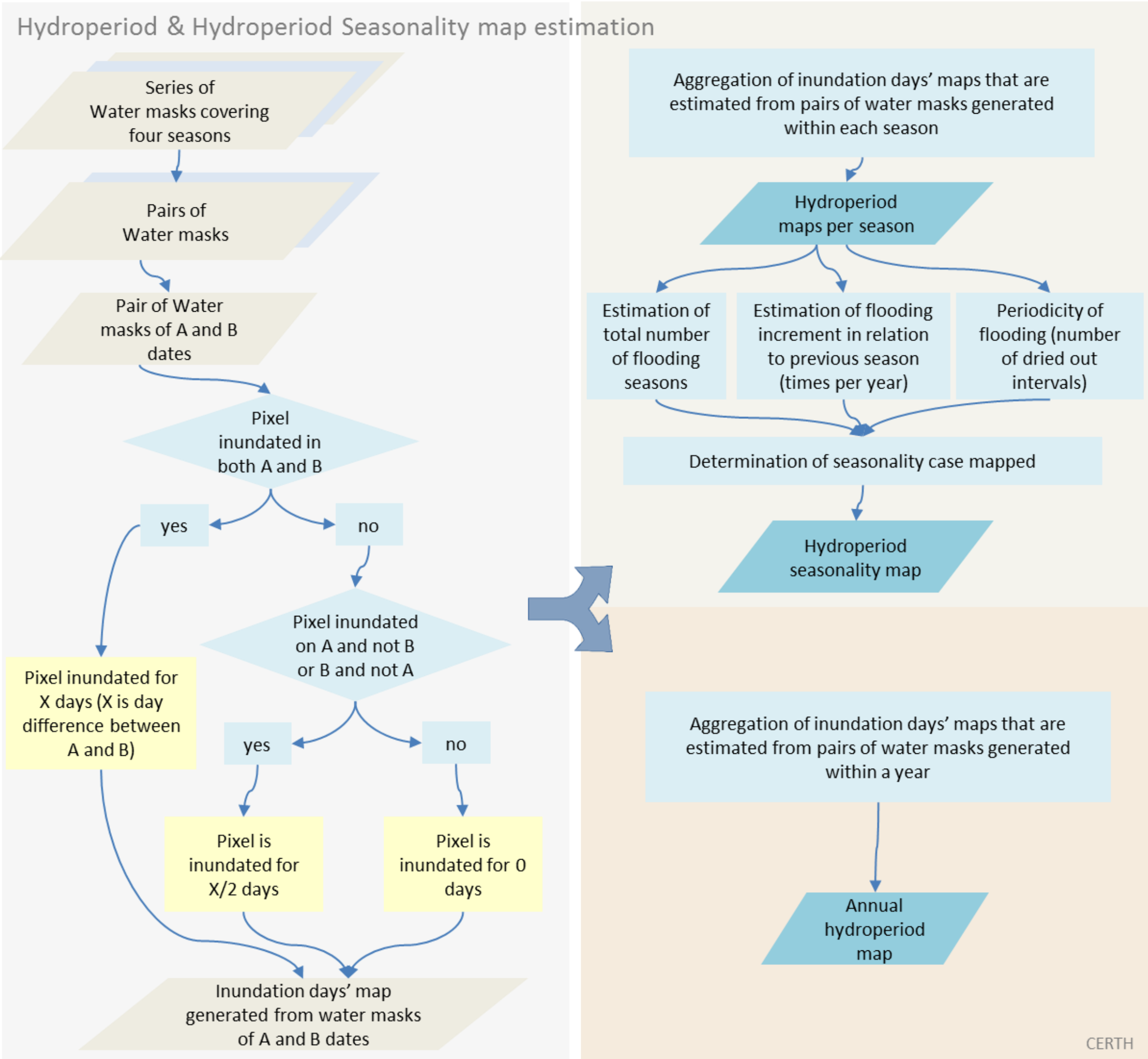

Figure 8.7. Flowchart of the hydroperiod and seasonality maps estimation

8.8 Water mask generation and uncertainty estimation

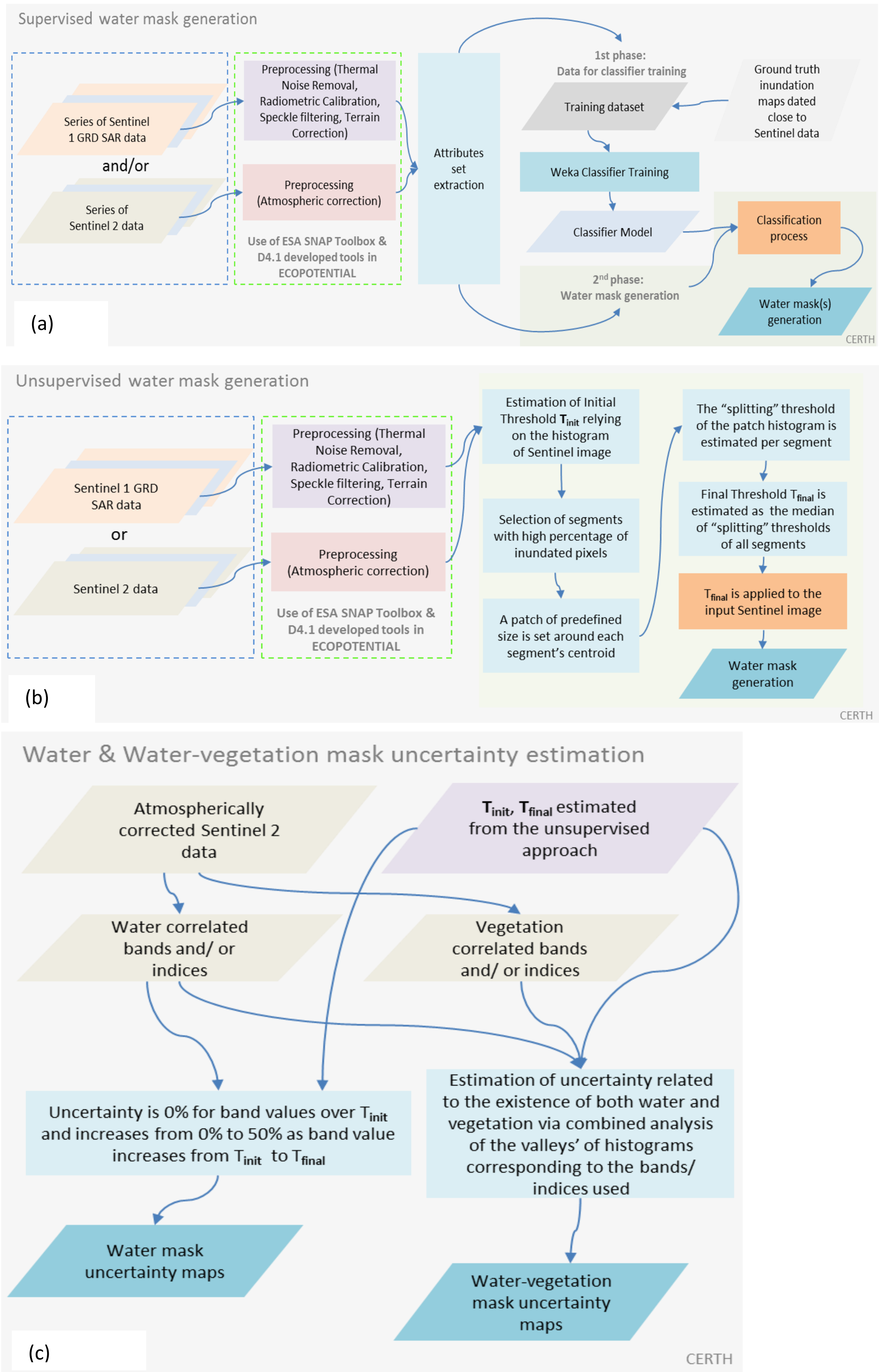

Figure 8.8. (a) Supervised water mask generation; (b) unsupervised water mask generation; (c) water and water – vegetation mask uncertainty estimation.

8.9 Sea Surface Wind Fields (SSW) - Marine

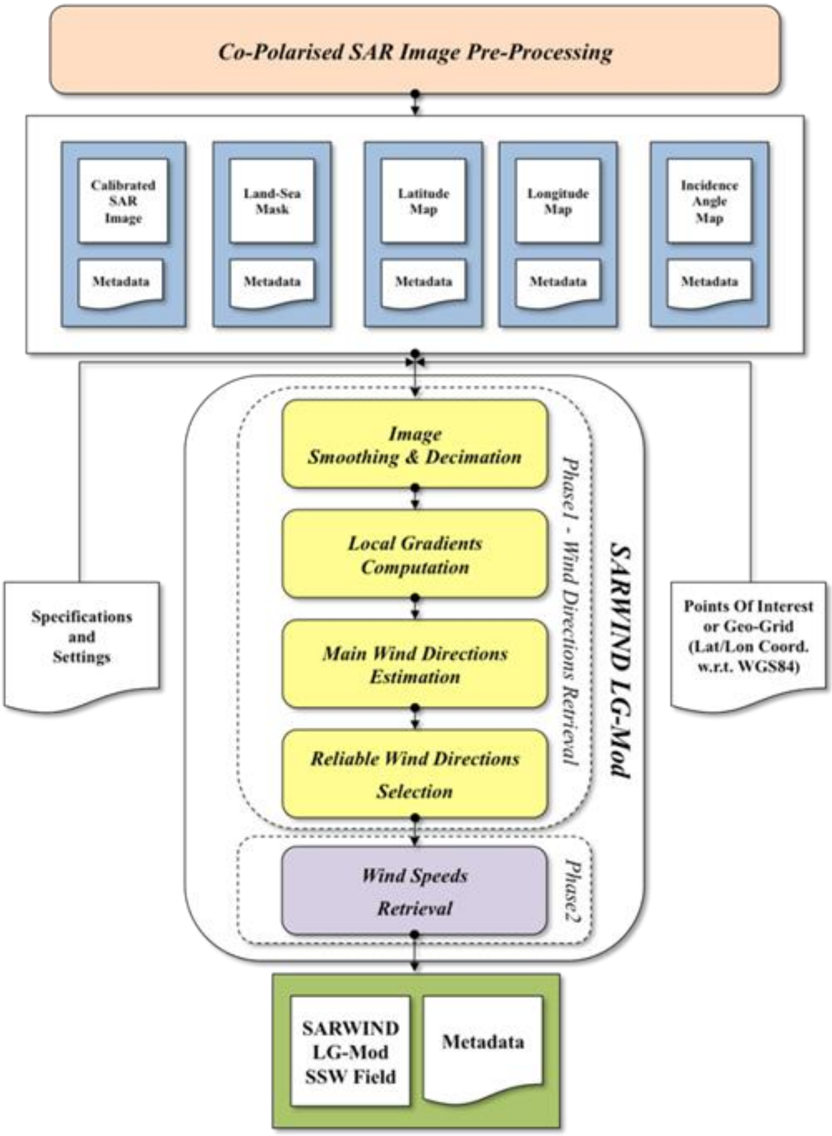

Figure 8.9. SSW algorithm's data flow

Co-funded by the European Union

8.10 Work Flow for Landscape Indicators and uncertainty estimation

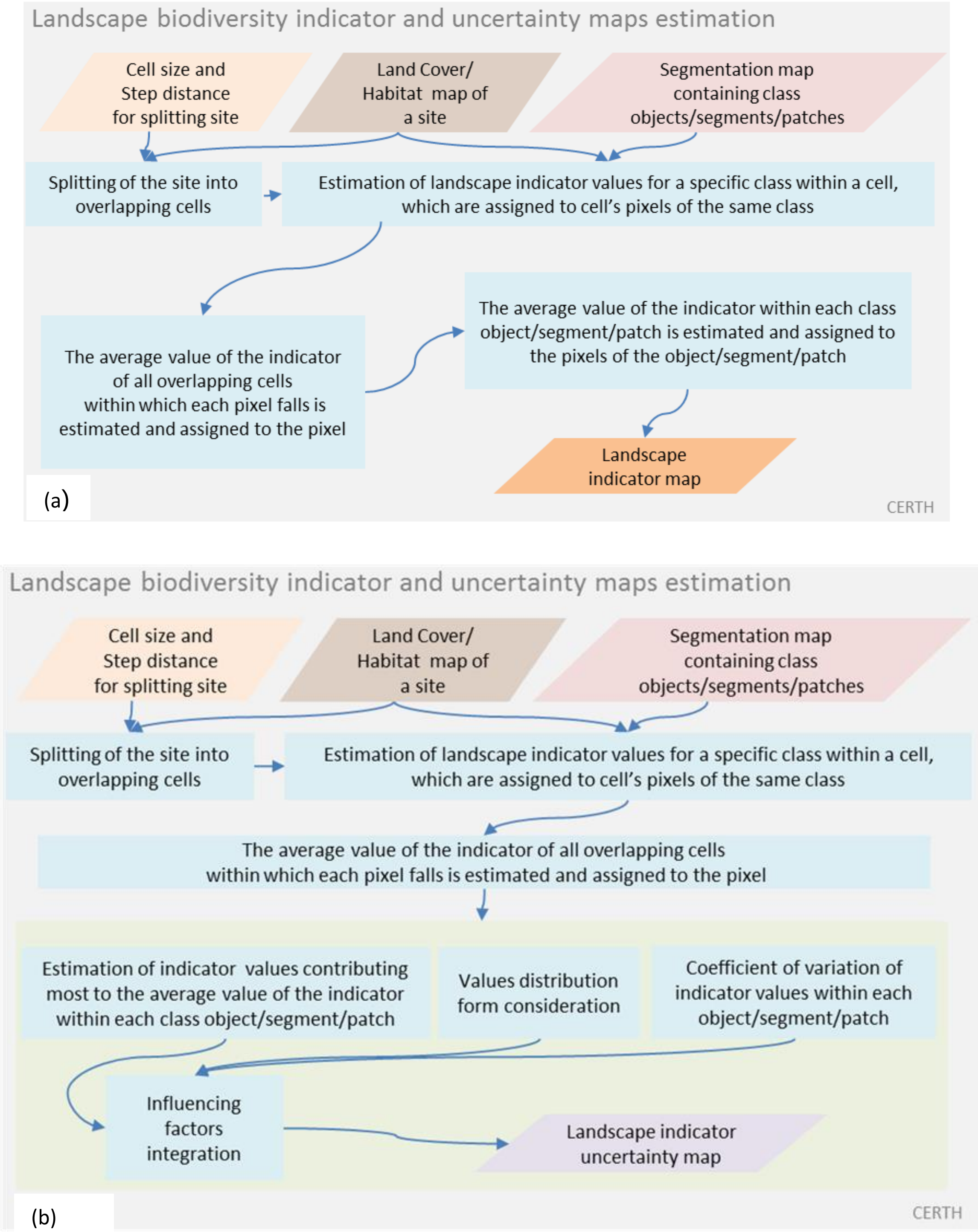

Figure 8.10. (a) Landscape indicator map generation work flow;
(b) uncertainty estimation work flow

8.11 Data driven image classification

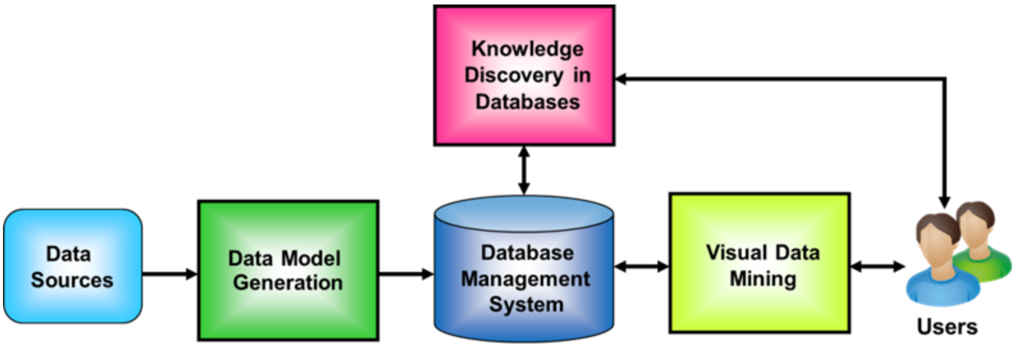

Figure 8.11. Flowchart of DLR data driven image classification system

9. Appendix 2. FAO-LCCS2 Guide

Richard Lucas, Valeria Tomaselli and Anthea Mitchell (6th March 2017)

The following provides an overview of the Food and Agricultural Organisation's (FAO) Land Cover Classification System (LCCS2) and its integration within the ECOPOTENTIAL Earth Observation Data for Habitat Monitoring (EODESM) System.

The Guide provides LCCS2 Level 4 descriptions and associated codes for the following LCCS2 Level 3 categories.

Cultivated Terrestrial Vegetated (A11)
Cultivated Aquatic Vegetated (A23)
Cultivated (Common Categories) (A11 and A23)
Natural/Semi-natural Terrestrial Vegetated (A12)
Natural/Semi-natural Aquatic Vegetated (A24)
Natural/Semi-natural (Common categories) (A12 & A24)
Artificial (B15)
Bare natural (B16)
Water (Common Categories) (B27 and B28)

The format of tables as follows:

Layer name Value LCCS2 Description LCCS2 Code

where:

Layer name: The the raster file name for input to the EODESM system.
Value: The value assigned to all pixels or objects within the layer representing each land cover described.
LCCS2 Description: Detailed descriptive name for the LCCS2 class
LCCS2 Code: Code for the LCCS2 class.

Note that the values often are derived from the LCCS2 Code but not always as some categories (e.g., herbaceous) are described differently depending on the Level 3 classification (e.g., A3 for A11; A2 for A12).

Cultivated Terrestrial Vegetated (A11)

A. Crop Lifeform (4 layers):
1. Crop Lifeform (lifeform)

LlifeForm	= 3	Trees	(A1)
LlifeForm	= 4	Shrubs	(A2)
LlifeForm	= 2	Herbaceous	(A3)
LlifeForm	= 6	Graminoids	(A4)
LlifeForm	= 5	Non-graminoids	(A5)

2. Crop Lifeform (leaf type)

LLeafType	= 1	Broadleaved (trees or shrubs)	(A7)
LLeafType	= 2	Needle-leaved (trees or shrubs)	(A8)

3. Crop Lifeform (phenology)

LPhenolog	= 1	Evergreen (trees or shrubs)	(A9)
LPhenolog	= 2	Deciduous (trees or shrubs)	(A10)

4. Crop Lifeform (urban vegetated)

LUrbanveg	= 6	Urban vegetated	(A6)	
LUrbanveg	= 11	Parks	(A11)	(Overwrites urban vegetated)
LUrbanveg	= 12	Parkland	(A12)	(Overwrites urban vegetated)
LUrbanveg	= 13	Lawns	(A13)	(Overwrites urban vegetated)

B. Crop combination (3 layers):
1. Crop combination (Crop number):

LCropcomb	= 1	Single Crop	(C1)
LCropcomb	= 2	Multiple Crop	(C2)
LCropcomb	= 3	Multiple crop (One additional crop)	(C3)
LCropcomb	= 4	Multiple crop (Two additional crops)	(C4)

2. Crop combination (lifeform):

LlifeForm	= 3	Trees	(C5)	(One additional crop; Multiple crop)
LlifeForm	= 4	Shrubs	(C6)	(One additional crop; Multiple crop)
LlifeForm	= 2	Herbaceous (terrestrial)	(C7)	(One additional crop; Multiple crop)
LlifeForm	= 2	Herbaceous (aquatic)	(C8)	(One additional crop; Multiple crop)
LlifeForm	= 3	Trees	(C9)	(Two additional crops; Multiple crop; first crop)
LlifeForm	= 4	Shrubs	(C10)	(Two additional crops; Multiple crop; first crop)
LlifeForm	= 2	Herbaceous (terrestrial)	(C11)	(Two additional crops; Multiple crop; first crop)
LlifeForm	= 2	Herbaceous (aquatic)	(C12)	(Two additional crops; Multiple crop; first crop)
LlifeForm	= 3	Trees	(C13)	(Two additional crops; Multiple crop; second crop)
LlifeForm	= 4	Shrubs	(C14)	(Two additional crops; Multiple crop; second crop)
LlifeForm	= 2	Herbaceous (terrestrial)	(C15)	(Two additional crops; Multiple crop; second crop)
LlifeForm	= 2	Herbaceous (aquatic)	(C16)	(Two additional crops; Multiple crop; second crop)

3. Crop combination (cropping sequences):

LCropsequ	= 17	Simultaneous cropping	(C17)	(trees, shrubs and herbaceous)
LCropsequ	= 18	Overlapping cropping	(C18)	(herbaceous terrestrial only)
LCropsequ	= 19	Sequential cropping	(C19)	(herbaceous aquatic only)

C. Cultural practices - water supply (2 layers):
1. Water supply:

LWatersup	= 1	Cultural Practice (Rainfed)	(D1)	
LWatersup	= 2	Cultural Practice (Post-flooding)	(D2)	
LWatersup	= 3	Irrigated	(D3)	
LWatersup	= 4	Irrigated Surface	(D4)	(Overwrites irrigated)
LWatersup	= 5	Irrigated Sprinkler	(D5)	(Overwrites irrigated)
LWatersup	= 6	Irrigated Drip	(D6)	(Overwrites irrigated)

2. time factor:

LTimefact	= 7	Shifting cultivation	(D7)
LTimefact	= 8	Fallow system	(D8)
LTimefact	= 9	Permanent cultivation	(D9)

Cultivated Aquatic Vegetated (A23)

Lifeform of the main crop

LlifeForm	= 6	Graminoids	(A1)
LlifeForm	= 5	Non-graminoids	(A2)
LlifeForm	= 1	Woody	(A3)

Water seasonality

LWaterday	= 1	Water (Persistent for whole day)	(C1)
LWaterday	= 2	Water (With daily variations)	(C2)
LWaterday	= 3	Waterlogged	(C3)

Cultural practices - fallow period

LCropsequ	= 1	Permanent cropping	(D1)
LCropsequ	= 2	Relay intercropping	(D2)
LCropsequ	= 3	Sequential cropping	(D3)

Cultivated (Common Categories) (A11 and A23)

Spatial aspect (size):

Lspatsize	= 1	Large to medium-sized fields (2 to > 5 ha)	(B1)
Lspatsize	= 2	Small-sized field(s) (< 2 ha)	(B2)
Lspatsize	= 3	Large-sized field(s) (> 5 ha)	(B3)
Lspatsize	= 4	Medium sized field(s) (2 to 5 ha)	(B4)

Spatial aspect (distribution):

Lspatdist	= 5	Continuous	(B5)
Lspatdist	= 6	Scattered (clustered)	(B6)
Lspatdist	= 7	Scattered (isolated)	(B7)

Natural/Semi-natural Terrestrial Vegetated (A12)

Lifeform:

LLifeform	= 1	Woody	(A1)
LLifeform	= 3	Trees	(A3)
LLifeform	= 4	Shrubs	(A4)
LLifeform	= 2	Herbaceous	(A2)
LLifeform	= 5	Forbs	(A5)
LLifeform	= 6	Graminoids	(A6)
LLifeform	= 7	Lichens/Mosses	(A7)
LLifeform	= 8	Lichens	(A8)
LLifeform	= 9	Mosses	(A9)

Spatial distribution/macropattern:

Lspatdist	= 1	Continuous	(C1)
Lspatdist	= 2	Fragmented	(C2)
Lspatdist	= 3	Parklike patches	(C3)
Lspatdist	= 4	Fragmented Striped	(C4)
Lspatdist	= 5	Fragmented Cellular	(C5)

Natural/Semi-natural Aquatic Vegetated (A24)

Lifeform - Natural Aquatic Vegetated
lifeform (2 layers) :

1. Lifeform main

LLifeform	= 1	Woody	(A1)
LLifeform	= 3	Trees	(A3)
LLifeform	= 4	Shrubs	(A4)
LLifeform	= 2	Herbaceous	(A2)
LLifeform	= 5	Forbs	(A5)
LLifeform	= 6	Graminoids	(A6)
LLifeform	= 7	Lichens/Mosses	(A7)
LLifeform	= 8	Lichens	(A10)
LLifeform	= 9	Mosses	(A11)

2. Lifeform main

MLifeform	= 8	Rooted Forbs	(A8)
MLifeform	= 9	Free floating forbs	(A9)

Water seasonality:

Lwatersea	= 1	Water more than three months	(C1)	
Lwatersea	= 2	Water < 3 months	(C2)	
Lwatersea	= 3	Waterlogged	(C3)	
Lwatersea	= 4	Water > 3 months	(C4)	(persistent whole day)
Lwatersea	= 5	Water > 3 months	(C5)	(with daily variations)

Natural/Semi-natural (Common categories) (A12 & A24)

Canopy cover (2 derivatives):

1. Broad cover types

LCanopyco	= 10	Closed (> 70-60 %)	(A10)
LCanopyco	= 11	Open (70-60 to 20-10 %)	(A11)
LCanopyco	= 20	Closed to open (100-15 %)	(A20)
LCanopyco	= 14	Sparse (20-10 - 1%)	(A14)

2. Sequential cover types (modifiers)

LCanopyco	= 21	Closed to open (100-40 %)	(A21)
LCanopyco	= 12	Open (70-60 to 40 %)	(A12)
LCanopyco	= 13	Open (40-20 to 10 %)	(A13)
LCanopyco	= 15	Sparse (<20-10 - 4%)	(A15)
LCanopyco	= 16	Scattered (4-1 %)	(A16)

Canopy height (2 derivatives)

Height (3 derivatives):

1. Broad height types

DCanopyht	= 1	(7-2 m)	(B1)
DCanopyht	= 2	(>30-3 m)	(B2)
DCanopyht	= 3	(5-0.3 m)	(B3)
DCanopyht	= 4	(3-0.03)	(B4)

2. Trees (30 - 3 m)

DCanopyht	= 5	(>14 m)	(B5)
DCanopyht	= 6	(14-7 m)	(B6)
DCanopyht	= 7	(7-3 m)	(B7)

3. Shrubs (5-0.3 m)

DCanopyht	= 8	(5-3 m)	(B8)
DCanopyht	= 9	(3-0.5)	(B9)
DCanopyht	= 10	(< 0.5 m)	(B10)
DCanopyht	= 14	(5-0.5 m)	(B14)

4 Forbs and graminoids (3-0.3 m)

DCanopyht	= 15	(3-0.3 m)	(B15)
DCanopyht	= 11	(3-0.8 m)	(B11)
DCanopyht	= 12	(0.8-0.3 m)	(B12)
DCanopyht	= 13	(0.03-0.3 m)	(B13)

Leaf Type

LLeafType	= 1	Broadleaved	(D1)
LLeafType	= 2	Needle-leaved	(D2)
LLeafType	= 3	Aphyllous	(D3)

Phenology (2 layers)

1. 'Pure' vegetation stands

LPhenolog	= 1	Evergreen	(E1)
LPhenolog	= 4	Semi-evergreen	(E4)
LPhenolog	= 2	Deciduous	(E2)
LPhenolog	= 4	Semi-deciduous	(E4)
LPhenolog	= 5	Mixed -forbs/graminoids	(E5)

2. Mixed vegetation stands

MPhenolog	= 3	Mixed (applicable to trees and shrubs)	(E3)
MPhenolog	= 6	Mixed herbaceous (annual)	(E6)
MPhenolog	= 7	Mixed herbaceous (perennial)	(E7)

Stratification second layer

LStrat2nd	= 1	2nd layer absent	(F1)
LStrat2nd	= 2	2nd layer present	(F2)

Lifeform second layer

LLifef2nd	= 3	2nd layer Woody	(F3)
LLifef2nd	= 4	2nd layer Herbaceous	(F4)
LLifef2nd	= 5	2nd layer Trees	(F5)
LLifef2nd	= 6	2nd layer Shrubs	(F6)

Cover second layer

DCover2nd	= 7	Closed (> 70-60) to open (70–60 - 15 %)	(F7)
DCover2nd	= 8	Closed (> 70-60 %)	(F8)
DCover2nd	= 9	Open (70-60 - 20-10 %)	(F9)
DCover2nd	= 10	Sparse (20-10 - 1 %)	(F10)

Height second layer

DHeigh2nd	= 1	(7-2 m - for Woody)	(G1)
DHeigh2nd	= 2	(> 30-3 m)	(G2)
DHeigh2nd	= 3	(5-0.3 m)	(G3)
DHeigh2nd	= 4	(3-0.03 m)	(G4)
DHeigh2nd	= 5	(>14 m)	(G5)

DHeigh2nd = 6	(14-7 m)		(G6)
DHeigh2nd = 7	(7-3 m)		(G7)
DHeigh2nd = 8	(5-2 m)		(G8)
DHeigh2nd = 9	(2-0.5 m)		(G9)
DHeigh2nd = 10	(<0.5 m)		(G10)
DHeigh2nd = 11	(3-0.3 m)		(G11)
DHeigh2nd = 12	(0.3-0.03 m)		(G12)

Artificial (B15)

Artificial surface aspect (A)

Lartisurf = 1	Built up		(A1)
Lartisurf = 3	Linear infrastructure		(A3)
Lartisurf = 4	Non-linear infrastructure		(A4)
Lartisurf = 2	Non-built up		(A2)

A. Built up

1. Linear infrastructure

Mlinearis = 7	Roads		(A7)
Mlinearis = 8	Paved roads		(A8)
Mlinearis = 9	Unpaved roads		(A9)
Mlinearis = 10	Railways		(A10)
Mlinearis = 11	Comm. Lines/Pipelines		(A11)

2. Non-linear infrastructure (2 layers)

Lnolinear = 12	Industrial a/o other		(A12)
Lnolinear = 13	Urban areas		(A13)

a. Urban areas (density)

D/Lurbanden= 14	Urban high density	(>75 %)	(A14)
D/Lurbanden= 15	Urban medium density	(50-75 %)	(A15)
D/Lurbanden= 16	Urban low density	(30-50 %)	(A16)
D/Lurbanden= 17	Scattered density	(15-30 %)	(A17)

B. Non built up.

MNonbuilt = 5	Waste dump deposit		(A5)
MNonbuilt = 6	Excavation site		(A6)

Bare natural (B16)

Bare surface aspect (A)

Lbaresurf = 1	Consolidated		(A1)
Lbaresurf = 2	Unconsolidated		(A2)
Lbaresurf = 3	Bare rock a/o coarse fragments		(A3)
Lbaresurf = 4	Hardpans		(A4)

Lbaresurf	= 5	Unconsolidated bare soil and	(A5) (other unconsolidated material)
Lbaresurf	= 6	Loose and shifting sands	(A6)

Bare rock a/o coarse fragments

Mbarematr	= 7	Bare rock	(A7)
Mbarematr	= 8	Gravel/stones/boulders	(A8)
Mbarematr	= 14	Gravel	(A14)
Mbarematr	= 15	Stones	(A15)
Mbarematr	= 16	Boulders	(A16)

Hardpans

Mhardpans	= 9	Ironpan/Laterite	(A9)
Mhardpans	= 10	Petrocalcic	(A10)
Mhardpans	= 11	Petrogypsic	(A11)

Unconsolidated material, soils and loose shifting sands

Munstones	= 12	Stony (5-40 %)	(A12)
Munstones	= 13	Very stony(40-80 %)	(A13)

Bare macropattern (sands) (B)

Lmacropat	= 1	Dunes	(B1)
Lmacropat	= 2	Barchans	(B2)
Lmacropat	= 5	Barchans (saturated)	(B5)
Lmacropat	= 8	Barchans (unsaturated)	(B8)
Lmacropat	= 3	Parabolic dunes	(B3)
Lmacropat	= 6	Parabolic dunes (saturated)	(B6)
Lmacropat	= 9	Parabolic dunes (unsaturated)	(B9)
Lmacropat	= 4	Longitudinal dunes	(B4)
Lmacropat	= 7	Longitudinal dunes (saturated)	(B7)
Lmacropat	= 10	Longitudinal dunes (unsaturated)	(B10)
Lmacropat	= 13	Salt flat	(B13)

Bare macropattern (soils) (B)

Lmacropat	= 11	Gilgai	(B11)
Lmacropat	= 12	Termite mounds	(B12)

Water (Common Categories) (B27 and B28)

B27 & B28 - water
A. physical status (A)

Lwaterstt	= 1	Water	(A1)
Lwaterstt	= 2	Snow	(A2)
Lwaterstt	= 3	Ice	(A3)

B. water dynamics (A)

Mwatermvt	= 4	Flowing water	(A4)
Mwatermvt	= 5	Standing water	(A5)

Mwatermvt	= 6	Moving ice	(A6)
Mwatermvt	= 7	Stationary ice	(A7)

C. water persistence (B)

Dwaterper	= 1	Perennial (> 9 months)	(B1)
Dwaterper	= 2	Non-perennial (< 9 months)	(B2)
Dwaterper	= 3	Tidal area	(B3)
Dwaterper	= 7	Perennial (9-7 months)	(B7)
Dwaterper	= 8	Perennial (6-4 months)	(B8)
Dwaterper	= 9	Perennial (3-1 months)	(B9)

a. Substrate material

Msubstrat	= 4	bare rock	(B4)
Msubstrat	= 5	bare soil	(B5)
Msubstrat	= 6	sand	(B6)

D. water depth

Lwaterdpt	= 1	Deep to medium (> 2 m)	(C1)
Lwaterdpt	= 2	Shallow (< 2 m)	(C2)

E. water sediment loads

Lwsedload	= 1	Almost no sediment	(D1)
Lwsedload	= 2	With sediment	(D2)

10. Appendix 3. Summary of LC and habitats, relation for selected protected areas and their translation to LCCS2 categories.

It is worth noting that only habitats characterized by one-to-one LC to habitat translation relation are considered in the Table reported hereafter.

A11: Herbaceous. Multiple Crop with simultaneous cropping, rainfed and permanent cultivation
Complex cultivation patterns
Cultivation and complex systems
Heterogeneous agricultural areas
Mixed crops of market gardens and horticulture
Arable land and market gardens
Other perennial crops
Temporary crops associated with permanent crops
Sunflower
A11: Herbaceous. Multiple Crop with simultaneous cropping, irrigation and permanent cultivation
Arable irrigated and non-irrigated land
Horticultural gardens
Irrigated vegetable crops in open fields and greenhouses
A11: Herbaceous. Single Crop with irrigation and permanent cultivation
Basins with irrigation as predominant use
A11: Herbaceous. Single Crop, rainfed and permanent cultivation
Agrarian culture with natural spaces
Agricultural land
Agricultural land
Agricultural production units
Agriculturally-improved, re-seeded and heavily fertilised grassland, including sports fields and grass lawns
Alfalfa
Alpine and subalpine enriched grassland
Annual crops
Corn
cultivated areas with vegetation
cultivated areas without vegetation
grazed pasture
Greenhouse crops
Herbaceous crops
Intensive unmixed crops
Land principally occupied by agriculture with significant areas of natural vegetation
Low and medium altitude hay meadows
Managed grassland
meadows
Mixing of natural vegetation and crops
Mountain hay meadows
Non-irrigated vegetable crops in open fields and greenhouses
Pastures and grasslands
Pastures and meadows including wastelands and warehouse corridors
Permanent crops
Permanent mesotrophic pastures and aftermath-grazed meadows
Permanent pastures
Simple non-irrigated arable land
Sorghum
Wheat
A11: Shrubs (broadleaved, deciduous). Single Crop with rainfed and permanent cultivation
Vineyards
A11: Shrubs (broadleaved). Single Crop with rainfed and permanent cultivation
Shrub plantations
A11: Shrubs (broadleaved deciduous). Multiple Crop with simultaneous cropping, rainfed and permanent cultivation
Fruit trees and berry plantations
A11: Shrubs (broadleaved deciduous). Single Crop with rainfed and permanent cultivation
Orchard
orchards
A11: Shrubs (broadleaved deciduous). Single Crop, rainfed and permanent cultivation
Vineyard
A11: Shrubs (broadleaved evergreen). Single Crop with rainfed and permanent cultivation
grape vines
A11: Shrubs (broadleaved, deciduous). Single Crop with rainfed and permanent cultivation
Shrub plantations for ornamental purposes or for fruit, other than vineyards
Vineyards
A11: Trees
trees, bush greenery

A23: Graminoids, large-sized field(s), water (persistent for whole day)
Rice
ricefields
A23: Non-graminoids, waterlogged
peat extraction plots
A24: Forbs, open (4-2 to 2-1 %), 2-5 m (for shrubs), aphyllous, annual, 2nd layer absent, water > 3 months (with daily variations)
Salt Marshes and Grasslands (inside Dykes)
Salt Marshes and Grasslands (outside Dykes)
A24: Forbs, open (4-2 to 2-1 %), 3-3 m (for herbaceous)
Salt plain (low Salicornia-type)
A24: Forbs, open (4-2 to 2-1 %), 3-3 m (for herbaceous),
open salicornia-type marshes
A24: Forbs, open (7-6 to 4 %)
dense salicornia-type marshes
A24: Forbs, open (7-6 to 4 %), 8-3 m (for herbaceous)
Salt plain (high Salicornia-type)
A24: Free floating forbs, open (4-2 to 2-1 %), 3-3 m (for herbaceous), broadleaved mixed (forbs, graminoids), 2nd layer absent, water > 3 months (with daily variations)
Transition mires to quaking bogs
A24: Graminoids, open (7-6 to 4 %)
Reedbeds
Water-fringing reed beds and tall helophytes other than canes
A24: Graminoids, open (7-6 to 4 %), 5-5 m (for shrubs)
Reed beds
A24: Graminoids, open (7-6 to 4 %), 5-5 m (for shrubs),
Cladium mariscus beds (sawgrass marsh)
A24: Graminoids, open (7-6 to 4 %), broadleaved evergreen, 2nd layer herbaceous, closed (> 7-6 %), waterlogged
Mediterranean tall humid grasslands of the Molinio-Holoschoenion
A24: Herbaceous
Wet areas
A24: Herbaceous
Inland wet areas
Wet coastal areas
A24: Herbaceous
Wetlands
A24: Herbaceous, aphyllous, annual, 2nd layer absent
Low - Young marshes
Silty Pioneer Vegetation
A24: Herbaceous, aphyllous, annual, 2nd layer absent
Medium and High - Old Saltmarshes
A24: Herbaceous, closed to open (1-15 %), 3-3 m (for herbaceous), aphyllous, evergreen, 2nd layer absent,
Salicornia and other annuals colonizing mud and sand
A24: Herbaceous, closed to open (1-15 %), mixed (forbs, graminoids), water < 3 months
salt meadows high level
A24: Herbaceous, closed to open (1-15 %), mixed (forbs, graminoids), water > 3 months (With daily variations)
salt meadows low level
A24: Herbaceous, open (7-6 to 4 %)
Base-rich fens and calcareous spring mires
Blanket bogs
Bog
Damaged, inactive bogs
Periodically inundated shores with pioneer and ephemeral vegetation
Raised and blanket bogs
Raised bog complexes
Raised bogs
Rich fens, including eutrophic tall-herb fens and calcareous flushes and soaks
Swamp
Transition mires and quaking bogs
Valley mires, poor fens and transition mires
Wetlands with or without wet woodlands
A24: Herbaceous, open (7-6 to 4 %)
Bog
Exploited peat bog
Inland saline marshes
Swamp

A11: Trees (broadleaved). Single Crop with rainfed and permanent cultivation

Annual crops + other broadleaf trees
Woody crops

A11: Trees (broadleaved evergreen). Single Crop with rainfed and permanent cultivation

Annual crops + oaks
Cork Oak
Cork Oak + Oak

A11: Trees (broadleaved evergreen). Single Crop, rainfed and permanent cultivation

Olive orchard

A11: Trees (broadleaved, deciduous). Multiple Crop with simultaneous cropping, rainfed and permanent cultivation

Orchards and small fruit farms

A11: Trees (broadleaved, deciduous). Single Crop with rainfed and permanent cultivation

orchards

A11: Trees (broadleaved, evergreen). Single Crop with rainfed and permanent cultivation

Olive groves

A11: Trees (needleaved, deciduous). Single Crop with rainfed and permanent cultivation

Coppice and early-stage plantations

A11: Trees (needleaved, evergreen). Single Crop with rainfed and permanent cultivation

Forests spruce dominated
Highly artificial coniferous plantations

A11: Trees, rainfed and permanent cultivation

Agriculture and forest areas

A11: Trees. Multiple Crop with simultaneous cropping, rainfed and permanent cultivation

Forests mixed broadleaf and conifers

A11: Trees. Single Crop, rainfed and permanent cultivation

orchards

A11: Urban Vegetated

Cultivated areas of gardens and parks
Open surfaces with anthropogenic vegetation
Playing surfaces and bushes
Small-scale ornamental and domestic garden areas
Sports grounds
Urban green areas
Urban parks, facilities for sports, leisure and cultural activities, historical areas

A11: Urban Vegetated in large-sized field(s)

fallows, wastelands, edges of pathways

A11: Urban Vegetated, rainfed and permanent cultivation

Urban (including green) spaces
urban vegetation

A12: Woody

Lines of trees
Lines of trees, small anthropogenic woodlands, recently felled woodland, early-stage woodland and coppice
Pasture woods (with a tree layer overlying pasture)

A12: Forbs

Subalpine moist or wet tall-herb and fern stands

A12: Forbs

Moist or wet tall-herb and fern fringes and meadows

A12: Forbs, open (7-6 to 2-1 %), < 5 m (for shrubs), continuous, needleleaved, annual,2nd layer absent,

Hydrophilous tall herb fringe communities of plains and of the montane to alpine levels

A12: Graminoids

Dense grass cover
Grassland
Humid and wet grasslands
Natural pastures, grasslands, uncultivated
Rough pastures (including wastelands)
Sandveld Communities

A12: Graminoids

[Festuca pallens] grassland
Acid alpine and subalpine grassland
Alpine and sub-alpine vegetation communities without trees
Alpine and subalpine grasslands
Alpine riverine [Carex maritima] ([Carex incurva]) swards
Arid and semi-arid grasslands with dry bushes, dwarf shrub heath and Nardus grasslands (including wastelands)
Arid subcontinental steppic grassland ([Festucion valesiacae])
Beds of large sedges normally without free-standing water
Central alpine arid grassland ([Stipo-Poion])
Closed non-Mediterranean dry acid and neutral grassland
Continental inland salt steppes
Dry grasslands
Dry sub-continental acid steppic grasslands
Euro-Siberian pioneer calcareous sand swards
Grassland with higher proportion of forest/woodland communities
Grasslands

A24: Herbaceous, open (7-6 to 4 %),

Juncus rush bed
Other marshes with emergent vegetation
water with vegetation

A24: Herbaceous, open (7-6 to 4 %), < 5 m (for shrubs), aphyllous semi-evergreen or semi-deciduous, 2nd layer herbaceous, open (7-6 to 2-1 %), 3 - 0.3 m (for herbaceous), water > 3 months (Peristent for whole day)

Oligotrophic waters containing very few minerals of sandy plains

A24: Herbaceous, scattered (4-1 %), 2-0.5 m (for shrubs), aphyllous annual, 2nd layer absent, water > 3 months (with daily variations)

Brackish Pioneer Vegitation (SALT MARSHES AND SALT MEADOWS)
Salt Pioneering Vegetation (Sea Bed) (SALT MARSHES AND SALT MEADOWS) [annuals]
Salty Pioneer Vegetation (Sea Wall) (SALT MARSHES AND SALT MEADOWS) [annuals]

A24: Rooted Forbs, open (4-2 to 2-1 %)

pond, marsh

A24: Rooted Forbs, open (4-2 to 2-1 %),

Open marshes
Pond, marsh or lagoon

A24: Shrubs, closed to open (1-15 %)

Mire
Mire deciduous

A24: Shrubs, open (7-6 to 4 %), 2-5 m (for shrubs), broadleaved evergreen, 2nd layer herbaceous, sparse to scattered (2-1 - 1%), 3 - m (for herbaceous), water > 3 months (With daily variations)

Spartina swards

A24: Trees, open (4-2 to 2-1 %), 2-5 m (for shrubs), needleleaved, evergreen, 2nd layer shrubs, open (7-6 to 2-1 %),waterlogged

Southern riparian galleries and thickets

A24: Trees, open (7-6 to 4 %)

River flood plain forests

A24: Trees, open (7-6 to 4 %), 7-3 m (for trees), broadleaved deciduous, 2nd layer trees, closed (> 7-6 %), 5-2 m (for shrubs), waterlogged

Gallieries

A24: Woody, open (7-6 to 4 %)

Inland freshwater marshes
Lowland forests and forests on damp and wet locations
Swamp in forest

A24: Woody, open (7-6 to 4 %), broadleaved

Broadleaved swamp forest

B15: Built up

airports
Ancient and continuous residential fabric
Anthropogenic locations
buildings
Buildings of cities, towns and villages
Cemeteries
Construction isolates
Discontinuous residential fabric
Disused settlements
heliports
Industry, markets and transports
Residential fabric (rarely nucleiforme)
Settlement
urbanised territory

B15: Comm. Lines/Pipelines

Technical Infrastructures

B15: Extraction site

Restored former salt works
Salt works (preconcentration of salt)
Salt works (salt harvest)

B15: Industrial and/or other areas

Airports and heliports
Cemeteries
Construction and excavation sites
Energy distribution, production and transport networks and areas
Hospital settlements
Industrial
industrial areas
Industrial or commerical area
Industrial or handicraft settlement with adjioning spaces
Industrial, commercial and military units
Landfills and quarry deposits, mines, industry
Large concentration and sorting good plants
Major private and public service systems
Mine extractions
Mineral extraction, dump and construction sites
Mining areas
Open cast scrap deposits, car cemetries
Port areas
Reworked soils and artifacts

Iberian montane [Nardus stricta] swards	Technological systems
Mesic grasslands	Telecommunications installations
Meso-xerophile subcontinental meadow-steppes ([Cirsio-Brachypodion])	Trade settlement
Moist or wet eutrophic and mesotrophic grassland	Wastelands (recent)
Moist or wet oligotrophic grassland	B15: Industrial and/or other areas
Pannonic loess steppic grassland	Extractive industrial sites
Perennial calcareous grassland and basic steppes	B15: Linear infrastructure
Reedbeds normally without free-standing water	Road/rail network and associated space
Seasonally wet and wet grasslands	Transport networks and other constructed hard-surfaced areas
Sedge and reedbeds, normally without free-standing water	Transportation infrastructures
Semi natural grassland without trees (TCD <30 %)	B15: Non-Built up
Serpentine steppes	building surroundings
Sparsely wooded grasslands	cemetery
Sub-Atlantic semi-dry calcareous grassland	dumping grounds
Sub-Atlantic very dry calcareous grassland	Gravel pit
Unmanaged xeric grassland	quarry
A12: Graminoids, < 5 m (for shrubs)	Saltworks (preconcentration of salt)
Rocky grasslands	Saltworks (salt havest)
A12: Graminoids, semi-evergreen or semi-deciduous	B15: Paved roads
Shrubby high vegetation and degraded or transition forest + other softwoods	runway
A12: Graminoids, open (4-2 to 2-1 %)	Unpaved roads
Embryonic dune	B15: Railways
A12: Graminoids, open (4-2 to 2-1 %), < 5 m (for shrubs)	Rail networks and adjoining surfaces
Mediterranean sub-steppe	Railways and associated land
A12: Graminoids, open (7-6 to 2-1 %,	B15: Roads
Open non-Mediterranean dry acid and neutral grassland, including inland dune grassland	Road networks and ancillary spaces
A12: Herbaceous	Road networks and associated land
Bare ground - fresh veg	roads
Basins without manifest productive uses	B15: Unpaved roads
Biotope complex	Firebreaks
Biotope complexes of montane to alpine slopes	pathways (gravel roads)
Forests with higher proportion of woody plants and/or grassland types	B15: Urban areas
pastures or grasslands	Urban pavillons
Pastures/meadows	B15: Urban areas
Rich small structures	Archaeological areas
unused land	Artificial territories
Vegetation	Disused settlements
A12: Herbaceous	Equipment for sport and leisure
Basic mountain flushes and streamsides, with a rich arctic-montane flora	Mixed urban
undefined low vegetation	Residential area
Water and herbaceous vegetation	Residential fabric (rarely nucleiforme)
Water with higher proportion of forests, shrubs and grasslands	stadiums and sports and recreation grounds
A12: Herbaceous,	Urban areas
Bare ground - patchy veg	Urban fabric
Biotope complexes of montane to alpine plateaux	Urban fabric (predominantly public and private units)
Meadows and marshes	B15: Urban areas of high density
A12: Herbaceous, broadleaved evergreen	Dense urban fabric
Bare areas with little or no vegetation + oak	Recent dense and high continuous residential fabric
A12: Herbaceous, closed (> 7-6 %), 2-5 m (for shrubs), striped, broadleaved semi-evergreen or semi-deciduous, 2nd layer absent,	Recent dense and low continuous residential fabric
Humid Dune slacks	B15: Urban areas of low density
A12: Herbaceous, closed (> 7-6 %), 3-0.3 m (for herbaceous), continuous, broadleaved perennial. 2nd layer absent, 3rd layer absent,	Green urban areas and leisure facilities
Mediterranean salt steppes	Low density buildings
A12: Herbaceous, closed to open (1-15 %)	Urban spaces without solid construction
sand, dune with vegetation	B15: Urban areas of medium density
A12: Herbaceous, closed to open (1-15 %), broadleaved evergreen	Discontinuous residential fabric
Meadow	B15: Urban areas of scattered density
A12: Herbaceous, open (4-2 to 2-1 %), < 5 m (for shrubs)	Scattered residential fabric
Vegetated dune	B15: Urban areasof scattered density
A12: Herbaceous, open (7-6 to 2-1 %), 0.8-0.3 m (for herbaceous), striped, broadleaved perennial, 2nd layer absent	Scattered residential fabric
Fixed coastal dunes with herbaceous vegetation (Grey Dunes) [hard/calcium]	B15: Waste dump deposit
Fixed coastal dunes with herbaceous vegetation (Grey Dunes) [soft]	Inert extraction areas, waste decomposition areas and construction sites
A12: Herbaceous, open (7-6 to 2-1 %), 2-5 m (for shrubs), parklike patches, broadleaved evergreen 2nd layer herbaceous, sparse to scattered (2-1 to 1%), 3 - 0.33 m (for herbaceous), 3rd layer absent,	Reworked soils and artifacts
Mediterranean salt meadows	Waste deposits
A12: Herbaceous, scattered (4-1 %), 0.8-0.3 m (for herbaceous), cellular, broadleaved evergreen 2nd layer absent, 3rd layer absent,	B16: Bare rock
Shifting dunes along the shoreline ('white dunes')	Calcareous and ultra-basic screes of warm exposures
A12: Herbaceous, scattered (4-1 %), 8-3 m (for herbaceous), cellular, broadleaved evergreen 2nd layer absent, 3rd layer absent,	Rock
Annual vegetation of drift lines	Rock
A12: Herbaceous, sparse to scattered (2-1 - 1%)	B16: Bare rock and/or coarse fragments
Sparsely vegetated areas	Bare rocks and rock debris
A12: Herbaceous, sparse to scattered (2-1 - 1%), cellular, broadleaved evergreen 2nd layer absent, 3rd layer absent,	Bare rocks, cliffs and outcrops
Fixed coastal dunes with herbaceous vegetation ('grey dunes')	Cave interiors
A12: Lichens	Foreland with rock and rubble
Bare ground - lichens	Loose rock and weathered formations
A12: Shrubs	Natural and artificial caves and tunnels
Arctic, alpine and subalpine scrub	Rock formations
Areas with natural recolonisation	Rock formations, caves, special weathering forms
Bushes	B16: Bare rock and/or coarse fragments
Debris in forest	Acid siliceous inland cliffs
Debris in open forest	Almost bare rock pavements, including limestone pavements
Disturbed areas (fires or other damaging events)	Basic and ultra-basic inland cliffs
Dry heaths	Inland cliffs, rock pavements and outcrops
Inland sand and rock with open vegetation	Weathered rock and outcrop habitats

Riverine and fen scrubs	B16: Bare soil a/o other uncons. material
Riverine scrub	Bare soil
Sclerophyllous vegetation	Dry
Scree with shrubbery	High silt and sand flats
Shrubland	Land without current use
Temperate and mediterranean-montane scrub	B16: Bare soil a/o other uncons. material
Temperate thickets and scrub	Bare soil
Thermo-Atlantic xerophytic scrub	B16: Consolidated
A12: Shrubs	Bare ground - no registered veg
Bushes and shrubs	Bare ground - no veg
Forest	Miscellaneous inland habitats with very sparse or no vegetation
Heathlands and moorlands	Unvegetated areas
hedgerows	B16: Consolidated
A12: Shrubs, aphyllous	unclassified
Dwarf Knob Thorn Savanna	B16: Gravel/stones/boulders
Knob Thorn/False-thorn Thorn Thickets	Scree
Knob Thorn/Large Marula Thorn veld	Temperate-montane acid siliceous screes
Knob Thorn/Sickle bush Thorn Thickets	Temperate-montane calcareous and ultra-basic screes
Mopane/Knob Thorn Savanna	B16: Gravel/stones/boulders
A12: Shrubs, broadleaved	Scree
Bushwillow/Guarri Bushveld	B16: Loose and shifting sands
Bushwillow/Knob Thorn Rugged Veld	Beaches
A12: Shrubs, broadleaved	Dunes
Bushwillow/Mopane Rugged Veld	B16: Loose and shifting sands
Cluster leaf/Rock Fig Sour Bushveld	Beach
Euphorbia/Baobab Mountain Bushveld	B16: Loose and shifting sands, dunes
Euphorbia/Bushwillow Mountain Bushveld	beaches, dunes , sand
Mixed Bushwillow Bush Savanna	Embrionic Dunes and Beach Area
Mixed Bushwillow/Mopane Bush Savanna	Pannonic inland dunes
Mopane Shrub Savanna	sands
A12: Shrubs, broadleaved mixed evergreen/deciduous	B16: Loose and shifting sands, longitudinal dunes (unsaturated)
Low quality rangeland and low shrubby vegetaiton + weeds	Colonizing Dunes
Shrubby high vegetation and degraded or transition forest + cork oak	White Dunes
Shrubby high vegetation and degraded or transition forest + eucalyptus	B16: Unconsolidated
Shrubby high vegetation and degraded or transition forest + other broadleaf	Rest area
A12: Shrubs, needleleaved, evergreen	River banks
Conifer scrub close to the tree limit	B27: Water
A12: Shrubs, closed (> 7-6 %), >3-3 m (for trees), needleleaved, evergreen	Highly artificial man-made waters and associated structures
Vegetaed dune (shrubs)	B27: Water, non-perennial (< 9 months), shallow, with sediment
A12: Shrubs, closed (> 7-6 %), 0.8-0.3 m (for herbaceous), striped, broadleaved perennial, 2nd layer absent	Salines
Sea Buckthorn Thickets	B27: Water, perennial (> 9 months)
A12: Shrubs, closed (> 7-6 %), 0.8-0.33 m (for herbaceous), fragmented, broadleaved evergreen 2nd layer absent, 3rd layer absent,	Canals and waterways
Temperate Atlantic wet heaths	Highly modified natural water courses and canals
A12: Shrubs, closed (> 7-6 %), 5-0.3 m (for shrubs), broadleaved deciduous	Intensively managed fish ponds
Shrublands and woodland	Ponds and lakes with completely man-made structure
A12: Shrubs, closed (> 7-6 %), 5-2 m (for shrubs), fragmented, needleleaved, evergreen 2nd layer shrubs, closed to open (1 - 15 %), 2-5 m (for shrubs), 3rd layer herbaceous, sparse to scattered (2-1 - 1%), 3 - 0.33 m (for herbaceous)	Standing water bodies of industrial sites
European dry heaths	B27: Water, perennial (> 9 months), shallow, with sediment
A12: Shrubs, closed (> 7-6 %), 5-3 m (for shrubs), striped, broadleaved, semi-evergreen or semi-deciduous, 2nd layer absent	Canal
Creeping Willow Thickets	B27: Water, perennial (> 9 months), deep to medium, almost no sediment
A12: Shrubs, deciduous	Dam
Subalpine deciduous scrub	B27: Flowing water, perennial (> 9 months),
Submediterranean deciduous thickets and brushes	reservoirs
A12: Shrubs, evergreen	B27: Standing water, perennial (> 9 months),
Evergreen alpine and subalpine heath and scrub	ponds and stagnant water bodies
A12: Shrubs, needleleaved, evergreen	B27: Water, tidal area, shallow, with sediment
Mountain pine scrub forest	Salt lakes
A12: Shrubs, open (4-2 to 2-1 %), 2-5 m (for shrubs), striped, broadleaved evergreen 2nd layer herbaceous, sparse to scattered (2-1 to 1%), 2-5 m (for shrubs), 3rd layer absent,	B28: Flowing water that is non-perennial (< 9 months), shallow and almost no sediment
Mediterranean and thermo-Atlantic halophilous scrubs	Constantly flowing Mediterranean rivers
A12: Shrubs, open (7-6 to 2-1 %)	B28: Flowing water that is perennial (> 9 months)
Open areas and with low vegetation cover	Flow
A12: Shrubs, open (7-6 to 2-1 %), 3-0.3 m (for herbaceous), fragmented, broadleaved evergreen 2nd layer shrubs, sparse to scattered (2-1 to 1%), 2-5 m (for shrubs), 3rd layer absent,	Interconnected running water courses
Dune sclerophyllous scrubs	Rivers, streams and ditches
A12: Shrubs, open (7-6 to 2-1 %), 5-0.3 m (for shrubs), broadleaved deciduous	Watercourse
Semi-open shrubland and woodland	B28: Flowing water that is perennial (> 9 months)
A12: Shrubs, open (7-6 to 2-1 %), 7-2 m (for woody)	Flow
Tamarix thickets	rivers
A12: Shrubs, sparse to scattered (2-1 - 1%)	Springs, spring brooks and geysers
Sparse vegetation	B28: Flowing water that is perennial (> 9 months),
A12: Trees	Surface running waters
Early growth forests (reforestation)	B28: Flowing water that is perennial (> 9 months),
Forest	Watercourse
Forests	B28: Flowing water that is perennial (> 9 months), shallow
Forests (successional)	streams, canal, drainage ditches
Forests and natural and semi-natural habitats	B28: Flowing water that is tidal area, deep to medium and with sediment
Forests on wet and damp locations	Saltiness
forrest	B28: Flowing water that is tidal area, deep to medium with sediment
Lines of trees and scrub	Gully (deeper than 5 m)
Moor	Submerged Tidal Flats (<-5m-1% sandbanks)
Riparian forests	B28: Flowing water that is tidal area, shallow and with sediment
Special locations	Tidal muds
trees	B28: Flowing water that is tidal area, shallow and with sediment

trees in agricultural areas
trees zone
Woods and forests on damp and wet locations
A12: Trees
Forest edge vegetation communities
Forests
Mixed riparian floodplain and gallery woodland
Semi natural grassland with trees (TCD >30 %)
Transitional woodland and scrub
tree-lined meadows, wooded pastures
Woodlands with grassland
Woodlands with shrublands
A12: Trees,
Forest
A12: Trees, >3-3 m (for trees), broadleaved deciduous
Deciduous forest
Mixed forest
Riparian forest
A12: Trees, >3-3 m (for trees), needleleaved, evergreen
Coniferous forest
A12: Trees, >3-3 m (for trees), broadleaved deciduous
riverine forest
A12: Trees, broadleaved
Knob thorn/Marula Tree Savana
Mixed bushwillow/Cluster leaf Tree Savanna
Mopane Tree Savanna
Oaks + other softwoods
A12: Trees, broadleaved deciduous
[Abies] and [Picea] woodland
[Fagus] woodland
Acidophilous [Quercus]-dominated woodland
Bare areas with little or no vegetation + other softwood
Broadleaved deciduous woodland
Broadleaved swamp woodland not on acid peat
Broadleaved swamp woodland on acid peat
Forest Deciduous
Meso- and eutrophic [Quercus], [Carpinus], [Fraxinus], [Acer], [Tilia], [Ulmus] and related woodland
Oak + annual crops
Oak + eucalyptus
Oak and Pinus pinaster
Oaks
Oaks + chestnut
Thermophilous deciduous woodland
A12: Trees, broadleaved evergreen
Bare areas with little or no vegetation + Pinus pinaster
A12: Trees, broadleaved mixed evergreen/deciduous
Bare areas with little or no vegetation + other broadleaves
Oak and other broadleaf
Other broadleaf trees
Other broadleaf trees + oaks
A12: Trees, broadleaved semi-evergreen or semi-deciduous
Mixed deciduous and coniferous woodland
Shrubby high vegetation and degraded or transition forest + oaks
Shrubby high vegetation and degraded or transition forest + Pinus pinaster
A12: Trees, broadleaved, deciduous
Other natural and semi natural broadleaved forest
A12: Trees, needleleaved, deciduous
[Pinus uncinata] woodland
Alpine [Larix] - [Pinus cembra] woodland
A12: Trees, needleleaved, evergreen
[Pinus nigra] woodland
[Pinus sylvestris] woodland south of the taiga
Bare areas with little or no vegetation + cork oak
Boreal bog conifer woodland
Conifeorus forest
Coniferous woodland
Forest Coniferous
Nemoral bog conifer woodland
A12: Trees, needleleaved, mixed evergreen/deciduous
Mixed coniferous and deciduous forest
Tall mixed woody forest with degradation or sucession + Pinus pinaster
A12: Trees, broadleaved deciduous
Broadleaved (hardwood) forests
Deciduous forests
Deciduous forests (other)
Mixed broadleaf forests beech dominated
A12: Trees, broadleaved, deciduous
Decidious forest
A12: Trees, broadleaved, semi-evergreen or semi-deciduous
Other natural and semi natural mixed forest
A12: Trees, closed (> 7-6 %), >3-3 m (for trees), needleleaved, evergreen
Pine forest
A12: Trees, closed (> 7-6 %), >3-3 m (for trees), broadleaved deciduous
deciduousforests
A12: Trees, closed (> 7-6 %), 14-7 m (for trees), striped, broadleaved, deciduous, 2nd layer absent
Wooded Dunes of the Atlantic and Continental Boreal Region (dry)
Wooded Dunes of the Atlantic and Continental Boreal Region (wet)

Exposed Tidal Flat - (1-33% sandbanks)
Exposed Tidal Flat - (33%-67% sandbanks)
Exposed Tidal Flat - (67-99% sandbanks)
Flooded During Spring Time (99% sandbanks)
B28: Flowing water that is tidal area, surface: bare soil, shallow and with sediment
Colonizing Mud and Sand Flats (North Sea Coastal Zone)
Colonizing Mud and Sand Flats (tidal)
Estuary
Mud
B28: Flowing water that is tidal area, surface: sand, shallow and with sediment
Coarse Sand
Standing Sandbanks (North Sea Coastal Zone)
Standing Sandbanks (tidal)
B28: Flowing water that is tidal, deep to medium and with sediment
Outer Delta
B28: Flowing water, tidal area, shallow and with sediment
Saltmarsh creeks and puddles
B28: Flowing water, tidal area. Surface: sand, shallow, and with sediment
Fine Sand
B28: Flowing water, tidal, deep to medium and with sediment
Shrimp Fishery intensity
Water Depth
B28: Flowing water, tidal, shallow and with sediment
Mud Flats
B28: Ice that is non-perennial (< 9 months)
Mediterranean temporary ponds
Natural eutrophic lakes with Magnopotamion or Hydrocharition -type vegetation
B28: Ice that is perennial (> 9 months)
Glacier
Rubble on glacier
B28: Ice that is perennial (> 9 months)
Glacier
Ice caps and true glaciers
Rubble on glacier
B28: Snow that is perennial (> 9 months)
Snow or ice-dominated habitats
B28: Standing water
Coastal lagoons
water without vegetation
B28: Standing water that is perennial (> 9 months)
Coastal lagoons
lagoons
Permanent dystrophic lakes, ponds and pools
Permanent eutrophic lakes, ponds and pools
Separated water bodies belonging to the river system (dead side-arms, flood ponds)
Surface standing waters
B28: Standing water that is perennial (> 9 months)
Littoral zone of inland surface waterbodies
B28: Standing water that is perennial (> 9 months), deep to medium
Baltic sea, Curonian lagoon
lakes
B28: Stationary ice that is perennial (> 9 months)
Glacier
B28: Water that is non-perennial (< 9 months), shallow and almost no sediment
Bare water
B28: Water that is perennial (> 9 months)
Inland water bodies
Lake
Marine (other)
Natural water bodies
Offshore and coastal areas
Water bodies
B28: Water that is perennial (> 9 months)
Freshwater
Lake
B28: Water that is perennial (> 9 months),
Water and aquatic vegetation

A12: Trees, closed to open (1-15 %), 5-3 m (for shrubs), cellular, needleleaved, evergreen 2nd layer trees, sparse to scattered (2-1 to 1%), 2-5 m (for shrubs), 3rd layer present, sparse to scattered (2-1 - 1%), 3 - 3 m (for herbaceous)
Coastal dunes
A12: Trees, mixed evergreen/deciduous
Forest Mixed
A12: Trees, needleleaved, evergreen
Coniferous forests (natural)
Mountain pine and scrub forest
Other natural and semi natural coniferous forest
A12: Trees, open (7-6 to 2-1 %)
Open forest
Open forests, herbaceous vegetation and shrubs
A12: Trees, open (7-6 to 2-1 %)
Open forest
A12: Trees, open (7-6 to 2-1 %), 7-3 m (for trees), fragmented, broadleaved deciduous 2nd layer trees, sparse to scattered (2-1 to 1%), 2-5 m (for shrubs), 3rd layer herbaceous, sparse to scattered (2-1 - 1%), 3 - 0.3 m (for herbaceous)
Woodlands
A12: Trees, open (7-6 to 4 %), 5-2 m (for shrubs), striped, broadleaved evergreen 2nd layer present, sparse to scattered (2-1 to 1%), 2-5 m (for shrubs), 3rd layer absent,
Thermo-Mediterranean and pre-desert scrub
A12: Woody
Lean and semi-dry grasslands, dry bushes, borstgras and dwarf shrub heath
Revegetation of trees and/or grassland
Trees/bush groups, copses, rows of trees, hedges, alleys, indiv tree rows, hedgerows, alleys, individual trees
A12: Woody
Other biotope complexes

11. Appendix 4. Technology Readiness Levels

Technology Readiness Levels (TRL) are a method of assessing technology maturity providing a metric for benchmarking, development goals and Key Performance Indicators (KPIs).

Within ECOPOTENTIAL TRLs can be a useful communication tool between work packages regarding EO module/ EV (Environmental Variable) outputs and identifying key feasibility and development criteria. This is particularly the case for communications between WP10 (Virtual Laboratory), WP11 (EO supported Policy Development & Integration) and WP12 (Capacity building and knowledge exchange) and the wider project.

There are 9 technology readiness levels progressing from level 1; basic scientific principles observed and reported, to level 9; Actual system proven through successful operations. These are accepted metrics for H2020 projects: (http://ec.europa.eu/research/participants/data/ref/h2020/wp/2014_2015/annexes/h2020-wp1415-annex-g-trl_en.pdf)

TRL 1 – basic principles observed

TRL 2 – technology concept formulated

TRL 3 – experimental proof of concept

TRL 4 – technology validated in lab

TRL 5 – technology validated in relevant environment (industrially relevant environment in the case of key enabling technologies)

TRL 6 – technology demonstrated in relevant environment (industrially relevant environment in the case of key enabling technologies)

TRL 7 – system prototype demonstration in operational environment

TRL 8 – system complete and qualified

TRL 9 – actual system proven in operational environment (competitive manufacturing in the case of key enabling technologies; or in space)

The purpose of this Appendix is to benchmark the TRLs of EO modules and track these to completion of the project. This exercise, made by ESL Partner, aids in clarifying EO module aims, development objectives of the technology system (hardware, software and data) and proposed market, including; user needs and requirements of EO module outputs.

11.1 Method

The assessment used an online questionnaire to ascertain the TRL of each module and circulated these to leads within WP4. Two weeks were given to gather responses and the results are compiled herein. The results have been reported in Table 5.1 within Section 5.

The Questionnaire can be viewed by following the link below:

https://docs.google.com/a/envsys.co.uk/forms/d/1d7oA-xbJRsAbS_p3F7fM5FzEmFJO3dvO0M0z2AUf5rU/edit

11.2 Limitations

1) There are 11 outstanding EO modules/ENVs TRL assessments.
2) Some modules include multiple ENVs that present challenges to overall TRL assessments.
3) Some module products rely heavily on supporting providers for data, software and hardware presenting difficulties to accurate assessment without clearly defined use cases.
    a. A wider assessment frame may be needed and this will be taken forward as an action based upon expected use cases of EO products.

11.3 Conclusions

The TRL assessment found the average score for respondents to be level 4 described as; 'Component and/or platform validation in laboratory environment.'

The range of scores extends form level 3 to 9 with one module; 'Indexes computation' scoring a level 9. This module supports other modules within ECOPOTENTIAL, thereby proving successful operational use case.

Having baselined module TRLs, user development plans can be tracked along with appropriate research and potentially policy and commercial exploitation strategies. Work should be continued to gather TRL scores for remaining modules and target scores set for the culmination of the project.